

---

**Exploring the Molecular Mechanisms of Action  
of Samoan Medicinal Plants  
via Chemical Genetic Analyses**

---

By

Seesei Molimau-Samasoni

A thesis  
submitted to the Victoria University of Wellington  
in fulfilment of the requirements for the degree of  
Doctor of Philosophy  
in Cell and Molecular Bioscience

Victoria University of Wellington  
2016



This thesis was conducted under the supervision of

**Dr. Andrew B Munkacsi (Primary Supervisor)**  
Victoria University of Wellington  
Wellington, New Zealand

and

**Professor Paul H Atkinson (Secondary Supervisor)**  
Victoria University of Wellington  
Wellington, New Zealand



---

## Abstract:

---

Natural products are a robust source of drug leads, and medicinal plants have been the source of natural products that are important pharmaceuticals in modern medicine. Samoan medicinal plants have been investigated in the past, but their potential as a source of new drug leads has not been realized. I hypothesized that determining the mechanism of action of Samoan medicinal plant extracts would provide insight into their pharmaceutical potential. The work described herein was carried out on 11 Samoan medicinal plants, from which 22 extracts were prepared. A bioactivity rate of 68% was determined when 15 of the 22 extracts inhibited the growth of yeast (*Saccharomyces cerevisiae*). The medicinal plant *Psychotria insularum* was the most potent, thus genome-wide analyses were completed using the haploid deletion mutant library of *S. cerevisiae*. Yeast strains deficient in iron transport were hypersensitive to the *P. insularum* aqueous extract. Further investigations showed that exogenous iron supplementation rescued the growth defect induced by *P. insularum* extracts, suggesting that *P. insularum* reduced intracellular iron. Fittingly, yeast cells treated with *P. insularum* extracts contained less intracellular iron than control cells. Paradoxically, the expression levels of iron transporter proteins were upregulated upon extract treatment. When we investigated iron-requiring cellular processes, we found that yeast cells treated with *P. insularum* extracts exhibited a respiratory deficient phenotype and reduced heme synthesis, indicative of an impaired cellular iron status. These findings suggested that *P. insularum* reduced bioavailable iron leading to the induction of the low iron response, and indeed the extracts of *P. insularum* were shown to chelate iron via the iron-chelating CAS assay. To translate results from yeast to mammalian cells, we treated primary murine macrophages with *P. insularum* extracts and detected an anti-inflammatory response, which we found to correlate with reduced activity of the iron-requiring aconitase enzyme. We further determined using pooled diploid mutant genetic analyses that the extracts of *P. insularum* did not have a genetic target. To identify the compound

mediating the iron chelation mechanism, bioassay-guided isolation was conducted. Fractionation of the crude aqueous extract of *P. insularum* produced a relatively pure fraction that NMR and the acid-butanol assay identified as a condensed tannin. Together, these results indicate a relationship between iron chelation, a condensed tannin and inflammation. Further, we established an iron chelation mechanism of action by which *P. insularum* extracts are used to treat inflammation-associated symptoms in traditional Samoan medicine. Lastly, the findings presented here substantiate the reliability of plants with ethnobotanical background as sources for bioactive natural products.

---

## Acknowledgements:

---

This work could not have been completed without the tremendous help of numerous people, and I would like to express my most heartfelt gratitude to them. First and foremost, I would not be here without the funding from the Victoria Doctoral Scholarship, under the VUW and Scientific Research Organisation of Samoa (SROS) memorandum of cooperation (MOC). Thank you for the PhD opportunity! Thank you specifically to Afioga Tilafono David Hunter for the push to apply for this.

To my primary supervisor Dr Andrew Munkacsi: thank you for giving me the opportunity to study here by agreeing to take me on as one of your first PhD students, and for your endless support throughout my project. I do not think I could have come across a more patient supervisor than you! Prof. Paul Atkinson, your appreciation of my small victories was a constant reassurance that there was a method to the madness. I thank you both for giving me free reign over the direction of my project, because it has taught me the invaluable lesson of project design and critical thinking, important skills one would hope to walk away with from having completed a PhD.

To the Chemical Genetics lab crew past and present, to say I have had a colorful experience working with you all would be an understatement. You have all contributed to a “culturally unique” experience during my studies in The Land of the Long White Cloud. I would especially like to thank Drs James Matthew, Peter Bircham and (pending Dr) Bede Busby for showing me the ropes around the lab. Peter and Bede, I’m pretty sure relaxing with you guys singing karaoke to Gangsta’s Paradise led to a subsequent week of brain light bulbs lighting up! To my fellow PhD colleague Namal Coorey, our early morning lab sessions were one of my more productive lab times. We have yet to take a “morning crew” selfie! Dini, you are truly a jack of all trades. From pinning out library master copies to putting together a computer so I could write my thesis – You’re a champ! To (pending Dr) Russian – Spasibo for the patient proof-reading; I know it was a painful task!

I also express my heartfelt gratitude to the other research groups that were involved in this work. In particular, I thank Dr Rob Keyzers, for your enthusiasm and for always having time to discuss the chemistry side of my project. Your help in deciphering my NMR spectra and your invaluable input to my chemistry chapter are sincerely acknowledged. To the student cohort in the chemistry labs: Benjamin Baker, Helen Woolner and Sarah Andreassand, (who helped out with running my LH20 column, TLCs and NMRs), your help in the chemistry lab is most appreciated. To Dr Daniel Sinclair from the School of Geography and Environmental Science, thank you for allowing

us to run our samples on your ICP-MS, despite its limited use in this area. To Associate Professor Anne La Flamme, Pirooz Zareie and Vimal Patel, thank you for taking on the macrophage work on my extracts. Thanks also to Associate Professor David Ackerley and Dr. Jeremy Owen for your kind assistance and putting up with my troubleshooting of CAS assay hiccups. I would also like to acknowledge the help I received from Associate Professor David Gresham and his PhD student Darach Miller for the Bar-seq work carried out at NYU.

To the Samoan support group at SROS, from the staff, to the management and the Board, my most heartfelt Faafetai tele lava! You have supported me right from the start, through prayers, encouragement and financial assistance. I would not have been able to leave home and travel to NZ to undertake this without your support. To the Ministry of Natural Resources and Environment, specifically Mr Talie Foliga – A huge thank you for taking the time out to assist with my sample collection. I hope the findings of this research can contribute to your conservation efforts. Faamoetaulua Dr Faale Tumaalii, thank you for your faith in me.

It has been a challenge to undertake a PhD, away from the motherland. In this aspect, my husband, daughter and I have been the recipient of the kindness of many who we now consider family. Katie & Viv Zeier, we thank you for your friendship and generosity – You have contributed to smoother sailing in the final year of my PhD. To the Teofilo, Lualua, Fruean and Poleta families, you took us in without any questions and your kind-heartedness will never be forgotten. To my dearest uncle Fitulua Utupo and his partner Virginia Fruean, we are unquestionably indebted to you both. From the moment we landed to our departure, you have been with us every step of the way. Through thick and thin, you have supported us unconditionally, and from the bottom of our hearts, we say THANK YOU!

Finally, to my dear husband and best friend, your endurance in raising our daughter by yourself for the most part of the time we've been here while I've been preoccupied with work is not unnoticed. Your endless support, prayers and encouragement has pushed me on to the finishing line. My dearest daughter Toeupu, I can only hope to provide you with a good example and a better future from this. Mum, thank you for encouraging me to take on this opportunity, and for pushing me to get the PhD I've always wanted. Last but not least, I dedicate this thesis to my late father Molimau Poleta – Dad, I've finally done it, Vi'ia le Ali'i!

---

## Table of Contents:

---

<b>Abstract</b> .....	i
<b>Acknowledgements</b> .....	iii
<b>Contents</b> .....	v
<b>List of Tables</b> .....	xi
<b>List of Figures</b> .....	xii
<b>Abbreviations</b> .....	xvi

---

<b>Chapter 1: Literature Review</b>	1-21
-------------------------------------	------

---

<b>1.1</b>	<b><i>Natural Products</i></b> .....	1
<b>1.2</b>	<b><i>The status of natural products research over the years</i></b> .....	2
<b>1.3</b>	<b><i>Microbial natural products</i></b> .....	4
<b>1.4</b>	<b><i>Marine natural products</i></b> .....	6
<b>1.5</b>	<b><i>Animal natural products</i></b> .....	7
<b>1.6</b>	<b><i>Plant natural products</i></b> .....	8
<b>1.7</b>	<b><i>Medicinal plants</i></b> .....	10
<b>1.8</b>	<b><i>Samoan medicinal plants</i></b> .....	12
1.8.1	<i>History</i> .....	12
1.8.2	<i>Previous studies on Samoan medicinal plants</i> .....	13
<b>1.9</b>	<b><i>Chemical genetics</i></b> .....	15
1.9.1	<i>Introduction</i> .....	15
1.9.2	<i>Yeast as a model organism</i> .....	16
1.9.3	<i>Yeast chemical genetics</i> .....	17
1.9.3.1	<i>Characteristics of the gene deletion mutant collection</i> .....	17
1.9.3.2	<i>Yeast chemical genetic profiling</i> .....	18
1.9.3.3	<i>Drug targets &amp; mechanism of action via yeast chemical genetic profiling</i> .....	20
1.9.3.4	<i>Yeast chemical genetic profiling of crude natural product extracts</i> .....	20
<b>1.10</b>	<b><i>Aims</i></b> .....	21

**Chapter 2: Bioactivity and Stability of Aqueous & Methanolic Extracts  
of Samoan Medicinal Plants**

22-51

---

<b>2.1</b>	<b>Introduction</b> .....	22
2.1.1	<i>Bischofia javanica</i> .....	22
2.1.2	<i>Clerodendrum inerme</i> .....	23
2.1.3	<i>Colubrina asiatica</i> .....	23
2.1.4	<i>Cordyline fruticosa</i> .....	24
2.1.5	<i>Cymbobogon citratus</i> .....	24
2.1.6	<i>Flakourtia rukam</i> .....	25
2.1.7	<i>Macropiper puberulum</i> .....	25
2.1.8	<i>Psychotria insularum</i> .....	25
2.1.9	<i>Syzygium corynocarpum</i> .....	26
2.1.10	<i>Vigna marina</i> .....	26
2.1.11	<i>Wollastonia biflora</i> .....	27
2.1.12	<i>Aim</i> .....	27
<b>2.2</b>	<b>Methods</b> .....	29
2.2.1	<i>Medicinal plant collection</i> .....	29
2.2.2	<i>Extract preparation</i> .....	30
2.2.3	<i>Liquid-based bioactivity assay</i> .....	31
2.2.4	<i>Agar-based bioactivity assay</i> .....	32
<b>2.3</b>	<b>Results</b> .....	33
2.3.1	<i>Two of 11 aqueous extracts are bioactive in SC media at pH 4.5</i> .....	33
2.3.2	<i>Five of 11 aqueous extracts are bioactive in SC media at pH 7.0</i> .....	35
2.3.3	<i>Five of 11 methanolic extracts are bioactive in SC media at pH 4.5</i> .....	37
2.3.4	<i>Ten of 11 methanolic extracts are bioactive in SC media at pH 7.0</i> .....	39
2.3.5	<i>Extracts from different plants exhibit varying bioactivity profiles</i> .....	41
2.3.6	<i>Aqueous extracts are not substrates of the PDR system</i> .....	42
2.3.7	<i>Methanolic extracts are not substrates of the PDR system</i> .....	44

2.3.8	<i>Aqueous extracts maintain bioactivity in agar</i> .....	46
2.3.9	<i>Methanolic extracts maintain bioactivity in agar</i> .....	47
<b>2.4</b>	<b>Discussion</b> .....	49

---

**Chapter 3: Mechanism of Action of *Psychotria insularum* is iron chelation** 52-93

---

<b>3.1</b>	<b>Introduction</b> .....	52
<b>3.2</b>	<b>Methods</b> .....	54
3.2.1	<i>Agar-based genome-wide analyses</i> .....	54
3.2.2	<i>Metal rescue assay</i> .....	54
3.2.3	<i>Quantification of intracellular iron</i> .....	55
3.2.4	<i>Protein expression</i> .....	55
3.2.5	<i>Heme assay</i> .....	56
3.2.6	<i>Aconitase assay</i> .....	56
3.2.7	<i>Iron chelation assay</i> .....	57
3.2.8	<i>Anti-inflammatory assays</i> .....	57
<b>3.3</b>	<b>Results</b> .....	59
3.3.1	<i>Genome-wide analysis of aqueous <i>P. insularum</i> extract</i> .....	59
3.3.2	<i>Validations implicate various biological processes in <i>P. insularum</i> MOA</i> .....	61
3.3.3	<i>Deletion of <i>CCC2</i> is hypersensitive to the aqueous <i>P. insularum</i> extract</i> .....	62
3.3.4	<i>Gene deletions of the iron transport system are hypersensitive to the aqueous extract of <i>P. insularum</i></i> .....	64
3.3.5	<i>Gene deletions of the iron transport system are hypersensitive to the methanolic extract of <i>P. insularum</i></i> .....	66
3.3.6	<i>Iron supplementation rescues the growth defect induced by the aqueous extract of <i>P. insularum</i></i> .....	68
3.3.7	<i>Iron rescue is specific to <i>P. insularum</i> extract treatments and is not a cytoprotective effect of iron supplementation</i> .....	69
3.3.8	<i>Supplementation with copper partially rescues the growth defect induced by <i>P. insularum</i> extracts in a <i>Fet3p</i> dependent manner</i> .....	71
3.3.9	<i>Supplementation with other metals does not rescue the growth defect induced by extracts of <i>P. insularum</i></i> .....	73

3.3.10	<i>Intracellular iron is decreased in the presence of P. insularum extracts.....</i>	74
3.3.11	<i>P. insularum extracts up-regulate the expression of iron transporters.....</i>	75
3.3.12	<i>P. insularum extracts induce a respiratory deficient phenotype.....</i>	79
3.3.13	<i>P. insularum extracts reduce heme synthesis.....</i>	80
3.3.14	<i>P. insularum extracts chelate iron.....</i>	81
3.3.15	<i>P. insularum extracts exhibit an anti-inflammatory response in murine macrophages.....</i>	83
3.3.19	<i>P. insularum extracts reduce aconitase activity in RAW 264.7 macrophages.....</i>	86
<b>3.4</b>	<b><i>Discussion.....</i></b>	<b>88</b>

---

**Chapter 4: Haploinsufficiency and Homozygous Profile Analyses of the Aqueous and Methanolic Extracts of *Psychotria insularum*** 94-128

---

<b>4.1</b>	<b><i>Introduction.....</i></b>	<b>94</b>
<b>4.2</b>	<b><i>Methods.....</i></b>	<b>96</b>
4.2.1	<i>Pooling the HET and HOM libraries.....</i>	96
4.2.2	<i>Competitive growth of HET and HOM libraries .....</i>	96
4.2.3	<i>Genomic DNA isolation.....</i>	97
4.2.4	<i>Barcode sequencing.....</i>	97
4.2.5	<i>Validation of fitness phenotype .....</i>	98
<b>4.3</b>	<b><i>Results.....</i></b>	<b>99</b>
4.3.1	<i>HIP analysis of the P. insularum aqueous extract .....</i>	99
4.3.2	<i>HOP analysis of the P. insularum aqueous extract.....</i>	104
4.3.5	<i>HIP analyses of the P. insularum methanolic extract .....</i>	109
4.3.7	<i>HOP analyses of the P. insularum methanolic extract .....</i>	114
<b>4.4</b>	<b><i>Discussion.....</i></b>	<b>124</b>

---

**Chapter 5: Identification of the Iron Chelating Condensed Tannin from the Aqueous Extract of *Psychotria insularum*** 129-154

---

<b>5.1</b>	<b><i>Introduction.....</i></b>	<b>129</b>
------------	---------------------------------	------------

<b>5.2</b>	<b>Methods</b> .....	132
5.2.1	<i>HP20 column chromatography fractionation</i> .....	132
5.2.2	<i>Back-loading</i> .....	132
5.2.3	<i>HP20ss column chromatography fractionation</i> .....	132
5.2.4	<i>LH20 column chromatography fractionation</i> .....	133
5.2.5	<i>Thin layer chromatography (TLC)</i> .....	133
5.2.6	<i>Nuclear magnetic resonance (NMR) spectroscopy</i> .....	133
5.2.7	<i>Tannin test</i> .....	134
5.2.8	<i>Condensed tannin test</i> .....	134
5.2.9	<i>Bioactivity assay</i> .....	134
5.2.10	<i>Iron supplementation assay</i> .....	134
5.2.11	<i>Protein expression</i> .....	134
<b>5.3</b>	<b>Results</b> .....	135
5.3.1	<i>The 30% and 75% acetone fractions are bioactive</i> .....	135
5.3.2	<i>The <sup>1</sup>H NMR analyses of the 30% and 75% fractions from HP20 fractionation show similar spectral profiles</i> .....	136
5.3.3	<i>Subfractions of HP20ss fractionation of 30% fraction are bioactive and variably potent</i> .....	137
5.3.4	<i>The NMR spectra of the 50% and 100% HP20ss fractions of the 30% aqueous extract fraction show highly similar profiles</i> .....	139
5.3.5	<i>Subfractions of the HP20ss fractionation of the 75% fraction are bioactive and variably potent</i> .....	140
5.3.6	<i>NMR spectra of the 50% and 60:100% HP20ss fractions of the 75% HP20 fraction display extremely similar profiles</i> .....	141
5.3.7	<i>The 75-50% LH20 pooled fractions A, E, F, G, H, I, K and P are not bioactive</i> .....	143
5.3.8	<i>The 75-50% LH20 1L bulk fractions are bioactive</i> .....	145
5.3.9	<i>Expression of Fet3p and Ftr1p iron transporters are up-regulated in the presence of the selected bioactive fractions</i> .....	146
5.3.10	<i>Fraction R from the LH20 column chromatography is a condensed tannin</i> .....	149
<b>5.4</b>	<b>Discussion</b> .....	150

**Chapter 6: Implications & Future Directions**

155-162

---

<b>6.1</b>	<b><i>Summary</i></b> .....	155
<b>6.2</b>	<b><i>Implications on <i>P. insularum</i> as a potential pharmaceutical</i></b> .....	155
<b>6.3</b>	<b><i>Implications on <i>P. insularum</i> application in Samoan medicine</i></b> .....	158
<b>6.4</b>	<b><i>Implications on the <i>P. insularum</i> plant</i></b> .....	159
<b>6.5</b>	<b><i>Implications on natural products in Samoa</i></b> .....	160
<b>6.6</b>	<b><i>Future Directions</i></b> .....	161
<b>6.7</b>	<b><i>Conclusions</i></b> .....	162

---

*References*

163-189

---

<i>Appendix I</i>	<i>Media Composition</i>	I
<i>Appendix II</i>	<i>Bioactivity of Aqueous Extracts at 70°C</i>	II
<i>Appendix III</i>	<i>Strains Genotypes</i>	III
<i>Appendix IV</i>	<i>List of Gene Deletions from Haploid Genetic Analysis</i>	IV
<i>Appendix V</i>	<i>Spot Dilutions of all Hits</i>	VII
<i>Appendix VI</i>	<i>Script for Acapella GFP Quantification</i>	IX
<i>Appendix VII</i>	<i>Optimized Concentrations for HIP HOP Analyses</i>	X
<i>Appendix VIII</i>	<i>Universal Primer Sequence</i>	XI
<i>Appendix IX</i>	<i>ICP-MS Data for Zinc Quantification</i>	XII

---

## List of Tables:

---

Table 2.1	Summary of bioactivity of aqueous and methanolic extracts	41
Table 3.1	Optimization of aqueous extract concentration for genome-wide analyses	59
Table 4.1	The 25 hypersensitive heterozygotes against the aqueous extract of <i>P. insularum</i> .....	101
Table 4.2	The 26 heterozygotes that grew better in the aqueous extract of <i>P. insularum</i> ...	102
Table 4.3	The 18 hypersensitive homozygous deletion mutants against the aqueous extract of <i>P. insularum</i> .....	106
Table 4.4	The 12 homozygous gene deletions that grew better in the presence of the aqueous <i>P. insularum</i> extract.....	107
Table 4.5	The 20 hypersensitive heterozygotes resulting from treatment with the methanolic extract of <i>P. insularum</i> .....	111
Table 4.6	The 31 heterozygous gene deletions with positive logFC and FDR < 0.05.....	112
Table 4.7	Hypersensitive homozygous deletions against treatment with the methanolic extract of <i>P. insularum</i> .....	116
Table 4.8	Top 90 gene deletions exhibiting improved growth in the presence of the methanolic extract of <i>P. insularum</i> .....	119

---

## List of Figures:

---

Figure 1.1	New chemical entities from or based on natural products .....	2
Figure 1.2	Original and total worldwide natural products patents, 1984-2003.....	3
Figure 1.3	FDA-approved drugs of natural sources from 2008-2012.....	4
Figure 1.4	New chemical entities based or derived from plant natural products.....	10
Figure 1.5	Construction strategy of the yeast deletion mutant collection.....	18
Figure 1.6	Chemical genetic interactions.....	18
Figure 2.1	Representations of the medicinal plants selected for this study.....	28
Figure 2.2	Location of collection of Samoan medicinal plants used in this study.....	29
Figure 2.3	Schematic of leaf juice sample preparation for analyses.....	30
Figure 2.4	Liquid-based bioactivity assay of aqueous plant extracts in SC at pH 4.5.....	34
Figure 2.5	Liquid-based bioactivity assay of aqueous plant extracts in pH 7.0 SC.....	36
Figure 2.6	Liquid-based bioactivity assay of methanolic extracts in pH 4.5 SC.....	38
Figure 2.7	Liquid-based bioactivity assay of methanolic extracts in pH 7.0 SC .....	40
Figure 2.8	Liquid-based growth assays of Y7092 WT and PDR-attenuated strain in aqueous extracts.....	43
Figure 2.9	Liquid-based growth assays comparing growth profiles in WT and PDR-attenuated strain in methanolic extracts.....	45
Figure 2.10	Agar-based growth assays of WT in aqueous extracts.....	47
Figure 2.11	Agar-based growth assays of WT against methanolic extracts.....	48

Figure 3.1	The scatterplot of gene deletion growth ratio against aqueous <i>P. insularum</i> extract.....	60
Figure 3.2	Spot dilution assay of five most hypersensitive gene deletions.....	62
Figure 3.3	<i>YDR269C</i> and <i>CCC2</i> .....	63
Figure 3.4	Growth profiles of gene deletions from the iron transport systems against the aqueous extract of <i>P. insularum</i> .....	65
Figure 3.5	Growth profiles of gene deletions from the iron transport systems against the methanolic extract of <i>P. insularum</i> .....	67
Figure 3.6	Iron supplementation against aqueous and methanolic extracts of <i>P. insularum</i> .....	69
Figure 3.7	Iron supplementation of atorvastatin and cycloheximide drug treatment of BY4741 WT yeast.....	70
Figure 3.8	Copper supplementation rescue profiles of WT and <i>fet3Δ</i> in the presence of aqueous and methanolic extracts of <i>P. insularum</i> .....	72
Figure 3.9	Growth profiles of WT against aqueous and methanolic extracts of <i>P. insularum</i> with metal supplementation.....	73
Figure 3.10	Comparison of relative intracellular iron between control and treated WT.....	74
Figure 3.11	Expression levels of iron transporters under extract treatment monitored via GFP-tagged proteins.....	77
Figure 3.12	Quantification of GFP intensity of iron transporters upon <i>P. insularum</i> treatment .....	78
Figure 3.13	Respiratory deficient phenotype of BY4741.....	80
Figure 3.14	Relative heme content of WT treated with <i>P. insularum</i> extracts.....	81
Figure 3.15	CAS assay illustrating iron chelation activity of <i>P. insularum</i> extracts.....	82
Figure 3.16	Macrophage response to treatment with <i>P. insularum</i> extracts.....	86

Figure 3.17	The aconitase activity of macrophages .....	87
Figure 3.18	Model of the mechanism of action of <i>P. insularum</i> extracts.....	91
Figure 4.1	Scatterplot of heterozygous mutants with false discovery rate values less than 0.05 against the aqueous extract of <i>P. insularum</i> , plotted as logCPM vs logFC....	100
Figure 4.2	Heterozygous genes validated to be hypersensitive to the aqueous extract of <i>P. insularum</i> .....	103
Figure 4.3	Scatterplot of the 30 homozygous deletion mutants with false discovery rate values less than 0.05 against the aqueous extract of <i>P. insularum</i> , plotted as logCPM vs logFC.....	105
Figure 4.4	Validations of the homozygous gene deletions detected to be hypersensitive to the aqueous extract of <i>P. insularum</i> .....	108
Figure 4.5	Scatterplot of the 51 heterozygous mutants with false discovery rate values less than 0.05 against the methanolic extract of <i>P. insularum</i> , plotted as logCPM vs logFC.....	110
Figure 4.6	Validations of the heterozygote genes detected to be hypersensitive to the methanolic extract of <i>P. insularum</i> .....	113
Figure 4.7	Scatterplot of 288 homozygous mutants with false discovery rate values less than 0.05 against the methanolic extract of <i>P. insularum</i> plotted as logCPM vs logFC .....	115
Figure 4.8	Validations of the HOP hits of the methanolic extract of <i>P. insularum</i> .....	122
Figure 5.1	Schematic of bioassay guided fractionation.....	130
Figure 5.2	Bioassays of the 30% and 75% HP20 fractions of the aqueous <i>P. insularum</i> extract.....	135
Figure 5.3	NMR spectra of the 30% and 75% HP20 fractions of the aqueous extract of <i>P.</i>	

	<i>insularum</i> .....	137
Figure 5.4	Bioactivity and iron rescue assays of the HP20ss fractions of the 30% HP20 fraction from the aqueous extract of <i>P. insularum</i> .....	138
Figure 5.5	NMR spectra of the 50% and 100% HP20ss fractions from the 30% HP20 fraction of the aqueous <i>P. insularum</i> extract .....	140
Figure 5.6	HP20ss fractions of the 75% HP20 fraction from the aqueous extract of <i>P. insularum</i> .....	141
Figure 5.7	NMR spectra of the 50% and 60:100% HP20ss fractions of the 75% HP20 fraction of the aqueous extract of <i>P. insularum</i> .....	142
Figure 5.8	Bioactivity assay and NMR spectra of the pooled fractions from the LH20 fractionation of the 75-50 fraction from the aqueous extract of <i>P. insularum</i> .....	144
Figure 5.9	Bioassays and NMR spectra of the 75-50-Q and 75-50-R LH20 fractions.....	145
Figure 5.10	Effects of the fractions leading to partially purified LH-20 bioactive fractions on the expression of the high affinity iron transporters Fet3p and Ftr1p .....	148
Figure 5.11	Tannin and condensed tannin tests .....	149
Figure 5.12	Summary of the bioassay guided fractionation of the crude aqueous extract of <i>P. insularum</i> .....	150
Figure 5.13	Basic concept of polar fractionation of crude extract material.....	151
Figure 5.14	Structure of a condensed tannin .....	153

---

## Abbreviations:

---

ACE	Angiotensin converting enzyme
AChE	Acetylcholinesterase
AD	Alzheimer's Disease
BBB	Blood brain barrier
BPS	Bathophenanthroline disulfonic acid
CAS	Chrome azurol S
CBD	Convention of biological diversity
CNS	Central nervous system
DMSO	Dimethylsulfoxide
DFN	Deferiprone
DFS	Deferasirox
DFX	Deferroxamine
ER	Endoplasmic reticulum
FDA	Food and Drugs Administration
FDR	False discovery rate
GFP	Green fluorescence protein
HDA	Histone deacetylase
HIP	Haploinsufficiency profiling
HIV	Human immunodeficiency virus
HOP	Homozygous profiling
ICP-MS	Inductively coupled plasma mass spectroscopy
ISC	Iron sulfur cluster
MOA	Mechanism of action

NCE	New chemical entity
NMR	Nuclear magnetic resonance
NP	Natural product
NPD	Natural product discovery
OD	Optical density
ORF	Open reading frame
PDR	Pleiotropic drug resistance
TCM	Traditional Chinese medicine
TLC	Thin layer chromatography
TOR	Target of rapamycin
WHO	World Health Organization
WT	Wild type

---

# Chapter 1:

## Literature Review

---

### 1.1. Natural Products

Nature has provided a vast source of structurally diverse natural product compounds of therapeutic significance from plants, microbes and animals. These bioactive chemicals have endured selection pressures of evolution to regulate fundamental molecular pathways, making them ideal templates for pharmaceuticals. It is undeniable that natural products are the most successful source of new drugs, drug leads, and new chemical entities (NCEs) in today's pharmacopoeia. In the three decades spanning 1981-2010, 75% of drugs approved by the United States Food & Drug Administration (FDA) were either derived or based on natural products (Harvey *et al.*, 2008). This is a testament to the reliability of natural products as drugs, or the basis of new drugs.

Historically, records of the use of natural products for medicinal purposes have been found as far back as 2900 BC (reviewed in Dias *et al.*, 2012). This included documentation of more than 700-plant based treatments such as potions, ointments and pills. The use of oils from *Cupressus sempervirens* and *Commiphora* species was noted as far back as 2600 BC, and is still being used in modern day applications for the treatment of inflammation, colds and coughs. The Indian Ayurvedic medicinal system which describes the use of various herbs and dietary prescriptions for disease management in a holistic and systematic manner, evolved into a science in 2500 BC and is still being used to date (Mishra *et al.*, 2001). In addition, multiple Chinese records documenting more than 1,000 drugs and prescriptions containing herbs and plants for traditional medicines exist from various periods including 1100 BC (Chinese Materia Medica), 100 BC (Shennong Herbal) and 659 AD (the Tang Herbal) (Dias *et al.*, 2012).

## 1.2. The status of natural products research over the years

The fortuitous discovery of penicillin from the filamentous fungus *Penicillium notatum* in 1928 spearheaded the natural products era, leading to pharmaceutical companies establishing individual natural products discovery programs. However, this area of research started waning in the 1990s due to several problems associated with natural products research, such as the lengthy period it takes from discovery to marketing, and issues involved with procuring sufficient material for studies and market supply.

Historically, natural products contributed close to half of NCEs in the six (6) decades spanning 1931-1990 (Fig 1.1, Patridge *et al.*, 2015). Specifically, in the decades between 1931-1940, and 1971-1980, natural products contributed to more than half of NCEs. However, since the 1990's, the contribution of natural products to NCEs decreased to a third, which can be attributed to the reasons mentioned above. More rigorous testing in relation to product safety may also have contributed to this decline, as well as the general movement away from natural products in the 1990s.

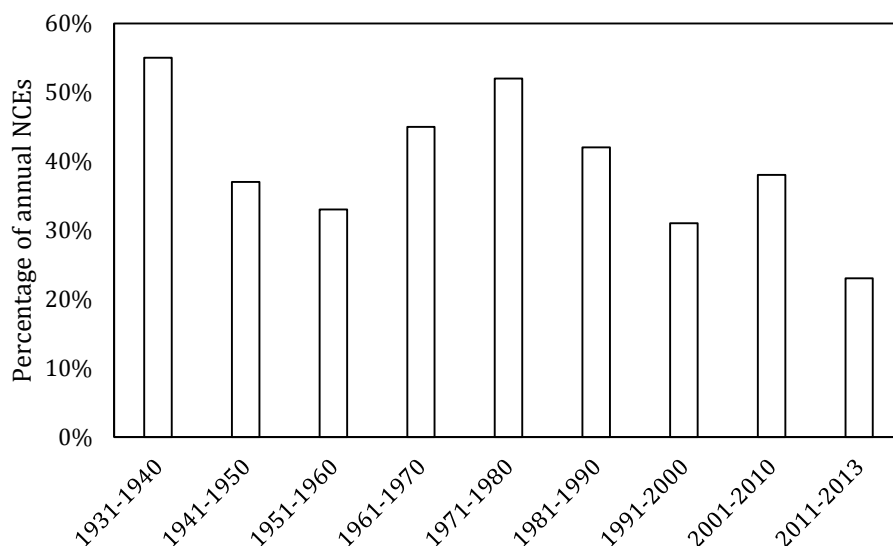


**Figure 1.1: New chemical entities from or based on natural products.** The percentage of approved new chemical entities (NCEs) derived or based on natural products, of microbial, plant or animal origin, for the decades between 1931-2013 (Adapted from Patridge *et al.*, 2015).

Another way to monitor the advances on natural products and their associated NCEs is an investigation of patents relating to such products. Koehn & Carter (2005) found that despite reported reduction in NCEs arising from natural products, the case was the opposite with registered patents on small molecule natural products, for the 20-year period from 1984-2003 (Fig 1.2). A comparison between 1984 and 2003 showed more than five-fold increase in total worldwide natural-product patents, and a three-fold increase in original natural-product patents, indicative of the advances in synthetic chemistry and the production of semi-synthetic derivatives and analogues of original natural product molecules (Koehn & Carter, 2005). Despite the variable number of patents on a year-by-year basis, a general increasing trend in total worldwide natural product patents is observed, thus painting a promising picture regarding natural product research.

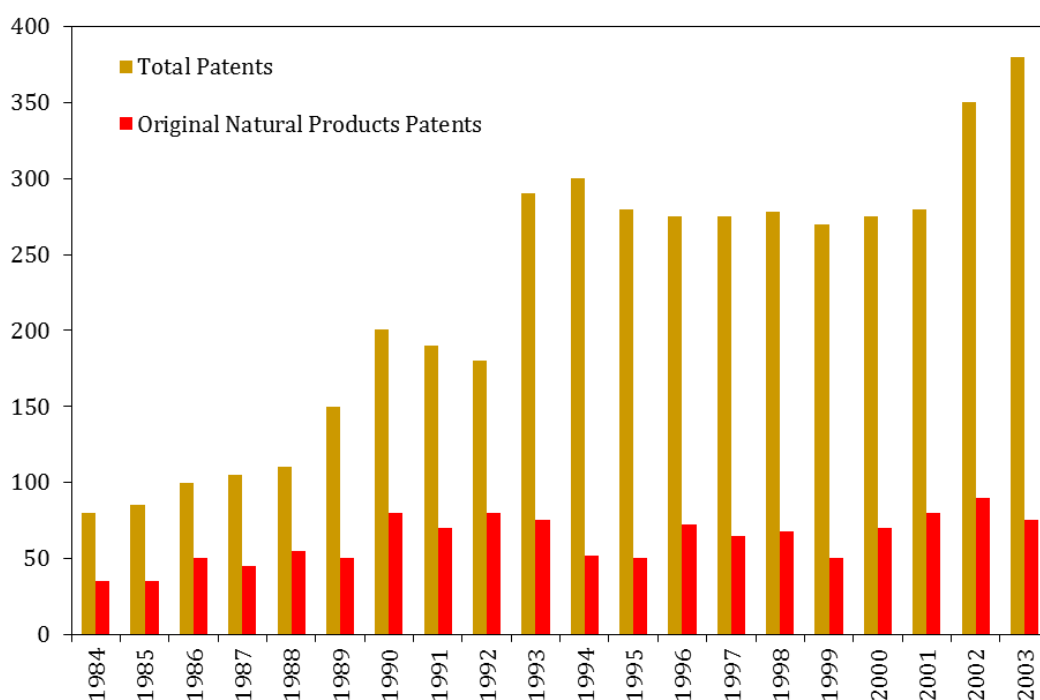


**Figure 1.2: Original and total worldwide natural product patents, 1984-2003.** Total worldwide natural product patents shown in gold represent patents of small molecules composed of (either partially or wholly) natural products as pharmaceuticals. Original natural product patents are shown in orange, and denote first-time novel composition of small molecular natural products as pharmaceuticals (Adapted from Koehn & Carter 2005).

However, given that a significant number of chemicals and molecules filed for patents do not pass through drug development and trials, a measure of the reliability of natural products for the production of new drugs is the number of new FDA approved drugs in recent years. Tao *et al.* (2014) noted that products of natural sources accounted for approximately 35% of FDA-approved drugs in 2008, whilst in 2010, the figure was approximately 80% (Fig 1.3). Drugs derived or based on natural sources contributed to approximately 50% of all FDA-approved drugs in both 2011 and 2012 (Tao *et al.*, 2014). These recent data continue to support a primacy of natural products in drug discovery, added to by advances in screening strategies and augmentation of existing traditional methods (Harvey *et al.*, 2015).

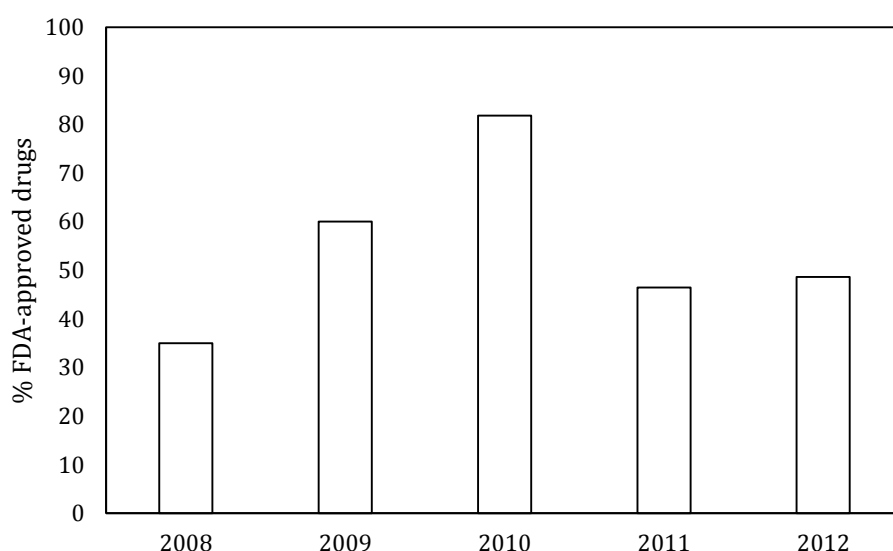


**Fig1.3: FDA-approved drugs of natural sources from 2008-2012.** Percentage of FDA-approved drug of natural sources, including natural product drugs and drugs based on natural products of microbial, marine, plant, and animal sources, for the years 2008-2012 (Adapted from Tao *et al.*, 2014).

### 1.3. Microbial Natural Products

The opportune discovery of penicillin from the filamentous fungus *Penicillium notatum* drove investigations into microorganisms as sources of drugs, and subsequently the “Golden Age of Antibiotics”, which was an era marked by exponential discoveries of antibiotics from natural

products, particularly of microbial sources. However, in spite of its revolutionary effect on drug discovery and natural product research, penicillin was not effective against all bacteria, and subsequent antibiotic resistance led to chemical modifications to the underlying penicillin structure, giving rise to more potent and wider spectrum antibiotics (Miller, 2002).

Tetracycline, another well-known antibiotic was isolated from the bacterium *Streptomyces aureofaciens*. As one of the first successful semi-synthetic pharmaceutical products derived from a natural product, tetracycline was produced from modifications to chlortetracycline (Aureomycin) by removal of its C7 chlorine. Indeed, the underlying naphthacene structure of chlortetracycline has been the basis of second generation tetracyclines, such as doxycycline (Vibramycin) (Nelson & Levy, 2011). Doxycycline is used as a broad spectrum antibiotic against community-acquired bacterial infections, malaria and *Bacillus anthracis*, the causative agent of anthrax infections (Nelson & Levy, 2011).

The bacterium *Streptomyces hygroscopicus* is the source of rapamycin, a well-known immunosuppressive agent used to reduce organ rejection in transplant cases. A secondary metabolite of *S. hygroscopicus*, rapamycin was first isolated in the 1970s, and was found to have antifungal, antitumor and immunosuppressive activities (Benjamin *et al.*, 2011). Interestingly, it was its antifungal activity that facilitated the discovery of the central regulatory molecule TOR (target of rapamycin), which in turn facilitated better understanding of TOR and its mechanisms (Benjamin *et al.*, 2011).

Cholesterol-lowering statin drugs were also sourced from microorganism NPs. Following the successful use of lovastatin in the clinical setting in the 1980s, two semi-synthetic statins (simvastatin and pravastatin) and four synthetic statins (fluvastatin, atorvastatin, rosuvastatine and pitavastatin) have been introduced and successfully used in lowering cholesterol levels (Endo, 2010). In addition, the extensively used anticancer drugs bleomycin A<sub>2</sub> and B<sub>2</sub> are also of a microorganism source, from the bacterium *Streptomyces verticillus* (Cragg & Newman, 2013).

In 2015, half of the Nobel Prize for Physiology or Medicine was awarded jointly to William C Campbell and Satoshi Ōmura for their discovery of avermectins that are produced solely by the bacterium *Streptomyces avermitilis* (Ōmura & Crump, 2004; Nobel Assembly, 2015). This species was first isolated in Japan 1973, and its anti-parasitic activity was detected in 1974. Later in the 1970s, the anti-helminthic activity of avermectin was discovered in the USA (Ōmura & Crump, 2004). Avermectin was subsequently found to have a broad range of anti-parasitic activity, with a highly potent and unique mechanism of action. A modification of the natural avermectins gave rise to a broader spectrum and less toxic compound that was marketed as ivermectin (Campbell, 2012). Ivermectin has since been used in 46 countries to treat cattle, sheep, horses and pigs; in New Zealand, avermectin is a front-line treatment for sheep roundworms without which the sheep industry would have difficulty surviving. Most importantly however, avermectin is used to treat river blindness and elephantiasis in humans and is undergoing trials for an ever-increasing number of applications against other parasitic diseases (Ōmura & Crump, 2004).

#### 1.4. Marine Natural Products

The oceans, which cover approximately 70% of the earth's surface, are another source of natural products. Whilst investigations into marine environments only started in the mid-1970s, multiple structures have been discovered since. For instance, 2,500 new metabolites were reported from 1977-1987, whilst up to 1,003 new compounds were recorded for the year 2010 alone (Blunt *et al.*, 2012; Faulkner, 2000). These results are indicative of the marine environment being a prolific source of natural products and NCEs.

Ziconotide, the first marine derived product to be approved as a drug was isolated from the venom used by the cone snail *Conus magus* to facilitate capture of its prey (Cragg & Newman, 2013); the drug is used for the management of severe chronic pain through intrathecal application (McGivern, 2007). Of particular note is its unique mechanism of action; ziconotide is the only clinically approved selective N-type channel (calcium channel) blocker (McGivern, 2007).

The alkaloid ecteinascidin 743, 40 years after its isolation from *Ecteinascidia turbinata*, was the first approved marine-derived anticancer drug (Molinski et al., 2009). It has been approved for the treatment of soft tissue sarcomas, and is currently undergoing various phases of clinical trials for the treatment of breast, prostate and pediatric sarcomas (Cragg & Newman, 2013).

Additional marine products with anticancer activity undergoing clinical trials are halichondrin B and its analogue eribulin mesylate (Cragg & Newman, 2013). Halichondrin B was discovered in 1986, but owing to limited compound availability as is common with natural products, its progress was delayed. Total synthesis of halichondrin B required 90 steps, however, further research found active synthetic analogues of halichondrin B with 30% less molecular mass that exhibited broad anti-proliferative activity against tumour cells, similar to that of halichondrin B (Towle et al., 2001).

## 1.5. Animal Natural Products

Drugs produced from natural sources also include those obtained from animal sources, although research on animal natural products is dwarfed in comparison to the volume of studies conducted on natural products from plant and microbial sources (Paavilainen, 2009). Whilst research on animal natural products is increasingly becoming more common, a significant number of these “medicinal” animals are listed as threatened species, largely due to their exploitation as a result of their use in traditional medicine (Alves & Albuquerque, 2013). While it is generally accepted that compounds insulin, trypsin and other human hormones are important animal products used for therapeutic applications, this section will present some examples of natural products discovered and isolated from animal sources that successfully entered the market for clinical use, or are currently undergoing trials for introduction into the pharmaceutical market.

The angiotensin converting enzyme (ACE) inhibitors captopril and enalapril were synthesized on the basis of the nonapeptide teprotide isolated from the venom of the Brazilian pit viper *Bothrops jararaca* in the 1970s (Ferreira et al., 1970; Ondetti et al., 1971; Ondetti et al., 1973).

This was a major breakthrough for antihypertension medications. However, whilst teprotide exhibited significant hypotension activity, its lack of oral activity led to the development of captopril and enalapril, which are used to treat not only hypertension but also congestive heart failure and diabetic nephropathy (Cushman & Ondetti, 1999).

The alkaloid epibatidine that was isolated from the skin of the poisonous frog *Epipedobates tricolor* forms the basis of the development of a novel class of potential painkillers (Spainhour, 2005). Additionally, the development of the injectable glucose extenatide polypeptide was based on exendin-4 isolated from venom of the Gila monster *Heloderma suspectum* (Eng *et al.*, 1992). Further to these drugs on the market, natural products from animals have also shown promise through antimicrobial peptides such as cecropins and defensins (Aerts *et al.*, 2008; Boman, 1991). Various bee products such as honey, venom and propolis (bee glue) have also showed varied activities, including but not limited to anti-cancer and anti-HIV properties (Molan, 1999; Park *et al.*, 2000; Wade *et al.*, 1992).

## 1.6. Plant Natural Products

Plants have played a significant contribution in the field of drug discovery. Whilst it is understood that plants have contributed to medicine as far back as 2900 BC, the earliest contribution of plants into modern medicine started with the discovery of digoxin from *Digitalis purpurea* (foxglove) in 1785. William Withering was first made aware of the plant's medicinal properties from patients who received a potion containing *D. purpurea* (Aronson, 1977). Since then, other *Digitalis* spp. have contributed their own chemical compounds to medicine such as acetyldigoxin, digitalin, digitoxin, deslanoside, and lanatosides A, B and C from *D. lanata* (Lahlou, 2013).

The bark of *Cinchona* trees was often chewed by South American natives to abate shivering while working in cold waters and to treat fevers (Meshnick & Dobson, 2001). Later in the 1600s, its antimalarial properties were accidentally discovered (Kaufman & Rúveda, 2005). Pure

quinine and cinchonine were later isolated from *Cinchona* bark in 1820 in Europe, and thereafter used by physicians to treat malaria (Meshnick & Dobson, 2001). Whilst references were made to an opium elixir with pain-relieving properties in the BC period, morphine was first isolated from *Papaver somniferum* in the early 1800s by the German pharmacist Friedrich Sertürner (Brune & Hinz, 2004). The *P. somniferum* extract also contained codeine (another analgesic), and papaverine (a muscle relaxant) which reduced cardiac muscle contraction (Davies & Hollman, 2002). A synthetic analogue of papaverine called verapamil was shown to be highly active as a calcium channel blocker, in its activity against arrhythmia (Davies & Hollman, 2002). Noscapine, another component of opium, is used as a cough suppressant and has also been shown to have anti-cancer activity (Mahmoudian & Rahimi-Moghaddam, 2008). An effort by the National Cancer Institute screening a large collection of plant extracts led to the discovery of the widely-used anti-cancer drug paclitaxel in 1971, from the Pacific yew tree, *Taxus brevifolia* (Rowinsky & Donehower, 1995). Other contributions of plants into medicine include vinblastine and vincristine from the Madagascar periwinkle *Catharanthus roseus*, and etoposide and teniposide-based on epipodophyllotoxin isolated from the root of the American mayapple plant *Podophyllum peltatum* (Itokawa *et al.*, 2008).

Nevertheless, despite these promising leads, plant natural products have shown a decline in recent years (Fig 1.4, Patridge *et al.*, 2015). Whilst they contributed to 15-20% of total approved annual NCEs in the three decades spanning 1931-1960, plant natural products contributed to less than 10% of total annual NCEs discovery from 1961-2013. In addition to the factors previously discussed (Section 1.1), another factor that may have contributed to this decline in plant natural product outputs was the Convention of Biological Diversity and the regulations it put in place to protect biodiversity and sustainability. Additionally, it is proposed that discoveries from plant natural products have slowed down because the “lower hanging fruit” of plant natural products have been picked, and what remains requires more perseverance, time and financial investment. Contrastingly, there was an increase in NCE/year, from 0.6 NCE/year from 2001-2010 to 1.5 NCE/year in the period 2011–2013 (Fig 1.4) suggesting that when effort is expended, plenty of plant NCEs remain to be

discovered. This prospect is broadened since 90% of species in the plant kingdom have yet to undergo any bioactivity assays for crude or purified fractions (Harvey, 2008), thus there is vast potential for NCEs in the plant kingdom yet to be mined and explored for therapeutic activity.

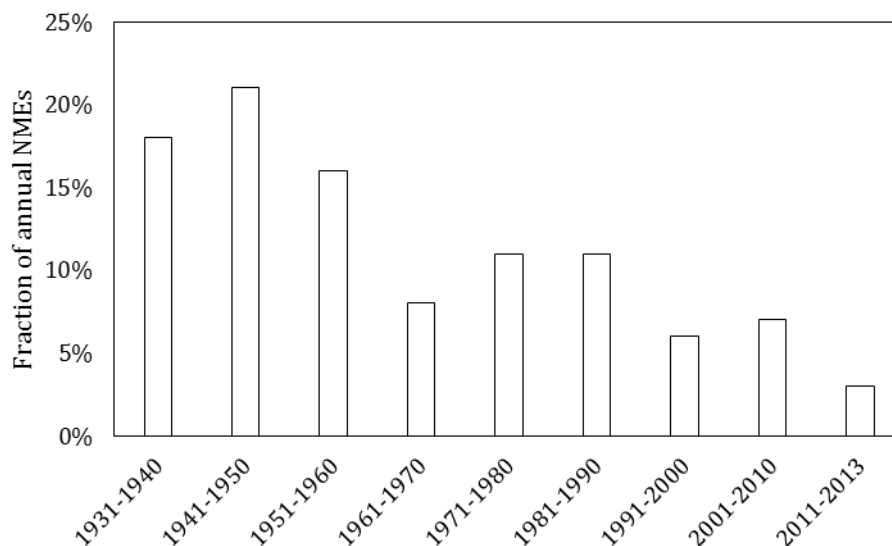


**Fig 1.4:** New chemical entities based or derived from plant natural products. The fraction of approved NCEs derived or based on plant natural products, from the years 1931-2013 (Adapted from Patridge *et al.*, 2015).

## 1.7. Medicinal Plants

Plants with extensive ethnobotanical usage for medicinal purposes (medicinal plants) have higher chances of demonstrating bioactivity and producing pharmacologically significant natural products (Cragg *et al.*, 1997; Cox *et al.*, 1988). As such, traditional medicinal plants have proven to be a reliable subgroup of plants to be explored for bioactivity and novel structures for development of pharmaceuticals. As discussed in the previous section, digoxin, quinine and morphine were all discovered from plants with well-established ethnobotanical applications.

Whilst much controversy initially surrounded the identity of *Colchicum autumnale* as the medicinal plant described in ancient Egyptian papyrus documents for the treatment of rheumatism, dropsy and gout, it was positively identified in the 1830s (Hartung, 1954). The alkaloid colchicine was subsequently isolated from the bulb of the plant, and identified as the bioactive component of *C.*

*autumnale*, with activity against gout attacks (Hartung, 1961). Colchicine inhibits the polymerization of tubulin and though too toxic for the treatment of cancer, it is however FDA approved for the treatment of gout and familial Mediterranean fever (Itokawa *et al.*, 2008). It is thought to be a mild anti-inflammatory agent and affects various components of the inflammation response (Terkeltaub, 2009).

In European traditional medicine, the use of *Galanthus woronowii* for the treatment of poliomyelitis can be found in literature as a second-hand report (Shellard, 2000). Early work on *G. woronowii* and other *Galanthus* spp. in the 1950s was primarily carried out in Bulgaria and Russia, where galanthamine (galantamine) was first isolated (Heinrich & Teoh, 2004). In the same decade, galanthamine was also isolated from *Leucojum aestivum* at higher quantities than other *Galanthus* spp, and its acetylcholinesterase (AChE) inhibiting and cholinesterase inhibiting activities were also determined (Heinrich & Teoh, 2004). While galanthamine was used clinically in the 1970s for its cholinesterase inhibiting activity (Shellard, 2000), it was investigated for Alzheimer's disease (AD) in the 1980s, as a result of its ability to cross the blood-brain barrier (BBB) and to fully utilize its cholinergic activity (Heinrich & Teoh, 2004). It was subsequently marketed in Austria in 1996 to slow down the progression of AD, and has since been launched in other countries such as the wider Europe (UK, Iceland, Sweden), Australia, Canada, Malaysia and the US in the early 2000s (Heinrich & Teoh, 2004).

In 2015, the other half of the Nobel Prize for Physiology or Medicine was awarded to Youyou Tu, for her work on Artemotil<sup>®</sup>, an antimalarial drug and a derivative of artemisinin (Cui & Su, 2009; Nobel Assembly, 2015). Artemisinin was isolated from *Artemisia annua*, a well-documented herb in traditional Chinese medicine (TCM) for which the dried aerial parts of which were used for the treatment of fever and malaria (Itokawa *et al.*, 2008). Although initial tablet formulations of artemisinin as a drug proved ineffective due to poor dissemination, a capsule form of artemisinin produced better results. However the dissemination of these positive findings was limited due to the political environment in China at the time (Tu, 2011). In further molecular

modifications of the original structure, a more stable and ten times more potent compound was synthesized, and both forms have been studied for applications to other diseases (Tu, 2011). All in all, medicinal plants have proven to be a fruitful investigative platform for the discovery of new drugs, drug leads, and NCEs.

## 1.8. Samoan Medicinal Plants

### 1.8.1. History

Samoan traditional medicine utilizing plants has relatively new beginnings, unlike Ayurvedic and traditional Chinese medicinal systems that have well-documented histories dating back to the ~2000 and ~1000 BC respectively. Whilst the missionaries and members of US expeditions to the Samoan islands during the 1800's had extensive periods of living with and observing Samoans, minimal reference was made to Samoan medical practices. At the time, it was noted that due to their isolation, the Samoan people did not suffer from diseases that were plaguing the Western world, such as measles, mumps, whooping cough, smallpox, tuberculosis and influenza. In contrast, Samoan people were often afflicted with diseases such as skin ulcers and infections, and several forms of eye ailments (Whistler, 1996).

During that time period, Samoan diseases were categorized into two groups: ailments with clear origins and manifestations (*e.g.* rashes, wounds, burns), and the other comprised ailments with internal or unclear origins (*e.g.* diseases often attributed to supernatural causes such as gods, spirits and ghosts) (Whistler, 1996). In the cases of rashes, wounds and burns, the extent of medical practices used to combat these included cleaning the site and wrapping with a plantain (*Musa spp.*) leaf (Whistler, 1996). Where ailments of unclear origins arose, Samoans attributed these to their gods, spirits and deities, and sought the assistance of a witch doctor to banish or appease the offended god, often achieved through prayers or the presentation of gifts (Harrington, 2001; Whistler, 1996).

Surprisingly, in recent years, detailed accounts of extensive Samoan medical practices, specifically their common use of approximately 84 available plants and herbs, have been published (Harrington, 2001; Han, 1998; Whistler, 1996; Whistler, 2000). This is a contrasting shift in paradigm; whilst other Pacific islands were adopting the European medical practices, Samoans were seeking medical relief from the plants and herbs available in their natural flora (Macpherson & Macpherson, 1990). Macpherson & Macpherson (1990) interpreted this as a response to the new diseases and epidemics that the Europeans and missionaries brought to the islands that could neither be attributed to gods and spirits, nor successfully remedied by Europeans medications.

In preparing plant material for traditional applications, Samoan healers use various parts of the selected plant including the plant bark, roots, leaves or shoots (Harrington, 2001; Han, 1998, Whistler, 1996). These are either mashed and rubbed onto the skin or wrapped onto the wound site, or the juice squeezed from the preparation and drunk as a potion or used as an ointment (Macpherson & Macpherson, 1990). In other instances, the plant material is mixed with coconut cream, or Samoan oil, and rubbed onto the skin or wrapped onto the affected area (Harrington, 2001; Macpherson & Macpherson, 1990). Additionally, some traditional healers chew the plant material, and squeeze the resulting juice onto a wound, with the belief that their “mana” as a selected healer, is transferred onto the wound (Whistler, 1996). In rarer cases, a dried plant material is used as a prop in chants for the treatment of some ailments, or is burnt and the resulting smoke is fanned onto the affected site (Macpherson & Macpherson, 1990). In the Samoan use of plants for medicinal purposes, the application is often targeted to the group of diseases mentioned earlier such as wounds, eye infections, boils, skin ulcers and infections, and supernaturally induced or hard to cure ailments of unseen origins (Whistler, 1996).

### 1.8.2. Previous studies on Samoan medicinal plants

Samoan medicinal plants as sources of bioactive compounds for drugs, drug leads and NCEs have been previously investigated. In 1973, a broad pharmacological study was undertaken on

34 Samoan medicinal plants, with samples taken from various parts including leaves, bark, stem and roots (Norton *et al.*, 1973). The two extracts prepared from each plant part (with polar and non-polar solvents) were analyzed for systemic effects in rats, as well as antibacterial, antiviral and antitumor activities. Although none of the tested extracts showed significant antiviral activity, several showed antibacterial and antitumor activity, with four exhibiting general systemic toxicity. Analyses also identified strongly hypotensive activities from 19 of 34 plant species, which is a 56% hit rate for hypotensive activity alone.

Another study was carried out in 1989 in which 104 extracts from 74 Samoan medicinal plant species were investigated for pharmacological activity via an *in vivo* Hippocratic screen and an *in vitro* ileum screen (Cox *et al.*, 1989). In this study, the Hippocratic screen was indicative of the extract effect on mice behavior which was measured by observing stimulant or depressant effects on the central nervous system, salivation and diarrhea; the ileum screen was a measure of induction or inhibition of smooth muscle contraction. This work showed that 86% of extracts inhibited ileum contraction and 41% exhibited significant effects from the Hippocratic screen while 19% of the extracts showed bioactivity in both tests.

Gustafon and associates (1992) isolated the bioactive phorbol prostratin from the Samoan medicinal plant *Homalanthus nutans*. Whilst prostratin was not a new chemical entity and had been previously referred to in literature, Gustafon *et al.* showed that unlike other phorbols, prostratin was not a tumor-promoting agent but rather a compound that exhibited strong cytoprotective activity against HIV. Medication against HIV/AIDS is limited to active HIV infection, whilst latently infected cells that act as reservoirs of the virus that exist intracellularly where drugs could not target; these reservoirs become reactive HIV infection when medication ceases (Archin & Margolis, 2014). Extraordinarily, prostratin not only reduces infection, but it also activates HIV replication in latent cells in a mechanism involving protein kinase C (PKC), allowing the destruction of HIV from these reservoirs by other therapeutic drugs (Hezareh, 2005; Potterat & Hamburger, 2008; Williams *et al.*, 2004). These results supported the progression of prostratin for further evaluation and drug

development where it is currently in Phase II clinical trials (Dias *et al.*, 2012). Significantly, it has been hailed as a pivotal compound in the fight to eradicate HIV.

Despite the clearly promising potential of Samoan plant natural products, investigations into Samoan medicinal plants came to a standstill as the American drug discovery groups involved opted out. The potential of Samoan medicinal plants discovered in these early works (aside from prostratin) was unrealized and thus the Government of Samoa via the Scientific Research Organization of Samoa (SROS) initiated the project subject of this thesis to further explore Samoan medicinal plants and their untapped potential, more than 20 years after the last investigative endeavor.

## 1.9. Chemical Genetics

### 1.9.1. Introduction

Historically, natural products and their derivatives often entered into human use and FDA approval without a clear understanding of their mechanism of action (MOA). This has changed, and understanding drug target and drug MOA has become more commonplace and though not required for FDA approval, greatly expedites the lengthy and cumbersome process. Chemical genetics, a relatively new discipline enabled by the genomics revolution of the last two decades, has played a huge role in recent drug discovery ventures, leading to a much enhanced understanding of drug MOA and drug targets. Simply, chemical genetics is a molecular technique that combines biology and chemistry through the utilization of chemical perturbations to investigate and understand protein function and underlying molecular mechanisms (Lopez *et al.*, 2008).

Model organisms that have been fully sequenced are another major facet of modern day drug discovery. Used with a well-defined toolbox of molecular and chemical techniques, model organisms have become powerful tools for exploratory efforts into drug target and MOA (Lopez *at al.*, 2008). One such model, the eukaryote *Saccharomyces cerevisiae* (Baker's yeast) has enabled several important natural product discoveries in the recent decade. For instance, artemisinin was

shown to mediate some of its antimalarial activity via disruption of normal mitochondrial function, elucidated through studies in yeast chemical genetics (Li *et al.*, 2005). Furthermore, better understanding of some molecular and cellular processes has been enabled by work in yeast. For example, investigations into the target of rapamycin in yeast led to the discovery of the well conserved TOR signaling pathway (Benjamin *et al.*, 2011).

### 1.9.2. Yeast as a model organism

*S. cerevisiae* yeast is a unicellular organism with ~6,300 genes that are readily amenable to genetic manipulations, a typical 90 minutes doubling time, and is very easy and cheap to culture. During the *Saccharomyces* Genome Deletion project, it was determined that ~15% of yeast genes are “essential”, and the remaining considered “non-essential” (Winzeler *et al.*, 1999). Essential genes are those wherein the null deletion results in cell death or an inviable strain, whilst non-essential genes are those wherein the deletion allowed a viable deletion mutant. Additionally, because yeast can exist in either haploid or diploid forms, a single copy of each essential genes can be individually deleted in its diploid form, giving rise to heterozygotes which permits essential genes to be studied (Winzeler *et al.*, 1999). The benefits of these features of yeast (gene deletions, haploid and diploid forms) will be further discussed in Section 1.5.3.1. The existence of yeast in two mating forms (MAT $\alpha$  and MAT $a$ ) permits investigations into gene-gene interactions and negative epistatic interactions, principally that of synthetic lethality (SL). SL occurs when two non-essential gene deletions individually form viable single deletion mutants, but when combined form a non-viable double mutant, which indicates the two genes are related in function (Boone *et al.*, 2007; Tong *et al.*, 2001). Significantly, 75% of yeast genes have high homology to human genes of similar function, with 30% of human disease genes possessing a homolog in yeast (Foury, 1997). With this high percentage of conservation between yeast and humans, much of the fundamental cellular processes and components of interest in humans are also present in yeast, making yeast an ideal model system.

### 1.9.3. Yeast Chemical Genetics

Multiple yeast methodologies, developed following the complete sequencing of the yeast genome in 1996 (Goffeau *et al.*, 1996), are largely adaptable to the study of bioactive compounds, in the determination of their MOA and molecular/cellular targets (Lopez *et al.*, 2008). Much progress has been made in yeast genomics and proteomics applications. For instance, libraries of individual yeast genes tagged with fluorescent protein probes exist (*e.g.*, GFP, RedStar, mCherry) facilitate studies into protein localization and protein expression levels in response to bioactive compounds (Bircham *et al.*, 2011; Ghaemmaghami *et al.*, 2003; Huh *et al.*, 2003; Niedenthal *et al.*, 1996). But perhaps one of the most significant developments in *S. cerevisiae* genomics applications was the generation of the yeast deletion mutant collection (Giaever *et al.*, 2002; Winzeler *et al.*, 1999).

#### 1.9.3.1. Characteristics of the gene deletion mutant collection

The creation of the yeast deletion mutant collection was the effort of an international consortium of 15 laboratories under the *Saccharomyces* Genome Deletion Project. The yeast deletion collection comprises several libraries, including two haploid deletion mutant libraries of ~5,000 non-essential genes, in both MAT $\alpha$  and MAT $\alpha$  mating types (Winzeler *et al.*, 1999). Additionally, a diploid library of the deletions in homozygous form is also available, as well as a diploid heterozygous library of ~6,300 strains, comprising both essential and non-essential genes, resulting from the deletion of a single copy of each gene. Of particular note is the feature of the library whereby each deleted gene/open reading frame (ORF) is replaced by a kanamycin resistance cassette (Fig 1.5), and a unique upstream and downstream barcode, that distinctively identifies each deleted ORF (Boone *et al.*, 2007; Giaever *et al.*, 2002; Winzeler *et al.*, 1999). These libraries are, arguably, the most relevant tool for determining MOA of a bioactive compound and its molecular target, through large scale genome wide chemical genetic analyses.

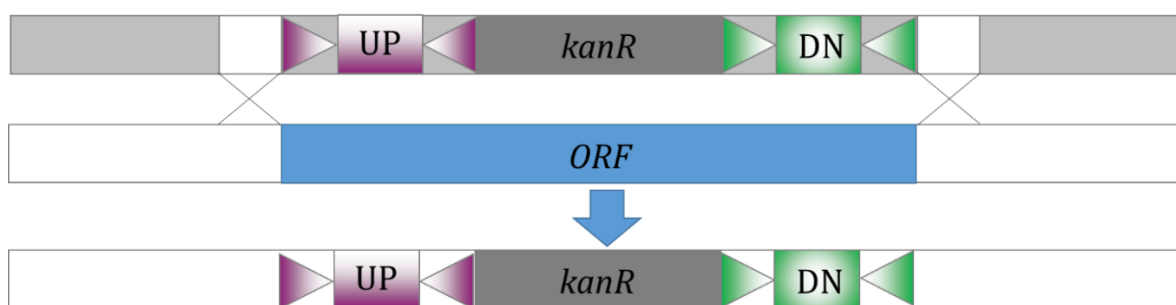


**Figure 1.5: Construction strategy of the yeast deletion mutant collection.** The ORF in the genomic DNA of yeast is replaced by the PCR product containing a kanamycin/G418 resistance cassette (*kanR*) flanked by up and down tags, via homologous recombination in yeast. The flanking tags (UP and DN) comprise 20-nucleotide molecular barcodes that uniquely identifies each ORF deletion mutant (Adapted from Boone *et al.*, 2007).

### 1.9.3.2. Yeast chemical genetic profiling

Large scale genome-wide chemical genetic analysis gives rise to the identification of a chemical genetic interaction, whereby a chemical probe (*e.g.*, a bioactive compound) results in the growth defect of a gene deletion mutant, compared to its growth in the absence of the chemical probe (Smith *et al.*, 2010). Logically then, the utilization of the gene deletion collection for the elucidation of compound MOA is subject to a chemical probe reducing yeast cell growth. In most genome-wide analyses of a compound, several gene deletions exhibit a growth defect or hypersensitivity as a result of exposure to the chemical perturbation, and these gene deletions and the chemical form the chemical genetic profile (Fig 1.6, Boone *et al.*, 2007; Lopez *et al.*, 2008). This profile provides important indications to the compound MOA or compound target.

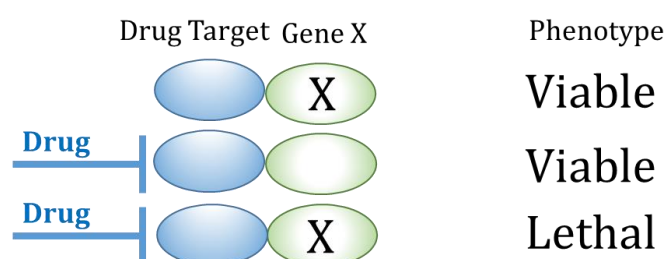


**Figure 1.6: Chemical genetic interactions.** The basis of a chemical genetic array whereby a gene deletion produces a viable mutant, and wild type yeast exposed to a drug treatment also produce a viable cell. However, the combination of the drug treatment and the gene deletion results in an inviable strain/lethal chemical genetic interaction (Adapted from Boone *et al.*, 2007).

Specifically, utilization of the heterozygous library results in a profile indicative of compound target, in what is referred to as drug-induced haploinsufficiency profiling (HIP) (Giaever *et al.*, 1999; Smith *et al.*, 2010). This is based on the theory that the deletion of one copy of the drug target conditions that particular heterozygote strain to hypersensitivity against the drug, and often the heterozygote strain exhibiting the highest growth defect in the presence of the drug is the drug target (Giaever *et al.*, 1999). Conversely, the utilization of the homozygous deletion collection (homozygous profiling, HOP) or the haploid deletion collections leads to the identification of buffering mechanisms against the activity of the drug probe (Dudley *et al.*, 2005; Fry *et al.*, 2005; Parsons *et al.*, 2004; Parsons *et al.*, 2006). In the homozygous or haploid deletion mutant collections, the genetic target of a drug is completely deleted and the corresponding deletion mutant subsequently becomes resistant to the drug (Smith *et al.*, 2010). However, the gene deletions exhibiting growth defects are identified as genes required for cell survival in the presence of the drug, suggesting that the genes function to protect and defend the cell against the effects of the drug (Hillenmeyer *et al.*, 2010). The resulting profile from a HOP (or haploid) assay subsequently imparts information on the drug mechanism of action, based on the cell buffering mechanisms.

Importantly, given the unique barcode feature of each ORF, the chemical genetic profile of a drug can be obtained from a pooled-liquid assay where all the deletion mutants are competitively grown together; comparing the growth of treated strains to their untreated counterparts, via microarray hybridization or barcode sequencing (Bar-seq), that allows for the identification of resistant or sensitive mutants (Boone *et al.*, 2007; Pitrowski *et al.*, 2015; Robinson *et al.*, 2014; Smith *et al.*, 2012). This pooled-liquid assay format is ideal where the compound/drug of interest is of limited availability. However, cost is markedly increased (because of the expense of microarray or Bar-seq analyses), compared to a cheaper approach of screening on agar, where the chemical genetic profile is obtained when colony sizes of treated and untreated mutants are compared (Smith *et al.*, 2010). Obtaining a chemical genetic profile utilizing the agar approach however requires larger

quantities of the drug probe. Notably, it is important to acknowledge that conclusive demonstration of drug target and MOA require further biological characterization, and cannot simply be inferred from yeast chemical genetic profiles obtained from agar, microarray or Bar-seq analyses.

### 1.9.3.3. Drug targets & MOA via yeast chemical genetic profiling

Since its invention, multiple studies have corroborated the reliability and robustness of yeast chemical genetics as a means of identifying drug target and elucidating drug MOA. Such studies employed a mixture of well characterized compounds (*e.g.*, tunicamycin), compounds with unknown targets, as well as various growth conditions (*e.g.*, different media, different temperature) and yeast chemical genetics profiling identified the drug targets, established buffering mechanisms as well as characterized responses to nutrient conditions. These studies were undertaken employing both HIP and HOP analyses in barcode-based pooled assays and in agar format (Baetz *et al.*, 2004; Carroll *et al.*, 2009; Giaever *et al.*, 1999; Giaever *et al.*, 2004; Hillenmeyer *et al.*, 2008; Lum *et al.*, 2004; Parsons *et al.*, 2004; Pierce *et al.*, 2007; Pitrowski *et al.*, 2015; Robinson *et al.*, 2014; Smith *et al.*, 2009). Multiple studies have also utilized yeast chemical genetic approaches to identify molecular targets and MOA of natural products. These natural products include, but are not limited to, products of marine sources such as sponge-derived drugs peloruside A, neothyonidioside, laulimalide and plakortide F, as well as plant sources such as artemisinin and curcumin (Azad *et al.*, 2013; Best *et al.*, 2013; Li *et al.*, 2005; Minear *et al.*, 2011; Wilmes *et al.*, 2012; Xu *et al.*, 2011; Yibmantasiri *et al.*, 2012).

### 1.9.3.4. Yeast chemical genetic profiling of crude natural product extracts

Yeast chemical genetic profiling has been shown to be a reliable technique in assessing MOA and biological activity of crude natural product extracts. For example, the chemical genetic profiles of two crude extracts and their respective isolated bioactive compounds were compared and it was determined that the profile of the isolated compound closely matched that of its respective

crude extract (Parsons *et al.*, 2006). Whilst this makes yeast chemical genetic profiling an even more important tool in natural product drug discovery by prioritizing extracts based on bioactivity, this approach is most ideal to crude extracts comprising one major bioactive compound.

## 1.10. Aims

This dissertation was based on the general question of whether Samoan medicinal plants had bioactive compounds of pharmaceutical potential, and whether their identified MOA correlate to their application in Samoan traditional medicine. Thus, the overall aim of this study was to investigate the bioactivity and mechanism of action of Samoan medicinal plants. Because yeast chemical genetics is a well-established and reliable method for such investigations, that methodology was implemented to accomplish the overall aim of this study. My attempt to address this overall aim was divided into four objectives:

1. To characterize the stability and bioactivity of aqueous and methanolic extracts of selected Samoan medicinal plants (Chapter 2).
2. To elucidate the MOA of the most potent medicinal plant by performing a haploid gene deletion-based genome-wide analysis and characterizing the implicated biological activity in order to correlate the determined MOA to its traditional application in Samoan medicine (Chapter 3).
3. To identify the target gene as well as establish both the haploinsufficiency and homozygous profiles of the extracts from the medicinal plant of interest via diploid-based genome-wide analyses (Chapter 4)
4. To identify the compound responsible for the MOA of the most potent medicinal plant (Chapter 5).

---

## Chapter 2:

# Bioactivity and Stability of Aqueous and Methanolic Extracts of Samoan Medicinal Plants

---

### 2.1. Introduction

In biological studies of natural products, sourcing quantities sufficient to ensure completion of structure and mechanism of action (MOA) studies is a major issue. Over-exploitation of natural sources such as plants and animals could lead to scarcity. For instance, paclitaxel was initially sourced from the bark of the slow growing Californian coastal yew tree, *Taxus brevifolia* and were it not for synthetic means of supply, *T. brevifolia* would have been threatened. In the interest of incurring minimal damage to Samoan plant species selected for this work, only leaves were sourced to ensure sufficient samples were collected from multiple plants per species without risking species viability. A major aim of this dissertation is to investigate the bioactivity of Samoan medicinal plants in the form that the plants are used in traditional medicine, thus pointing a focus to aqueous plant leaf extracts as this is the most common form of application. Here we selected 11 medicinal plants (Fig 2.1), and assessed their bioactivity against Baker's yeast, *Saccharomyces cerevisiae*. Bioactivity was assessed as the ability of the extracts to affect yeast metabolism measured as reduced yeast growth. In this work, yeast was used as the model organism primarily due to the existence and the robustness of the yeast deletion collection in identifying the genetic target or the MOA of a compound or extract.

#### 2.1.1. *Bischofia javanica*

The leaves of *B. javanica* are used in Samoan traditional medicine to treat eyelid infections, blurry vision and eye injuries, where the leaf juice is dripped directly into the eyes (Whistler, 1996). The bark is used for skin sores, mouth infections and mouth sores (Harrington, 2001; Whistler,

1996). Less commonly, the plant is also used to treat fevers, coughs, tooth-aches and gastrointestinal upsets (Uhe, 1974). In Fiji, a potion is prepared from the bark and given to children who have not walked by the time they reach two years of age; it is also used for stomach and mouth ulcers and athlete's foot (WHO, 1998). In the Solomon Islands, the stem is used to treat tuberculosis (WHO, 1998). The application of the plant to treat mouth and eye infections is common between Samoa, Tonga and Futuna Islands (WHO, 1998) and may denote some validity to the therapeutic effects of the plant. Work by Norton *et al.* (1974) showed that extracts from *B. javanica* did not display any antiviral, antimicrobial, hypotensive or antitumor activity. However, Cox and associates (1989) showed *B. javanica* bark extract to possess modest effects on mouse behaviour including a depressant effect on the central nervous system (CNS) and also showed activity as a muscle relaxant. In a later study, it was determined that *B. javanica* bark extract had a moderate inhibitory effect on prostaglandin synthesis (Dunstan *et al.*, 1997).

### 2.1.2. *Clerodendrum inerme*

Samoa healers use the juice from crushed leaves of *C. inerme* to treat wounds, inflammation, post-partum sickness and internal injuries (Uhe, 1974; Whistler, 1996). In American Samoa, *C. inerme* is used externally in combination with other medicinal plants to treat impetigo (Harrington, 2001). The use of this plant for medicinal purposes has not been reported from other South Pacific islands. In the study by Norton and associates (1974), it was determined that whilst *C. inerme* leaf extracts had neither antiviral nor antitumor activities, the leaf extracts exhibited mild hypotensive activity as well as antimicrobial activity against *Nocardia* spp and *Staphylococcus aureus*. It was later determined to also have modest muscle relaxant activity (Cox *et al.*, 1989).

### 2.1.3. *Colubrina asiatica*

Whistler (1996) reported only a single use for this plant in Samoan medicine. The leaves, either boiled or fresh, are used to prepare a potion taken to treat postpartum sickness. In American

Samoa, more extensive use of the plant in traditional medicine is reported to include treatment of gonorrhoea, abscesses and a Samoan ailment literally translated to spreading inflammation rash; this ailment often results in death if not treated immediately and is postulated to be the result of septicaemia (Harrington, 2001). Methanol and ethanol extracts of *C. asiatica* leaves exhibited antiviral, antitumor and strong hypotensive activities although no antimicrobial activity was detected (Norton *et al.*, 1974). When applied *in vivo*, *C. asiatica* extracts caused death in mice, while *in vitro* studies showed a significant muscle relaxant activity (Cox *et al.*, 1989).

#### 2.1.4. *Cordyline fruticosa*

The leaves of *C. fruticosa* are widely used by Samoan healers for massages (Whistler, 1996). In American Samoa, it is taken internally in combination with other plants for the treatment of intestinal upset in children that have the specific symptoms of loose greenish stool and difficulty in defecating (Harrington, 2001). Across the Pacific, the various plant parts are used to treat lower chest pains, filariasis, postpartum sickness, ear ache, eye infections, colds, coughs, eczema, laryngitis, gum abscesses, inflammations, aching limbs and fevers (WHO, 1998). In addition, Cox *et al.* (1989) reported a significant muscle relaxant activity from *C. fruticosa* leaf extracts.

#### 2.1.5. *Cymbobogon citratus*

*C. citratus* is used by both Samoan healers and lay people to treat ailments involving children, particularly mouth sores and mouth infections. The leaves are crushed or chewed, and the juice dripped onto the mouth sores or taken as a potion (Whistler, 1996). This application is also observed in American Samoa and Tonga (Harrington, 2001; Whistler, 1996). Less commonly, it is used to treat filariasis (Uhe, 1974). A significant muscle relaxant activity and mild central nervous system depressant (CNS) activity has been reported from a stem extract of *C. citratus* (Cox *et al.*, 1989).

#### 2.1.6. *Flacourtia rukam*

Whistler (1996) reported the application of the *F. rukam* bark for the treatment of inflammation, and its leaves in the treatment of sores in Samoan traditional medicine. McCuddin (2001) reported the use of the inner bark of *F. rukam* in combination with other plants in a potion taken for the treatment of an ailment exhibiting specific symptoms, including soreness and difficulty in opening eyes, the feeling of having a swollen head, cold sweat, dizziness, and leg numbness. Extracts from *F. rukam* did not demonstrate any antiviral, antitumor or antibacterial activities; however, the ethanol extract from its leaves proved hypotensive (Norton *et al.*, 1974). Further, extracts from the stem and bark exhibited mild to moderate CNS depressant and muscle relaxant activities (Cox *et al.*, 1989).

#### 2.1.7. *Macropiper puberulum*

Potions made from the leaves of *M. puberulum* are used to treat diseases believed to be of ghost or supernatural origins in Samoan traditional medicine (Whistler, 1996). In American Samoa, its use has been reported for the treatment of cellulitis and various other forms of inflammation (McCudden, 2001). The leaves and stems have also been used to treat influenza, convulsions, swellings of the testicles, swollen breasts, toothache and scabies in Fiji, whilst in Tonga, *M. puberulum* leaves are used to treat inflammation and boils (WHO, 1998). Although no scientific analyses have been done of *M. puberulum*, other members of the *Piperaceae* family, such as *Piper graeffi* and *P. methysticum*, have been shown to have mild CNS depressant activity, a significant muscle relaxant activity and moderate inhibitory effects on prostaglandin biosynthesis (Cox *et al.*, 1989; Dunstan *et al.*, 1997).

#### 2.1.8. *Psychotria insularum*

One of the most commonly used medicinal plants in Samoa against ailments attributed to ghosts and spirits (supernatural sources) is *P. insularum*, wherein the leaves or bark are crushed and

used to make a potion (Whistler, 1996). The leaves are also used to treat ailments such as burning fever, abdominal distress, abscess, incontinence, and scrotal swelling in elephantiasis (Cox *et al.*, 1989). Additionally, crushed leaves of the plant are applied directly to skin infections or wounds, and the plant is also used for the treatment of general body aches and swellings (Whistler, 1996). In American Samoa, *P. insularum* is often taken in combination with other medicinal plants for the treatment of vomiting or coughing up blood (unrelated to tuberculosis or gastrointestinal upset) and cellulitis (Harrington, 2001). *P. insularum* is not used for medicinal purposes elsewhere. Norton and associates (1974) detected mild hypotensive activity from extracts of *P. insularum*, although no antiviral, antitumor or antimicrobial activity was identified. In another study, *P. insularum* severely reduced motor function in mice, and proved toxic at high concentrations producing death in mice (Cox *et al.*, 1989). An anti-inflammatory effect of *P. insularum* extract has also been reported, exhibiting a strong inhibitory effect on both prostaglandin biosynthesis and rat ear oedema (Dunstan *et al.*, 1997).

#### 2.1.9. *Syzygium corynocarpum*

Samoan traditional medicine makes use of *S. corynocarpum* leaves for the treatment of skin sores as well as urinary tract problems (Whistler, 1996). Less commonly, it is used for the treatment of tuberculosis, sore throats, wounds and high fever (Uhe, 1974). McCuddin (2001) has recorded its use for erythraemia and fever in American Samoan traditional medicine. Leaf extract of *S. corynocarpum* caused death in mice and produced a strong muscle relaxant activity (Cox *et al.*, 1989). Mild inhibition of prostaglandin and rat ear oedema was detected by Dunstan and associates (1997).

#### 2.1.10. *Vigna marina*

Potions prepared from crushed *V. marina* leaves are used to treat infants that present with various ailments whereby the leaf juice is taken as a potion dripped into the ears, nose, mouth and

eyes, or alternatively rubbed onto the skin (Whistler, 1996). American Samoan traditional medicine uses *V. marina* in combination with other plants for the treatment of cellulitis and supernaturally induced ailments whereby the patient cannot sleep and is very talkative all day and night (Harrington, 2001). Leaf extracts of *V. marina* have been shown to exhibit mild muscle relaxant activity (Cox *et al.*, 1989).

#### 2.1.11. *Wollastonia biflora*

Whistler (1996) reported the most common application of this plant is for the treatment of urinary tract problems, for which the juice from the leaves of the plant is taken as a potion. Sometimes, the juice is taken to treat hepatitis and stomach ache (Whistler, 1996). In addition to the above applications, American Samoan healers also use *W. biflora* to treat gonorrhoea (Harrington, 2001). Leaf extracts of *W. biflora* did not exhibit antiviral, antitumor or antimicrobial activity, but did exhibit mild hypotensive activity (Norton *et al.*, 1974). In an *in vivo* study, administration of *W. biflora* leaf extracts at high concentrations proved toxic in mice, while *in vitro* studies showed the extracts exhibited strong muscle relaxant activity and mild inhibitory effects on prostaglandin biosynthesis (Cox *et al.*, 1989; Dunstan *et al.*, 1997).

#### 2.1.12. Aim

The aim of this chapter was to investigate and determine the bioactivity of the selected medicinal plants, establish their amenability to genome-wide analyses in yeast as a first step in determination of MOA, and to identify the medicinal plant producing the most potent extracts. This was achieved through monitoring the growth profiles of yeast in the presence of aqueous and methanolic extracts from the above 11 medicinal plants.

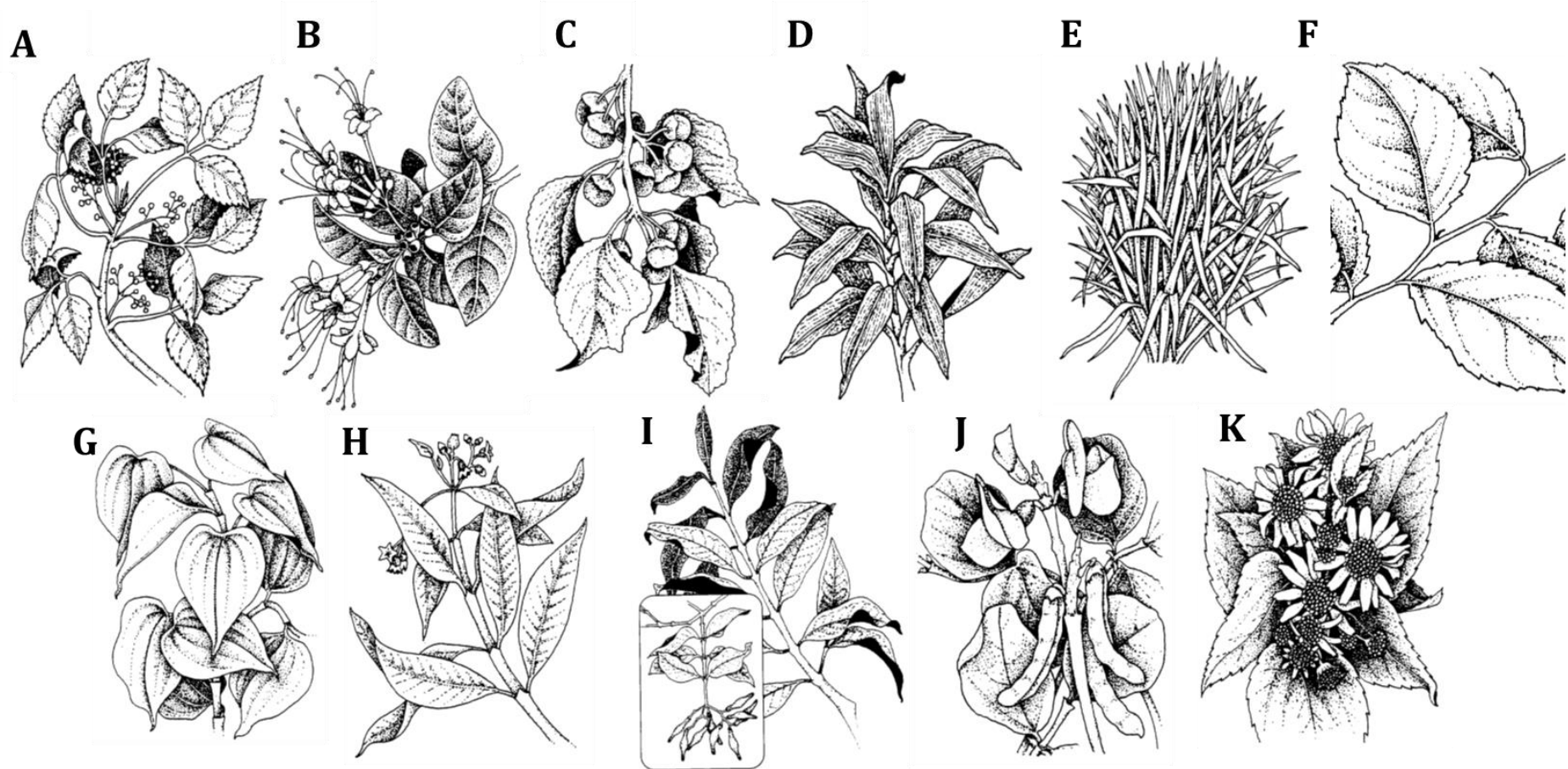


**Figure 2.1:** Representations of the medicinal plants selected for this study. A: *B. javanica* B: *C. inerme* C: *C. asiatica* D: *C. fruticosa* E: *C. citratus* F: *F. rakum* G: *M. puberulum* H: *P. insularum* I: *S. corynocarpum* J: *V. marina* K: *W. biflora* (Adapted from Harrington, 2001).

## 2.2. Methods

### 2.2.1. Medicinal plant collection

Permission was sought and obtained from the Ministry of Natural Resources and Environment (MNRE) Samoa in agreement with the Convention of Biological Diversity stipulations for the collection and export of Samoan medicinal plant material. Approval was also sought and acquired from the Ministry of Primary Industries (MPI NZ) for the importation of the plant material into New Zealand for research purposes. Sample identification and collection was carried out with the assistance of the Environment and Conservation Division within MNRE, specifically the Principal National Parks officer Mr Talie Foliga who worked extensively with Dr Arthur Whistler, the scientist that documented the extensive ethnobotany of Samoa (Atherton & Jefferies, 2012; Whistler, 1996; Whistler, 2000). Upon positive plant identification, leaves were collected from national parks and reserves managed by MNRE, as well as some private properties. Because a comparison of plant populations was not a factor in this study, leaves were collected from plants in one location (Fig 2.2). Once the leaves were washed, quantity required (weight was not measured) to produce 1 L of juice was juiced using an industrial juicer (Breville Juicer BJE410). The collected juice was stored at 4°C and shipped on ice to the Chemical Genetics Laboratory at Victoria University of Wellington.

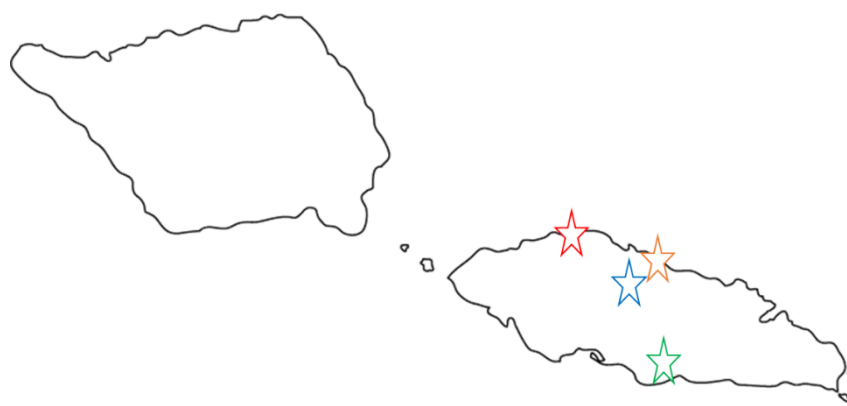


**Figure 2.2: Location of collection of Samoan medicinal plants used in this study.** The red star indicates village of Saleimoa, where *B. javanica*, *C. inerme*, *C. asiatica*, *P. insularum*, *S. corynocarpum*, *V. marina* and *W. biflora* were collected from various private properties. The orange star marks Vaivase from where *C. corynocarpum* was collected from a single private property. The blue star marks the Vailima Botanical Gardens, where *F. rukam* was collected from. The green star marks the Pupu-Pue National Park, which was the collection site of *C. fruticosa* and *M. puberulum*.

### 2.2.2. Extract preparation

Because this work focused on studying the plant extracts in the form used in traditional Samoan medicine, the juices from fresh leaves were prepared for biological analyses. As the yeast liquid-based growth assays were quantified via absorbance (spectrophotometric) measurements, the solid material from each leaf juice sample was removed by centrifugation at 10,000 x g for 30 min. The supernatant was collected and sequentially filtered through 7  $\mu\text{m}$ , 1.2  $\mu\text{m}$ , 0.45  $\mu\text{m}$  and 0.22  $\mu\text{m}$  filters to remove any solid particles and to ensure sterility. The resultant solutions were labelled aqueous extracts and stored at  $-20^{\circ}\text{C}$  in 1 mL aliquots.

The solid material removed from centrifugation was extracted in methanol at a ratio of 1 g solid plant material to 9 mL methanol; extraction was carried out at  $30^{\circ}\text{C}$  whilst shaking overnight. The solution was centrifuged at 10,000 x g for 30 min, and the supernatant was collected and filtered through 0.22  $\mu\text{m}$  filters to ensure sterility. Methanol was removed using a cold trap system (Labconco Centrivap), and the solid methanol extract was resuspended in DMSO (1 mL methanol extraction mass to 200  $\mu\text{L}$  DMSO). Aliquots were stored at  $-20^{\circ}\text{C}$ . The aqueous and methanol extractions are summarized in Fig 2.3.

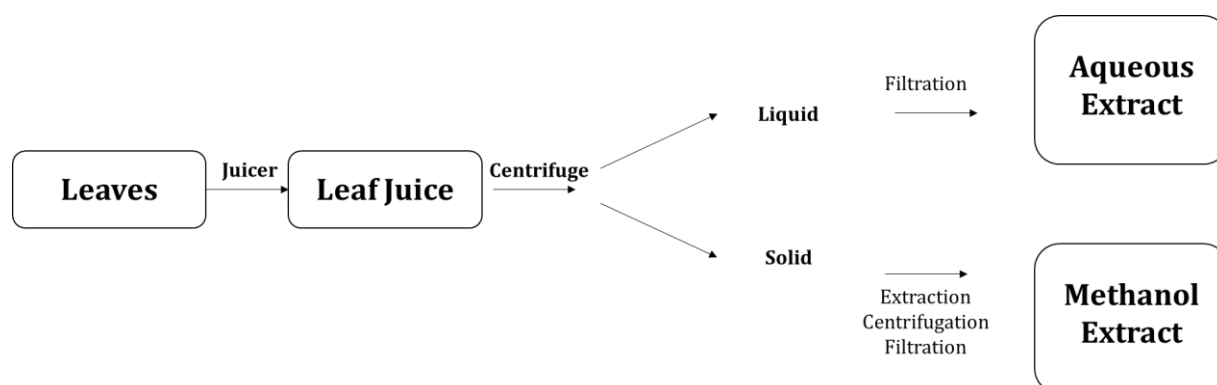


**Fig 2.3: Schematic of leaf juice sample preparation for analyses.** Leaves were collected, washed and homogenized to obtain leaf juice, which was then centrifuged to separate the liquid from the solid part. The liquid was filtered to generate the aqueous extracts. The solid part was extracted in methanol overnight, then centrifuged to remove the solid fraction, and the supernatant was filtered. The methanol was removed and the resulting dried methanol extract mass was resuspended in DMSO.

### 2.2.3. Liquid-based bioactivity assays

Determination of extract bioactivity was achieved by monitoring the growth of yeast as previously described (Amberg *et al.*, 2005) with the specification that the wild-type (WT) yeast strain BY4741 was quantified in the presence and absence of the extracts. Briefly, BY4741 that was streaked on a Yeast Peptone Dextrose (YPD – Appendix I) agar plate was used to inoculate 5 mL YPD and incubated at 30°C in a rotating drum overnight for 15–18 h. Optical density (OD) was determined at 660 nm using a UNICAM 8625 UV/VIS spectrometer and cell density was subsequently calculated using the OD to cell count conversion, before the cells were washed with water to remove YPD. Cells were resuspended in dH<sub>2</sub>O and used to inoculate 10 mL of Synthetic Complete (SC) media at 5x10<sup>5</sup> cells/mL. The experimental suspension was then set up to a final volume of 100 µL by adding the relevant volume of extract to the relevant volume of cell suspension (*e.g.*, 99 µL cell suspension + 1 µL of extract, or 95 µL cell suspension + 5 µL of extract). The plate was shaken at 1000 rpm for 30 s using a MixMate plate shaker (Eppendorf), before absorbance was measured at 590 nm for t<sub>0</sub> using the Envision 2102 Multilabel plate reader (Perkin Elmer). After 15 h of incubation at 30°C, the plate was shaken at 1,000 rpm for 30 s before the absorbance was read at 590 nm for t<sub>15</sub>. Experiments were carried out with three biological replicates, and each biological replicate had three technical replicates. Residual growth of yeast was calculated by normalizing absorbance (to remove any colour-associated absorbance interference due to the extract) by subtracting the absorbance of t<sub>0</sub> from t<sub>15</sub> (n-Abs). The absorbance of each individual extract treatment was then divided by the normalized absorbance of the vehicle control, multiplied by 100. Because the yeast system was used, the residual growth determined to be cut-off point for determination of bioactivity was 80%, as 20% growth reduction allowed for sufficient growth inhibition to identify buffering mechanisms, but not too high that a general cell-defence response is

$$\text{RG (\%)} = \frac{\text{Treatment (n-Abs)}}{\text{Control (n-Abs)}} \times 100$$

detected.

#### 2.2.4. Agar-based bioactivity assays

Relevant volumes of extracts and controls for the relevant concentrations tested were aliquoted separately into wells of a 24-well plate. Then 1 mL molten agar (~ 50°C) was added to each well, gently mixed by pipetting, and allowed to set at room temperature (RT) for 2 h. Once set, 2 µL of diluted BY4741 WT cells were spotted onto each well three times. Spots were allowed to dry before plates were inverted and incubated at 30°C for 24 h. The plates were photographed using a Canon EOS 600D camera, then re-incubated for an additional 24 h, photographed again, and visually analysed for growth defect in extract treatments compared to their relevant control.

## 2.3. Results

### 2.3.1. Two of 11 aqueous extracts are bioactive at pH 4.5

To determine if extracts reduced yeast growth in liquid, the growth of BY4741 WT yeast in the presence of the plant extracts was investigated. A defined quantity of cells ( $5 \times 10^5$  cells/mL) was inoculated into SC media at pH 4.5 containing either the vehicle control or a range of concentrations of the aqueous extracts. Absorbance was measured before ( $t_0$ ) and after 15 h ( $t_{15}$ ) of growth at 30°C. The highest tested concentration of aqueous extract was 5% v/v, with 1 in 5 serial dilutions to the lowest tested concentration of  $3.2 \times 10^{-4}$  % v/v.

The residual growth of BY4741 in the presence of the 11 tested aqueous extracts was calculated (Fig 2.4). Residual growth of BY4741 in most aqueous extracts remained around 100% despite increasing extract concentrations. Residual growth of 100% reflects growth of extract treated cells relative to control cells, thus indicative of no growth inhibition and no bioactivity. This lack of bioactivity was observed from the aqueous extracts of *C. inerme*, *C. asiatica*, *C. fruticosa*, *C. citratus*, *F. rukam*, *M. puberulum*, *S. corynocarpum*, *V. marina* and *W. biflora*. Contrastingly, two growth profiles exhibited residual growth of 80%, indicative of growth inhibition greater than 20%. These aqueous extracts were isolated from *F. rukam* and *P. insularum*. These findings are positive regarding bioactivity of Samoan medicinal plants, with two from 11 aqueous extracts producing bioactivity in yeast at pH 4.5.

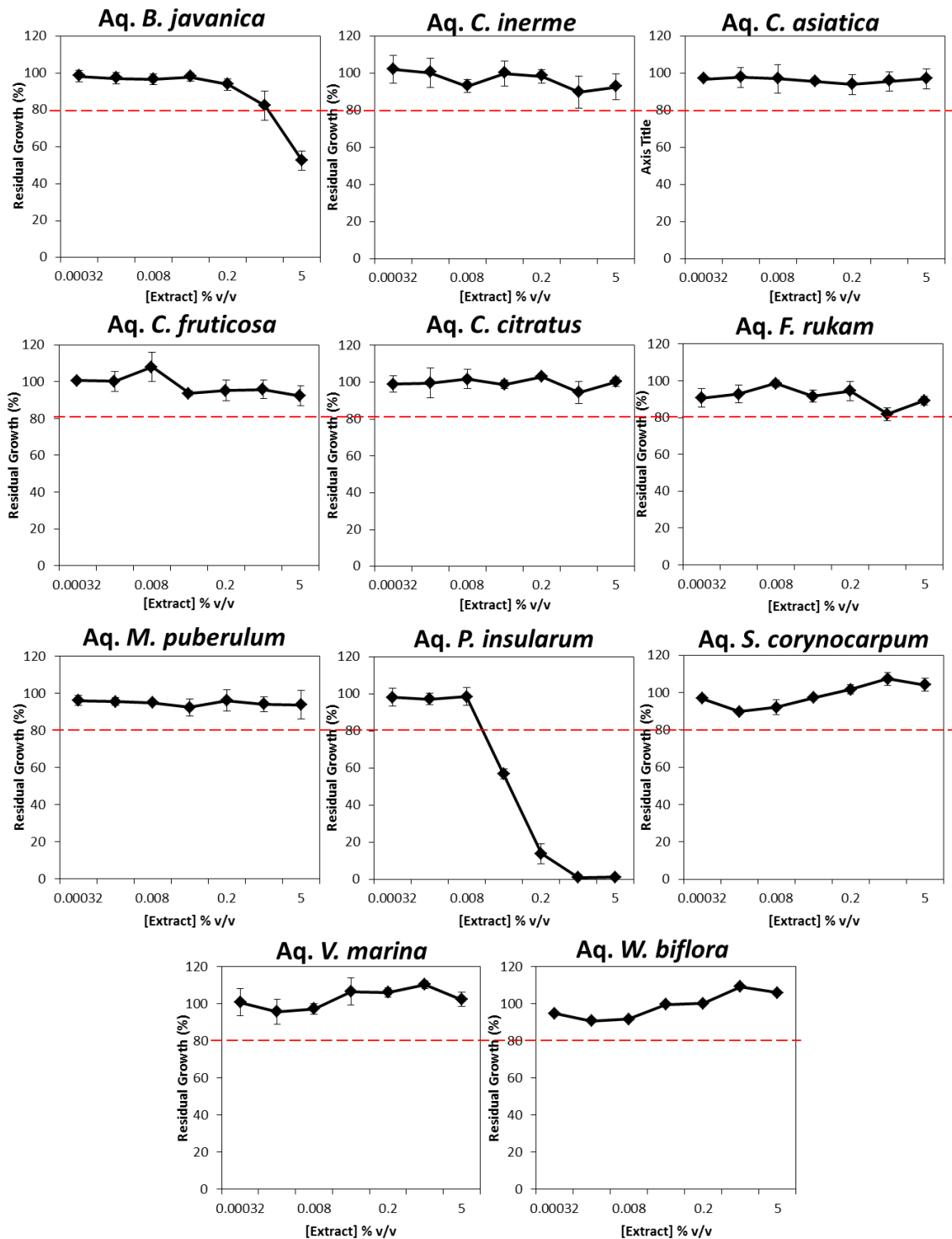


**Figure 2.4:** Liquid-based bioactivity assays of aqueous plant extracts in SC at pH 4.5. Residual growth of BY4741 (WT) in the presence of the 11 aqueous extracts of Samoan medicinal plants. BY4741 cells inoculated into SC were treated with increasing concentrations of aqueous extracts from  $3.2 \times 10^{-4}$  to 5% v/v, and growth was compared against vehicle control grown cells (SC + water). Red dashed lines mark threshold for indication of bioactivity (*i.e.* residual growth decreasing lower than 80% and exhibiting greater than 20% growth inhibition).

### 2.3.2. Five of 11 aqueous extracts are bioactive at pH 7.0

Various factors can affect extract bioactivity, pH being a major one. Given that the leaf extracts were often taken as potions in their application in traditional Samoan medicine, it was postulated that assessment of bioactivity may be enhanced if analyses were carried out at a pH closer to physiological pH. To determine if pH affected bioactivity of aqueous extracts, cells were treated similarly to the previous experiment, except the SC media used was buffered to pH 7.0 with 25 mM HEPES buffer.

The residual growth of BY4741 showed varied growth profiles at pH 7.0 across the 11 aqueous extracts (Fig 2.5). Aqueous extracts from six plants produced growth profiles whereby residual growth was maintained at control levels (100%); these extracts were obtained from *C. asiatica*, *C. fruticosa*, *C. citratus*, *F. rukam*, *S. corynocarpum*, and *V. marina*. Conversely, aqueous extracts from five plants (*B. javanica*, *C. inerme*, *M. puberulum*, *P. insularum* and *W. biflora*) produced growth profiles whereby residual growth progressed lower than 80% indicative of bioactivity. These latter aqueous extracts were thus bioactive in SC media buffered to pH 7.0 with HEPES, providing an enhanced bioactive profile compared to that obtained in SC media at pH 4.5. Therefore, experimental studies conducted with aqueous extracts were carried out in SC pH 7.0 from this point forth.

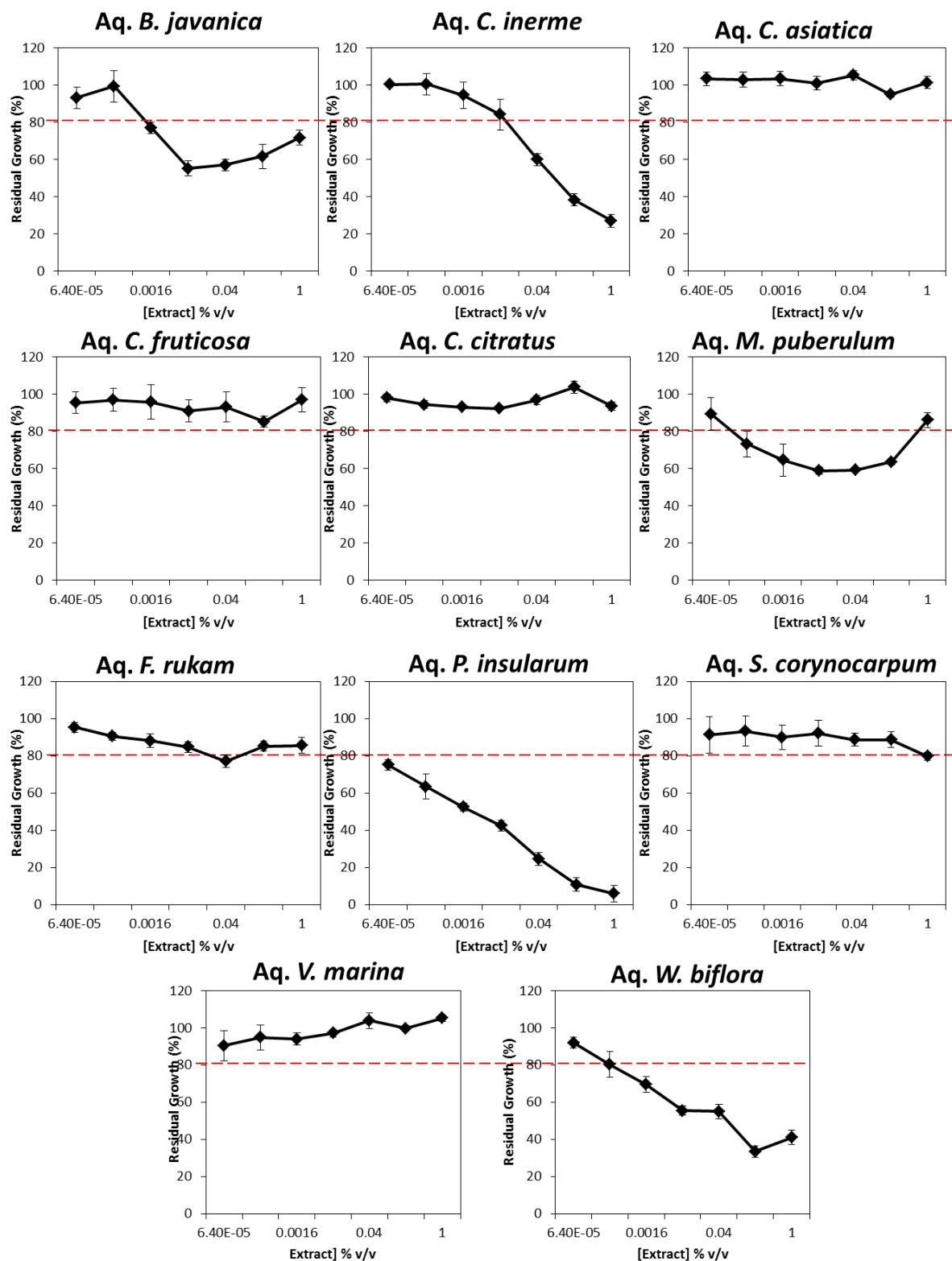


**Figure 2.5:** Liquid-based bioactivity assay of aqueous extracts in pH 7.0 SC. Residual growth assays of the 11 aqueous extracts of Samoan medicinal plants; cells inoculated into SC buffered to pH 7.0 with 25mM HEPES (SCH), were treated with increasing concentrations of aqueous extracts from  $3.2 \times 10^{-4}$  to 5% v/v, and growth was compared against control cells. Red dashed lines mark threshold for indication of bioactivity (*i.e.*, residual growth decreasing lower than 80% and exhibiting greater than 20% growth inhibition).

### 2.3.3. Five of 11 methanolic extracts are bioactive at pH 4.5

To assess the bioactivity of the methanolic plant extracts, BY4741 was grown in the presence of increasing concentrations of methanolic extracts in SC media at pH 4.5. Concentrations tested for methanolic extracts ranged from  $6.4 \times 10^{-5}$  to 1% v/v at five-fold serial dilutions. The maximum concentration tested was 1% v/v as it is established that DMSO at higher concentrations can affect the growth profile of yeast (Sadowska-Bartosz *et al.*, 2013).

In line with the results from the aqueous extracts, the residual growth of BY4741 in the presence of methanolic extracts was recovered compared to growth in vehicle control (1% v/v DMSO) (Fig 2.6). Whilst BY4741 showed a growth profile around 100% in the presence of some extracts, it also showed a decreasing growth profile in the presence of other extracts. Specifically, six methanol plant extracts produced BY4741 growth profiles that remained between 80 and 100% residual growth. These methanol extracts were from *B. javanica*, *C. fruticosa*, *C. citratus*, *F. rukam*, *V. marina* and *W. biflora*. The remaining five extracts produced BY4741 growth profiles that declined past the 80% residual growth line. These extracts were from *C. inerme*, *C. asiatica*, *M. puberulum*, *P. insularum* and *S. corynocarpum*. Interestingly, *P. insularum*, growth was nearly completely inhibited at 1% v/v of these extracts.

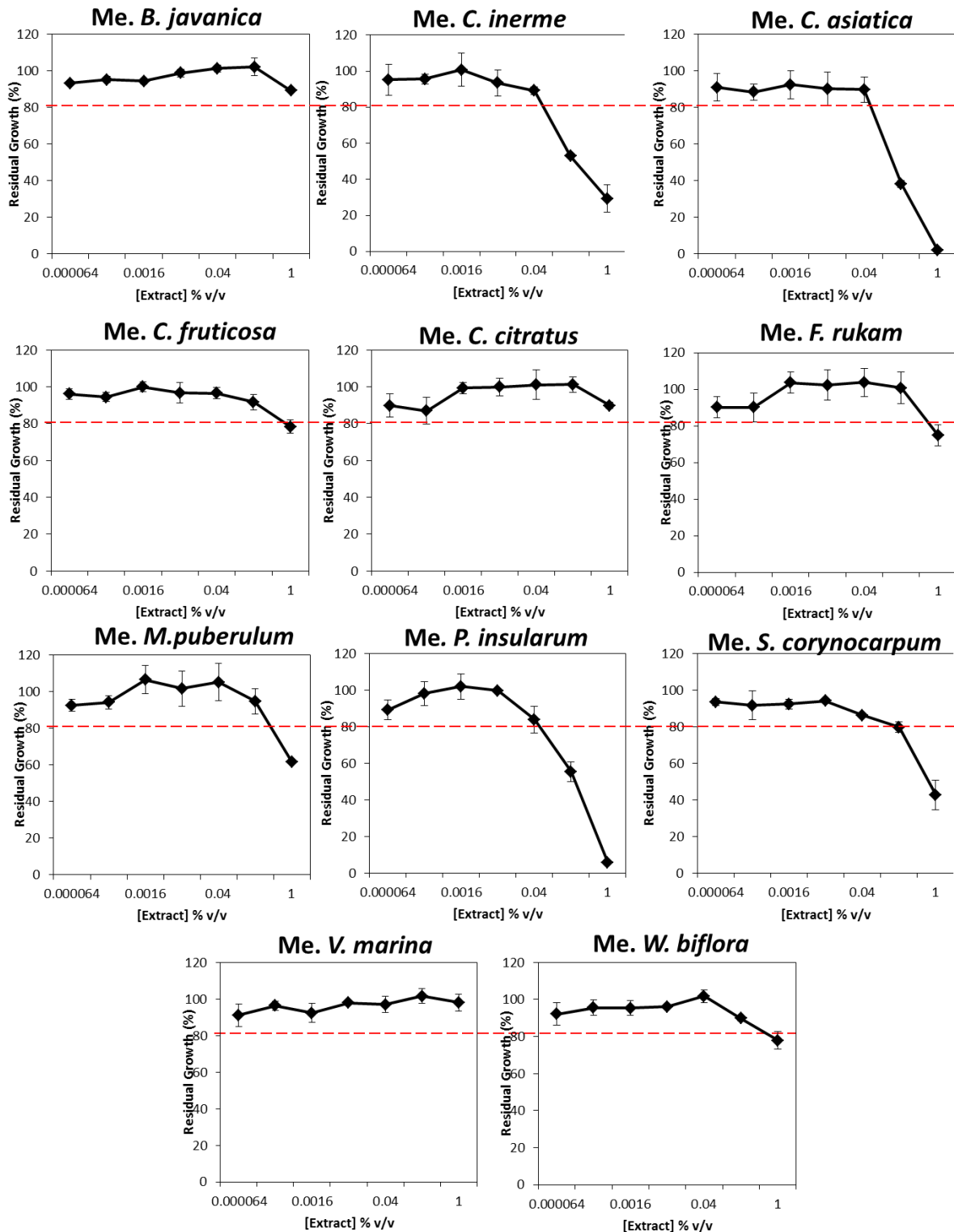


**Figure 2.6:** Liquid-based bioactivity assay of methanol extracts in pH 4.5 SC. Residual growth assays of the 11 methanol extracts of Samoan medicinal plants. BY4741 (WT) inoculated into SC were treated with increasing concentrations of methanol extracts from  $6.4 \times 10^{-5}$  to 1% v/v, and growth was compared against DMSO control cells. Red dashed lines mark threshold for indication of bioactivity (*i.e.*, residual growth decreasing lower than 80% and exhibiting greater than 20% growth inhibition).

#### 2.3.4. Ten of 11 methanolic extracts are bioactive at pH 7.0

Since pH was shown to play a significant role in the bioactivity of aqueous extracts of Samoan medicinal plants (Fig 2.4), we investigated if this was the same for the methanolic extracts. The previous experiment at pH 4.5 was repeated in SC media buffered to pH 7.0 with 25 mM HEPES. Residual growth of BY4741 was then measured and compared to growth in DMSO control (Fig 2.7). Impressively, 10 out of 11 methanol extracts reduced BY4741 growth past the 80% residual growth line; these methanolic extracts were from *B. javanica*, *C. inerme*, *C. asiatica*, *C. fruticosa*, *F. rukam*, *M. puberulum*, *P. insularum*, *S. corynocarpum*, *V. marina* and *W. biflora*. In these profiles, *B. javanica* extract consistently produced a BY4741 growth profile whereby growth decreases, but before it reaches complete or close to complete inhibition, growth improves again. Extracts that reduced BY4741 growth significantly, but did not reach the point of complete inhibition at 1% v/v include *C. inerme*, *M. puberulum* and *S. corynocarpum*. Methanolic extracts from *C. asiatica* and *P. insularum* showed profiles that reached close to 0% residual growth by 1% v/v. The *P. insularum* extract significantly reduced growth close to complete inhibition at 0.008% v/v, the lowest concentration producing close to complete inhibition observed from either aqueous or methanol extracts.

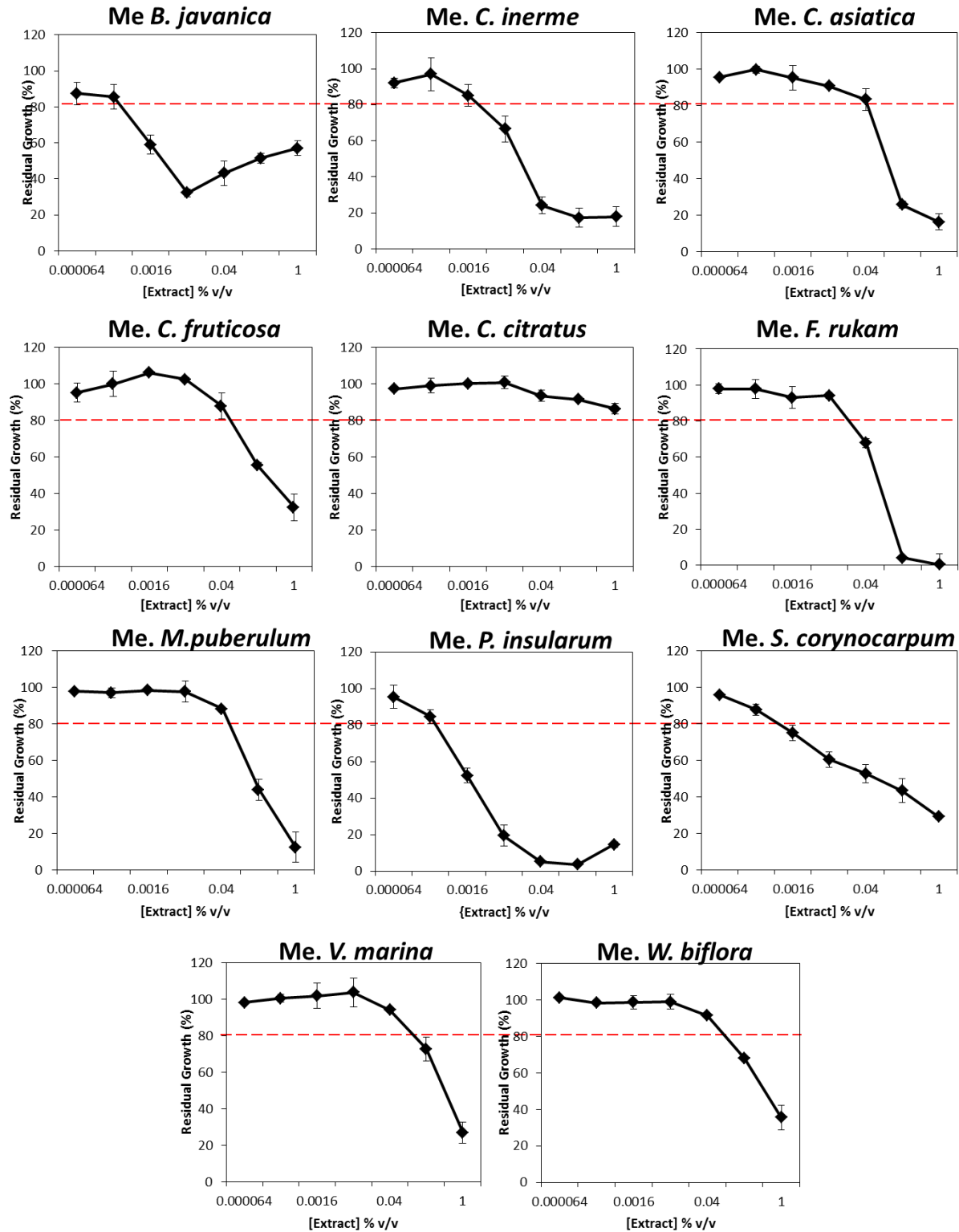


**Figure 2.7:** Liquid-based bioactivity assay of methanol extracts in pH 7.0 SC. Residual growth assays of the 11 methanol extracts of Samoan medicinal plants; cells inoculated into SC buffered to pH 7.0 with 25mM HEPES were treated with increasing concentrations of methanol extracts from  $6.4 \times 10^{-5}$  to 1% v/v, and growth was compared against DMSO control cells. Red dashed lines mark threshold for indication of bioactivity (*i.e.*, residual growth decreasing lower than 80% and exhibiting greater than 20% growth inhibition).

### 2.3.5. Extracts from different plants exhibit varying bioactivity profiles

To bring the extract bioactivity profile into context, the bioactivity results of the aqueous and methanolic extracts at two defined pH levels tested (Fig 2.4-2.7) were compiled (Table 2.1). The aqueous and methanolic extracts of *B. javanica* only demonstrated bioactivity in SC at pH 7.0 whilst only the methanolic extracts of *C. fruticosa*, *V. marina* and *W. biflora* were active in both pH 4.5 and pH 7.0. The *C. asiatica* and *S. corynocarpum* methanol extracts were active at either pH levels, whilst the aqueous extracts did not exhibit any bioactivity. The extracts of *C. inerme*, *F. rukam* and *M. puberulum* were bioactive in three of the four conditions, although these conditions varied from plant to plant. For instance, the aqueous extract of *F. rukam* was active at pH 4.5 and pH 7.0, while its methanolic extract was only active at pH 7.0. Conversely, *C. inerme* and *M. puberulum* aqueous extracts were only active at pH 7.0, and their methanolic extracts were active at both pH 4.5 and pH 7.0. Only *P. insularum* extracts were bioactive across all four conditions, as the aqueous and methanolic extracts were bioactive at both pH 4.5 and pH 7.0. In contrast, neither the aqueous nor the methanol extract from *C. citratus* reduced yeast growth at either pH.

**Table 2.1: Summary of bioactivity of aqueous and methanol extracts.** The table summarizes the concentration (% v/v) of extract required to inhibit 20% of yeast growth. NB indicates extracts which did not reduce yeast growth by 20% at the highest tested concentration. NT indicates extracts which were not tested. Red indicates lowest concentration producing bioactivity.

	Aqueous Extract			Methanolic Extract		
	Liquid pH 4.5	Liquid pH 7.0	Agar pH 7.0	Liquid pH 4.5	Liquid pH 7.0	Agar pH 7.0
<i>B. javanica</i>	1.5	0.0016	4	NB	0.0032	0.2
<i>C. inerme</i>	NB	0.016	7	0.06	0.0064	0.2
<i>C. asiatica</i>	NB	NB	NT	0.35	0.05	0.1
<i>C. fruticosa</i>	NB	NB	NT	NB	0.08	0.2
<i>C. citratus</i>	NB	NB	NT	NB	NB	NT
<i>F. rukam</i>	NB	NB	5	NB	0.024	0.5
<i>M. puberulum</i>	NB	0.00032	15	0.6	0.08	0.2
<i>P. insularum</i>	0.024	0.000064	3	0.05	0.0005	0.5
<i>S. corynocarpum</i>	NB	NB	NT	0.2	0.00096	1
<i>V. marina</i>	NB	NB	NT	NB	0.12	0.2
<i>W. biflora</i>	NB	0.00032	NT	NB	0.08	1
	5/11	10/11	5/11	5/11	10/11	10/11

### 2.3.6. Aqueous extracts are not substrates of the PDR system

Yeast undoubtedly is a powerful tool for investigating drug mechanism of action (Giaever *et al.*, 2004; Parsons *et al.*, 2004; Yibmantasiri *et al.*, 2012). However, it is often the case that studies in yeast require higher concentrations of a drug than that required in mammalian cell studies (Coorey *et al.*, 2015). Whilst the yeast cell wall contributes to this phenomenon, the major reason is the pleiotropic drug resistance (PDR) system (Coorey *et al.*, 2015). The yeast PDR system, as the name suggests, functions to effectively remove toxic drug compounds out of the cell via ABC transporters located in the plasma membrane. This defence system in yeast is regulated by two main transcription factors, *PDR1* and *PDR3*. Deletion of these transcription factors results in a strain with reduced drug reflux capabilities (Coorey *et al.*, 2015).

To determine if the aqueous plant extracts were substrates of the PDR system, the *pdr1Δpdr3Δ* double deletion mutant was grown in the presence of increasing concentrations of plant extracts in SC at pH 7.0. The growth profile of *pdr1Δpdr3Δ* in the presence of the extracts was compared to the growth profile of WT (Fig 2.8). Differences were observed in the growth of WT and *pdr1Δpdr3Δ* in the different aqueous extracts. For instance, WT exhibited a lower growth profile (*i.e.*, more sensitive growth profile) than *pdr1Δpdr3Δ* in the presence of the aqueous extract from *C. asiatica*. A similar difference between WT and the PDR attenuated strain was observed when treated with the aqueous extracts from *C. fruticosa*, *C. citratus*, *M. puberulum* and *V. marina*. The differences between WT and *pdr1Δpdr3Δ* do not appear to be statistically significant. When treated with the aqueous extracts of *B. javanica*, *C. inerme*, *F. rukam*, *P. insularum* and *W. biflora*, the growth profiles of WT and *pdr1Δpdr3Δ* were comparable. However, treatment with the aqueous extracts of *S. corynocarpum* resulted in a worse growth profile from *pdr1Δpdr3Δ* compared to WT, although the difference did not appear significantly different.

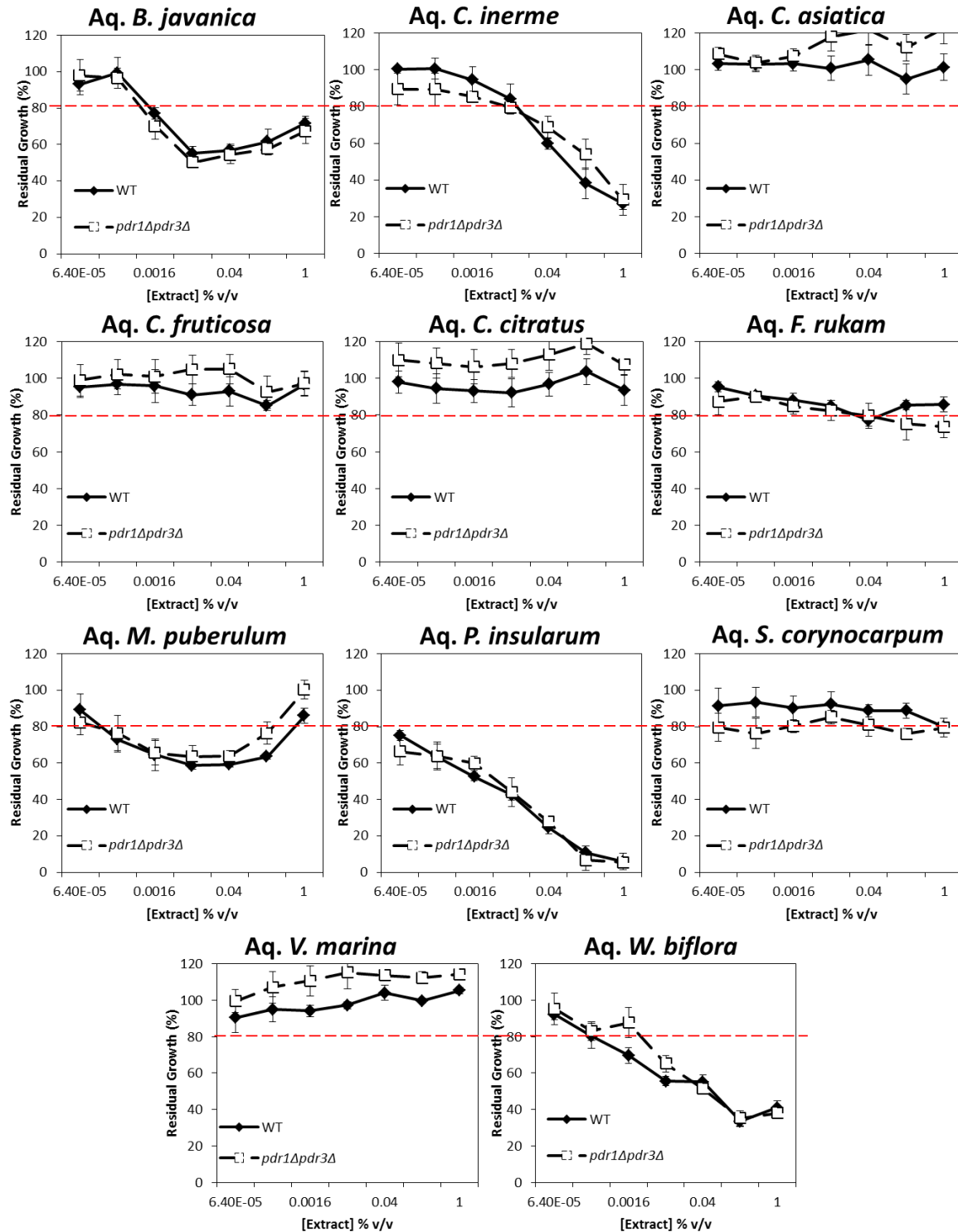


**Figure 2.8:** Liquid-based growth assays of Y7092 WT and PDR-attenuated strain in aqueous extracts. Residual growth assays of the 11 aqueous extracts of Samoan medicinal plants. Y7092 (WT) and *pdr1Δpdr3Δ* cells were inoculated into SC at pH 7.0 and treated with increasing concentrations of aqueous extracts from  $6.4 \times 10^{-5}$  to 1% v/v. Growth was compared against untreated cells, and residual growth calculated. Red dashed lines mark threshold for indication towards bioactivity (*i.e.*, residual growth decreasing lower than 80% and exhibiting greater than 20% growth inhibition).

### 2.3.7. Methanolic extracts are not substrates of the PDR system

To determine if the methanolic extracts obtained from the leaves of the selected Samoan medicinal plants were substrates of the yeast PDR system, Y7092 WT and *pdr1Δpdr3Δ* were grown in the presence of the methanolic extracts over a concentration range of  $6.4 \times 10^{-5}$  to 1% v/v in SC at pH 7.0. SC at pH 7.0 media was maintained in this experiment because it enhanced bioactivity of the extracts compared to that obtained from SC at pH 4.5. The growth of both strains in the presence of the extract was compared to growth in the presence of the vehicle control (1% v/v DMSO) to determine their residual growth (Fig 2.9).

Different patterns of growth comparison between WT and *pdr1Δpdr3Δ* were observed under treatment with methanolic extracts. For instance, treatment with the methanolic extracts from *C. inerme*, *C. asiatica*, *C. fruticosa*, *C. citratus*, *F. rukam*, *S. corynocarpum*, *V. marina* and *W. biflora* produced comparable growth profiles between WT and *pdr1Δpdr3Δ*. However, there were three methanolic extracts that produced varying growth profiles between WT and *pdr1Δpdr3Δ*, including the methanolic extracts from *B. javanica*, *M. puberulum* and *P. insularum*. However, while there appears to be statistical significance in some of these differences, whether there is biological relevance or not requires further investigation. Across all the extracts though, none produced a *pdr1Δpdr3Δ* growth profile that was more sensitive than WT, suggesting that the methanolic extracts were not substrates of the PDR system.

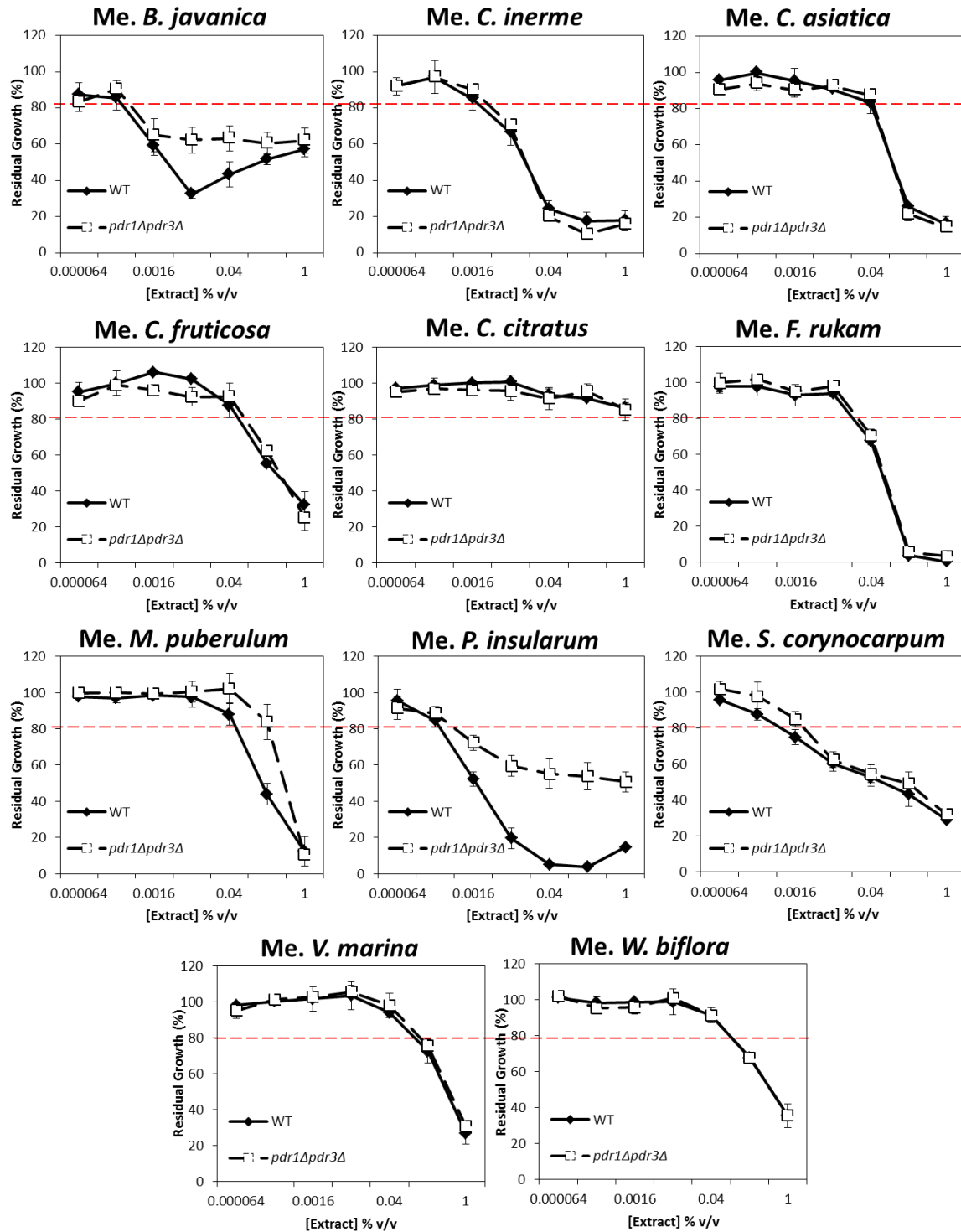


**Figure 2.9: Liquid-based growth assays comparing growth profiles in WT and PDR-attenuated strain in methanol extracts.** Residual growth assays of the 11 methanol extracts of Samoan medicinal plants. Y7092 (WT) and *pdr1Δpdr3Δ* cells were inoculated into SC buffered to pH 7.0 with 25mM HEPES, and treated with increasing concentrations of methanol extracts from  $6.4 \times 10^{-5}$  to 1% v/v. Growth was compared against vehicle control cells, and residual growth was calculated. Red dashed lines mark threshold for indication of bioactivity (*i.e.* residual growth decreasing lower than 80% and exhibiting greater than 20% growth inhibition).

### 2.3.8. Aqueous extracts maintain bioactivity in agar

Performing genome-wide analyses using the yeast deletion library on agar is more cost effective than performing microarray- or barcode sequencing-based genomic analyses. However, extracts that show bioactivity in liquid may not necessarily display bioactivity in agar, nor may there be sufficient compound depending on the potency of the compound in agar. To determine whether the extracts were amenable to agar-based genome-wide analyses, we ascertained if extract bioactivity was maintained in agar-based growth assays. This was achieved by spotting BY4741 cells on agar containing various concentrations of one of the five bioactive aqueous extracts, and comparing their growth to BY4741 grown in the vehicle control (Fig 2.10).

Although the extracts exhibited bioactivity at low concentrations in liquid, these concentrations did not reduce yeast growth in agar (data not shown). The experiment was therefore carried out at higher concentrations of the extracts to induce a growth defect. It was observed that *B. javanica* reduced growth of BY4741 at the 4% v/v concentration. As concentrations of aqueous *B. javanica* extract increased, BY4741 growth improved, similar to the profile observed in the liquid-based assays. In the cases of *C. inerme*, *F. rukam*, *M. puberulum* and *P. insularum*, BY4741 growth decreased in a dose-dependent manner. The aqueous extract from *C. inerme* reduced growth at 7% v/v. The *F. rukam* aqueous extract inhibited growth at 5% v/v, whilst this was only achieved at 15% v/v of the aqueous *M. puberulum* extract. In contrast, the *P. insularum* aqueous extract inhibited BY4741 growth at 3% v/v. These results show that *P. insularum* required the least amount of extract to inhibit growth in an agar-based growth assay (3% v/v), followed by the *B. javanica* aqueous extract at 4% v/v. The *F. rukam* extract is ranked third in bioactivity with a requirement of 5% of its aqueous extract to inhibit growth, and the *C. inerme* aqueous extract is ranked fourth via growth inhibition at 7% v/v. *M. puberulum* was the least bioactive requiring 15% v/v to inhibit yeast growth.

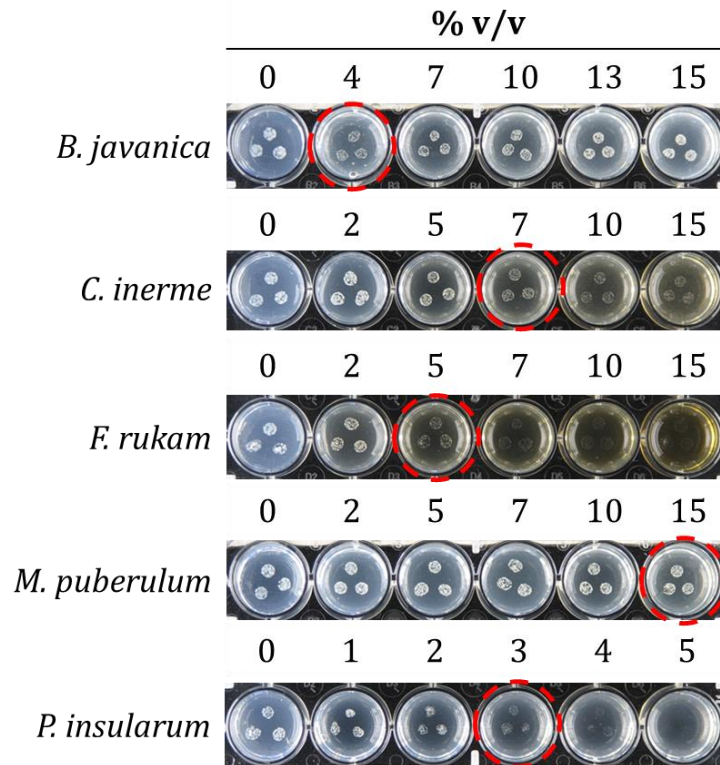


**Figure 2.10: Agar-based growth assays of WT in aqueous extracts.** WT yeast strain was grown on agar in the presence or absence of aqueous plant extracts. Agar was inoculated with yeast in spots. Growth was then compared between control agar well (0% v/v) and wells with various concentrations of extracts. Wells where aqueous extracts start to induce a growth defect are highlighted with red-dashed circles. Different volumes of extract had the relevant volume of vehicle control, but did not induce any change (data not shown) and a representative well is shown as control (0% v/v extract).

### 2.3.9. Methanolic extracts maintain bioactivity in agar

To determine if the bioactivity of methanol extracts were stable in agar and thus amenable to agar-based genome-wide analyses, we performed an experiment similar to that described above for aqueous extracts, utilizing increasing concentrations of the 10 bioactive methanolic extracts (Fig 2.11). The same phenomenon observed in the aqueous extracts whereby higher concentrations of extract was required to induce a growth defect in agar was again observed (data not shown), and the concentrations tested were therefore increased for these experiments. The methanolic extracts of *B. javanica*, *C. inerme*, *C. fruticosa*, *M. puberulum* and *V. marina* reduced growth of BY4741 at 0.2% v/v on agar. The methanolic extract of *C. asiatica* produced minimal growth reduction of

BY4741 at 0.04% v/v and completely inhibited its growth at 0.2% v/v, thus a titration experiment across the range of 0.04% v/v and 0.2% v/v to determine the concentration to detect approximately 10–20% growth inhibition of BY4741 (the amount of inhibition required for genome-wide analysis on agar) should work proceed with this extract. The same case was observed for both *F. rukam* and *P. insularum*, requiring concentration titration across the range of 0.2% v/v and 1% v/v. Methanolic extractions from *S. corynocarpum* and *W. biflora* were required at 1% v/v to induce growth inhibition of BY4741 on agar. Interestingly, while the methanolic extract of *P. insularum* was the most potent in liquid-based growth assays, it did not appear to be the most potent in agar, suggesting reduced activity of the extract in this form of growth assay.

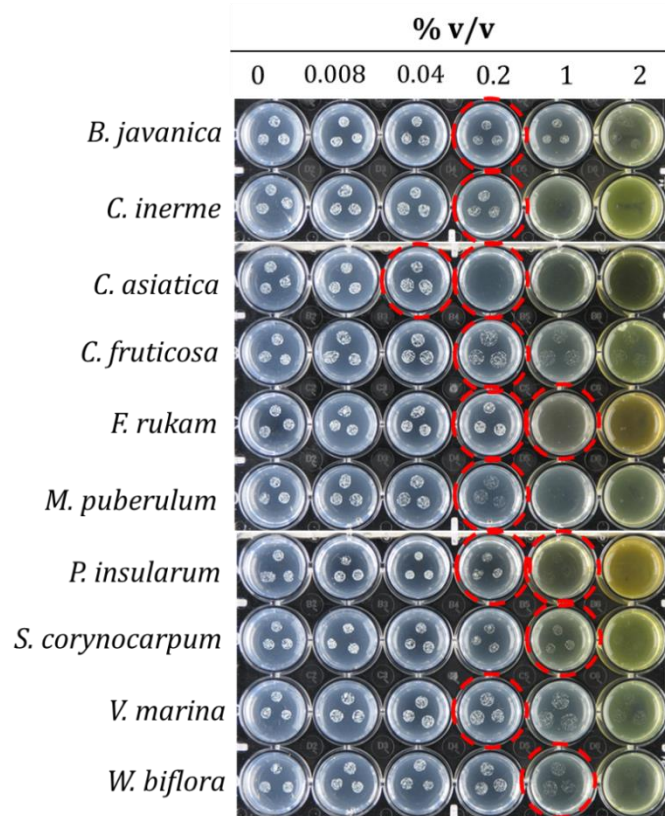


**Figure 2.11: Agar-based growth assays of WT against methanol extracts.** WT yeast strain was grown on agar in the presence or absence of plant methanol extracts. Agar was inoculated with yeast in spot-format. Growth was then compared between BY4741 WT on control agar well (0% v/v) and BY4741 WT in wells with various concentrations of extracts. Wells with extracts exhibiting a visually detectable reduction in growth are highlighted with red-dashed circles. Two circles per extract indicate a requirement to titrate between two concentrations.

## 2.4. Discussion

Our findings have clearly demonstrated that most of the 11 Samoan medicinal plants displayed bioactivity in yeast. Of the 22 extracts prepared from the 11 plants, five aqueous and 10 methanolic extracts inhibited yeast growth, a 68% bioactivity rate (Table 2.1). Previous pharmacological screens of Samoan medicinal plants for bioactivity produced varied bioactivity rates; Norton *et al.* (1973) had a 58% bioactivity rate from 208 plant extracts, Cox *et al.* (1989) had a 78% bioactivity rate from 104 plant extracts, and Dunstan *et al.* (1997) tested 50 Samoan medicinal plant extracts and had a 32% bioactivity rate, making the bioactivity rate obtained here comparable to those previous studies. However, studies previously carried out on Samoan medicinal plants utilized multiple assays to determine bioactivity (*e.g.*, Dunstan *et al.* (1997) used an *in vitro* assay assessing prostaglandin biosynthesis and rat ear oedema) which may subsequently result in a higher bioactivity rate, compared to the study reported herein, whereby only one assay (yeast growth inhibition) was used to evaluate bioactivity. In this context, our study on Samoan medicinal plants produced a higher bioactivity rate than those previously reported. A study on 61 Indian plant extracts produced a 34% bioactivity rate (Kumar *et al.*, 2006), suggesting that the bioactivity rate detected from the yeast liquid-based assay carried out in this work on Samoan plant extracts was comparable to studies of plants outside of Samoa. It is important to note that the bioactivity detected here from the crude aqueous and methanolic extracts of the selected medicinal plants, may be a consequence of a single bioactive compound, a mixture of compounds, or the synergistic activities of more than one compound. Also of significance from these results was the conclusion that only *C. citratus* produced aqueous and methanolic extracts that did not reduce yeast growth in SC at pH 4.5 and pH 7.0. However, this conclusion was drawn on the basis of the parameters tested here, and that *C. citratus* extracts may be bioactive if tested at higher concentrations, in a different system, or if extracted using a different solvent.

Also of note is the significantly higher concentration of extracts necessary to inhibit yeast growth in agar compared to that in liquid. For instance,  $6.5 \times 10^{-5}$  % v/v of *P. insularum* aqueous extract was required to inhibit approximately 20% of BY4741 growth in liquid (Fig 2.5) whilst in the agar assay, it was required at 3% v/v to induce a similar level of growth inhibition (Fig 2.10). One explanation could be the 50°C temperature needed to liquefy agar, however extract activity was maintained after heating at 70°C overnight for 15 h (Appendix II). A more likely explanation is the form of the assay because in liquid, yeast cells are surrounded by media containing the tested extracts whereas in agar, the plant extracts are in much more limited contact with yeast cells.

Bioactivity of the plant extracts was affected when HEPES was added to buffer pH from 4.5 to 7.0, regardless of whether the extracts were aqueous or methanolic. For instance, the aqueous extracts of *C. inerme* that did not inhibit yeast growth at pH 4.5 reduced yeast growth at pH 7.0. Furthermore, methanolic extracts that were shown to have marginal inhibitory effects on yeast growth at pH 4.5 showed increased inhibition at pH 7.0, such as the methanolic extracts from *B. javanica* and *C. fruticosa*. Whether this phenotype is common with all plant extracts remains unknown, as most studies into plant crude extracts have not considered pH as a variable (Alanis-Garza *et al.*, 2007; Ali-Shtayeh & Ghdeib, 1999; Hammer *et al.*, 1999; Kumar *et al.*, 2006; Quiroga *et al.*, 2001; Rauha *et al.*, 2000; Satish *et al.*, 2007; Webster *et al.* 2008; Weckesser *et al.*, 2007; Wilson *et al.*, 1997). This aside, these results suggest that either pH 7.0 or the HEPES buffer used increased potency of the extracts. Importantly, Quek *et al.* (2013) showed that pH does affect potency, when pH 7.0 reduced the bioactivity of their compound TA-289 2-fold compared to its activity at pH 4. Whilst this trend is opposite to the one observed here, it shows that pH does affect potency of bioactive compounds. Further, Tanaka *et al.* (1996) showed the activity of the antimicrobial agent DU-6859a was also affected by pH, where its MIC was reduced as pH increased. Furthermore, Palm *et al.* (1999) showed that pH affected drug transport. These works provide evidence that pH does affect the potency however, to fully discount the possibility that the increased potency was a

consequence of HEPES addition, we propose the pH of the media be adjusted to 7.0 using a different buffer (*e.g.*, MOPs) or using NaOH.

Another promising finding from the results presented in this chapter is the lack of hypersensitivity of the PDR-attenuated strain (*pdr1Δpdr3Δ*) to the extracts of the Samoan medicinal plants. Although hypersensitivity would have allowed further studies to be carried out at lower concentrations (Coorey *et al.*, 2015), it would have also indicated extract unsuitability for application as antifungals. However, our findings suggested that the bioactive compounds in the plant extracts were not substrates of the yeast drug efflux system, further inferring that the plant extracts could be exploited as antifungals. Intriguingly, whilst the PDR attenuated strain did not appear hypersensitive to the extracts, in some cases, they appeared more resistant towards the extracts, as the WT exhibited more sensitivity. This suggests that *PDR1* and/or *PDR3* contribute to the mechanism of action of the extracts, such as the methanolic extracts of *B. javanica*, *M. puberulum* and *P. insularum*.

In summary, 15 out of 22 extracts from 11 Samoan medicinal plants were established as bioactive in *S. cerevisiae*, and the optimal media condition for the most potency was elucidated. The amenability of the extracts for agar-based genome-wide analyses was also determined, and the extracts were further shown to not be substrates of the PDR system. From this chapter, it was also ascertained that *P. insularum* was the only medicinal plant that produced bioactivity across the aqueous and methanolic extracts at two different pH levels. The *P. insularum* extracts were the most potent aqueous extract and thus became the medicinal plant of most interest for the remainder of this thesis.

---

## Chapter 3:

# The Mechanism of Action of *Psychotria insularum* is Iron Chelation

---

### 3.1 Introduction

Plants have been the source of many significant contributions to human medicine, including drugs such as aspirin and paclitaxel. Plants with extensive ethno-botanical background are even more successful as sources of drugs, for instance digoxin, quinine, morphine and artemisinin. However, a large portion of medicinal plants remain unstudied, and the mechanisms of action (MOA) of the majority remaining are largely unknown. Samoan medicinal plants were the subject of several investigative endeavours in the 1970s and 1980s (Cox *et al.*, 1989; Norton *et al.*, 1973). However, only their activities were explored, but how the plant extracts mediated their activity, or more specifically their MOA, remains largely unknown.

In Chapter 2, leaf extracts of the Samoan medicinal plant *Psychotria insularum* produced the most potent inhibition of yeast growth. Leaf extracts of *P. insularum* are one of the most prescribed medicinal remedies in Samoan traditional medicine against supernaturally induced ailments (Whistler, 1996). The plant is also administered in cases involving inflammation, such as fever, abdominal distress, skin infections, wounds, as well as general body aches and swellings (Dunstan *et al.*, 1995; Whistler, 1996). Extracts of *P. insularum* reduced blood pressure, motor activity, prostaglandin synthesis and the development of rat ear oedema (Cox *et al.*, 1989; Dunstan *et al.*, 1995; Norton *et al.*, 1973). Despite these multiple studies, the underlying MOA, notably the genes and pathways of how the extracts mediate these activities, are unknown.

The findings in the preceding chapter demonstrated that *P. insularum* was the only plant that produced an aqueous extract that was bioactive at both pH 4.5 and pH 7.0. Further, the aqueous extract of *P. insularum* was the most potent in agar compared to other aqueous extracts. As

aqueous extracts are of particular interest in this thesis in the interest of correlating MOA to application in traditional Samoan medicine, the genetic analysis utilizing the Mata haploid deletion library of *S. cerevisiae* was carried out on the aqueous extract of *P. insularum*. We elucidated that *P. insularum* extracts possessed iron-chelating activity regulated an anti-inflammatory activity, correlating its MOA to how the plant is used in the Samoan traditional medicine setting.

## 3.2 Methods

### 3.2.1 Agar-based genome-wide analysis

Rectangular petri plates (Singer Instrument Co. Ltd) were prepared with 40 mL of SC agar containing either the relevant concentration of the aqueous extract of *P. insularum* or water. The Mata haploid deletion mutants subset of the Yeast Knockout Collection (Open Biosystems) in the 1,536 format (*i.e.* 1,536 colonies per plate arrayed as quadruplicates of 384 mutants) was pinned in triplicate on control agar and on agar containing the aqueous extract. The plates were incubated at 30°C for 24 h, photographed using a Canon Powershot S3IS digital camera, further incubated for an additional 24 h, and photographed again. For each time point (24 and 48 h), colony sizes were measured using Gitter (Wagih & Parts, 2014) and ScreenMill (Dittmar *et al.*, 2010) was used to quantify colony fitness of each gene deletion strain including statistical evaluation using z-scores and p-values. To confirm mutant growth was reduced in the presence of the extract, all deletion mutant strains with p-values less than 0.05 in two or more replicates were selected for validations via serial dilution growth analyses. Five-fold serial dilutions of  $5 \times 10^5$  cells/mL were spotted on SC agar containing aqueous extract of *P. insularum* or vehicle control. Plates were incubated at 30°C for 24 h, photographed, further incubated for an additional 24 h, and photographed again.

### 3.2.2 Metal rescue assay

Amelioration of *P. insularum*-induced growth defects was evaluated with the addition of various metals. Cultures were prepared by inoculating experimental cultures at  $5 \times 10^5$  cells/mL in SC with the presence or absence of 100  $\mu$ M of metal solutions of interest ( $\text{FeCl}_3$ ,  $\text{FeSO}_4$ ,  $\text{ZnCl}_2$ ,  $\text{CaCl}_2$ ,  $\text{CuCl}_2$ ,  $\text{MgCl}_2$  and  $\text{MnCl}_2$ ). Concurrently, cultures with and without exogenous metal supplementation were treated with increasing concentrations of *P. insularum* extract, incubated at 30°C for 15 h, and quantified via absorbance at 590 nm using an EnVision 2102 multilabel plate reader (Perkin Elmer).

Percentage of residual growth (treated OD<sub>590</sub>/untreated OD<sub>590</sub> x 100) was then calculated for each treatment.

### 3.2.3 Quantification of intracellular iron

Intracellular iron was quantified using inductively coupled plasma mass spectroscopy (ICP-MS) as previously described (Tamarit *et al.*, 2006). Cultures were prepared by inoculating experimental cultures at 5x10<sup>5</sup> cells/mL in SC with the relevant treatment (extracts or controls at the prescribed concentration). At mid-log growth, 10 OD units were collected by centrifugation. Cells were digested in 3% nitric acid at 96°C for 16h and clarified by centrifugation at 13,000 rpm for 5 min. Levels of iron, copper, zinc, calcium and magnesium were measured in the supernatant using ICP-MS (Element 2 Magnetic Sector Field, ThermoFisher). Metal standards were run in conjunction with samples, as well as the relevant equipment blanks to monitor potential contamination at each step of the process. Spike samples were also prepared to ensure that cell lysate was not interfering with metal quantification, and each sample was analysed by ICP-MS 10 times. Where changes were observed, the statistical significance of an increase or decrease was assessed using a one-tailed Student's t-test, and the same was carried throughout this thesis.

### 3.2.4 Protein expression

Protein expression was quantified by fluorescence of a GFP-tagged protein of interest relative to the fluorescence of internal markers of the cytoplasm and nucleus (mCherry and RedStar, respectively). Experimental cultures were prepared by inoculating with 5x10<sup>5</sup> cells/mL of the relevant strain (Appendix III) and grown in the relevant treatment and grown at 30°C for 15 h, diluted to approximately 1 x 10<sup>9</sup> cells/mL, transferred to 384 clear bottom microtitre plates (Perkin Elmer), and visualized using the Evo-Tec OPERA high throughput spinning disc confocal microscope (Perkin Elmer) at room temperature, with the 60X water immersion lens (NA 1.2). GFP excitation was at 488 nm and detected with a 520/35 filter. mCherry and RedStar excitation was at 561nm and detected

with a 600/40 filter. An exposure of 400ms with 5 Z-stacks 0.5µm apart was used for all images (Bircham *et al.*, 2011). GFP quantification was achieved using ACAPELLA software v2.0 (Perkin Elmer) that identified cells based on the mCherry and RedStar signals and the quantification of GFP as previously described (Bircham *et al.*, 2011). Fluorescence was compared between treatments using a Student's t-test.

### 3.2.5 Heme assay

Heme was quantified by the triton-methanol protocol as previously described (Pandey *et al.*, 1999). Cells were treated overnight as described before, lysed by glass-bead agitation, and protein extracted as described in Dunn & Wobble (2001) and Zhang *et al.* (2011). Briefly, cells were washed, pre-treated with 2M lithium acetate, washed, pre-treated with 0.4M NaOH, before lysis with acid-washed glass beads. The cell lysate was then collected by centrifugation. Protein was quantified using the BCA protein assay kit (Pierce) according to manufacturer instructions. Heme was then quantified by the triton-methanol protocol (Pandey *et al.*, 1999) where 20µL of clarified cell lysate was added to 180µL triton-methanol (2.5% triton in methanol), and absorbance was read at 405 nm using an Envision plate reader (Perkin Elmer). Hemin (Sigma) was prepared at concentrations ranging from 10-500 nM for the standard curve. Heme content of yeast protein samples was calculated using the hemin standard curve, normalized to protein content, and reported as relative heme content  $[(\text{treated heme}_{\text{nM}/\mu\text{g protein}} / \text{untreated heme}_{\text{nM}/\mu\text{g protein}}) \times 100]$ .

### 3.2.6 Aconitase assay

Aconitase activity was measured using the Aconitase Assay Kit (Cayman Chemical) according to manufacturer's instructions. Briefly, RAW 264.7 cells were washed in cold 1 X PBS, resuspended in Assay Buffer and lysed by sonication 20 times with 5 s bursts. The cell suspension was then centrifuged at 500 x g for 10 min at 4°C to remove cell debris and the supernatant was transferred to a fresh tube and frozen at -80°C until use. Then 50 µL of sample containing 1 mg/ mL

protein was aliquoted in a 96-well plate in triplicate, followed by the addition of 5  $\mu\text{L}$  Assay Buffer, 50  $\mu\text{L}$  of  $\text{NADP}^+$  Reagent, 50  $\mu\text{L}$  isocitric dehydrogenase and 50  $\mu\text{L}$  substrate solution. A positive control was prepared using a manufacturer-supplied aconitase control, and blank wells were also prepared. Absorbance was measured at 340 nm every 30 min at 37°C. Aconitase activity was then calculated using the following equation:

$$\text{Aconitase Activity (nmol/min/mL)} = \left[ \frac{\Delta A/\text{min (sample)} - \Delta A/\text{min (sample background)}}{0.00313 \mu\text{M}^{-1}} \right] \times \frac{0.205 \text{ mL}}{0.05 \text{ mL}} \times \text{Sample Dilution}$$

wherein  $\Delta A$  is the change in absorbance,  $0.00313 \mu\text{M}^{-1}$  is the extinction coefficient of aconitase based on pathlength of the well, 0.205 mL is the final reaction volume, and 0.05 mL is the aconitase sample used. Aconitase activities were ultimately compared between different treatments and the control.

### 3.2.7 Iron chelation assay

Iron chelation was directly measured using a modified chrome azurol S (CAS) assay as previously described (Alexander & Zuberer, 1991). Briefly, the CAS assay solution was prepared by the addition of 7.5 mL of 2 mM CAS and 1.5 mL of 1 mM  $\text{FeCl}_3$  dissolved in 10 mM HCl to 21.9 mg of HDTMA (hexa-decyl-tri-methy-ammonium bromide) dissolved in 25 mL water. To this solution, MES (2-(N-morpholino)ethanesulfonic acid) buffer (pH 5.6) was added and made up to 100 mL with  $\text{dH}_2\text{O}$ . Then 100 $\mu\text{L}$  of the prepared CAS solution was aliquoted into a 96-well plate, to which 100  $\mu\text{L}$  of various dilutions of the extracts were added. A colour change reaction from blue to yellow was indicative of iron chelation activity.

### 3.2.8 Anti-inflammatory assays

Markers of inflammation were measured using enzyme-linked immunosorbent assays (O'Sullivan *et al.*, 2014). Briefly, bone marrow-derived macrophages from C57BL/6 mice (for MTT, cytokine and NO work) and RAW 264.7 cells (for aconitase work) were seeded at  $1 \times 10^5$  or  $5 \times 10^4$

cells/well respectively in 96-well plates, primed with 20 U/mL interferon gamma (IFN $\gamma$ ) and incubated at 37°C with 5% CO $_2$  for 18 h, before 200 ng/mL LPS and relevant treatment were added simultaneously to each well. Plates were incubated for a further 24 h, before 170  $\mu$ L of supernatants were collected for cytokine and NO analyses, and cells were used for MTT (3-[4,5-dimethylthiazoyl-2—yl]-2,5-diphenyltetrazolium bromide) assays.

The MTT assay measures the metabolic activity of the cells, using the MTT tetrazolium salt which is converted from yellow to purple via the activity of metabolically active cells. Essentially, upon removal of supernatant for cytokine and NO analyses, 50  $\mu$ L of CTCM (complete T cell media) and 20  $\mu$ L of 5 mg/mL MTT solution in PBS were added to the 96-well plate. The plates were incubated at 37°C with 5% CO $_2$  for 2 h, before 100  $\mu$ L of MTT solubilizer solution (10% SDS [sodium dodecyl sulfate], 45% DMF [dimethylformamide] in ddH $_2$ O pH 4.5) was added. Plates were incubated overnight at 37°C, before reading at 570nm using an Enspire Multi-Plate reader (Perkin Elmer). NO is an indicator of the inflammatory response, and is rapidly degraded to nitrite and nitrate in the supernatant. These products are measured as an indicator of NO production in macrophages. This was achieved by mixing 50  $\mu$ L of cell supernatant with 50  $\mu$ L of Griess reagents in 96-well plates, together with a standard curve prepared from NaNO $_2$  (sodium nitrite). Absorbance was read at 570nm. Enzyme-linked immunosorbent assays (ELISA) were used to determine levels of IL-10, IL-12 and TNF $\alpha$  from supernatants, conducted as per manufacturer's instructions (BD Bioscience). Briefly, 96-well ELISA plates were coated overnight at 4°C with a capture antibody, and excess antibody was removed after incubation, and the plates were blocked with 5% or 10% FCS in PBS for 2 h. The plates were subsequently washed three times with 0.05% tween in PBS, before being loaded with 50  $\mu$ L cell supernatant or standards. Plates were washed four times, followed by the addition of 50  $\mu$ L of detection antibody, before plates were incubated at room temperature for 1 h, washed eight times, and then 100  $\mu$ L of TMB reagent (BD Bioscience) was added into each well. After colour development, the reaction was stopped with 100  $\mu$ L of stop solution, and absorbance was read at 460 nm.

### 3.3 Results

#### 3.3.1 Genome-wide analyses of aqueous *P. insularum* extract

Genome-wide analyses using mutant libraries of yeast have been used to successfully identify MOA of compounds (Baetz *et al.*, 2004; Carroll *et al.*, 2009; Giaever *et al.*, 1999; Giaever *et al.*, 2004; Hillenmeyer *et al.*, 2008; Lumet *et al.*, 2004; Parsons *et al.*, 2004; Robinson *et al.*, 2014; Smith *et al.*, 2009). To determine the mechanism of action of the aqueous extract of *P. insularum*, we first identified a concentration to conduct the viability-based genome-wide analysis; this is a concentration that resulted in 10-20% growth inhibition in the wild-type BY4741 strain. With a 10-20% inhibition in mutant strains, there will be a large window to detect growth inhibitions up to 80-90% in the deletion strains. Via growth analysis of a representative library plate in 1,536 format, we conducted an image analysis using Gitter (Wagih & Parts, 2014) and identified that 6% v/v of the aqueous extract inhibited approximately 15% of yeast growth across the entire plate compared to agar vehicle control (Table 3.1).

**Table 3.1: Optimization of aqueous extract concentration for genome-wide analysis.** Colony sizes were measured using R-Gitter (arbitrary units) and residual growths were calculated by comparison to control median colony size.

	Control	Aq. <i>P. insularum</i>		
		2% v/v	4% v/v	6% v/v
Conoly size (median, AU)	516.3	525.3	488.7	440.5
Residual Growth (%)	100.0	101.7	94.6	85.3
Standard Deviation (%)	3.1	6.2	4.3	3.5

We thus grew the ~4,300 haploid deletion strains in the deletion library (~70% of the yeast genome) in the presence or absence of 6% v/v of the aqueous extract of *P. insularum*. Specifically, these strains were either grown on SC agar with the aqueous extract at 6% v/v or with dH<sub>2</sub>O at 6% v/v, in triplicate per treatment. After 24 h, colony sizes were calculated using Gitter (Wagih & Parts, 2014), from which growth ratios were calculated using ScreenMill (Dittmar *et al.*, 2010). The growth ratio was a comparison of the colony size of each vehicle-treated deletion mutant against the colony

size of each *P. insularum*-treated deletion mutant. Essentially, a growth ratio of 1 suggests the treated deletion mutant grew comparatively to its control counterpart. A growth ratio lower than 1 suggests the treated deletion mutant grew better than its control equivalent, while a growth ratio greater than 1 indicates the treated deletion mutant exhibited less growth compared to control. The majority of gene deletions exhibited a growth ratio between 0.8 and 1.2 (Fig 3.1) suggesting that the treatment with the aqueous extract of *P. insularum* did not drastically improve or reduce growth compared to growth under control conditions. There were 23 deletion mutants that exhibited a growth ratio less than 0.8 indicating the treatment with the aqueous extract of *P. insularum* improved their growth by at least 10% compared to control conditions. The increased growth of these gene deletions suggested that the deletion of the gene suppressed the effect of the extract. There were 88 gene deletions that exhibited a growth ratio greater than 1.2, indicative of 10% growth inhibition of the deletion mutants in the presence of the aqueous extract of *P. insularum*. The hypersensitivity of these gene deletions suggested that these genes are required to buffer the effect of the *P. insularum* aqueous extract.

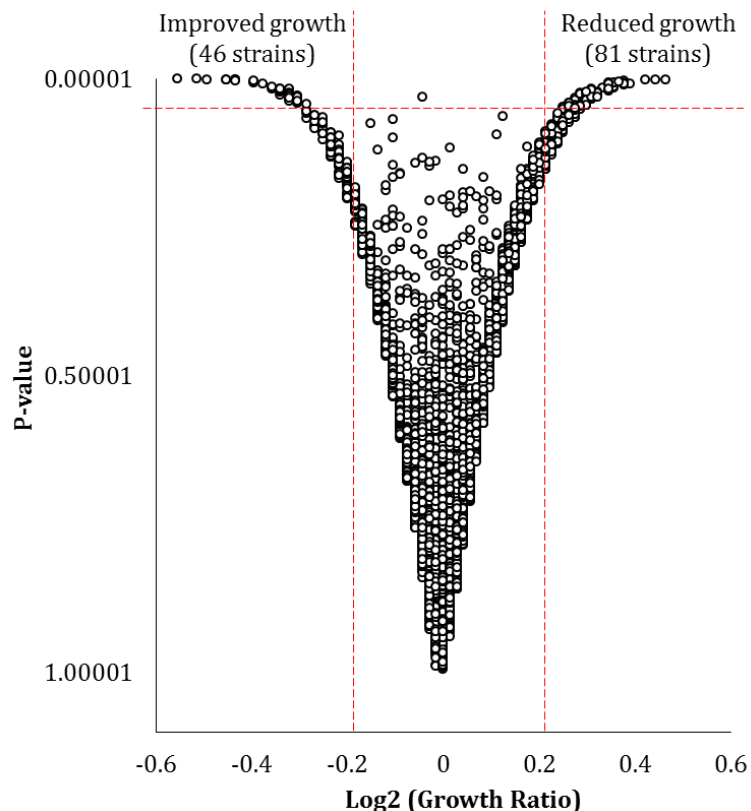


**Figure 3.1: The scatterplot of gene deletion log<sub>2</sub> growth ratio against aqueous *P. insularum* extract versus p-value.** The haploid deletion mutant collection was analyzed against the aqueous extract of *P. insularum* extract in triplicate, and the growth of each deletion mutant was compared against its control counterpart. The average of the resulting fitness score across all three replicates was calculated and plotted as log<sub>2</sub>, against their corresponding p-values. The red-dashed lines mark the cut-off points of strains with improved and reduced growth, while the black-dashed line marks the p-value 0.05. Based on this selection system, 46 strains had log<sub>2</sub> growth ratio less than -0.2 and p-value less than 0.05 (improved growth) and 81 strains with log<sub>2</sub> growth ratio greater than 0.2 and p-value less than 0.05 (reduced growth).

---

### 3.3.2 Validations implicate various biological processes in *P. insularum* MOA

Using the statistical evaluation of p-value cut-off of <0.05, we determined that the growth of 204, 227 and 239 deletion mutants were significantly altered compared to the control, in replicates 1, 2 and 3 respectively. Across these 670 gene deletions, 128 mutants (Appendix IV) were present in two or more replicates. Sensitivity of these 128 gene deletion mutants was independently evaluated using a spot dilution assay. The gene deletion strains were grown in overnight cultures, and then serially diluted five-fold and inoculated on control agar or agar containing 2% v/v aqueous extract of *P. insularum*. The plates were visually analysed after 48 h of growth at 30°C, and 29 of the 128 mutants were sensitive to the aqueous extract of *P. insularum* (Appendix V). Based on comparisons of growth at specific dilutions (red dashed circles in Fig 3.2), the most hypersensitive gene deletions to the aqueous *P. insularum* extract were *bem1Δ*, *bem4Δ*, *snf5Δ*, *tef4Δ*, and *ydr269cΔ*. The *BEM* genes are involved in bud emergence. Specifically, *BEM1* encodes a protein involved in establishing cell polarity and morphogenesis, while *BEM4* encodes a protein involved in the establishment of cell polarity and bud emergence (Bender & Pringle, 1991; Mack *et al.*, 1996). *SNF5* encodes a protein of the subunit of the SWI-SNF chromatin remodelling complex, while *TEF4* encodes the gamma subunit of the eEF1B translational elongation factor (Kinzy *et al.*, 1994; Peterson *et al.*, 1994). *YDR269C* is a dubious open reading frame that overlaps *CCC2* (Fig 3.3A), a copper transporter at the Golgi apparatus (Fisk *et al.*, 2006; Fu *et al.*, 1995).

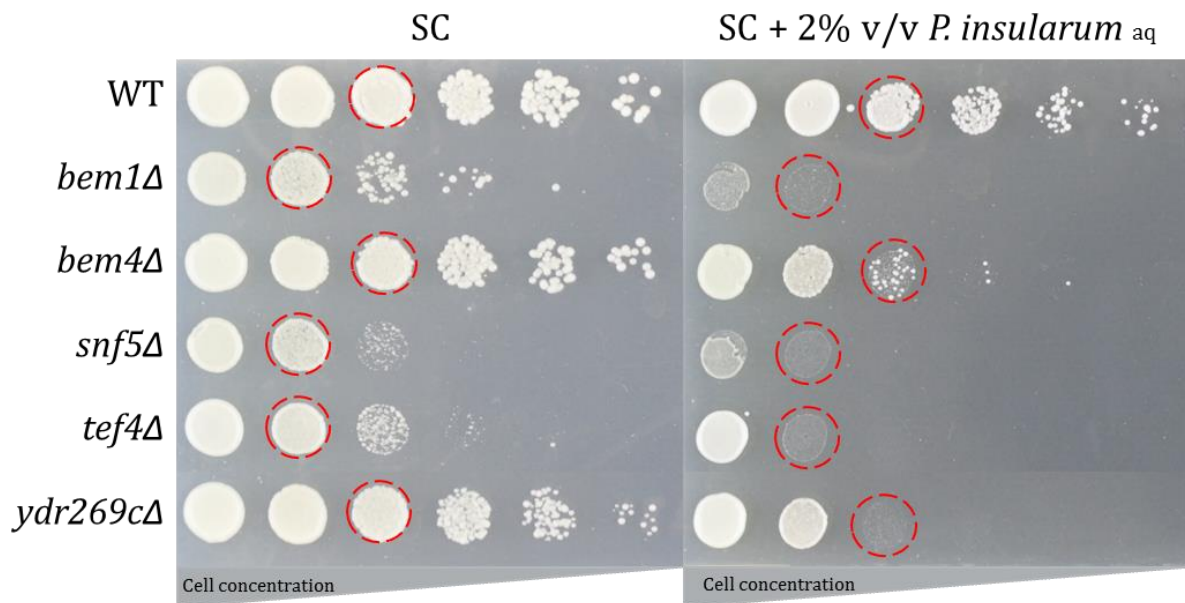


**Figure 3.2: Spot dilution assay of five most hypersensitive gene deletions.** Gene deletions were grown overnight then serially diluted, and subsequently spotted onto SC control agar, or SC agar containing 2% v/v aqueous extract of *P. insularum* (*P. insularum*<sub>aq</sub>). Images for visual comparison were taken after 48 h growth at 30°C. Gene deletions showing the most hypersensitivity to the aqueous extract of *P. insularum* are illustrated, including *bem1Δ*, *bem4Δ*, *snf5Δ*, *tef4Δ* and *ydr269cΔ*. Spots with red dashed circles indicate the circles that were compared against WT growth and treatment counterpart to illustrate degree of growth reduction.

### 3.3.3 Deletion of *CCC2* is hypersensitive to the aqueous *P. insularum* extract

As we determined above that *ydr269cΔ* is hypersensitive to the *P. insularum* aqueous extract (Fig 3.2) and that *YDR269C* is a dubious ORF that overlaps with *CCC2* (Fig 3.3A), we sought to determine if *ccc2Δ* was also hypersensitive to the *P. insularum* aqueous extract. WT, *ydr269cΔ* and *ccc2Δ* were grown in increasing concentrations of *P. insularum* aqueous extract for 15 h at 30°C. At concentrations less than 0.05% v/v, there was not a dramatic difference in residual growth (treated/untreated) between the three strains; all strains exhibited residual growth values between 90-100% (0-10% growth inhibition). In contrast, growth of *ydr269cΔ* and *ccc2Δ* was significantly reduced at concentrations greater than 0.05% v/v compared to the WT, with residual growth values between 20-60% (40-80% growth inhibition). These results suggest that the hypersensitivity of

*ydr269cΔ* may be attributed to the deletion of nucleotides overlapping with *CCC2*, particularly since *YDR269C* is a dubious ORF that does not encode a protein. These findings warranted further investigations into *CCC2* and associated pathway(s).

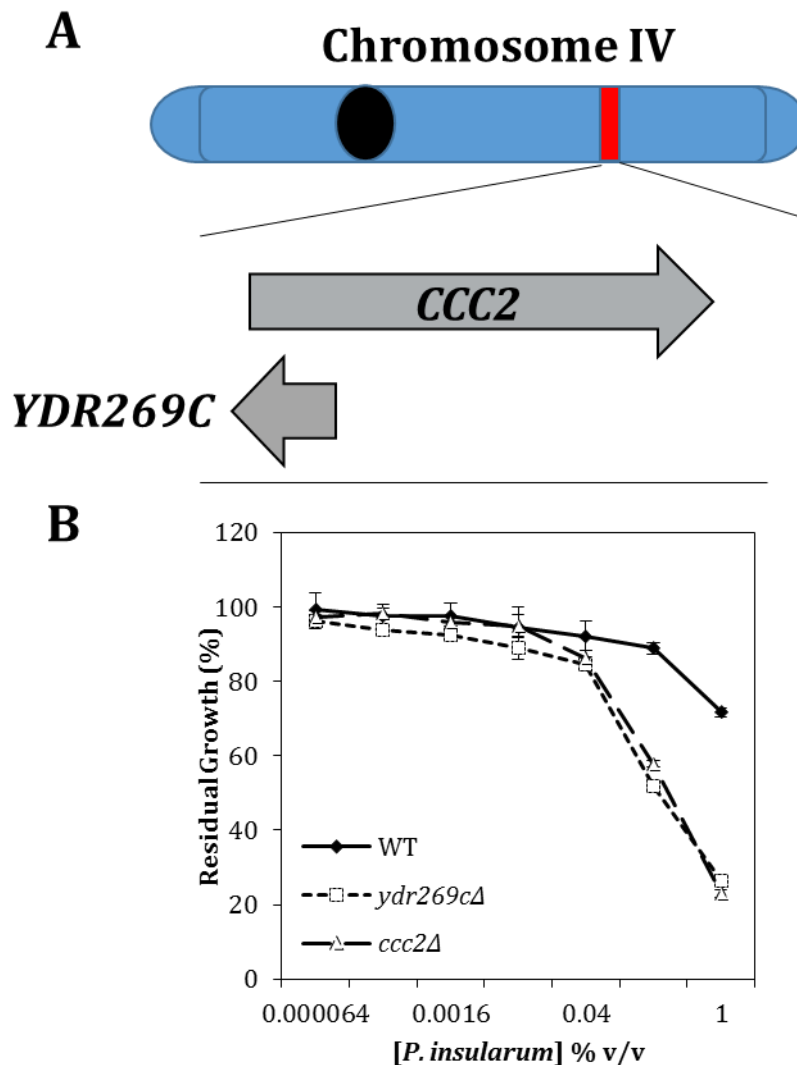


**Figure 3.3: *YDR269C* and *CCC2*.** **A.** The relationship between *YDR269C* and *CCC2*, and how the two ORFs overlap. It is illustrated here that the deletion of *YDR269C* leads to the deletion of the starting sequence of *CCC2*. **B:** The residual growths of WT (solid black line), compared to the residual growths of *ccc2Δ* and *ydr269cΔ* (dashed black lines). WT and deletion strains were grown in the presence of increasing concentrations of the aqueous extract of *P. insularum*, at a concentration range of  $6.4 \times 10^{-5}$  to 1% v/v with five-fold dilutions.

*CCC2* encodes a copper transporter at the Golgi apparatus that is not under the control of the copper-sensing transcription factor Mac1p but is regulated by the iron-sensing transcription factor Aft1p. Indeed, *CCC2* is primarily involved in iron transport into the cell (Yamaguchi-Iwai *et al.*,

1996). Iron transport in yeast occurs via three pathways: high-affinity iron transport, low-affinity iron transport, and an iron siderophore transport system (reviewed in Eide, 1998; van Ho *et al.*, 2002). The high-affinity iron transport system involves the Fet3p-Ftr1p complex at the plasma membrane (Askwith *et al.*, 1994; de Silva *et al.*, 1995; Eide *et al.*, 1994; Stearman *et al.*, 1996). It is at this branch of iron transport that Ccc2p is required as it functions to pump copper into the Golgi apparatus for its subsequent incorporation into Fet3p for its oxidase activity (Gaxioliola *et al.*, 1998; Lin *et al.*, 1997; Pufahl *et al.*, 1997; Yuan *et al.*, 1997). At the plasma membrane, Fet3p oxidase activity converts Fe<sup>2+</sup> to Fe<sup>3+</sup>, which is successively transported into the cell by Ftr1p; this is specific as Ftr1p only transports Fe<sup>3+</sup> from Fet3p (Askwith *et al.*, 1994; de Silva *et al.*, 1995; Stearman *et al.*, 1996). The low-affinity iron transport system is composed solely of Fet4p, a non-specific metal transporter that pumps iron, zinc and copper into the cell (Dix *et al.*, 1994; Dix *et al.*, 1997; Hassett *et al.*, 2000; Portnoy *et al.*, 2001; Waters & Eide, 2002). The iron siderophore transport system is composed of cell wall transporters (Fit1p, Fit2p, Fit3p and Fit4p) that scavenge iron siderophores, which are thenceforth taken into the cell via iron siderophore transporter vesicles (Arn1p, Arn2p, Arn3p and Arn4p) (Heymann *et al.*, 2000; Philpott *et al.*, 2002; Protchenko *et al.*, 2001; Yuan *et al.*, 2000). The involvement of Ccc2p in iron transport necessitated an investigation of the iron transport systems and how it is affected by the aqueous *P. insularum* extract.

### 3.3.4 Gene deletions of the iron transport systems are hypersensitive to the aqueous *P. insularum* extract

To determine if the high-affinity iron transport system was sensitive to the aqueous extract of *P. insularum*, growth profiles of *fet3Δ* and *ftr1Δ* were compared to WT in the presence of the extract. The growth of *fet3Δ* and *ftr1Δ* was reduced at concentrations greater than 0.05% v/v compared to WT with residual growth values between 10%-80% (20%-90% growth inhibition) (Fig 3.4A). To determine if the low-affinity iron transport system was sensitive to the aqueous extract of *P. insularum*, the growth profile of *fet4Δ* was compared to WT in the presence of the extract. The

growth profile of *fet4Δ* also exhibited a prominent growth defect compared to WT at concentrations greater than 0.05% v/v with residual growth values between 80-10% (20%-90% growth inhibition). To determine if the iron siderophore transport system was sensitive to the aqueous extract of *P. insularum*, the growth profiles of *arn1Δ*, *arn2Δ*, *arn3Δ* and *arn4Δ* as well as *fit1Δ*, *fit2Δ*, *fit3Δ* and *fit4Δ* were compared to WT in the presence of the extract. All six representative gene deletions of the iron siderophore transport system were also all shown to be hypersensitive to the aqueous extract of *P. insularum* in comparison to WT at concentrations greater than 0.05% v/v with residual growth values between 80-10% (20%-90% growth inhibition). Although all gene deletions of the iron transport systems showed varying degrees of sensitivity to the aqueous extract of *P. insularum*, all exhibited pronounced growth defects compared to WT, suggesting each of these genes are required to buffer the effects of the extract.

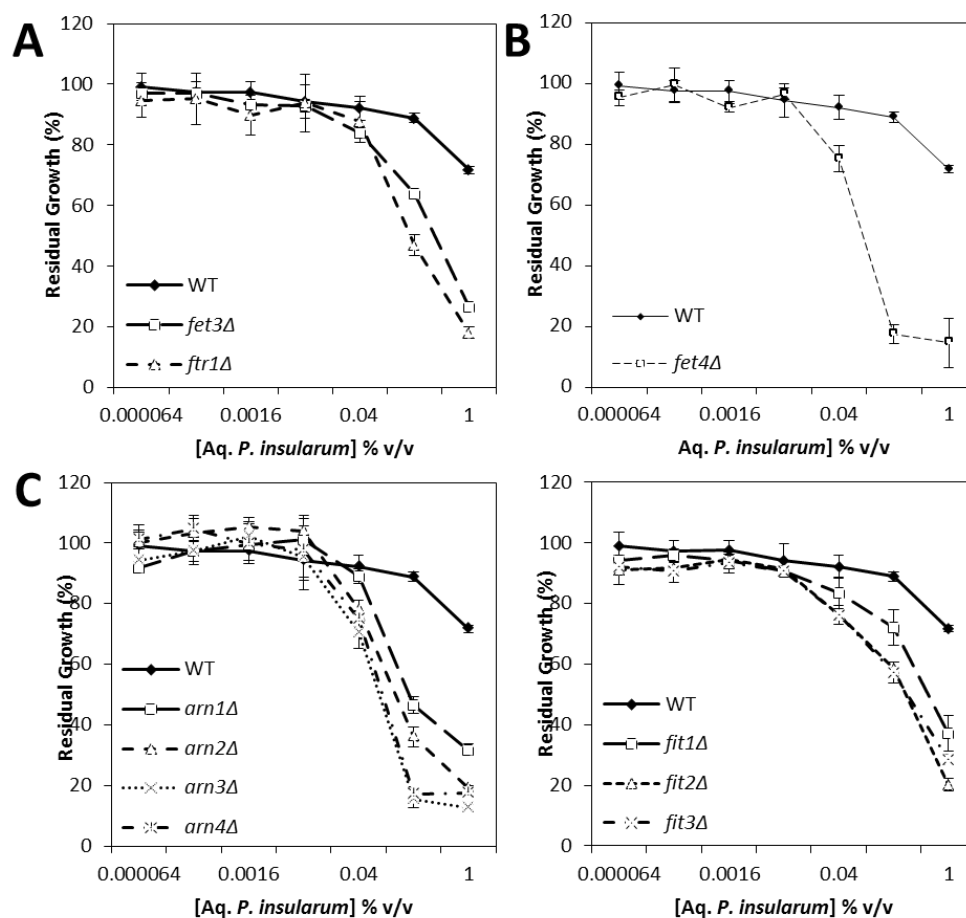


**Figure 3.4: Growth profiles of gene deletions from the iron transport systems against the aqueous extract of *P. insularum*.** Liquid based assays were carried out using the aqueous extract of *P. insularum* over increasing concentrations from  $6.4 \times 10^{-5}$  to 1% v/v with five-fold dilutions. Absorbance readings at 590 nm after 15 h growth at 30°C compared to their control treated counterparts were used to calculate residual growths. **A:** Residual growth comparison of WT to gene deletions of the high affinity iron transport system, *fet3Δ* and *ftr1Δ*. **B:** Residual growth comparison of WT to gene deletions of the low affinity iron transport system *fet4Δ*. **C:** Residual growth comparison of WT to gene deletions of the iron siderophore transport system *arn1-4Δ* and *fit1-3Δ*.

---

### 3.3.5 Gene deletions of the iron transport systems are hypersensitive to the methanolic *P. insularum* extract

On the principle that the bioactivity of crude extracts are often accounted for by a single bioactive compound or a single class of bioactive compounds such as peloruside A and B which are antitumor compounds that promote microtubule polymerisation and isolated from *Mycale hentscheli* (Singh *et al.*, 2010), we proposed that the methanolic extract, which was shown to be bioactive in Chapter 2 (Figs 2.6 & 2.7), may follow a similar mechanism as that of the *P. insularum* aqueous extract. To determine if this was the case, the growth profiles of gene deletion strains involved in the high affinity transport system including the initially detected deletions of *YDR269C* and *CCC2* (*ydr269cΔ*, *ccc2Δ*, *fet3Δ* and *ftr1Δ*), the low affinity iron transport system (*fet4Δ*) and the iron siderophore transport systems (*arn1Δ*, *arn2Δ*, *arn3Δ*, *arn4Δ* and *fit1Δ*, *fit2Δ* and *fit3Δ*) were monitored over a range of concentration of the methanolic extract ( $6.4 \times 10^{-5}$  to 1% v/v) relative to a WT control. Similar to their growth profiles in the presence of the aqueous extract of *P. insularum*, the gene deletions of the three iron transport systems all exhibited hypersensitivity to the methanolic extract indicated by their more pronounced growth defect compared to WT (Fig 3.5). Gene deletions of the high affinity iron transport system and those from the iron siderophore transport systems exhibited residual growth values of 80%-20% (20%-80% growth inhibition) at concentrations greater than 0.005% v/v compared to WT residual growth. The gene deletion of the low-affinity iron transport system (*fet4Δ*) showed residual growth ranging from 80%-20% (20%-80%

growth inhibition) at concentrations greater than 0.0005% v/v compared to WT. These results suggest that both the aqueous and methanolic extracts of *P. insularum* mediate their bioactivity via a similar mechanism involving iron transport. Although it was observed that all iron transporters tested were hypersensitive to the extracts of *P. insularum* compared to WT, it was unlikely that this was a general metal transporter phenotype, as gene deletions of zinc transporters did not exhibit hypersensitivity (data not shown).

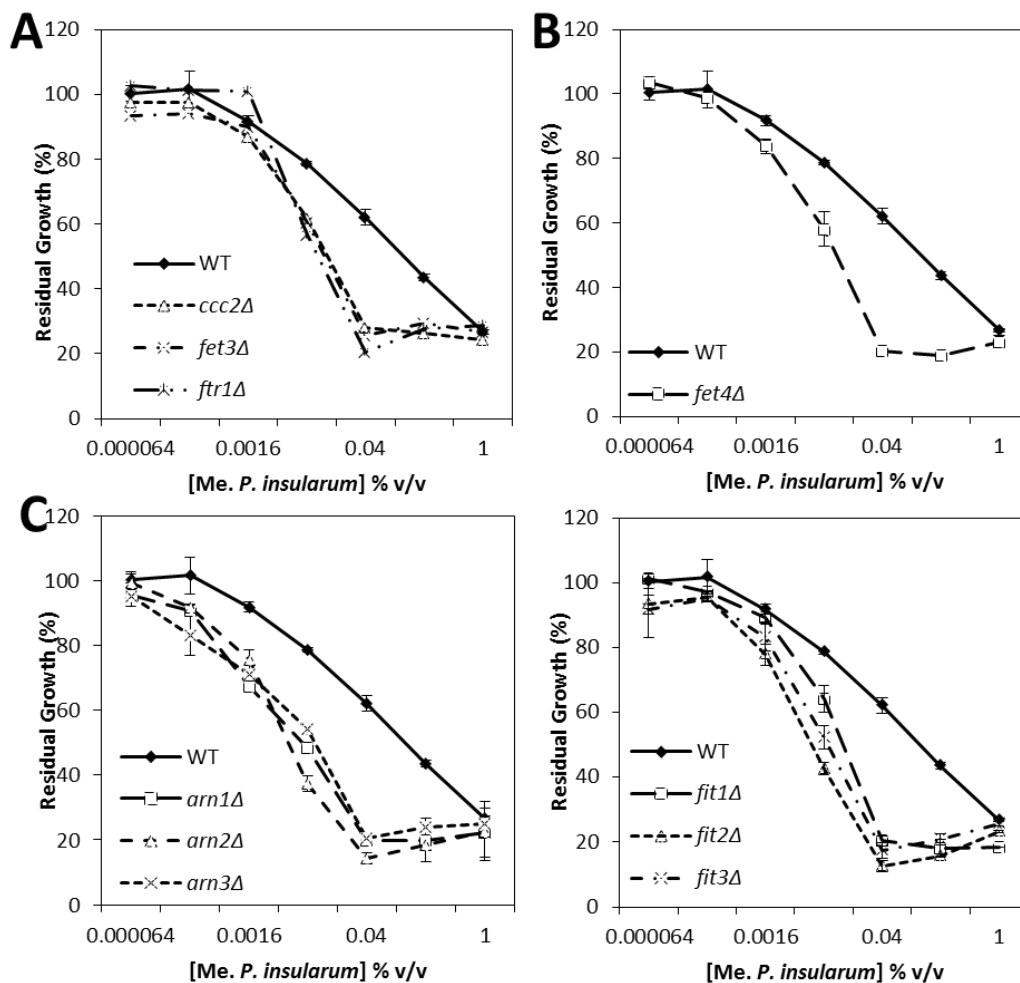


**Figure 3.5: Growth profiles of gene deletions from the iron transport systems against the methanolic extract of *P. insularum*.** Liquid-based growth assays were carried out using the methanolic extract of *P. insularum* over increasing concentrations from of  $6.4 \times 10^{-5}$  to 1% v/v with five-fold dilutions. Absorbance readings at 590 nm after 15 h growth at 30°C compared to their control treated counterparts were used to calculate residual growths **A:** Residual growth comparison of WT to gene deletions of the high affinity iron transport system, *ydr269cΔ*, *ccc2Δ*, *fet3Δ* and *ftr1Δ*. **B:** Residual growth comparison of WT to gene deletion of the low affinity iron transporter *fet4Δ*. **C:** Residual growth comparison of WT to gene deletions of the iron siderophore transport system *arn1-4Δ* and *fit1-3Δ*.

### 3.3.6 Iron supplementation rescues the growth defect induced by aqueous *P. insularum* extract

The hypersensitivity of gene deletions of the iron transport systems to the aqueous and methanolic extracts of *P. insularum* suggests that the iron transport genes are required to buffer the effects of the *P. insularum* extracts. Because the genes function to provide iron to the cell and their deletions led to hypersensitivity, we hypothesized the addition of iron will reduce the growth defect induced by extract treatment. To test this hypothesis, three sets of liquid-based assays using BY4741 WT were carried out with increasing concentrations of either the aqueous or methanolic extract of *P. insularum*, with supplementation of either 100  $\mu\text{M}$   $\text{FeCl}_3$ , 100  $\mu\text{M}$   $\text{FeSO}_4$ , or no supplement at all. Supplementation with  $\text{FeCl}_3$  and  $\text{FeSO}_4$  ensured that both forms of iron (ferric and ferrous respectively) were investigated, each at the previously established 100  $\mu\text{M}$  iron concentration for optimal yeast growth (Shakoury-Elizeh *et al.*, 2010). The BY4741 WT used here showed 70%-10% residual growth (30%-90% growth inhibition) at aqueous extract concentrations greater than 0.005% v/v (Fig 3.6A). On the other hand, BY4741 WT grown in the presence of the methanolic *P. insularum* extract exhibited residual growth values ranging from 70%-10% (30%-90% growth inhibition) at concentrations greater than 0.0001% v/v (Fig 3.6B). Supplementation with 100  $\mu\text{M}$   $\text{FeCl}_3$  resulted in a shift of growth of WT in media containing the aqueous extract, indicating  $\text{FeCl}_3$  reduced the aqueous extract treatment-induced growth defect by 80% at 0.2% v/v, and by 50% at 1% v/v. Similarly, the growth profile of WT cells grown in the aqueous extract of *P. insularum* supplemented with 100  $\mu\text{M}$  of  $\text{FeSO}_4$  also exhibited a shift, however, it did not match the shift observed from  $\text{FeCl}_3$ . For instance, 100  $\mu\text{M}$   $\text{FeCl}_3$  was able to rescue WT growth from 20% residual growth to 100% residual growth at 0.2% v/v aqueous extract treatment, while  $\text{FeSO}_4$  was only able to rescue to approximately 70% residual growth (Fig 3.6A, dashed lines). Likewise,  $\text{FeCl}_3$  and  $\text{FeSO}_4$  supplementation variable rescued the methanolic extract treatment-induced growth defect. Specifically, 100  $\mu\text{M}$   $\text{FeCl}_3$  fully rescued growth of WT (from 80% growth inhibition to 0% growth

inhibition) from treatment with 0.008% v/v of methanolic extract, while 100  $\mu\text{M}$   $\text{FeSO}_4$  supplementation partially rescued growth of WT (80% growth inhibition to 20% growth inhibition) (Fig 3.6B). These results suggest that supplementation of extract treatment with exogenous iron reduced the effect of the extract and improved yeast growth. Further, these findings showed that ferric iron ( $\text{FeCl}_3$ ) rescued yeast growth slightly better than ferrous iron ( $\text{FeSO}_4$ ).

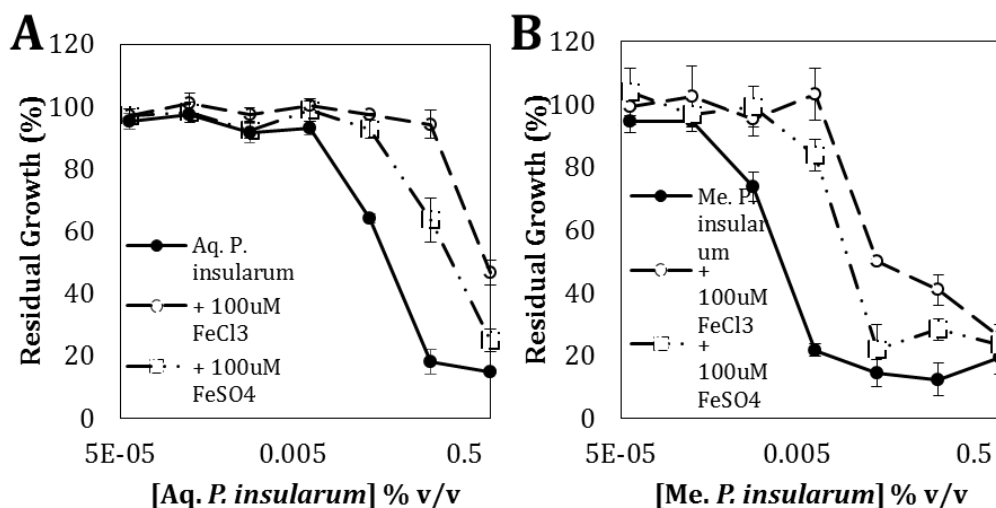


**Figure 3.6: Iron supplementation against aqueous and methanolic extracts of *P. insularum*.** Liquid-based growth assays of BY4741 WT were prepared as previously described with increasing concentrations of extract without iron supplementation, compared to metal supplemented extract treatments with 100  $\mu\text{M}$  of the relevant metal salt solution. **A:** Growth profiles of BY4741 WT in the presence of aqueous *P. insularum* extract (solid line) without iron supplementation, with 100  $\mu\text{M}$   $\text{FeCl}_3$  (dashed line with circle) or with 100  $\mu\text{M}$   $\text{FeSO}_4$  (dashed line with square) **B:** Growth profiles of BY4741 WT in the presence of methanol *P. insularum* extract without iron supplementation (solid line), with 100  $\mu\text{M}$   $\text{FeCl}_3$  (dashed line with circle) or with 100  $\mu\text{M}$   $\text{FeSO}_4$  (dashed line with square).

### 3.3.7 Iron rescue is specific to *P. insularum* extract treatment and is not a cytoprotective effect of iron supplementation

Iron has been shown to contribute to drug susceptibility and resistance (Prasad *et al.*, 2006) suggesting that iron may exhibit a cytoprotective effect against a drug treatment independent of the drug's MOA. To investigate if the cytoprotective phenomenon of iron in suppressing sensitivity of WT cells to *P. insularum* extracts (Fig 3.6) is conserved for other drugs, BY4741 WT

yeast cells were grown in the presence of two well characterized drugs, cycloheximide (which disrupts translation, Schneider-Poestch *et al.*, 2010) and atorvastatin (which targets ergosterol synthesis, Callegari *et al.*, 2010), with and without exogenous iron supplementation (100  $\mu\text{M}$   $\text{FeCl}_3$ ). Whilst BY4741 demonstrated sensitivity to atorvastatin at increasing concentrations, no difference was observed between BY4741 growth in drug alone compared to the drug treatment with iron supplementation. For example, aqueous *P. insularum* extract treatment of WT with 0.2% v/v caused an 80% growth inhibition and supplementation with 100  $\mu\text{M}$   $\text{FeCl}_3$  diminished the extract-induced growth inhibition, however, iron supplementation of atorvastatin treatment (Fig 3.7A) or cycloheximide treatment (Fig 3.7B) failed to rescue even a growth inhibition of 20%. These findings demonstrate that iron supplementation did not rescue the growth defects induced by atorvastatin or cycloheximide. Subsequently, these results indicate that the rescue observed from iron supplementation in *P. insularum* extract treatments was unlikely a consequence of iron playing a general cytoprotective role, but rather a specific function relating to the MOA of the *P. insularum* extracts.

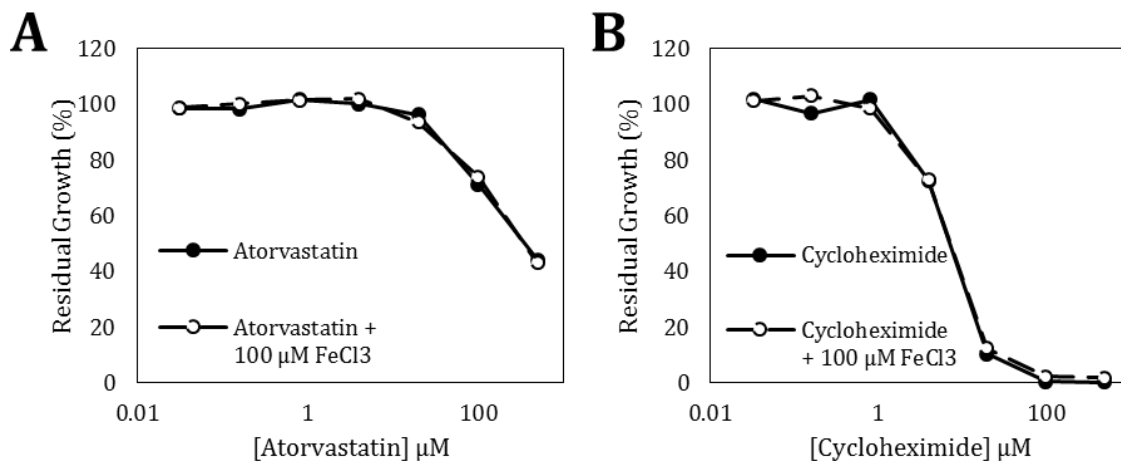


**Figure 3.7: Iron supplementation of atorvastatin and cycloheximide drug treatment of BY4741 WT yeast.** **A:** BY4741 WT treatment with atorvastatin. **B:** BY4741 WT treatment with cycloheximide. BY4741 cells were inoculated into SC media at  $5 \times 10^5$  cells/mL and treated at increasing concentrations of drug, or drug with 100  $\mu\text{M}$   $\text{FeCl}_3$  supplementation. Residual growths were calculated by comparison to the control. Solid lines indicate treatment with drug alone, dashed lines correspond to treatment with drug and iron supplementation.

### 3.3.8 Copper supplementation partially rescues the growth defect induced by *P. insularum* extracts in a Fet3p-dependent manner

Copper is required in the high affinity iron transport pathway for the oxidase activity of Fet3p (Askwith *et al.*, 1994). We thus hypothesized that the addition of copper to *P. insularum* extract treatments may also rescue the extract-induced growth defect. To test this hypothesis, both WT and *fet3Δ* yeast strains were grown in the presence of both aqueous and methanolic extracts of *P. insularum*, with or without the presence of copper supplementation (100μM CuCl<sub>2</sub>). Supplementation with CuCl<sub>2</sub> modestly reduced the growth defect resulting from aqueous extract treatment (Fig 3.8A). For instance, at 0.2% v/v extract treatment, copper supplementation was only able to rescue growth from 20% to 40% residual growth while FeCl<sub>3</sub> was able to completely rescue at this concentration from 20% to 100% residual growth. A stronger rescue was observed from copper supplementation of WT treatment with the methanolic extract of *P. insularum* (Fig 3.8B). Similar to FeCl<sub>3</sub> rescue, CuCl<sub>2</sub> supplementation was able to rescue the growth defect induced by 0.008% v/v treatment with methanolic extract from 20% residual growth to 80%. Contrastingly, CuCl<sub>2</sub> supplementation failed to reduce the effect of the aqueous extract on *fet3Δ* growth, while FeCl<sub>3</sub> supplementation rescued the *fet3Δ* growth defect resulting from treatment with the aqueous extract of *P. insularum* (Fig 3.8C). A similar result was obtained from *fet3Δ* treated with the methanolic extract of *P. insularum*, whereby supplementation with CuCl<sub>2</sub> did not clearly exhibit a rescue phenotype, while supplementation with FeCl<sub>3</sub> reduced the growth defect induced by the methanolic extract (Fig 3.8D). These findings suggest that the moderate rescue observed from copper supplementation in BY4741 WT but not *fet3Δ* was mediated through the copper-dependent oxidase activity of the high-affinity iron transporter Fet3p, in the case of the aqueous extract of *P. insularum*. Further, the greater rescue observed from CuCl<sub>2</sub> supplementation of the methanolic extract compared to the aqueous extract suggests the methanolic extract component responsible for the iron transport-related phenotype may also affect copper transport in yeast cells, given that the deletion of *FET3* did not completely remove the copper rescue.

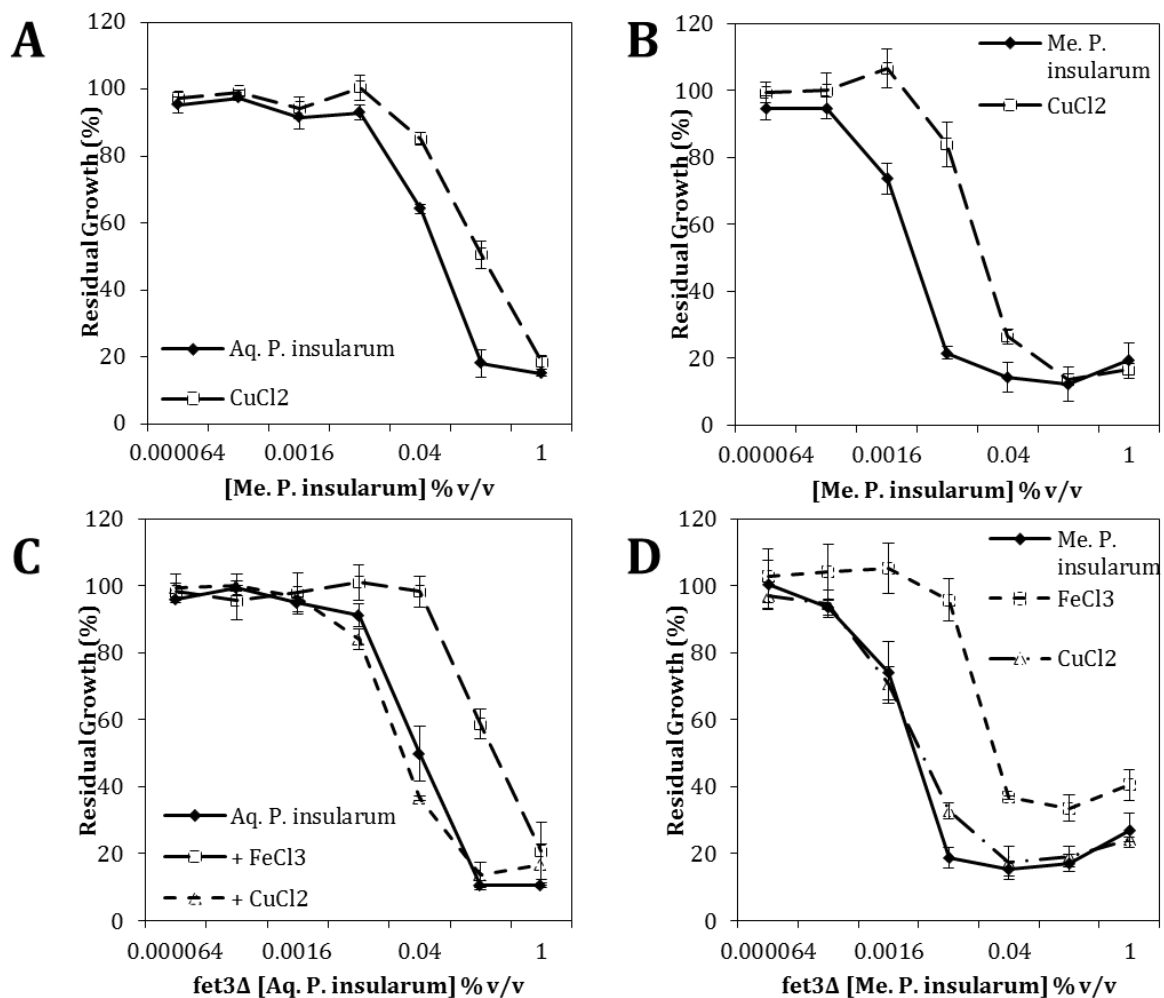


**Figure 3.8: Copper supplementation rescue profiles of WT and *fet3Δ* in the presence of aqueous and methanolic extracts of *P. insularum*.** Liquid-based growth assays of BY4741 WT cells in increasing concentrations of extract, compared to metal supplemented extract treatments with 100  $\mu$ M of the relevant metal salt solution. **A:** Comparison of WT growth profiles in the presence of aqueous *P. insularum* extract (solid black line), and exogenous copper supplementation (dashed line). **B:** Comparison of WT growth profiles in the presence of methanolic *P. insularum* extract (solid black line) and WT growth with exogenous copper supplementation (dashed line). **C:** Growth profiles of *fet3Δ* deletion mutant grown in the presence of aqueous *P. insularum* extract (solid black line), with exogenous FeCl<sub>3</sub> supplementation (dashed line with square markers) or copper supplementation (dashed lines with triangle markers). **D:** Growth profiles of *fet3Δ* deletion mutant grown in the presence of methanolic *P. insularum* extract (solid black line), with exogenous FeCl<sub>3</sub> supplementation (dashed line with square markers), or copper supplementation (dashed lines with triangle markers).

### 3.3.9 Supplementation with other metals does not rescue the growth defect induced by extracts of *P. insularum*

Given that iron and copper supplementation rescued WT cells from the activity of *P. insularum* extracts, it was obligatory to investigate the effects of other metals on the activity of *P. insularum* extracts. This was achieved through growth assays of WT in the presence of either the aqueous or methanolic extracts of *P. insularum* supplemented with 100  $\mu\text{M}$   $\text{CaCl}_2$ ,  $\text{MgCl}_2$ ,  $\text{MnCl}_2$  or  $\text{ZnCl}_2$ . Supplementation with  $\text{CaCl}_2$ ,  $\text{MgCl}_2$ ,  $\text{MnCl}_2$  or  $\text{ZnCl}_2$  did not exhibit any significant effects on aqueous extract activity, as the growth profiles of BY4741 treated with aqueous extract alone followed the same growth pattern as those with metal supplementation (Fig 3.9A). The same lack of difference was observed from BY4741 grown in the methanolic extract of *P. insularum*, suggesting that calcium, magnesium, manganese and zinc do not exert any effects on the activity of *P. insularum* extracts, unlike iron and copper.

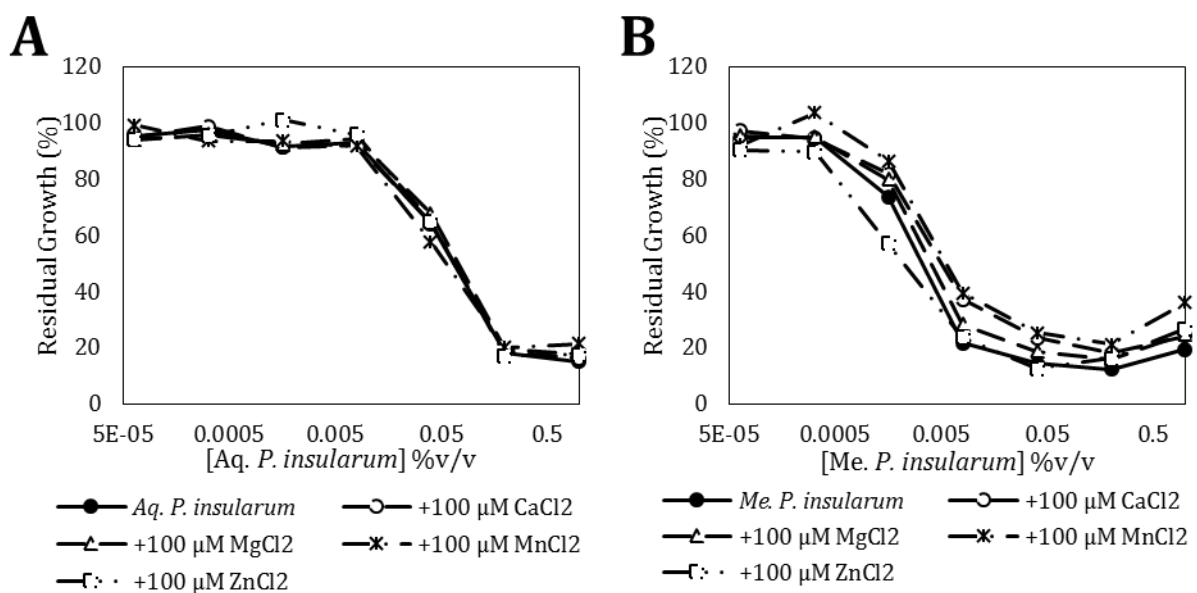


**Figure 3.9: Growth profiles of WT against aqueous and methanolic extracts of *P. insularum* with metal supplementation.** Liquid-based growth assays of BY4741 WT cells in increasing concentrations of extract, compared to metal supplemented extract treatments with 100  $\mu\text{M}$  of the relevant metal salt solution. A: Metal supplementation of WT grown in the aqueous extract of *P. insularum*. B: Metal supplementation of WT grown in the methanol extract of *P. insularum*. Extract treatment (solid line) and metal supplementation (dashed lines) of  $\text{CaCl}_2$  (circle marker),  $\text{MgCl}_2$  (triangle marker),  $\text{MnCl}_2$  (asterisk marker) and  $\text{ZnCl}_2$  (square marker).

### 3.3.10 Intracellular iron is decreased in the presence of *P. insularum* extracts

Iron supplementation rescued the growth defect induced by the extract of *P. insularum* (Fig 3.6), implying that the treatment of cells with the extracts reduced intracellular iron. To determine if this was the case, inductively coupled plasma mass spectrometry (ICP-MS) was used to quantify intracellular iron in WT cells treated with the extracts of *P. insularum*. For comparison, cells were also grown in iron-free media, or treated with the iron chelator bathophenanthroline disulfonic acid (BPS). Treatment of WT BY4741 cells led to an approximate 50% reduction in growth of cells treated with the aqueous *P. insularum* extract, the methanolic *P. insularum* extract or the iron chelator compared to control cells (Fig 3.10). Additionally, cells grown in iron-free media showed an approximate 80% reduction in total intracellular iron compared to the control cells. These results indicate that the *P. insularum* extracts chelate iron as effectively as an established iron chelator.

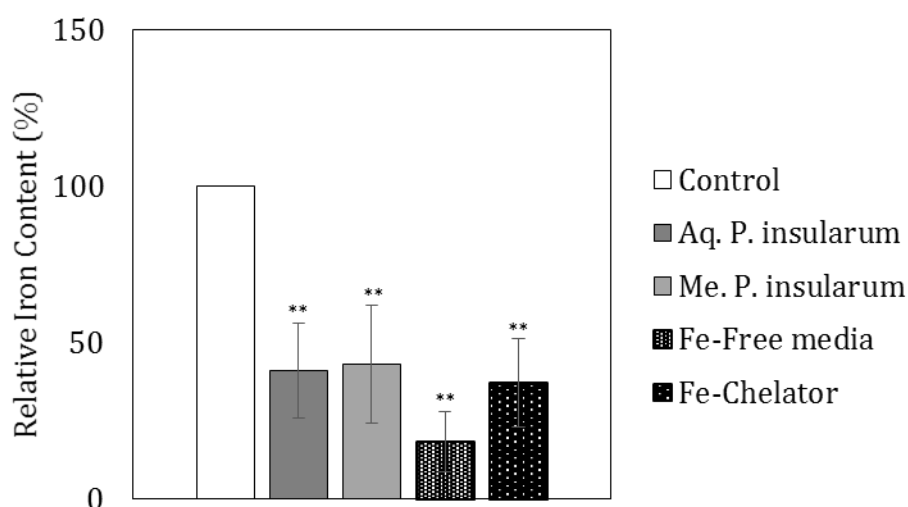


**Figure 3.10: Comparison of relative intracellular iron between control and treated WT.** BY4741 cells were grown in control media (Control), as well as in treatment media containing 0.05% v/v of aqueous extract (Aq. *P. insularum*) and 0.005% v/v of methanol extract (Me. *P. insularum*), as well as iron-free media (Fe-free media) and media containing 0.1  $\mu$ M bathophenanthroline disulfonic acid (Fe-Chelator). Quantified iron is reported as relative total intracellular iron, compared to control BY4741, obtained from the average and standard deviation of two biological replicates (\*\*: p-value < 0.01).

### 3.3.11 *P. insularum* extracts up-regulate the expression of iron transporters

To determine if the expression of iron transporters is affected by extract treatment, the fluorescence of GFP-tagged iron transporters was quantified using fluorescent microscopy. A special feature of the GFP strains utilized here was the incorporation of an mCherry nuclear localising signal, a high intensity red fluorescence tag, and a RedStar2 cytoplasmic signal, a low intensity red fluorescence tag (Bircham *et al.*, 2011), two signals that identified the nucleus and the cell periphery, allowing the quantification of GFP signal per cell per treatment relative to control. In these experiments, the green fluorescence intensity was an indicator of the protein expression of the iron transporters which the GFP tag was attached to. Contrary to the reduced intracellular iron content of extract-treated cells (Fig 3.10), proteins representative of the three iron transporter systems were significantly increased compared to control cells, when the green fluorescence intensity was assessed visually (Fig 3.11), and quantified (Fig 3.12).

Fet3p and Ftr1p were chosen to represent the high-affinity transport system. The fluorescence of GFP tagged onto both Fet3p and Ftr1p increased when the strains were treated with the extracts of *P. insularum*, the iron-chelator and when grown in iron-free media. Indeed, when quantified, the aqueous extract treatment induced a significant 50% increase in Fet3p-GFP fluorescence, while methanolic extract treatment caused a significant 30% increase compared to the control. Fet3p-GFP cells grown in iron-free media resulted in a significant 100% increase in GFP intensity, while the iron chelator treatment induced a significant 70% increase. The aqueous extract treatment of Ftr1p-GFP showed a modest but significant 30% increases in GFP fluorescence. Both iron-free media and iron chelator treatments resulted in 50% and 40% increases in GFP fluorescence, respectively.

Fet4p represented the low-affinity iron transport system. The fluorescence of GFP tagged onto Fet4p increased when the strain was treated with the extracts of *P. insularum*, the iron-chelator and when grown in iron-free media. This was statistically quantified to a 30% increase when

treated with *P. insularum* extracts. When grown in iron-free media, a significant 80% increase in GFP fluorescence was seen, while growth in iron chelator treatment induced a significant 60% increase.

Arn1p and Arn3p were chosen to represent the iron siderophore transport system. The fluorescence of GFP tagged onto both Arn1p and Arn3p increased when the strains were treated with the extracts of *P. insularum*, the iron-chelator and when grown in iron-free media. When quantified, Arn1p-GFP showed a significant 30% increase in fluorescence intensity when treated with the aqueous extract of *P. insularum*. However, the 10% increase observed from the methanolic extract treatment was not statistically significant. Arn1p-GFP exhibited an extraordinary and significant 180% increase in fluorescence when grown in iron-free media, while a significant 50% increase was observed when grown in the presence of the iron chelator. Arn3p-GFP showed modest yet not significant 12-15% increases in GFP intensity from aqueous and methanolic extract treatments. Significant and dramatic increases of 80% and 50% in Arn1p-GFP fluorescence were observed in cells grown in iron-free media and the iron chelator, respectively.

Intriguingly, the increased expression of proteins representative of the three iron transport systems in extract-treated cells was significantly reduced to control levels with exogenous iron supplementation. These findings thus reveal that yeast cells, specifically iron transport proteins, respond to *P. insularum* extract in a comparable manner to responding to iron-free media or the presence of an iron chelator. The cells increase expression of the iron transporters as a cellular response to low iron, further supporting our hypothesis that there is low available iron in the cell as a consequence of *P. insularum* extract treatment.

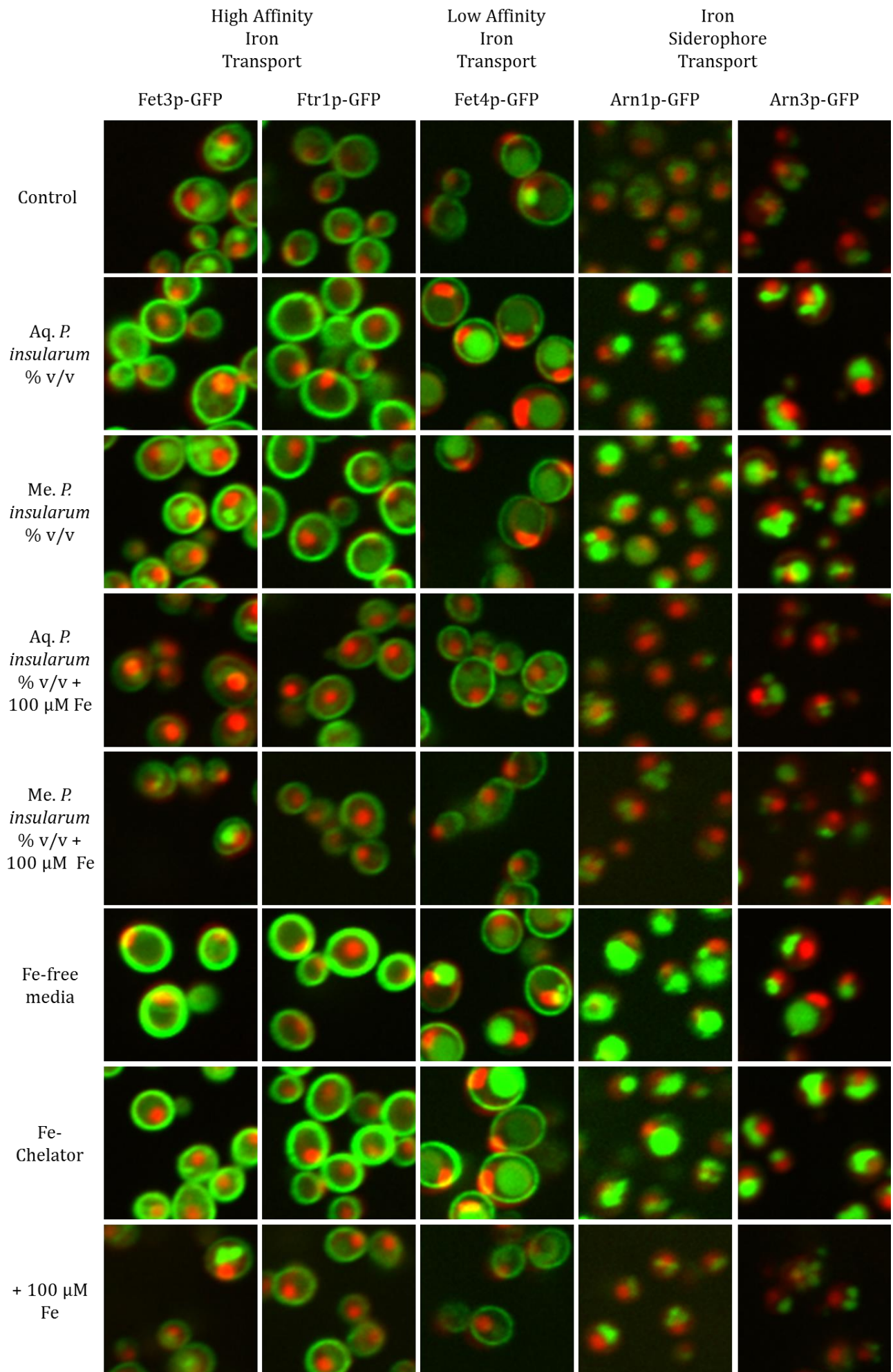


**Figure 3.11: Expression levels of iron transporters under extract treatment, monitored via GFP tagged proteins.** Expression levels of iron transporters from the high affinity transport system (Fet3p and Ftr1p), low affinity iron transport system (Fet4p), and iron siderophore transport system (Arn1p and Arn3p) were monitored through their GFP-tagged counterparts, and grown under 8 treatment conditions, including control, aqueous *P. insularum* extract (0.05% v/v), methanol *P. insularum* extract (0.005% v/v), aqueous extract treatment supplemented with 100µM FeCl<sub>3</sub>, methanol extract treatment supplemented with 100µM FeCl<sub>3</sub>, cells grown in iron-free media, iron chelator control (0.1µM), and a 100µM FeCl<sub>3</sub> supplementation. The GFP-tagged strains were grown overnight, then inoculated into the relevant treatment media at 5 x 10<sup>5</sup> cells/mL, and incubated at 30°C whilst shaking overnight for 15 h. Cell were diluted into fresh treatment media and 50 µL were visualized using the Opera EvoTec spinning disc confocal microscope, where GFP and mCherry/RedStar2 were excitation was achieved at 488 and 561 nm, and detection was through 520/35 and 600/40 filters respectively.

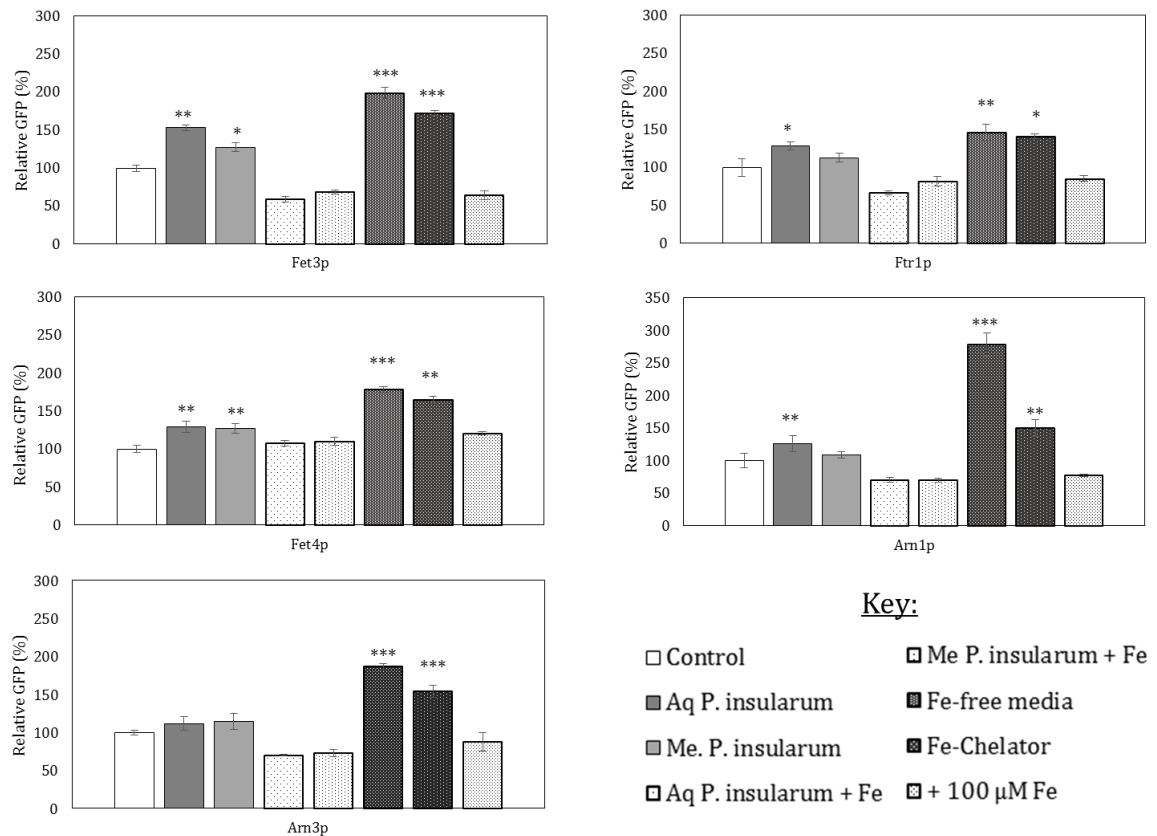


**Figure 3.12: Quantification of GFP intensity of iron transporters upon *P. insularum* treatment.**

Images obtained from confocal microscopy of iron transporters tagged with GFP were exposed to Acapella software to quantify GFP intensity, utilizing the mCherry and RedStar2 nuclear localising and the cytoplasmic signals respectively. Identification of the cellular periphery allowed for the quantification of the GFP signal, and the median GFP intensity was determined. Average of 3 replicates per treatment was calculated, and compared to control GFP intensity to determine relative GFP (%) as illustrated. The 8 treatments tested were control, aqueous extract (0.05% v/v), methanol extract (0.005% v/v), aqueous extract treatment supplemented with 100  $\mu$ M FeCl<sub>3</sub>, methanol extract treatment supplemented with 100  $\mu$ M FeCl<sub>3</sub>, iron free media, iron chelator control (0.1  $\mu$ M), and 100  $\mu$ M FeCl<sub>3</sub> supplementation control. Statistical analyses using a one-tailed Student's t-test was carried out to identify if the increase in GFP signal from treatment was statistically significant compared to control (\* = p-value < 0.05, \*\* = p-value < 0.01, \*\*\* = p-value < 0.001).

---

### 3.3.12 *P. insularum* extracts induce a respiratory deficient phenotype

The growth pattern of yeast strains under specific media conditions often provides information regarding the effect of a growth condition on the strain; for instance, an extended lag phase and a lower stationary phase often indicates a defect in the respiratory system of yeast (Xu *et al.*, 2012). Given that *P. insularum* extracts reduce intracellular iron in the cell (Fig 3.10), and the requirement of iron in heme and iron sulfur cluster (ISC) cofactors needed for respiration (Philpott, 2012), we hypothesized that the extracts of *P. insularum* would induce a growth profile indicative of respiratory deficiency. To test this hypothesis, BY4741 WT yeast was grown in the presence and absence of the aqueous (0.05% v/v) and methanolic (0.005% v/v) extracts of *P. insularum*. The growth pattern of BY4741 grown in the presence of *P. insularum* extracts compared to BY4741 grown under control conditions followed the predicted pattern, whereby extract treated cells exhibited a modestly extended lag phase, with a discernible reduced stationary phase. These findings support the hypothesis that the extracts of *P. insularum* induce a respiratory deficient phenotype.

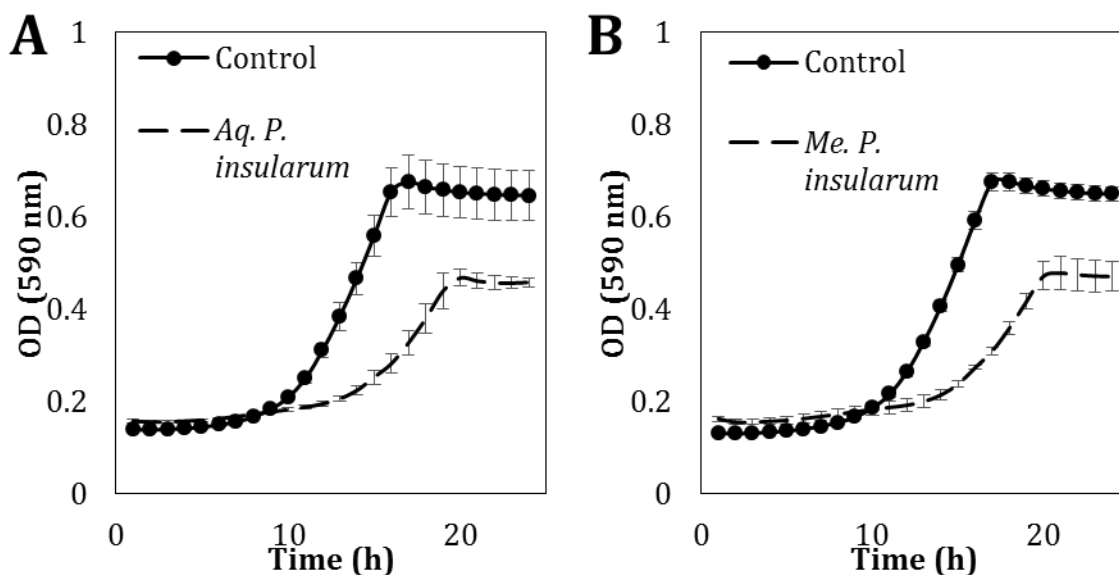


**Figure 3.13: Respiratory deficient phenotype of BY4741.** Cells grown to log phase were inoculated into the relevant media at  $5 \times 10^5$  cells/mL and grown at 100  $\mu$ L in 96-well plates, with absorbance readings every hour for 48 h at 30°C. **A:** Growth curve of BY4741 WT under control conditions compared to growth in the presence of the aqueous extract of *P. insularum* at 0.05% v/v (dashed line). **B:** Growth curve of BY4741 WT under control conditions (solid black line) and in the presence of the methanol extract of *P. insularum* at 0.005% v/v (dashed line).

### 3.3.13 *P. insularum* extracts reduce heme synthesis

The quantified low levels of iron in the cell (Fig 3.10), in conjunction with the respiratory deficient phenotype (Fig 3.13) in the presence of the extracts of *P. insularum* suggested that the treatment of cells with the extracts led to reduced synthesis of iron-requiring co-factors and a down-regulation of iron-requiring pathways. Given that iron is utilized in the cell as an essential transition metal in the activity of heme-dependent and iron-sulfur cluster (ISC) -dependent enzymes and protein complexes (Philpott, 2012) in cellular respiration, we quantified heme in cells that were grown in the presence and absence of *P. insularum* extracts. This was achieved by using the triton methanol method (Padney *et al.*, 1999) on cell lysates of cells harvested from several treatments, including control, aqueous extract treatment, methanolic extract treatment, iron-free media and iron chelator treatment. The quantified heme content of BY4741 WT cells showed marked differences between the control and the four treatments (Fig 3.14). Cells treated with aqueous and

methanolic *P. insularum* extract showed approximately 50% reduction in heme content compared to control cells. Likewise, cells grown in iron-free media or in the presence of the iron chelator showed approximately 30% reduction in heme content compared to control cells. These findings suggest that the reduced levels of heme detected from the four treatments were a consequence of low bioavailable iron, although this is not reflection in status of iron-requiring proteins.

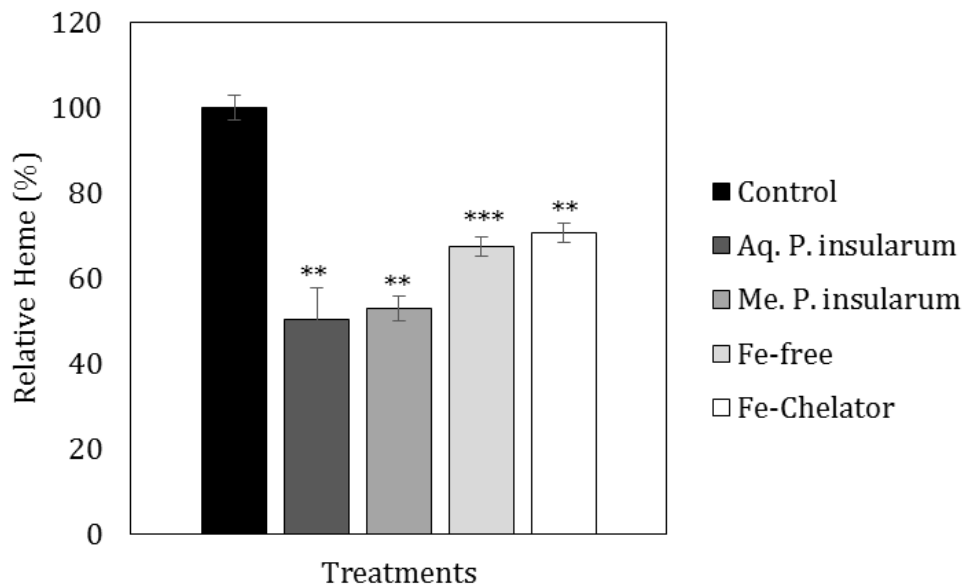


**Figure 3.14: Relative heme content of WT treated with *P. insularum* extracts.** BY4741 WT cells were grown in five (5) conditions, including control, aqueous *P. insularum* extract treatment, methanol *P. insularum* extract treatment, iron free media and BPS chelator treatment. Cells were harvested and protein prepared. The protein content was assayed for heme content using the triton methanol method. The standard curve was used to calculate total heme, and the protein content per sample was used to normalize heme content. Relative heme was calculated using the control heme content. Statistical analyses was carried out using Microsoft Excel paired two sample for means, one tailed t-test (\* = p-value < 0.05, \*\* = p-value < 0.01, \*\*\* = p-value < 0.001).

### 3.3.14 *P. insularum* extracts chelate iron

Our findings thus far have shown comparable results between the *P. insularum* extracts and the iron chelator BPS. For instance, both *P. insularum* extracts and iron chelator decreased total intracellular iron content (Fig 3.10). Further, treatment of cells with extracts as well as iron chelator caused an up-regulation of iron transporters (Fig 3.11 & 3.12), indicative of the induction of the low iron response in yeast. Moreover, we have shown that treatment with *P. insularum* extracts and iron

chelator led to reduced synthesis of heme (Fig 3.14) that was indicative of low bioavailable iron yeast. Therefore, we hypothesized that the bioactive component of the aqueous and methanolic extracts of *P. insularum* mediate its therapeutic effect via an iron chelation mechanism. To test this hypothesis, we employed the chrome azurol S (CAS) assay, a colorimetric assay that indicates whether a compound chelates iron (Alexander & Zuberer, 1991). The assay was carried out over a concentration range of the *P. insularum* aqueous extract (0.005%-10% v/v) and the *P. insularum* methanolic extract (0.0005%-1% v/v), as well as EDTA as an established iron chelator to give the required blue-to-yellow colour reaction. The BPS iron chelator used in previous experiments was not used since it produced a different colour reaction as it forms a red complex with iron. The CAS assay results against the aqueous and methanolic extracts of *P. insularum* show moderate blue-to-yellow colour change as soon as the extracts were added to the CAS solution (Fig 3.15 A), and this colour change intensified after 1 h incubation (Fig 3.15B). However, unlike EDTA that showed this positive blue-to-yellow colour change down to 0.0001  $\mu$ M EDTA, the aqueous extract of *P. insularum* was only able to induce a colour change down to 0.5% v/v, while the methanol extract of *P. insularum* was able to induce a colour change at concentrations as low as 0.1% v/v. These findings show that although the extracts of *P. insularum* chelate iron, their iron chelation activity was not as potent as that of EDTA. However, these findings are not directly comparable as the *P. insularum* extracts tested are crude extracts and may contain miniscule amounts of the bioactive component.

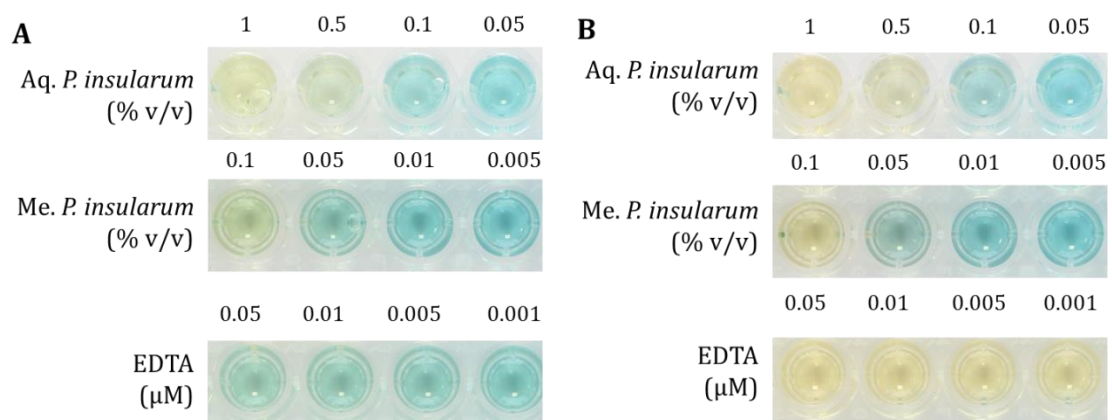


**Figure 3.15: CAS assay illustrating iron chelation activity of *P. insularum* extracts.** 100  $\mu\text{L}$  of CAS assay solution was aliquot in replicate into 96-well plates, to which 100  $\mu\text{L}$  of the relevant dilution of extract (% v/v) or EDTA ( $\mu\text{M}$ ) was added, and images were taken at 0 min and 1 h after leaving at RT. **A:** CAS assay at  $t_0$ , soon after extracts and EDTA were added to the CAS solution. **B:** CAS assay at 1 h after extracts and EDTA were added to the CAS solution. Color change from blue to yellow indicates a positive iron chelation activity.

---

### 3.3.15 *P. insularum* extracts exhibit an anti-inflammatory response in murine macrophages

Aside from its extensive use in ailments generally attributed to spirits and ghosts, the aqueous extract from *P. insularum* leaves is also used to treat skin infections, skin wounds and general body aches and swellings in Samoa (Whistler, 1996) indicative of the extracts playing a modulating role in inflammation. To test if *P. insularum* targets inflammation as it is currently prescribed in traditional Samoan medicine, the effects of varying concentrations of the aqueous and methanolic extracts of *P. insularum* on the cellular metabolic rate (MTT), the anti-inflammatory cytokine interleukin-10 (IL-10), the pro-inflammatory cytokine interleukin-12 (IL-12), tumour necrosis factor  $\alpha$  (TNF $\alpha$ ) and nitrous oxide (NO) levels were monitored in activated primary macrophages derived from mice (C57BL/6). Primary macrophages were also treated with varying concentrations of the iron chelator BPS to ascertain if the results obtained from each extract treatment were a consequence of its iron chelator activity. Additionally, varying concentrations of Risperidone, an anti-inflammatory control (O'Sullivan *et al.*, 2014) was included to determine if the *P. insularum* extracts exhibited the hallmark phenotypes of an anti-inflammatory compound particularly in increasing IL-10 and decreasing IL-12 levels.

All four concentrations of the aqueous *P. insularum* extract (0.5, 1, 2 and 3% v/v) and the two higher concentrations of the methanolic extract (0.05 and 0.1% v/v) increased levels of MTT by 50-75% compared to untreated macrophages (Fig 3.16A). In contrast, the two lower concentrations of the methanolic *P. insularum* extract (0.005 and 0.01% v/v), the three lower concentrations of iron chelator (0.01, 0.1 and 1  $\mu\text{M}$ ) and all four Risperidone concentrations (6.25, 12.5, 25 and 50  $\mu\text{M}$ ) did

not increase MTT levels, suggesting that these treatments did not alter metabolic activity of treated cells compared to the control. However, the highest tested concentration of iron chelator (10  $\mu$ M) showed reduced metabolic activity, which may indicate reduced viability. While it is ideal that MTT levels were not lower compared to control in extract treatments, the increased MTT levels suggest that a component of the crude extracts may function to increase the metabolic activity of macrophages. The increased metabolic activity of macrophages in the presence of the extracts can also be interpreted as a bioactivity marker, aside from cytokine measurements.

Levels of the anti-inflammatory cytokine IL-10 were markedly increased in a dose-dependent manner with the four concentrations of the aqueous extract of *P. insularum* (Fig 3.16B), with increases from 50% at the lowest concentration tested (0.5% v/v) to 800% at the highest concentration tested (3% v/v). Interestingly, the *P. insularum* methanolic extract did not alter IL-10 levels at any concentration compared to untreated macrophages. The two higher concentrations of the iron chelator BPS increased IL-10 levels by 600-700% (6-7-fold) compared to control macrophages, a result that is comparable to the 800% increase in IL-10 levels observed from the highest concentration tested of the aqueous extract of *P. insularum*. The four Risperidone concentrations increased IL-10 levels by 100% compared to untreated macrophages.

Levels of the pro-inflammatory cytokine IL-12 were markedly reduced with the four treatments of the aqueous or methanolic extracts of *P. insularum*, compared to untreated macrophages (Fig 3.16C). The lowest dose of the aqueous extract reduced IL-12 levels by 40%, while the three other doses reduced IL-12 levels by 95-100% compared to untreated macrophages. The four *P. insularum* methanolic extract concentrations significantly reduced IL-12 levels by 25-80% compared to untreated macrophages. The two higher concentrations of the iron chelator as well as the two higher concentrations of Risperidone reduced IL-12 levels by 60-75% compared to untreated macrophages.

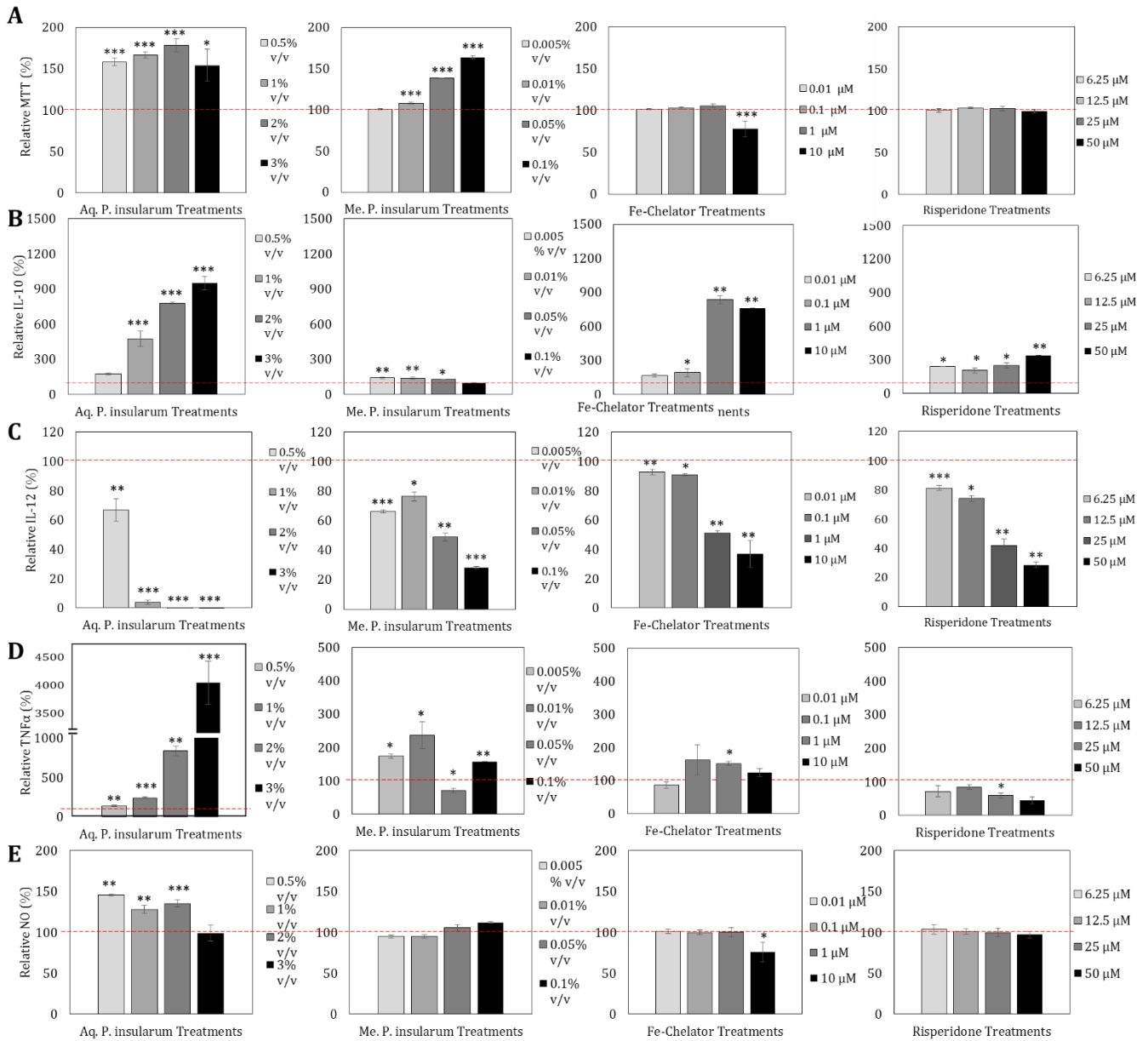
Levels of TNF $\alpha$  were dramatically increased with the two higher concentrations of the aqueous *P. insularum* extract with increases of 650-4000% compared to untreated macrophages (Fig

3.16D). Three of the four *P. insularum* methanolic extract treatments (0.005, 0.01, 0.1% v/v) increased TNF $\alpha$  levels by 20-110% compared to untreated macrophages. The iron chelator at all four tested concentrations and Risperidone at the two lower concentrations did not significantly alter TNF $\alpha$  levels compared to untreated macrophages, while the two higher risperidone concentrations reduced TNF $\alpha$  levels by approximately 50% compared to untreated macrophages. Interestingly, NO levels were increased in cytokines from macrophages treated with the aqueous extract of *P. insularum*, yet were unaltered in macrophages treated with the methanolic extract of *P. insularum*, the iron chelator or risperidone (Fig 3.16E).

The analyses of cytokine analyses from primary macrophages treated with the aqueous and methanolic extracts of *P. insularum* produced varied responses. The aqueous extract increased IL-10 levels and decreased IL-12 levels, hallmark indicators of an anti-inflammatory compound, consistent with the anti-inflammatory application of the plant in Samoan traditional medicine. However, the methanolic extract was only able to reduce IL-12 levels without affecting IL-10 levels. Further, these findings showed that the aqueous extract of *P. insularum* was more potent in regulating IL-10, IL-12, TNF $\alpha$  and NO levels compared to the methanolic extract.

---

**Figure 3.16: Macrophage response to treatment with *P. insularum* extracts.** Primary macrophages were isolated from mice and treated with LPS to induce the inflammatory response for 24 h. The macrophages were then treated with the relevant aqueous (Aq. *P. insularum*) or methanolic (Me. *P. insularum*) extract concentration as well as the iron chelator control (Fe-Chelator) and the anti-inflammatory control (Risperidone) at various concentrations. **A:** MTT results for the extract and control treatments. **B:** IL-10 levels from the macrophages reported as relative IL-10 compared to the relevant treatment control. **C:** IL-12 levels from the macrophages reported as relative IL-12 compared to the relevant treatment control. **D:** TNFA levels from the macrophages reported as relative TNFA compared to the relevant control. **E:** NO levels from the treated macrophages reported as relative NO compared to the relevant control. Statistical analyses were carried out using a one-tailed Student's t-test (\*: p-value < 0.05; \*\*: p-value < 0.01; \*\*\*: p-value < 0.001).



### 3.3.16 *P. insularum* extracts reduce aconitase activity in RAW 264.7 macrophages

We previously determined from analyses in yeast that the extracts of *P. insularum* affected mitochondria respiration (Fig 3.13) via reduced heme synthesis (Fig 3.14). To investigate if mitochondrial function was affected by *P. insularum* extracts in murine macrophages, the enzymatic activity of aconitase, an iron-sulfur dependent enzyme involved in the TCA cycle, was measured in macrophages treated with the extracts of *P. insularum*, the iron chelator BPS or the anti-

inflammatory control Risperidone. Compared to untreated control, the relative aconitase activity was significantly decreased with the aqueous *P. insularum* extract, the methanolic *P. insularum* extract, and the iron chelator treatments (Fig 3.17). Importantly, Risperidone-treated macrophages had aconitase activity levels that were significantly increased compared to the control. These results implied that similar to yeast cells, treatment of mammalian cells with extracts of *P. insularum* affected the mitochondrial machinery involved in cellular respiration.

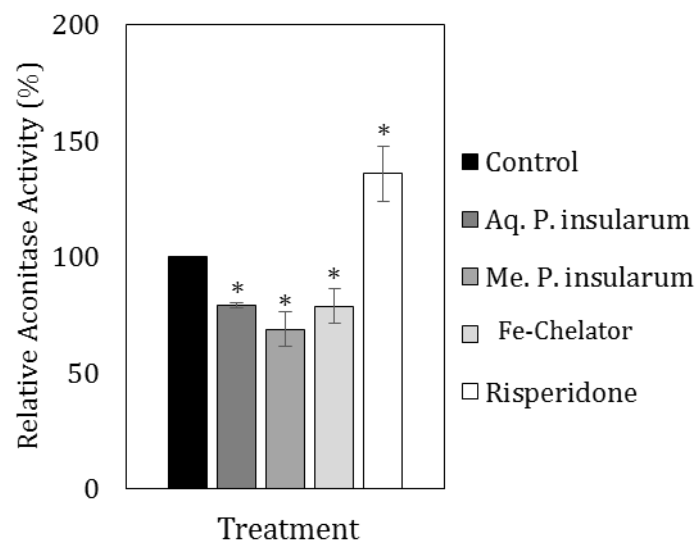


**Figure 3.17: The aconitase activity of macrophages.** Macrophages were induced with LPS followed by treatment with extracts, BPS or risperidone. Protein was isolated from the macrophages, which were used for the aconitase assay. Activity of aconitase from protein samples were calculated, followed by comparisons between each treatment and its relevant vehicle control. Presented is the relative aconitase activity per treatment normalized to its vehicle control. Statistical analyses were carried out using a one-tailed Student's t-test (\*: p-value < 0.05).

### 3.4 Discussion

This chapter aimed to elucidate the MOA of the leaf extracts from the plant *P. insularum*, administered in traditional Samoan medicine to treat illnesses accredited to supernatural causes as well as inflammation related ailments. Results that have been presented herein have indicated that the extracts of *P. insularum*, despite different preparations as aqueous and methanolic extractions, exhibited an iron chelator MOA. It is postulated that despite the different extractions, the bioactive components of the crude extracts may belong to the same group of compounds with the same underlying iron chelating mechanism, as has been observed from other natural products isolated from the same source, such as the microtubule stabilizing mechanism of Peloruside A (extracted with aqueous methanol) and B (extracted with methanol) from *Mycale hentscheli* (Brakovic & Harvey, 2015; Singh *et al.*, 2010; West *et al.*, 2000).

In yeast cells, the extracts of *P. insularum* were shown to induce a hypersensitive growth phenotype in strains lacking iron transport genes (Figs 3.3, 3.4 & 3.5), which indicated that iron transporters were required to buffer the effects of the extracts. This suggested that either iron transport into the cell was blocked, or that iron was not available for cellular processes. However, because all iron transporters were shown to exhibit the hypersensitive phenotype (Figs 3.4 & 3.5), it was unlikely that an iron transporter was a physical target of the extracts because deletion of the extract target would render the deletion mutant resistant to the extract (Smith *et al.*, 2010). We therefore proposed the extracts exhibited their activity by making iron unavailable to the cell via the chelation of iron. This hypothesis was supported when the addition of exogenous iron rescued the extract-induced growth defect (Fig 3.6), the interpretation being that iron pools which have been depleted by the extract would have been replenished to some extent depending on the concentration of the extract treatment. Our iron chelator hypothesis was further corroborated when we determined that extracts reduce intracellular iron compared to control cells to the same extent that the established iron chelator BPS reduced intracellular iron by (Fig 3.10). This phenotype was also observed in yeast cells treated with curcumin, which was also proposed to possess iron

chelating activity (Minear *et al.*, 2011). Interestingly, data from the ICP-MS quantification of iron did not allow for the determination of whether iron was chelated inside the cell or outside the cell.

Theoretically, the chelation of iron intracellularly would suggest the complex remained inside the cell, and complexed iron would be released upon treatment for quantification, leading to increased intracellular total iron (Tamarit *et al.*, 2006). However, despite the internalization of curcumin by the cell, its iron content remained reduced (Minear *et al.*, 2011), suggesting that the curcumin-iron complex is removed before iron was quantified by ICP-MS possibly when insoluble cell debris is removed. Further, the iron chelator control used in this study chelates iron extra-cellularly, which may suggest that the reduced iron content determined from the extract treatment, similar to that obtained for the chelator control, was a consequence of extracellular iron chelation. However, because both internalized curcumin iron chelation and extracellular BPS iron chelation produce reduced iron content in treated cells, our results were thus unable to provide insight into the site of iron chelation by the *P. insularum* extracts.

Yeast cells undergo a molecular response under low iron conditions that includes the down-regulation of iron-requiring pathways, and the up-regulation of iron transporter expression (Chen *et al.*, 2004; Kaplan *et al.*, 2006; Philpott *et al.*, 2012; Philpott & Protchenko, 2008; Puig *et al.*, 2005; Shakoury-Elizeh *et al.*, 2004; Shakoury-Elizeh *et al.*, 2012). When yeast strains with GFP-tagged iron transporters were treated with *P. insularum* extracts, it was determined that the expression levels of the iron transporters were noticeably increased similar to cells treated with the iron chelator control as well as cells grown in iron-free media (Fig 3.11). Our results are consistent with previous work that monitored the expression of the iron transporter Fet3p using a *lacZ* reporter system and found that Fet3p expression was upregulated under low iron conditions (Chen *et al.*, 2004; Puig *et al.*, 2005).

As proposed by Xu *et al.* (2012), an extended lag-phase and lower stationary phase were indicative of a defect in cellular respiration. This phenotype was observed from the growth curves of yeast treated with *P. insularum* extracts, indicating that the extracts caused a defect in cellular

respiration. The requirement of iron in cellular respiration in the form of iron sulfur cluster proteins and heme is well understood (reviewed in Philpott *et al.*, 2012). Thus, heme was quantified and our findings showed that heme levels were significantly reduced in extract treated cells compared to control cells, a result that is consistent with the downregulation in heme biosynthesis (Puiget *et al.*, 2005; Shakoury-Elizeh *et al.*, 2010). The reduced heme (Fig 3.14), and presumably reduced activity of iron sulfur cluster dependent enzymes (Puig *et al.*, 2005) contribute to the reduced stationary phase of extract-treated cells, as it is during this phase that yeast cells are shunted to cellular respiration as the more readily fermented glucose carbon source is depleted (Shakoury-Elizeh *et al.*, 2010).

Results from the CAS assay definitively showed that the *P. insularum* extracts chelate iron (Fig 3.17). The CAS solution turned from blue (with complexed iron) to yellow (iron is removed by a chelator) upon the addition of both the aqueous and methanolic extracts of *P. insularum*. Interestingly, the CAS assay carried out here showed a similar chelating strength between the aqueous and methanolic extracts, although it appeared that the aqueous extract chelated iron more readily than the methanolic extract, as the aqueous extract caused a colour change more readily than the methanolic extract. These findings may suggest that the aqueous extract iron chelating component more readily chelates iron, while its variant in the methanolic extract, present at higher concentrations may not readily chelate iron, and may explain its higher potency yet slower iron chelating activity as observed. It is important to note here that given the well documented metal-chelating activity of plant natural products such as plant polyphenols and flavonoids (Hatcher *et al.*, 2008; Hider *et al.*, 2001; Morel *et al.*, 1993), it would be unsurprising to obtain a positive colour change if we were to include another plant extract in the CAS assay.

In addition to iron transport gene deletions, the deletions of *TEF4*, *SNF5*, *BEM1* and *BEM4* that were determined to be hypersensitive to the aqueous extract in the genome-wide analysis (Fig 3.2) may be secondarily affected by the low iron condition resulting from the *P. insularum* extracts. The *tef4* strain exhibits fragmented vacuoles (Esposito & Kinzy, 2010) and deletion mutants with fragmented vacuoles are hypersensitive to low iron conditions (Szczypka *et al.*, 1997). *SNF4* is a

component of the SWI/SNF (SWITCH/Sucrose Non-Fermentable) complex, which is important for transcriptional regulation of iron uptake at the chromatin level (Monahan *et al.*, 2008). *BEM1* and *BEM4* are involved in cell budding and therefore the cell cycle, a process that can be arrested by iron chelators (Fu *et al.*, 2007; Rao, 2013; Siriwardana & Seligman, 2013; Zhang, 2014).

Collectively, we use our results in yeast to propose a model wherein the bioactive compound from the aqueous and methanolic extracts of *P. insularum* chelates iron either intracellularly or extracellularly, leading to reduced bioavailable iron for cellular processes required for growth, such as cellular respiration (Fig 3.18). The cell subsequently responds by upregulating the expression of iron transporters to import more iron into the cell and downregulate iron-requiring cellular processes. This is a working model that requires further investigation in mammalian cells, such as the measurements of intracellular iron in murine macrophages. As heme is required for ergosterol synthesis (Lewis *et al.*, 1985), it would be interesting to incorporate ergosterol synthesis into this model.

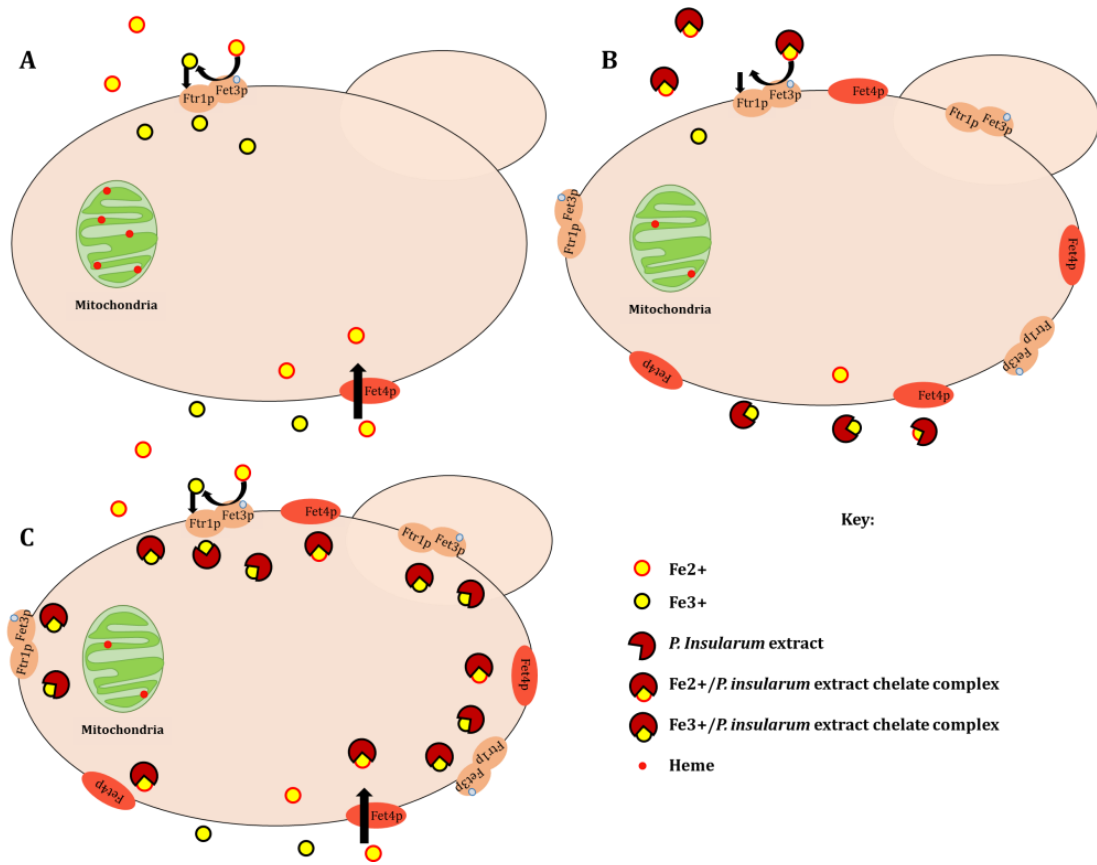


**Figure 3.18: Model of the mechanism of action of *P. insularum* extracts.** **A:** Iron replete conditions. The cell has sufficient iron for iron requiring proteins, enzymes and co-factors. **B:** Extracellular iron chelation. *P. insularum* extracts chelate iron outside of the cell, and the cell subsequently is unable to internalize more iron, despite up-regulation of iron transporter expression; reduced heme production results from low iron. **C:** Intracellular iron chelation. *P. insularum* extracts chelate iron inside of the cell, and the cell subsequently is unable to access the iron complexed in the chelate complex, leading to reduced heme production. Despite up-regulation of iron transporter expression, iron that is internalized is chelated.

---

Investigations into the effects of the *P. insularum* extracts on inflammation in murine macrophages clearly showed a strong anti-inflammatory activity for the aqueous extract of *P. insularum* and a mild anti-inflammatory activity for the methanolic extract (Fig 3.16). Interestingly, the responses from the iron chelator control in the macrophages closely mirrored the trends observed from the extracts, suggesting the anti-inflammatory activity observed from the extracts was a consequence of iron chelation. These results are consistent with the intimate connection between iron and inflammation (Ganz & Nemeth, 2015; Wessling-Resnick, 2010). It has been generally reported that high iron promotes infection and subsequently inflammation (Jurado, 1997). Indeed, various iron chelators have been reported to possess anti-inflammatory activities, such as ibuprofen, and curcumin (Islam *et al.*, 2016; Kennedy *et al.* 1990; Menon & Sudheer, 2007).

The mechanisms by which iron chelators mediate inflammation are not completely understood. The anti-inflammatory effects of iron chelators were largely attributed to their reactive oxygen species (ROS) scavenging ability, as free iron has the ability to generate ROS and other oxidative stressors (Lehmann *et al.*, 2015). However, evidence has revealed that iron plays a role in the activation of the NF- $\kappa$ B, which drives the inflammatory response (Xiong *et al.*, 2003). Logically then, the removal of iron via iron chelation leads to reduced activation of NF- $\kappa$ B, resulting in an anti-inflammatory phenotype.

Intriguingly, the results obtained from the positive anti-inflammatory control Risperidone (O'Sullivan *et al.*, 2014), although similar for IL-10 and IL-12 trends, proved variant in the case of the TNF $\alpha$  results. Reduced TNF $\alpha$  levels are expected under anti-inflammatory conditions, so it is

paradoxical that despite the anti-inflammatory activity of the extracts of *P. insularum*, the extracts induced increased TNF $\alpha$  levels, indicative of an inflammatory response arising from its pivotal role in the inflammatory response (Esposito & Cuzzocrea, 2009). However, Zakharova & Ziegler (2005) showed that injection of mice with TNF $\alpha$  led to the down-regulation of the pro-inflammatory cytokine IL-12, suggesting that TNF $\alpha$  may also possess anti-inflammatory effects, as observed from the macrophage response in *P. insularum* treatment.

In summary, this chapter has proposed a mechanism by which the aqueous extract of *P. insularum* is used in traditional medicine in Samoa. Using yeast as a model organism, we identified that the deletion of iron transporters in the presence of *P. insularum* extracts markedly reduced growth, which was rescued upon supplementation with exogenous iron. Reduced intracellular iron, upregulated iron transporter expression, and reduced heme synthesis together with a respiratory deficient phenotype were the effects the extracts had on yeast cells. These findings were collated to present a model by which the extracts chelate iron away from iron-requiring cellular processes. Additionally, this iron chelation has been further shown to mediate an anti-inflammatory activity in murine macrophages, which can attest to how the plant is used to treat inflammation-related ailments in traditional medicine.

---

## Chapter 4:

# Haploinsufficiency and Homozygous Profile Analyses of the Aqueous and Methanolic Extracts of *Psychotria insularum*

---

### 4.1. Introduction

Thus far, we have identified the extracts of *Psychotria insularum* as the most potent extracts from the 11 Samoan medicinal plants collected for this work. We used an agar-based analysis of ~4,300 non-essential genes to identify iron transport and iron chelation as the mechanisms by which the extracts of *P. insularum* mediated its anti-inflammatory activity. Despite these findings, the agar-based genome-wide analysis of the non-essential genes comprised only ~70% of the yeast genome against only the aqueous extract of *P. Insularum*, leaving the remaining non-essential genes to be screened against the aqueous extract, and both essential and non-essential genes to be investigated against the methanolic extract of *P. Insularum*. In this chapter, we aimed to utilize the diploid yeast libraries, both in heterozygous and homozygous forms to obtain complete chemical-genetic profiles of both the aqueous and methanolic extracts, via the haploinsufficiency profiling (HIP) and homozygous profiling (HOP techniques.

Complete genome-wide analyses conducted in yeast via the HIP technique utilizes heterozygous diploid mutants of essential and non-essential genes. This approach identifies the most hypersensitive mutant as the genetic target of the compound tested (Giaever *et al.*, 1999). For instance, Giaever *et al.* (1999) used this approach in a proof-of-concept work using tunicamycin and benomyl, where the correct targets of these two drugs (*ALG7* and *TUB1*, respectively) were identified. Further, multiple other compounds have been tested using this approach, as well as several other growth conditions such as media, pH and temperature (Giaever *et al.*, 2004; Hillenmeyer *et al.*, 2008; Pierce *et al.*, 2007; Yan *et al.*, 2008).

Complementary to HIP analysis is the utilization of HOP technique, utilizing diploid deletion mutants of non-essential genes. This approach, given its nature, inherently does not allow for the incorporation of essential genes and therefore only determines the fitness of the deletion mutants against a compound. Instead of identifying genetic targets, the HOP technique identifies gene deletions that are hypersensitive in the presence of a compound, thereby indicating that the gene products are required to buffer the effects of the compound. This in turn provides an outlook to the compound's mechanism of action, based on the buffering pathways identified from the hypersensitive deletion mutants. This approach has been used for instance, by Parsons *et al.* (2006) to identify calcium disruption as the mechanism of action of the breast cancer drug tamoxifen. The buffering mechanisms of yeast against many other compounds have been determined using this approach (Giaever *et al.*, 2004; Hillenmeyer *et al.*, 2008; Pierce *et al.*, 2007; Yan *et al.*, 2008).

In this chapter, we aim to use the competitive pooled HIP and HOP analyses of the aqueous and methanolic extracts of *P. insularum* to identify genetic targets of both, and any further buffering mechanisms that were not previously identified in the agar-based genome-wide analysis of haploid deletion mutants. The HIP analyses did not identify genetic targets for either the aqueous or methanolic extracts of *P. insularum*, while the HOP analyses identified buffering genes that complemented the iron chelating mechanism of action identified in Chapter 3.

## 4.2. Methods

### 4.2.1. Pooling the HET and HOM libraries

The heterozygous (HET) and homozygous (HOM) diploid libraries (Open Biosystems) were pinned on YPD+G418 (100 µg/mL) plates in 384 colony format on rectangular petri plates (Singer). After 24 h incubation at 30°C, the colonies were pooled twice with 5 mL of YPD+G418 by agitation with a glass rod across the agar surface and collected in a sterile conical flask on ice. Glycerol was added to a final concentration of 15% v/v before cell density was calculated using a Coulter counter. Aliquots of each library were prepared at  $1 \times 10^9$  cells and stored at -80°C.

### 4.2.2. Competitive growth of HET and HOM libraries

A single aliquot of the pools of HET and HOM libraries was used to inoculate 10 mL SC and each culture was grown whilst shaking at 30°C. After 18 h, this 10 mL overnight culture was used to inoculate fresh 100 mL SC that was incubated at 30°C whilst shaking for a further 5 h. This was to ensure cells were in log phase of growth at the initiation of the treatment. Fresh 2 mL SC with the relevant concentration of extract (optimized at 0.005% v/v for aqueous extract, and 0.001% v/v for methanolic extract, optimized in Appendix VI); was then inoculated to a final concentration of  $5 \times 10^6$  cells/mL (*i.e.*, approximately 1000 representations of each strain) and incubated at 30°C whilst shaking for 15 h. This became the first 10 generations. The OD<sub>600</sub> was measured to ensure cells were at log phase (OD<sub>600</sub>= 4-6) and to ensure the concentration of the extract was sub-lethal (10-20% growth inhibition), and cell density was calculated using a Coulter counter. Then the relevant volume of 10 generation culture was used to inoculate fresh 2 mL SC containing the relevant treatment (*P. insularum* extract or control) to a final concentration of  $5 \times 10^6$  cells/mL and incubated at 30°C for 15 h (second 10 generations). After 15 h, cell density was again determined using a Coulter counter, before cells were harvested for genomic DNA isolation.

#### 4.2.3. Genomic DNA Isolation

Genomic DNA (gDNA) was isolated using the YeaStar Genomic DNA Kit (ZymoResearch), according to Protocol I in the manufacturer's instructions. Briefly,  $5 \times 10^7$  cells were harvested by centrifugation at  $500 \times g$  for 2 min, the pellet was resuspended in 120  $\mu\text{L}$  of YD digestion buffer and 5  $\mu\text{L}$  of R-Zymolase by vortexing, and the tubes were incubated at  $37^\circ\text{C}$  for 40-60 min. Then 120  $\mu\text{L}$  of lysis buffer was added, followed by gentle mixing by inversion, and 250  $\mu\text{L}$  of chloroform was then added, followed by mixing for 1 min. Tubes were then centrifuged at 10,000 rpm for 2 min, and the upper layer (gDNA) was transferred onto a Zymo spin III column. The gDNA was bound to the column, the liquid phase was removed by centrifugation at 10,000 rpm for 1 min, and 300  $\mu\text{L}$  of DNA wash buffer was added and removed twice by centrifugation at 10,000 rpm for 1 min. The Zymo column was then transferred into a sterile 1.5 mL centrifuge tube and the gDNA was eluted with 60  $\mu\text{L}$  sterile  $\text{dH}_2\text{O}$  onto the membrane, incubated for 1 min at room temperature, and centrifuged at 10,000 rpm for 10 s to yield 10-20  $\mu\text{g}$  of gDNA.

#### 4.2.4. Barcode Sequencing

The unique 20 bp barcodes flanking each gene deletion (UPTAG upstream and DNTAG downstream of each gene deletion) were amplified and sequenced as previously described (Robinson *et al.*, 2014). In brief, 10 ng/ $\mu\text{L}$  of gDNA was used as a template in a PCR using universal primers that are upstream and downstream of every barcode. All UPTAG amplicon libraries were pooled separately from all the DNTAG amplicon libraries, and 60 ng of each pool underwent PCR amplification for the incorporation of the Illumina P5 adapter sequence (primer sequences in Appendix VII). The multiplexed UPTAG and DNTAG libraries were mixed together at a 1:1 ratio and 50 bp single end reads were sequenced on an Illumina flow cell using an IlluminaHiSeq 2000 platform. Read matching and statistical analyses were carried out as previously described to record logFC (measure of change in mutant barcode sequence abundance in treatment compared to

control), FDR (false discovery rate) and logCPM (quality of barcode sequencing results) for every gene deletion in the HET and HOM diploid libraries (Robinson *et al.*, 2014).

#### 4.2.5. Validation of Fitness Phenotype

Heterozygous or homozygous strains that were selected for validations were arrayed and grown in 96-format on YPD agar at 30°C overnight, which was subsequently used to inoculate a fresh 96-well plate containing 100 µL of YPD and incubated at 30°C overnight. Cells were centrifuged, washed, and resuspended in 100 µL of dH<sub>2</sub>O, of which 1 µL was used to inoculate fresh SC containing the relevant amount of extract or control. All validations and controls were carried out in triplicate and grown at 30°C. Absorbance readings at 590 nm using an Envision plate reader (Perkin Elmer) were recorded at 0, 15, 18 and 24 h. Growth comparisons of treated and control cells were conducted to quantify growth inhibition and determine the heterozygous and homozygous deletion strains that were sensitive to *P. insularum* extracts.

## 4.3. Results

### 4.3.1. HIP Analysis of the *P. insularum* Aqueous Extract

To determine the haploinsufficiency profile (HIP) of *S. cerevisiae* in the presence of the aqueous extract of *P. insularum*, the pooled heterozygous library was exposed to the aqueous extract (0.001% v/v), and grown for 20 generations. The gDNA was harvested and the barcodes flanking each gene deletion were amplified, sequenced and quantified using next-generation sequencing and bioinformatics analyses. Comparison of the growth profiles of the heterozygous mutants in the presence and absence of the aqueous extract resulted in calculations of logCPM and logFC. In our analyses, logCPM is the log counts per million, and is a measure of the reliability of the results. If an ORF does not produce sufficient reads/counts, it is discounted from the analyses. Conversely, logFC is the log fold change, and is a measure of the effect of the extract treatment. In this work, a negative logFC correlated to a reduction in read counts from ORFs treated with the extract compared to those without extract treatment, indicative of hypersensitivity and reduced growth of a particular deletion strain in the presence of the extract. A positive logFC correlated to an increase in read counts from ORFs treated with the extract compared to those without extract treatment, indicative of improved growth when treated with extract. Of the 5,814 heterozygous mutants, the majority exhibited logCPM greater than 3 indicative of a high quality of sequencing (Fig 4.1). While a logFC value at 0 indicates the treated heterozygous strain grew comparatively to the control, positive logFC values indicate the treated heterozygous mutants grew better than the control and negative logFC values show the treated heterozygous mutants grew worse than the control and are hypersensitive to the extract treatment. Using a False Discovery Rate (FDR) cutoff of  $< 0.05$ , 26 strains were identified with positive logFC and 25 strains with negative logFC. When the 51 genes were analysed through GO enrichment, no biological processes, molecular functions or cellular components were enriched.

The 25 heterozygous deletions that exhibited hypersensitivity (negative logFC) to the aqueous extract of *P. insularum* treatment are involved in gene expression at the genomic,

transcription and translation stages, as well as trafficking in the cell involving the ER, the Golgi and the vacuole (Table 4.1). Interestingly, the iron-transporter *FET4* was identified as one of the most hypersensitive genes in the HIP analysis, a result that is consistent with our previous finding that the *FET4*-deficient haploid deletion strain was hypersensitive to the extracts of *P. insularum* (Chapter 3).

There were 26 heterozygous strains that exhibited better growth in the presence of the *P. insularum* aqueous extract compared to the control (Table 4.2). Heterozygous mutations that conferred better growth included genes involved in histone structure, autophagy, and cell trafficking involving the Golgi. Of most interest from this set of results is the better growth profile of *FRA1*, (Fe Repressor of Activation) which is a negative regulator of the iron regulon.

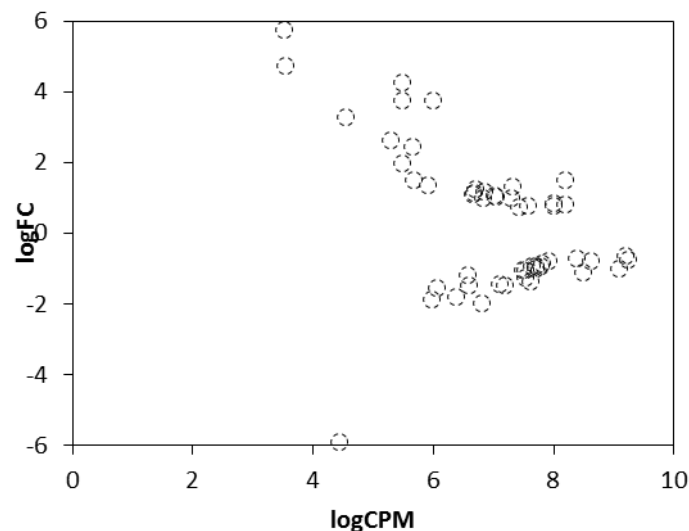


**Figure 4.1:** Scatterplot of heterozygous mutants with false discovery rate values less than 0.05 against the aqueous extract of *P. insularum*, plotted as logCPM vs logFC. Read count of treated mutants were compared to read count of control mutants and is represented as the logFC, whereby logFC 0 indicates no change/difference between control and treated strains, while a positive or negative logFC indicates that treated heterozygotes grew better or worse (respectively) compared to the control. The plotted logCPM is a measure of data quality, whereby higher logCPM (*e.g.*, greater than 2) is considered good quality data.

**Table 4.1: The 25 hypersensitive heterozygotes against the aqueous extract of *P. insularum*.** The data summarized herein are sorted by the logFC, with the lowest logFC at the top of the table, indicating the genes are sorted from most hypersensitive to the least hypersensitive true hits. logCPM, p-value and FDR values for all gene hits are shown, together with their gene names and biological functions obtained from the Saccharomyces Gene Database.

	logFC	logCPM	PValue	FDR	Gene	Biological Function
YER157W	-5.89255	4.425087	7.07E-05	2.25E-02	COG3	Essential component of the conserved oligomeric Golgi complex
YMR319C	-1.97577	6.788245	7.23E-05	2.25E-02	FET4	Low affinity iron transporter at the plasma membrane
YJL172W	-1.84687	5.951847	6.20E-05	2.25E-02	CPS1	Vacuolar carboxy peptidase S
YPL260W	-1.78916	6.365672	9.43E-06	8.68E-03	YPL260W	Putative substrate of cAMP-dependent protein kinase
YAL007C	-1.54478	6.046772	1.52E-04	3.19E-02	ERP2	Member of the p24 family involved in ER to Golgi transport
YLR315W	-1.45443	7.183376	1.18E-05	8.78E-03	NKP2	Central kinetochore protein and subunit of the Ctf19 complex
YOL069W	-1.44614	6.574941	3.57E-04	4.82E-02	NUF2	Component of the kinetochore-associated Ndc80 complex
YCR028C	-1.40387	7.084485	1.64E-04	3.25E-02	FEN2	Plasma membrane H <sup>+</sup> -pantothenate symporter
YGL207W	-1.34066	7.596771	2.08E-05	1.37E-02	SPT16	Subunit of the heterodimeric FACT complex
YEL054C	-1.22951	7.527092	1.15E-04	2.84E-02	RPL12A	Ribosomal 60S subunit protein L12A
YCR020W-B	-1.18159	6.560867	1.56E-04	3.19E-02	HTL1	Component of the RSC chromatin remodeling complex
YJL211C	-1.07773	8.472511	1.19E-09	7.07E-06	YJL211C	Dubious open reading frame, overlaps with <i>PEX2</i>
YPL021W	-1.02942	7.511751	7.85E-05	2.33E-02	ECM23	Non-essential protein of unconfirmed function
YJL190C	-1.00397	7.478848	3.50E-04	4.82E-02	RPS22A	Protein component of the small (40S) ribosomal subunit
YML104C	-0.99336	7.691982	5.22E-05	2.22E-02	MDM1	PtdIns-3-P binding protein that tethers the ER to vacuoles at NVJs
YHL027W	-0.96755	9.066119	6.56E-05	2.25E-02	RIM101	Cys2His2 zinc-finger transcriptional repressor
YLR068W	-0.91841	7.770453	1.53E-04	3.19E-02	FYV7	Essential protein required for maturation of 18S rRNA
YOR340C	-0.91718	7.622687	2.19E-04	3.71E-02	RPA43	RNA polymerase I subunit A43
YCR102W-A	-0.9145	7.691793	3.78E-04	4.85E-02	YCR102W-A	Dubious open reading frame
YNR068C	-0.82746	7.787097	2.11E-04	3.71E-02	YNR068C	Putative protein of unknown function
YMR220W	-0.77389	8.612453	4.01E-04	4.85E-02	ERG8	Phosphomevalonate kinase involved in ergosterol synthesis
YLL044W	-0.76131	7.898162	2.30E-04	3.79E-02	YLL044W	Dubious open reading frame
YDL240W	-0.7137	9.219504	8.90E-05	2.39E-02	LRG1	GTPase-activating protein
YNL044W	-0.69931	8.372763	1.84E-04	3.52E-02	YIP3	Protein localized to COPII vesicles
YGL213C	-0.63938	9.175094	1.26E-04	2.88E-02	SKI8	Ski complex component and WD-repeat protein

**Table 4.2: The 26 heterozygotes that grew better in the aqueous extract of *P. insularum*.** The data summarized herein are sorted by the logFC, with the lowest logFC at the top of the table, indicating the genes are sorted from least resistant to the most resistant to the aqueous extract of *P. insularum*. logCPM, p-value and FDR values for all gene hits are shown, together with their gene names and biological functions obtained from the Saccharomyces Gene Database. NA: no associated gene, simply an identified ORF.

	logFC	logCPM	PValue	FDR	Gene	Biological Function
YDL170W	0.779259	7.561222	9.28E-05	2.39E-02	UGA3	Transcriptional activator for GABA (gamma-aminobutyrate) genes
YOR304C-A	0.802629	7.981128	3.08E-04	4.68E-02	BIL1	Protein that binds Bud6p, role in actin cable assembly
YLR150W	0.830896	8.188551	1.02E-05	8.68E-03	STM1	Protein required for optimal translation under nutrient stress
YLR262C-A	0.877725	7.993725	3.87E-04	4.85E-02	TMA7	Unknown function, associates with ribosomes
YDL134C-A	1.009552	6.809188	3.36E-04	4.82E-02	NA	NA
YLL029W	1.013686	7.273951	3.07E-04	4.68E-02	FRA1	Involved in negative regulation of iron regulon transcription
YGR071C	1.050189	7.035567	5.61E-05	2.22E-02	ENV11	Protein proposed to be involved in vacuolar functions
YIL005W	1.100702	7.00332	2.82E-04	4.52E-02	EPS1	ER protein with chaperone and co-chaperone activity
YNL051W	1.133584	6.636807	2.13E-04	3.71E-02	COG5	Component of the conserved oligomeric Golgi complex
YFL014W	1.175569	6.663223	3.57E-04	4.82E-02	HSP12	Plasma membrane protein involved in maintaining membrane organization
YPR026W	1.186516	6.824689	1.02E-05	8.68E-03	ATH1	Acid trehalase required for the utilization of extracellular trehalose
YBL002W	1.2581	6.675206	2.09E-04	3.71E-02	HTB2	Histone H2B
YOL019W	1.34473	7.306941	5.42E-05	2.22E-02	YOL019W	Protein of unknown function
YOR365C	1.361513	5.897571	1.24E-04	2.88E-02	YOR365C	Putative protein of unknown function
YPR049C	1.512557	5.667632	3.99E-04	4.85E-02	ATG11	Adapter protein for pexophagy and the Cvt targeting pathway
YNL062C	1.523893	8.168126	1.20E-06	2.86E-03	GCD10	Subunit of the tRNA methyltransferase with Gcd14p
YBR133C	2.006621	5.468299	4.24E-04	4.93E-02	HSL7	Arginine N-methyltransferase
YBL003C	2.458397	5.633028	2.35E-06	3.48E-03	HTA2	Histone H2A
YBL005W	2.634583	5.273181	3.48E-05	2.03E-02	PDR3	Transcriptional activator of the pleiotropic drug resistance network
YPL158C	3.295032	4.53157	4.19E-04	4.93E-02	AIM44	Regulates Cdc42p and Rho1p
YFL033C	3.757344	5.987579	1.45E-06	2.86E-03	RIM15	Protein kinase involved in cell proliferation in response to nutrients
YPR021C	3.778685	5.467699	4.07E-05	2.03E-02	AGC1	Mitochondrial amino acid transporter
YDR506C	4.265256	5.474882	4.11E-05	2.03E-02	GMC1	Involved in meiotic progression
YEL072W	4.765103	3.5177	3.93E-04	4.85E-02	RMD6	Required for sporulation
YGR062C	5.773421	3.49702	8.57E-05	2.39E-02	COX18	Required for membrane insertion of C-terminus of Cox2p

As false positives are inherent in high throughput analyses such as the genome-wide Bar-seq analyses conducted in this chapter, results of such analyses must be validated using independent methods. We previously focussed on the haploid mutants with impaired growth in the presence of the extracts (in Chapter 3) and validation work in this chapter also only investigates the validity of diploid mutants on that basis. We thus grew the 25 heterozygous strains with negative logFC in the presence of the aqueous extract or the control treatment, and measured their growth (absorbance at 590 nm) at 15 h, a time point where yeast strains are at mid-log phase of growth. Growth (percent residual growth) of six of the 25 strains was significantly reduced by the aqueous *P. insularum* treatments compared to the BY4743 WT control (Fig 4.2). These mutants were Fet4p (the low-affinity iron transporter), Cps1p (the vacuolar caboxypeptidase S), Lrg1p (a GTPase activating protein), Yip3p (a protein localised to COP II vesicles), and two uncharacterized genes *YPL260W* and *YNR068C* (Bordallo *et al.*, 1991; Dix *et al.*, 1994; Fitch *et al.*, 2004; Genget *et al.*, 2005).

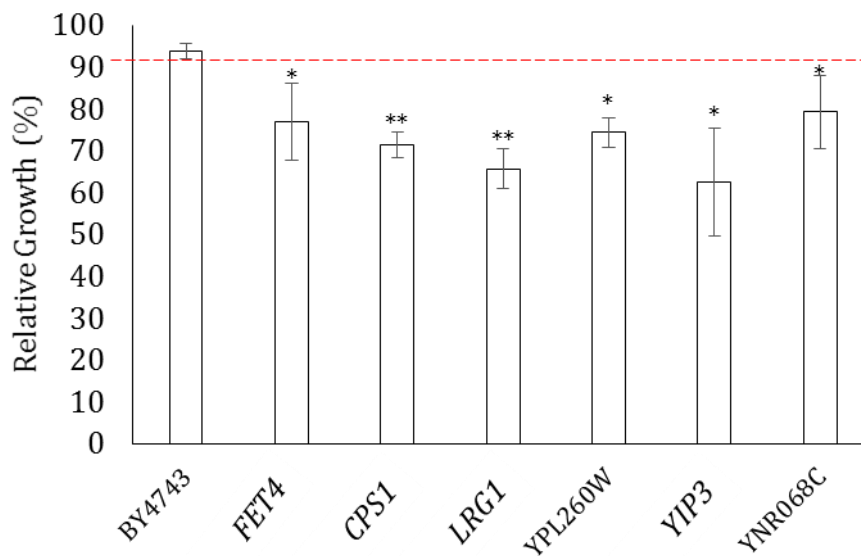


**Figure 4.2: Heterozygous genes validated to be hypersensitive to the aqueous extract of *P. insularum*.** Heterozygous mutants were individually grown in the presence of the aqueous extract in triplicate, and compared to the control treatment. Mutants exhibiting growth less than 90% consistently across the three triplicates compared to the WT (BY4743) are plotted as residual growth as mean  $\pm$  SD. The p-values were calculated using one tailed Student's t-test (\*: p-value < 0.05, \*\*: p-value < 0.01).

#### 4.3.2. HOP Analysis of the *P. insularum* Aqueous Extract

To determine the homozygous profile of the aqueous extract of *P. insularum*, the pooled collection of homozygous deletion mutants was exposed to 0.001% v/v of the aqueous extract and the growth profiles (barcode abundance) of each deletion mutant in the presence of the extract was compared to their control counterparts. The logFC and logCPM values for each deletion mutant were determined and the majority of the deletion mutants were largely unaffected by the extract treatment with most of the ORFs scattered around a logFC value of 0 (Fig 4.3). Using FDR < 0.05 as a cutoff for significance, there were 18 deletion mutants with negative logFC values ranging from 0.5 to -5.5 (Table 4.3) indicative of impaired growth in the presence of the extract, and 12 deletion mutants with positive logFC values ranging from 0.3 to 3.5 (Table 4.4) indicating better growth in the presence of the extract. When the 30 genes were analysed through GO enrichment, no biological processes, molecular functions or cellular components were enriched.

The 18 genes with negative logFC values function in a variety of cellular processes (Table 4.2). The gene deletion most hypersensitive (*i.e.*, the lowest logFC value) to the aqueous extract treatment was *ERG2*, an enzyme involved in ergosterol synthesis (Arthington *et al.*, 1991). Interestingly, the ergosterol synthesis pathway requires the co-factor heme at the Erg11p step of the pathway (Turi & Loper, 1992). Several genes can be observed as belonging to distinct molecular components and functions. For instance, several gene deletions involved in ribosomal structure were detected (*e.g.*, *rpp1aΔ*, *rpl37aΔ*, *rps4bΔ*, *jjj1Δ*, *rpl17bΔ* and *rpl4aΔ*) (Cyr *et al.*, 1994; Planta & Mager, 1998; Stolc & Altman, 1997). Several gene deletions were determined to be involved in cellular transport (*e.g.*, *ubp3Δ*, *srn2Δ*, *eps1Δ*, *jjj1Δ* and *pex8Δ*) (Agne *et al.*, 2003; Baker *et al.*, 1992; Robinson *et al.*, 1988; Wang & Chang, 1999). Two deletion mutants were observed to regulate transcription of specific genes and pathways, including *mtq2Δ* and *fyv5Δ* (Bianchi *et al.*, 1999; Polevoda *et al.*, 2006). Dubious ORFs and putative proteins were also detected, including *ynl338wΔ*, *ydl242wΔ* and *yil001wΔ*.

The 12 gene deletions that showed improved growth exhibited varied functions (Table 4.4). Some are involved in the pleiotropic drug response (*PDR3*), autophagy (*ATG11*), oxidative stress (*YAP1*) and protein breakdown (*PNG1*). Interestingly, the null deletion mutant of *ROX1*, a heme-dependent repressor of hypoxic genes, exhibited improved growth in the presence of the aqueous extract.

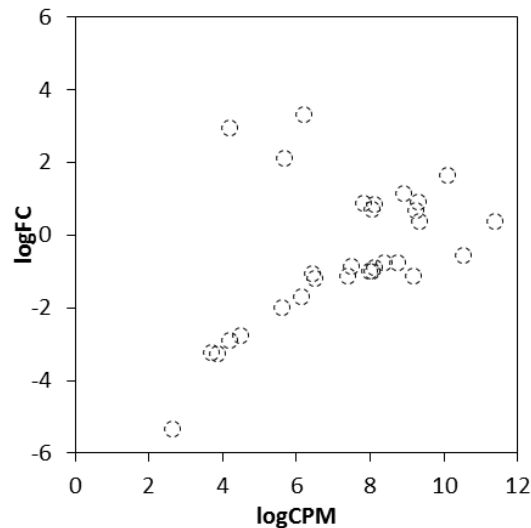


**Figure 4.3:** Scatterplot of the 30 homozygous deletion mutants with false discovery rate values less than 0.05 against the aqueous extract of *P. insularum*, plotted as logCPM vs logFC. Pooled homozygous mutants were treated with 0.001% v/v aqueous extract of *P. insularum* and exposed to a total of 20 generations, DNA extracted and barcode sequenced. Charted are deletion mutants with FDR values calculated to be less than 0.05, plotted using logCPM vs logFC.

**Table 4.3: The 18 hypersensitive homozygous deletion mutants against the aqueous extract of *P. insularum*.** The data summarized herein are sorted by the logFC, with the lowest logFC at the top of the table, indicating the genes are sorted from most hypersensitive to the least hypersensitive true hits. logCPM, p-value and FDR values for all gene hits are shown, together with their gene names and biological functions obtained from the Saccharomyces Gene Database.

	logFC	logCPM	PValue	FDR	Gene	Biological Function
YMR202W	-5.32403	2.627291	1.58E-04	3.60E-02	ERG2	C-8 sterol isomerase, involved in ergosterol synthesis
YDR140W	-3.25781	3.847427	7.41E-05	2.44E-02	MTQ2	S-adenosylmethionine-dependent methyltransferase
YER151C	-3.22246	3.67191	1.06E-04	3.13E-02	UBP3	Ubiquitin-specific protease involved in transport and osmotic response
YCL058C	-2.87062	4.177405	8.70E-06	7.04E-03	FYV5	Protein involved in regulation of the mating pathway
YDL081C	-2.73501	4.471486	1.32E-04	3.26E-02	RPP1A	Ribosomal stalk protein P1 alpha
YLR185W	-1.96176	5.587265	1.57E-06	1.86E-03	RPL37A	Ribosomal 60S subunit protein L37A
YHR203C	-1.66012	6.116239	4.32E-05	1.97E-02	RPS4B	Protein component of the small (40S) ribosomal subunit
YLR119W	-1.18286	6.46769	1.46E-04	3.46E-02	SRN2	Component of the ESCRT-I complex
YIL005W	-1.115	9.141387	2.31E-04	4.57E-02	EPS1	ER protein with chaperone and co-chaperone activity
YOR275C	-1.11443	7.373076	2.01E-04	4.26E-02	RIM20	Protein involved in proteolytic activation of Rim101p; part of response to alkaline pH
YNL227C	-1.02762	6.398809	1.21E-04	3.13E-02	JJJ1	Co-chaperone that stimulates the ATPase activity of Ssa1p, ribosome biogenesis
YJL177W	-0.98441	8.021737	5.66E-05	2.24E-02	RPL17B	Ribosomal 60S subunit protein L17B
YNL338W	-0.97276	7.958258	1.16E-04	3.13E-02	YNL338W	Dubious open reading frame
YKR027W	-0.88167	8.102546	1.07E-06	1.58E-03	BCH2	Member of the ChAPs (Chs5p-Arf1p-binding proteins) family
YBR031W	-0.85451	7.458257	6.14E-05	2.27E-02	RPL4A	Ribosomal 60S subunit protein L4A
YGR077C	-0.7311	8.359912	1.71E-04	3.75E-02	PEX8	Intraperoxisomal organizer of the peroxisomal import machinery
YDL242W	-0.72361	8.735494	9.50E-06	7.04E-03	YDL242W	Dubious open reading frame
YIL001W	-0.53614	10.49215	2.29E-04	4.57E-02	YIL001W	Putative protein of unknown function

**Table 4.4: The 12 homozygous gene deletions that grew better in the presence of the aqueous *P. insularum* extract.** The data summarized herein are sorted by the logFC, with the lowest logFC at the top of the table, indicating the genes are sorted from least resistant to the most resistant to the aqueous extract of *P. insularum*. logCPM, p-value and FDR values for all gene hits are shown, together with their gene names and biological functions obtained from the Saccharomyces Gene Database.

	logFC	logCPM	PValue	FDR	common	Function
YFL033C	0.391197	11.37304	2.78E-05	1.50E-02	RIM15	Protein kinase involved in cell proliferation in response to nutrients
YBL005W	0.404761	9.318519	1.18E-04	3.13E-02	PDR3	Transcriptional activator of the pleiotropic drug resistance network
YLR150W	0.698048	9.211196	6.96E-05	2.43E-02	STM1	Protein required for optimal translation under nutrient stress
YLR187W	0.740099	8.034502	8.89E-05	2.77E-02	SKG3	Protein of unknown function
YPL096W	0.857543	8.109192	3.84E-07	7.58E-04	PNG1	Conserved peptide N-glycanase
YPR049C	0.894325	7.810629	2.98E-06	2.95E-03	ATG11	Adapter protein for pexophagy and the Cvt targeting pathway
YPR064W	0.919732	9.279071	3.06E-05	1.51E-02	YPR064W	Dubious ORF
YML007W	1.173474	8.876484	2.77E-05	1.50E-02	YAP1	Transcription factor required for oxidative stress tolerance
YPR065W	1.652044	10.08996	8.59E-14	5.09E-10	ROX1	Heme-dependent repressor of hypoxic genes
YDL225W	2.135633	5.651854	1.25E-05	8.23E-03	SHS1	Component of the septin ring required for cytokinesis
YDR401W	2.984504	4.179569	4.96E-05	2.10E-02	YDR401W	Dubious ORF
YDR392W	3.34067	6.188196	9.27E-10	2.75E-06	SPT3	Subunit of the SAGA transcriptional regulatory complexes

To validate the results of the Bar-seq analysis, we grew the 18 homozygous gene deletion mutants with negative logFC values (between -0.5 and -5.5) and FDR < 0.05 in the presence and absence of the *P. insularum* aqueous extract and measured growth (absorbance 590nm) at 15 h, a time point where cells were at mid-log of growth. The residual growth (treated/untreated x 100) for each deletion mutant was calculated and then compared to that of the BY4743 WT (Fig 4.4). Seven homozygous deletion mutants were hypersensitive to the extract compared to the WT control. The most sensitive gene was the ergosterol synthesis gene *ERG2* (Arthington *et al.*, 1991), a result that is consistent with the *ERG2* mutant being the most sensitive strain in the Bar-seq analyses. Also sensitive were *JJJ1*, *RPL4b* and *RPS4B* that are all involved in ribosomal biogenesis (Planta & Mager, 1998; Walsh *et al.*, 2004), the dubious ORFs *YGR151C* and *YDL242W*, and the putative protein encoded for by *YIL007W*.

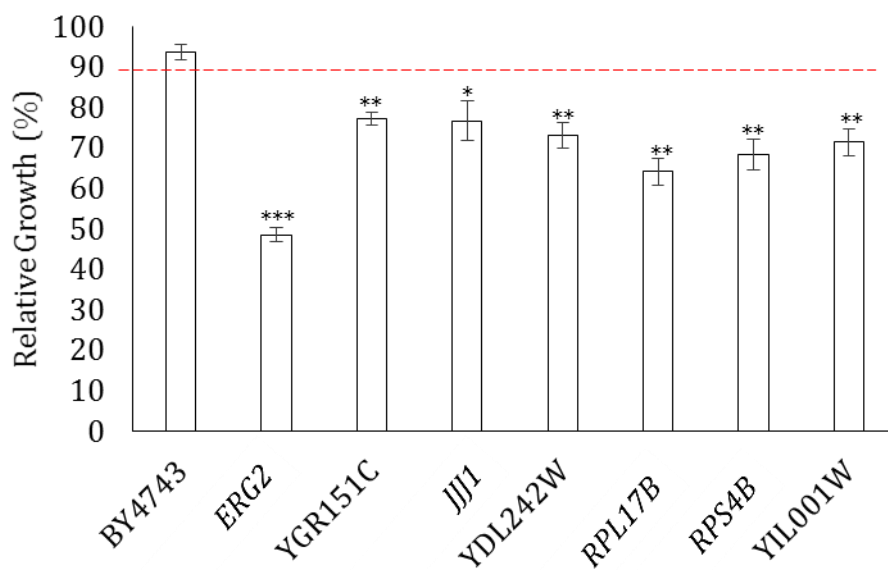


**Figure 4.4: Validations of the homozygous gene deletions detected to be hypersensitive to the aqueous extract of *P. insularum*.** Homozygous deletion mutants were individually grown in the presence of the aqueous extract in triplicate, and compared to the control treatment. Mutants exhibiting growth less than 90% consistently across the three triplicates compared to the WT (BY4743) are plotted as mean residual growth  $\pm$  SD. The p-values were calculated using a one tailed Student's t-test (\*: p-value < 0.05, \*\*: p-value < 0.01, \*\*\*: p-value < 0.001).

### 4.3.3. HIP Analysis of the *P. insularum* Methanolic Extract

As the priority aim of this thesis is primarily gaining understanding of the biological and chemical mechanisms of action of *P. insularum* as it is prepared by traditional healers in Samoa, it was only the aqueous extract that was used in the agar-based genome-wide analyses in Chapter 3. To explore the haploinsufficiency profile of the methanolic extract of *P. insularum*, the pooled heterozygous library was grown in the presence and absence of 0.0001% v/v of the methanolic extract. Similar to the previous Bar-seq results collected for the aqueous *P. insularum* extract, the majority of the mutant strains showed logFC values around 0, indicating that the *P. insularum* methanolic extract did not affect growth compared to the control (Fig 4.5). Using FDR < 0.05 as a cutoff for significance, there were 20 heterozygous mutants that exhibited impaired growth in the presence of the methanolic extract compared to the control, with negative logFC values ranging from -0.75 to -2.65. On the same basis, there were 31 heterozygous mutants that grew better in the presence of the methanolic extract compared to the control, with logFC values ranging from 0.75 to 1.65. When the 51 genes detected here were analysed for GO enrichment, no enrichment was detected from biological processes, molecular functions or cellular components.

Of the 20 genes with negative logFC with FDR < 0.05 (Table 4.5), the heterozygous ORF shown to be the most hypersensitive with the lowest logFC was *IRC7*, which encodes a  $\beta$ -lyase that exhibits increased expression in response to copper levels (Gross *et al.*, 2000; Roncoroni *et al.*, 2011). Several ORFs were observed to be clearly implicated in specific pathways. For instance, *RPL10*, *RPL24B* and *RPS29A* are involved in ribosomal structure (Planta & Mager, 1998), while *SWC5*, *SPT16*, *ITC1* and *SET5* are involved in chromatin remodelling (Krogan *et al.*, 2003; Malone *et al.*, 1991; Nislow *et al.*, 1997; Sugiyama & Nikawa, 2001). Interestingly, *HEM2* that encodes aminolevulinate dehydratase, an enzyme involved in heme synthesis (Gollub *et al.*, 1977), was also detected. Several other ORFs involved in autophagy (*ATG15*), cell cycle (*BUB1* and *SFI1*), transcriptional regulation (*CDC39*), translational control (*SBP1*), as well as proteins found at the plasma membrane (*STL1*) and the cell wall (*FLO11*) were recovered (Breter *et al.*, 1983; Hoyt *et al.*,

1991; Jong *et al.*, 1986; Klonsky *et al.*, 2003; Lo & Dranginis, 1996; Ma *et al.*, 1999; Zhao *et al.*, 1994). Dubious ORFs and putative proteins of unknown functions were also detected, including *YAR043C* and *YKL036C*.

The 31 heterozygous mutants that grew better in the presence of the methanolic extract of *P. insularum* were involved in a variety of functions (Table 4.6), a few of which were intriguing. For instance, *STM1* required for optimal translation under nutrient stress (van Dyke *et al.*, 2006) and *BIL1* which binds Bud6p and is involved in actin cable assembly (Graziano *et al.*, 2013) were detected in the HIP of the aqueous extract of *P. insularum*, were also detected in the HIP of the methanolic extract. Other genes were detected from pathways involving cellular transport and trafficking (*MUK1*, *PEP12* and *EXO84*), mitochondrial ribosomal structure (*RSM25* and *MRPL22*), transcriptional regulation (*RSF2*, *SPN1* and *SPT6*), as well as protein recycling and degradation (*UBP6*, *CDC34* and *HRD3*) (Carbrera *et al.*, 2013; Gracck & Wittmann-Liebold, 1998; Gardener *et al.*, 2000; Goebel *et al.*, 1988; Guo *et al.*, 1999; Krogan *et al.*, 2002; Park *et al.*, 1997; Rothman & Stevens, 1986; Saveanu *et al.*, 2001; Tkach *et al.*, 2012; Youdell *et al.*, 2008).

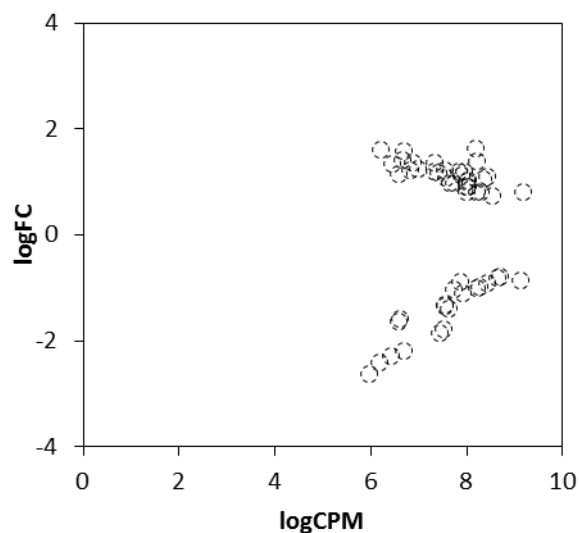


**Figure 4.5:** Scatterplot of the 51 heterozygous mutants with false discovery rate values less than 0.05 against the methanolic extract of *P. insularum*, plotted as logCPM vs logFC. Pooled heterozygous mutants were treated with 0.0001% v/v of methanolic extract over 20 generations, DNA extracted and barcode sequenced. The mutants with FDR < 0.05, are plotted using logCPM against logFC.

**Table 4.5: The 20 hypersensitive heterozygotes resulting from treatment with the methanol extract of *P. insularum*.** The data summarized herein are sorted by the logFC, with the lowest logFC at the top of the table, indicating the genes are sorted from most hypersensitive to the least hypersensitive true hits. logCPM, p-value and FDR values for all gene hits are shown, together with their gene names and biological functions obtained from the Saccharomyces Gene Database.

	logFC	logCPM	PValue	FDR	Gene	Biological Function
YFR055W	-2.60733	5.959965	2.74E-05	0.010818	IRC7	Beta-lyase involved in the production of thiols
YHL034C	-2.39046	6.17154	1.92E-05	0.009467	SBP1	Protein that binds eIF4G and has a role in repression of translation
YAR043C	-2.29016	6.416529	2.20E-04	0.040517	YAR043C	Does not encode a protein
YBR281C	-2.18888	6.670253	5.70E-05	0.016075	DUG2	Component of glutamine amidotransferase (GATase II)
YBR231C	-1.84337	7.406921	4.19E-07	0.001242	SWC5	Component of the SWR1 complex
YCR068W	-1.76099	7.493509	2.17E-05	0.009467	ATG15	Putative lipase required for lysis of autophagic and Cvt bodies
YDR156W	-1.62516	6.570473	4.22E-04	0.049541	RPA14	RNA polymerase I subunit A14
YLR075W	-1.58644	6.587466	8.90E-05	0.021095	RPL10	Ribosomal 60S subunit protein L10
YGL207W	-1.3877	7.596771	2.34E-04	0.040719	SPT16	Subunit of the heterodimeric FACT complex (Spt16p-Pob3p)
YGR148C	-1.32513	7.529734	4.21E-04	0.049541	RPL24B	Ribosomal 60S subunit protein L24B
YCR093W	-1.30638	7.517605	4.26E-04	0.049541	CDC39	Component of the CCR4-NOT1 core complex
YGR188C	-1.09262	7.911316	1.28E-04	0.027152	BUB1	Protein kinase involved in the cell cycle checkpoint into anaphase
YLR388W	-1.02036	7.70285	2.26E-04	0.040517	RPS29A	Protein component of the small (40S) ribosomal subunit
YIR019C	-0.98499	8.187611	5.28E-05	0.016	FLO11	GPI-anchored cell surface glycoprotein (flocculin)
YKL036C	-0.9641	8.243288	1.90E-04	0.03639	YKL036C	Dubious open reading frame
YDR536W	-0.90094	8.406403	2.40E-04	0.040719	STL1	Glycerol proton symporter of the plasma membrane
YGL040C	-0.88203	7.855504	4.05E-04	0.049541	HEM2	Aminolevulinatase; a homo-octameric enzyme, heme synthesis
YGL133W	-0.84329	9.108457	2.02E-05	0.009467	ITC1	Subunit of ATP-dependent Isw2p-Itc1p chromatin remodeling complex
YHR207C	-0.81185	8.620949	5.40E-05	0.016	SET5	Methyltransferase involved in methylation of histone H4 Lys5, -8, -12
YLL003W	-0.77468	8.670692	2.93E-04	0.044455	SFI1	Centrin (Cdc31p)-binding protein required for SPB duplication

**Table 4.6: The 31 heterozygous gene deletions with positive logFC and FDR < 0.05.** The data summarized herein are sorted by the logFC, with the lowest logFC at the top of the table, indicating the genes are sorted from least resistant to the most resistant to the methanolic extract of *P. insularum*. logCPM, p-value and FDR values for all gene hits are shown, together with their gene names and biological functions obtained from the Saccharomyces Gene Database.

	logFC	logCPM	PValue	FDR	common	Function
YHL019C	0.8082392	9.15137	3.11E-04	0.045973049	APM2	Protein of unknown function
YLR150W	0.8150514	8.188551	1.76E-04	0.035772533	STM1	Protein required for optimal translation under nutrient stress
YLR207W	0.8223704	7.986241	7.66E-05	0.018915263	HRD3	ER membrane protein that plays a central role in ERAD
YOR084W	0.8265312	8.28	1.19E-04	0.026229726	LPX1	Peroxisomal matrix-localised lipase
YJR127C	0.9049082	7.996086	4.00E-04	0.04954053	RSF2	Zinc-finger protein involved in transcriptional control
YOR304C-A	0.9281514	7.981128	2.48E-04	0.040821618	BIL1	Protein that binds Bud6p, role in actin cable assembly
YDR078C	0.9837623	7.645733	3.24E-04	0.045973049	SHU2	Component of the SHU complex, functions in promoting error-free DNA repair
YLR241W	0.9923575	7.711077	3.67E-04	0.048372791	CSC1	Calcium permeable gated cation channel
YLR262C-A	1.0079829	7.993725	3.26E-04	0.045973049	TMA7	Protein of unknown function, associates with ribosomes
YKR037C	1.046689	7.997847	1.12E-04	0.025605971	SPC34	Essential subunit of the Dam1 complex
YKR019C	1.0715253	8.323317	1.32E-07	0.000783566	IRS4	Protein involved in regulating phosphatidylinositol 4,5-biphosphate levels
YNL138W	1.0798731	7.540887	1.81E-04	0.035772533	SRV2	Cyclase-associated protein
YGR116W	1.1179655	8.407091	4.41E-05	0.014538754	SPT6	Nucleosome remodelling protein
YPL070W	1.1331816	7.868743	4.42E-05	0.014538754	MUK1	Guanine nucleotide exchange factor, involved in transport and trafficking
YOL052C	1.151685	6.55401	3.63E-04	0.048372791	SPE2	S-adenosylmethioine decarboxylase, biosynthesis of spermidine and spermine
YNL126W	1.1862742	7.383182	9.37E-06	0.009255003	SPC98	Component of the microtubule-nucleating gamma-tubulin complex
YIL093C	1.2049165	7.832839	2.81E-06	0.003462807	RSM25	Mitochondrial ribosomal protein of the small subuni
YPR133C	1.2066575	7.915618	3.87E-04	0.04954053	SPN1	Protein involved in RNA polymerase II transcription
YGL008C	1.2176259	7.3241	1.62E-05	0.009466682	PMA1	Plasma membrane P2-type H <sup>+</sup> -ATPase, pumps protons out of the cell
YOR036W	1.2323278	7.533333	2.10E-05	0.009466682	PEP12	Target membrane receptor, t-SNARE, transport and trafficking
YBR102C	1.2350682	6.803939	7.12E-05	0.018885621	EXO84	Exocyst subunit with dual roles in exocytosis and spliceosome assembly
YBR265W	1.2465347	6.964784	3.52E-04	0.048372791	TSC10	3-ketospinganine reductase
YMR072W	1.3562235	6.439788	2.24E-05	0.009466682	ABF2	Mitochondrial DNA-binding protein
YOL019W	1.3691733	7.306941	2.70E-04	0.042688993	YOL019W	Protein of unknown function
YFR010W	1.3863256	6.847775	7.33E-05	0.018885621	UBP6	Ubiquitin-specific protease
YIL141W	1.4026674	8.192527	8.90E-07	0.001757784	YIL141W	Dubious ORF
YDR054C	1.4332071	6.6478	1.64E-05	0.009466682	CDC34	Ubiquitin-conjugation enzyme
YGL232W	1.5966002	6.65792	3.79E-05	0.01405686	TAN1	Putative tRNA acetyltransferase
YNL177C	1.6220951	6.186091	2.23E-05	0.009466682	MRPL22	Mitochondrial ribosomal protein of the large subunit
YNL062C	1.6388785	8.168126	2.92E-06	0.003462807	GCD10	Subunit of tRNA (1-methyladenosine) methyltransferase with Gcd14p

To ascertain the legitimacy of the mutants identified with negative logFC < -0.75 and FDR < 0.05, the 20 heterozygous mutants mentioned above (Table 4.5) were grown in the presence and absence of the *P. insularum* methanolic extract (0.0002% v/v). Seven mutants were shown to be significantly hypersensitive compared to the WT BY4743 control in the presence of the extract (Fig 4.6). These strains include *RPL10* involved in ribosomal biogenesis (Planta & Mager, 1998), *SPT16* involved in FACT(facilitator of chromatin transactions) complex (Malone *et al.*, 1991), *FLO11* involved in flocculation (Lo & Dranginis, 1996), *SET5* involved in methylation of histones (Nislow *et al.*, 1997), *CDC39* involved in the CCR4-NOT complex, which is a complex involved in mRNA metabolism, including the repression and activation of mRNA initiation (Breter *et al.*, 1983), and *ATG15* involved in the lysis of autophagic and Cvt (cytoplasm-to-vacuole) transport bodies (Klonsky *et al.*, 2003). The growth of the dubious ORF *YKL036C* was also shown to be significantly impaired in the presence of the methanolic extract of *P. insularum*.

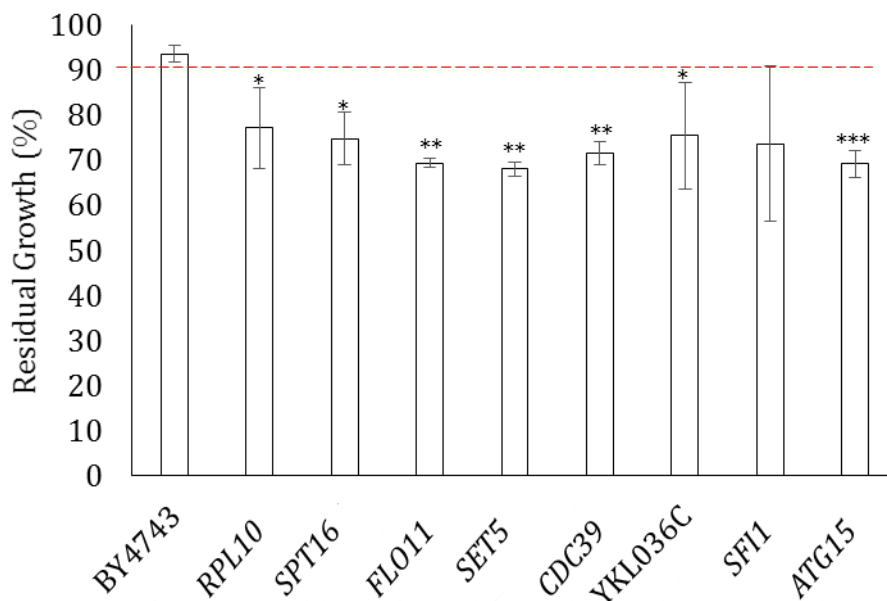


**Figure 4.6: Validations of the heterozygote genes detected to be hypersensitive to the methanolic extract of *P. insularum*.** Heterozygous mutants were individually grown in the presence of the methanolic extract in triplicate, and compared to the control treatment. Mutants exhibiting growth less than 90% consistently across the three triplicates are plotted compared to WT (BY4743), are reported as mean residual growth  $\pm$  SD. The p-values were calculated using a one tailed Student's t-test (\*: p-value < 0.05, \*\*: p-value < 0.01, \*\*\*: p-value < 0.001).

#### 4.3.4. HOP Analysis of the *P. insularum* Methanolic Extract

To identify the genes buffering the bioactivity of the methanolic extract from *P. insularum* leaves, a HOP analysis was conducted using Bar-seq analysis. The pooled homozygous library was grown in the presence and absence of 0.0001% v/v of the methanolic extract for 20 generations. Using FDR < 0.05 as a cutoff for statistical significance, there were 106 deletion mutants with positive logFC ranging from 0.5 to 4.6, and 182 deletion mutants with negative logFC ranging from 0.5 to -5.3, suggesting these homozygous deletion strains grew significantly different from that of WT as a result of the methanolic extract treatment (Fig 4.7). The recovery of 288 total mutants sensitive in the HOP analysis of the methanolic *P. insularum* extract was markedly greater than the 30 mutants that were sensitive in the HOP analysis of the aqueous *P. insularum* extract. Analysis of this list of 306 genes for GO enrichment found 4 biological processes were enriched, including the negative regulation of transcription from RNA polymerase II promoter (21 genes, p-value 0.006881), cytoplasmic translation (23 genes, p-value 0.020136), histone deacetylation (8 genes, 0.023809) and protein deacetylation (8 genes, p-value 0.046855). One molecular function was enriched, which involved structural constituent of ribosome (26 genes, p-value 0.010379). Eight molecular components were enriched, including cytosolic large ribosomal subunit (18 genes, p-value 1.084534<sup>-4</sup>), cytosolic ribosome (24 genes, p-value 2.613199<sup>-4</sup>), Set3 complex (5 genes, p-value 0.003051), large ribosome subunit (20 genes, p-value 0.003838), ribosomal subunit (27 genes, p-value 0.006386) and cytosolic part (26 genes, p-value 0.014001).

The 182 gene deletions with reduced growth due to the *P. insularum* methanolic extract are involved in a variety of functions (Table 4.7), including cytoplasmic translation, ribosomal biogenesis, and transcriptional regulation (*NOT3*, *NAP1*, *HDA2*, *HDA3*, *RRM3* and *SWP82*) (Cairns *et al.*, 1994; Collart & Struhl, 1994; Ishimi & Kikuchi, 1991; Ivessa *et al.*, 2000; Wu *et al.*, 2000; Inadome *et al.*, 2005; Muren *et al.*, 2001; Piper *et al.*, 1995; Rothman *et al.*, 1989; Wichmann *et al.*, 1992; Yompakdee *et al.*, 1996). Several dubious ORFs and proteins of unknown functions were also detected to be hypersensitive, including *YLR407W*, *RIM9*, *YPL261C*, *YCR050C*, *YCR049C*, *FYV1*,

*YER084W* and *YDR417C*. Interestingly, both *YCR049C* and *YCR050C* detected as hypersensitive hits overlap *ARE1*, which encodes acyl-CoA:sterolacyltransferase, an ER enzyme involved in sterol esterification (Yang *et al.*, 1996; Yu *et al.*, 1996).

The 106 genes corresponding to the deletion mutants with improved growth in the presence of the extract (Table 4.8) are involved in a variety of biological processes, including DNA-templated regulation of transcription (31 genes, *e.g.* *SIF2*, *MRC1*, *SNT1*, *GIS1*, *HTA1*, *YAP6*, *SPT2*, *SPT3*, *MIG3*, *LRS4*, *IES1* and *PGD1*), regulation of cellular macromolecule biosynthetic pathway (32 genes) and the regulation of nitrogen compound metabolic process involving 33 genes. As these processes are related, genes were detected from all three enriched biological processes, such as *SIF2*, *SPT2* and *SPT3*.

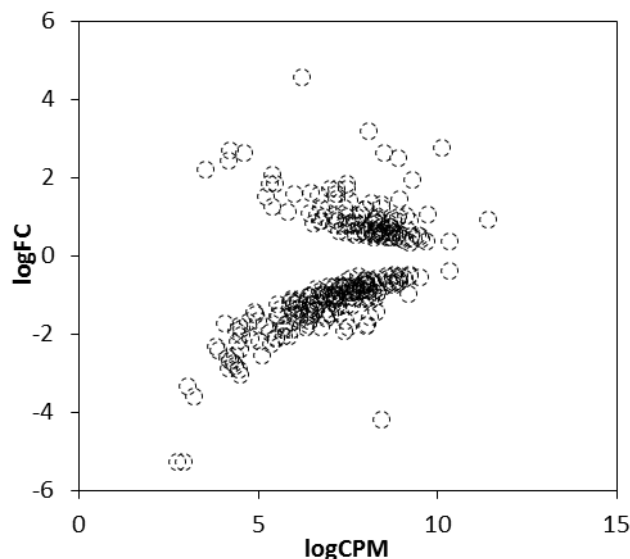


**Figure 4.7:** Scatterplot of 288 hypersensitive homozygous mutants against the methanolic extract of *P. insularum*. Pooled homozygous deletion mutants were grown in the presence of 0.0001% v/v of methanolic *P. insularum* extract over 20 generations, before DNA extraction and barcode sequenced. Mutants with calculated FDR values less than 0.05 were plotted, using logCPM vs logFC.

**Table 4.7: Hypersensitive homozygous deletions against treatment with the methanol extract of *P. insularum*.** The data summarized herein are sorted by the logFC, with the lowest logFC at the top of the table, indicating the genes are sorted from most hypersensitive to the least hypersensitive true hits. logCPM, p-value and FDR values for all gene hits are shown, together with their gene names and biological functions obtained from the Saccharomyces Gene Database.

	logFC	logCPM	PValue	FDR	Gene	Biological Function
YLR131C	-4.17683	8.402519	9.20E-05	4.83E-03	ACE2	Transcription factor required for septum destruction after cytokinesis
YFL025C	-3.57606	3.189629	1.08E-04	5.26E-03	BST1	GPI inositol deacylase of the endoplasmic reticulum (ER)
YDL047W	-3.336	3.010566	2.85E-04	1.08E-02	SIT4	Type 2A-related serine-threonine phosphatase
YDL081C	-3.0367	4.471486	3.21E-05	2.29E-03	RPP1A	Ribosomal stalk protein P1 alpha
YML001W	-2.88744	4.426691	1.12E-06	1.64E-04	YPT7	Rab family GTPase
YML073C	-2.88005	4.1334	6.02E-05	3.43E-03	RPL6A	Ribosomal 60S subunit protein L6A
YOL052C	-2.79799	4.312444	1.07E-03	2.71E-02	SPE2	S-adenosylmethionine decarboxylase; required for the biosynthesis of spermidine and spermine
YJL121C	-2.74276	4.292456	1.03E-03	2.63E-02	RPE1	D-ribulose-5-phosphate 3-epimerase
YCL058C	-2.66391	4.177405	1.85E-05	1.46E-03	FYV5	Protein involved in regulation of the mating pathway
YNL055C	-2.59417	4.104447	6.75E-04	1.95E-02	POR1	Mitochondrial porin (voltage-dependent anion channel)
YKL184W	-2.54098	4.340093	1.33E-03	3.15E-02	SPE1	Ornithine decarboxylase; catalyzes the first step in polyamine biosynthesis
YLL043W	-2.53832	5.065306	3.81E-05	2.54E-03	FPS1	Aquaglyceroporin, plasma membrane channel
YBL027W	-2.40995	3.853045	2.00E-05	1.56E-03	RPL19B	Ribosomal 60S subunit protein L19B
YNR006W	-2.38934	4.473799	8.20E-05	4.38E-03	VPS27	Endosomal protein that forms a complex with Hse1p
YJR074W	-2.29337	3.781547	2.77E-04	1.06E-02	MOG1	Conserved nuclear protein that interacts with GTP-Gsp1p
YBR106W	-2.2413	5.333605	6.13E-04	1.82E-02	PHO88	Probable membrane protein; involved in phosphate transport, secretory protein maturation
YOR070C	-2.1744	5.012808	1.52E-03	3.48E-02	GYP1	Cis-golgi GTPase-activating protein (GAP) for yeast Rabs
YMR269W	-2.16336	4.381987	2.18E-05	1.62E-03	TMA23	Nucleolar protein implicated in ribosome biogenesis
YJL204C	-2.1117	5.473082	4.81E-06	4.68E-04	RCY1	F-box protein involved in recycling endocytosed proteins
YGL124C	-2.09976	4.765319	3.48E-05	2.37E-03	MON1	Subunit of a heterodimeric guanine nucleotide exchange factor (GEF)
YDR435C	-2.08545	5.45808	6.05E-06	5.78E-04	PPM1	Carboxyl methyltransferase
YIL038C	-2.06305	5.678219	2.65E-06	2.90E-04	NOT3	Subunit of CCR4-NOT global transcriptional regulator
YEL054C	-2.04165	5.827001	2.66E-04	1.02E-02	RPL12A	Ribosomal 60S subunit protein L12A
YNR051C	-2.02342	4.5108	2.30E-03	4.71E-02	BRE5	Ubiquitin protease cofactor
YAL053W	-1.95589	5.273208	2.38E-05	1.74E-03	FLC2	Putative calcium channel involved in calcium release under hypotonic stress
YOR275C	-1.9199	7.373076	1.54E-09	5.38E-07	RIM20	Protein involved in proteolytic activation of Rim101p
YPL065W	-1.90951	4.342689	1.04E-03	2.65E-02	VPS28	Component of the ESCRT-I complex
YKL149C	-1.88056	5.683507	1.27E-06	1.80E-04	DBR1	RNA lariat debranching enzyme
YLR407W	-1.87084	5.886563	1.95E-04	7.99E-03	YLR407W	Putative protein of unknown function
YMR063W	-1.85593	4.48586	4.50E-04	1.48E-02	RIM9	Plasma membrane protein of unknown function

**Table 4.7: Cont'd**

	logFC	logCPM	PValue	FDR	Gene	Biological Function
YKL176C	-1.82436	5.671488	2.19E-06	2.64E-04	LST4	Subunit of the Lst4p-Lst7p GTPase activating protein complex for Gtr2p
YPL261C	-1.82045	6.729207	3.79E-09	1.12E-06	YPL261C	Dubious open reading frame
YIL110W	-1.81577	7.487026	5.88E-05	3.39E-03	HPM1	AdoMet-dependent methyltransferase
YKR007W	-1.80334	6.279483	1.66E-07	3.51E-05	MEH1	Component of the EGO and GSE complexes
YCR050C	-1.80029	4.444633	7.75E-04	2.17E-02	YCR050C	Non-essential protein of unknown function
YOR043W	-1.78456	7.960328	4.74E-04	1.53E-02	WHI2	Protein required for full activation of the general stress response
YIL148W	-1.77135	5.131166	1.56E-04	6.68E-03	RPL40A	Ubiquitin-ribosomal 60S subunit protein L40A fusion protein
YPL170W	-1.762	8.022655	2.02E-10	9.22E-08	DAP1	Heme-binding protein; involved in regulation of cytochrome P450 protein Erg11p
YKR048C	-1.74429	6.358735	4.28E-04	1.42E-02	NAP1	Histone chaperone
YML017W	-1.73984	5.710861	3.81E-04	1.31E-02	PSP2	Asn rich cytoplasmic protein that contains RGG motifs, role in mitochondria mRNA splicing
YDR195W	-1.71316	4.04087	2.33E-03	4.72E-02	REF2	RNA-binding protein; involved in the cleavage step of mRNA 3'-end
YAR014C	-1.68019	4.691206	2.55E-03	4.98E-02	BUD14	Protein involved in bud-site selection
YOR030W	-1.66988	5.887894	2.60E-04	1.01E-02	DFG16	Probable multiple transmembrane protein, possible involvement with Rim proteins
YDR389W	-1.65668	4.984338	1.84E-04	7.59E-03	SAC7	GTPase activating protein (GAP) for Rho1p
YFR008W	-1.6454	6.388552	2.44E-06	2.83E-04	FAR7	Protein involved in recovery from pheromone-induced cell cycle arrest
YPR179C	-1.64492	7.404422	3.07E-08	7.28E-06	HDA3	Subunit of the HDA1 histone deacetylase complex
YDR025W	-1.63371	6.100309	6.03E-07	9.93E-05	RPS11A	Protein component of the small (40S) ribosomal subunit
YBR296C	-1.5986	6.867357	1.62E-06	2.09E-04	PHO89	Plasma membrane Na <sup>+</sup> /Pi cotransporter
YKR027W	-1.56471	8.102546	2.01E-16	1.32E-13	BCH2	Member of the ChAPs (Chs5p-Arf1p-binding proteins) family
YHL007C	-1.54929	6.260396	1.11E-05	9.39E-04	STE20	Cdc42p-activated signal transducing kinase
YDR500C	-1.53462	5.55685	1.23E-03	3.00E-02	RPL37B	Ribosomal 60S subunit protein L37B
YGL031C	-1.52388	6.817099	5.54E-07	9.39E-05	RPL24A	Ribosomal 60S subunit protein L24A
YDL130W	-1.51924	6.441736	5.34E-05	3.13E-03	RPP1B	Ribosomal protein P1 beta
YNL294C	-1.51679	6.352535	6.13E-05	3.43E-03	RIM21	pH sensor molecule, component of the RIM101 pathway
YHR031C	-1.50966	5.511805	2.20E-04	8.75E-03	RRM3	DNA helicase involved in rDNA replication and Ty1 transposition
YCR049C	-1.50055	6.98131	2.53E-07	4.84E-05	YCR049C	Dubious open reading frame
YDR024W	-1.49943	6.121972	1.06E-04	5.24E-03	FYV1	Dubious open reading frame
YNL323W	-1.4747	4.880125	1.99E-03	4.25E-02	LEM3	Membrane protein of the plasma membrane and ER
YDR295C	-1.47261	7.262973	6.50E-07	1.04E-04	HDA2	Subunit of the HDA1 histone deacetylase complex
YER177W	-1.47016	6.978217	9.66E-04	2.50E-02	BMH1	14-3-3 protein, major isoform

**Table 4.7: Cont'd**

	logFC	logCPM	PValue	FDR	Gene	Biological Function
YER084W	-1.45349	6.405747	6.31E-06	5.94E-04	YER084W	Protein of unknown function
YKR035W-A	-1.42932	4.860043	1.35E-03	3.17E-02	DID2	Class E protein of the vacuolar protein-sorting (Vps) pathway
YKL190W	-1.39118	6.582962	1.04E-04	5.23E-03	CNB1	Calcineurin B; regulatory subunit of calcineurin which regulates Crz1p
YGL045W	-1.37923	6.536361	1.08E-04	5.26E-03	RIM8	Protein involved in proteolytic activation of Rim101p
YDR417C	-1.36016	6.395482	4.43E-05	2.79E-03	YDR417C	Dubious open reading frame
YOR246C	-1.34796	6.075999	5.75E-04	1.72E-02	ENV9	Protein proposed to be involved in vacuolar functions
YLR185W	-1.34586	5.587265	4.15E-04	1.39E-02	RPL37A	Ribosomal 60S subunit protein L37A
YMR238W	-1.34429	6.092986	1.84E-04	7.59E-03	DFG5	Putative mannosidase
YGL253W	-1.34219	6.855512	1.79E-04	7.47E-03	HXK2	Hexokinase isoenzyme 2
YLR047C	-1.32811	5.868224	1.23E-03	3.00E-02	FRE8	Protein with sequence similarity to iron/copper reductases; involved in iron homeostasis
YHR203C	-1.32	6.116239	7.89E-04	2.19E-02	RPS4B	Protein component of the small (40S) ribosomal subunit
YMR052C-A	-1.29154	7.172126	2.43E-06	2.83E-04	YMR052C-A	Dubious open reading frame
YAR042W	-1.29037	7.200968	4.12E-04	1.39E-02	SWH1	Protein similar to mammalian oxysterol-binding protein
YHR200W	-1.27628	6.365135	1.51E-04	6.62E-03	RPN10	Non-ATPase base subunit of the 19S RP of the 26S proteasome
YNL032W	-1.26573	7.451078	4.57E-07	8.47E-05	SIW14	Tyrosine phosphatase involved in actin organization and endocytosis
YMR071C	-1.2503	7.572523	4.43E-05	2.79E-03	TVP18	Integral membrane protein; localized to late Golgi vesicles along with the v-SNARE Tlg2p
YCR087W	-1.24338	6.654061	1.73E-04	7.28E-03	YCR087W	Dubious open reading frame
YGL005C	-1.24176	5.510767	2.35E-03	4.74E-02	COG7	Component of the conserved oligomeric Golgi complex
YGR133W	-1.24127	6.420837	8.45E-04	2.28E-02	PEX4	Peroxisomal ubiquitin conjugating enzyme
YHR066W	-1.24042	5.988224	1.96E-03	4.22E-02	SSF1	Constituent of 66S pre-ribosomal particles
YGL046W	-1.2401	6.4959	1.97E-03	4.22E-02	YGL046W	Merged ORF, does not encode a protein, overlaps with <i>RIM8</i>
YGL035C	-1.23062	7.198744	9.40E-07	1.47E-04	MIG1	Transcription factor involved in glucose repression
YGR054W	-1.20427	7.077133	1.41E-06	1.94E-04	YGR054W	Eukaryotic initiation factor (eIF) 2A
YBR277C	-1.19526	6.067662	1.15E-03	2.88E-02	YBR277C	Dubious open reading frame
YFL049W	-1.19309	6.652561	1.22E-04	5.59E-03	SWP82	Member of the SWI/SNF chromatin remodeling complex
YBR077C	-1.1619	5.891383	9.79E-04	2.51E-02	SLM4	Component of the EGO and GSE complexes, microautophagy and amino acid sorting
YEL053C	-1.15791	5.880754	2.30E-03	4.71E-02	MAK10	Non-catalytic subunit of N-terminal acetyltransferase of the NatC type
YBR300C	-1.12914	8.095591	4.36E-06	4.31E-04	YBR300C	Dubious open reading frame
YIL133C	-1.11967	6.087205	5.20E-04	1.64E-02	RPL16A	Ribosomal 60S subunit protein L16A
YNR032W	-1.10894	8.115949	6.60E-09	1.78E-06	PPG1	Putative serine/threonine protein phosphatase

**Table 4.8: Top 90 gene deletions exhibiting improved growth in the presence of the methanolic extract of *P. insularum*.** The data summarized herein are sorted by the logFC, with the lowest logFC at the top of the table, indicating the genes are sorted from most hypersensitive to the least hypersensitive true hits. logCPM, p-value and FDR values for all gene hits are shown, together with their gene names and biological functions obtained from the Saccharomyces Gene Database.

	logFC	logCPM	PValue	FDR	Gene	Biological Function
YDR392W	4.5919828	6.188196	8.80E-17	7.00E-14	SPT3	Subunit of the SAGA and SAGA-like transcriptional regulatory complex
YGL255W	3.2012021	8.034208	1.72E-04	7.28E-03	ZRT1	High-affinity zinc transporter of the plasma membrane
YPR065W	2.7891216	10.089961	2.01E-36	1.19E-32	ROX1	Heme-dependent repressor of hypoxic genes
YDR401W	2.718588	4.179569	2.33E-04	9.21E-03	YDR401W	Dubious ORF
YLR055C	2.6536338	8.470276	1.29E-21	2.55E-18	SPT8	Subunit of the SAGA transcriptional regulatory complex
YGL025C	2.6302753	4.555716	7.39E-04	2.10E-02	PGD1	Subunit of the RNA polymerase II mediator complex
YML007W	2.5193522	8.876484	8.08E-20	1.20E-16	YAP1	Transcriptional factor required for oxidative stress tolerance
YNL236W	2.441835	4.138878	1.00E-06	1.52E-04	SIN4	Subunit of the RNA polymerase II mediator complex
YNL107W	2.2009873	3.504036	2.51E-03	4.94E-02	YAF9	Subunit of the NuA4 histone H4 acetyltransferase and SWR1 complexes
YML010C-B	2.0865442	5.373827	1.53E-04	6.64E-03	YML010C-B	Dubious ORF
YPR064W	1.9660034	9.279071	1.05E-19	1.25E-16	YPR064W	Dubious ORF
YDL002C	1.8663376	7.433041	9.44E-17	7.00E-14	NHP10	Non-essential INO80 chromatin remodeling complex subunit
YBL047C	1.8554673	5.274969	3.37E-04	1.22E-02	EDE1	Scaffold protein involved in the formation of early endocytic sites
YNL079C	1.8413202	5.446698	1.23E-04	5.59E-03	TPM1	Major isoform of tropomyosin, stabilizes cables and filaments
YGR102C	1.7393452	7.425531	3.67E-13	2.18E-10	GTF1	Subunit of the trimeric GatFAB Amido Transferase (AdT) complex
YBL065W	1.73587	7.144636	4.68E-04	1.53E-02	YBL065W	Dubious ORF
YDL082W	1.7347822	6.987405	1.97E-03	4.22E-02	RPL13A	Ribosomal 60S subunit protein L13A
YDR268W	1.6410044	6.431576	2.37E-07	4.69E-05	MSW1	Mitochondrial tryptophanyl-tRNA synthetase
YKL032C	1.5996274	7.160644	2.60E-09	8.55E-07	IXR1	Transcriptional repressor that regulates hypoxic genes during normoxia
YML094W	1.5928865	5.975458	2.57E-03	4.98E-02	GIM5	Subunit of the heterohexameric cochaperone prefoldin complex
YDR439W	1.5765991	6.641002	3.09E-06	3.21E-04	LRS4	Nucleolar protein that forms complex with Csm1p
YLR233C	1.5382738	5.194209	5.75E-04	1.72E-02	EST1	TLC1 RNA-associated factor involved in telomere length regulation
YLL013C	1.4729478	8.923422	4.06E-18	4.01E-15	PUF3	Protein of the mitochondrial outer surface
YEL050C	1.4576679	7.15631	8.10E-04	2.22E-02	RML2	Mitochondrial ribosomal protein of the large subunit (L2)
YDL146W	1.4153258	7.523979	5.19E-05	3.11E-03	LDB17	Protein involved in the regulation of endocytosis
YBR216C	1.3548683	8.137438	3.07E-09	9.59E-07	YBP1	Protein involved in cellular response to oxidative stress
YCR033W	1.3379052	8.412615	1.39E-12	7.50E-10	SNT1	Subunit of the Set3C deacetylase complex
YOR002W	1.2553948	5.371411	4.89E-04	1.57E-02	ALG6	Alpha 1,3 gluosyltransferase
YER028C	1.2424489	8.419123	2.92E-10	1.24E-07	MIG3	Transcriptional regulator
YDR314C	1.2295853	6.720442	1.59E-03	3.62E-02	RAD34	Protein involved in nucleotide excision repair (NER)

**Table 4.8 Cont'd**

	logFC	logCPM	PValue	FDR	Gene	Biological Function
YBR103W	1.2090631	7.931573	4.56E-10	1.80E-07	SIF2	WD40 repeat-containing subunit of Set3C histone deacetylase complex
YFL013C	1.189818	7.957044	8.59E-08	1.89E-05	IES1	Subunit of the INO80 chromatin remodeling complex
YKL114C	1.1306098	5.80748	4.77E-04	1.54E-02	APN1	Major apurinic/apyriminidinic endonuclease
YDR225W	1.0936336	6.400817	2.32E-03	4.72E-02	HTA1	Histone H2A
YGL043W	1.0738261	6.622582	3.79E-04	1.31E-02	DST1	General transcription elongation factor TFIIIS
YJL052W	1.0688412	9.686078	2.58E-08	6.38E-06	TDH1	Glyceraldehyde-3-phosphate dehydrogenase (GAPDH) isozyme 1
YKL115C	1.0546653	7.845915	8.45E-08	1.89E-05	YKL115C	Dubious ORF
YIR037W	1.0424254	9.106641	1.41E-08	3.62E-06	HYR1	Thiol peroxidase
YOR251C	1.0382226	7.098727	9.24E-04	2.43E-02	TUM1	Rhodanese domain sulfur transferase
YOR189W	1.0197604	8.262246	5.00E-05	3.05E-03	IES4	Component of the INO80 chromatin remodeling complex
YMR156C	1.0159901	7.44248	3.90E-04	1.33E-02	TPP1	DNA 3'-phosphatase
YKL134C	1.0111059	6.797414	1.37E-03	3.19E-02	OCT1	Mitochondrial intermediate peptidase
YFL013W-A	0.9959433	8.886304	1.21E-10	5.99E-08	YFL013W-A	Dubious ORF
YJL169W	0.9917292	7.714283	1.44E-06	1.94E-04	YJL169W	Dubious ORF
YER092W	0.9706077	8.25769	2.51E-06	2.86E-04	IES5	Non-essential INO80 chromatin remodeling complex subunit
YFL033C	0.9464532	11.37304	4.19E-25	1.24E-21	RIM15	Protein kinase involved in cell proliferation in response to nutrients
YGR012W	0.9434509	7.120897	4.03E-05	2.63E-03	MCY1	Putative cysteine synthase
YHR009C	0.9346516	8.731417	5.17E-10	1.92E-07	TDA3	Putative oxidoreductase involved in late endosome to Golgi transport
YGL028C	0.9106868	6.718832	6.42E-04	1.88E-02	SCW11	Cell wall protein with similarity to glucanases
YPL049C	0.9062566	7.204247	1.16E-03	2.90E-02	DIG1	MAP kinase-responsive inhibitor of the Ste12p transcription factor
YGL087C	0.9054502	8.186316	2.77E-06	2.98E-04	MMS2	Ubiquitin-conjugating enzyme variant
YCL060C	0.9043242	6.676263	1.96E-03	4.22E-02	<NA>	Merged ORF with MRC1: S-phase checkpoint protein
YLR150W	0.9013719	9.211196	2.24E-07	4.58E-05	STM1	Required for optimal translation under nutrient stress
YIL035C	0.8969374	8.202944	1.53E-06	2.02E-04	CKA1	Alpha catalytic subunit of casein kinase 2 (CK2)
YER161C	0.8947903	8.848305	4.83E-07	8.68E-05	SPT2	Protein involved in negative regulation of transcription
YPL182C	0.8799259	7.697786	1.21E-04	5.59E-03	YPL182C	Dubious ORF
YBR058C	0.858321	8.38698	1.21E-05	1.01E-03	UBP14	Ubiquitin-specific protease
YDR158W	0.8485721	7.555994	2.47E-03	4.89E-02	HOM2	Aspartic beta semi-aldehyde dehydrogenase
YIL093C	0.8481479	8.633073	2.09E-06	2.58E-04	RSM25	Mitochondrial ribosomal protein of the small subunit

**Table 4.8 Cont'd**

	logFC	logCPM	PValue	FDR	Gene	Biological Function
YCL005W	0.8322289	6.525532	1.68E-03	3.78E-02	LDB16	Protein involved in lipid droplet assembly
YDR391C	0.8199758	7.870653	9.87E-05	5.00E-03	YDR391C	Putative protein of unknown function
YPL150W	0.8107782	7.097978	3.35E-05	2.34E-03	YPL150W	Protein kinase of unknown cellular role
YIL112W	0.8104066	8.153484	8.47E-05	4.48E-03	HOS4	Subunit of the Set3 complex
YPL202C	0.8015511	7.422982	1.81E-03	4.01E-02	AFT2	Iron-regulated transcriptional activator
YOR371C	0.7975345	7.529178	3.31E-04	1.20E-02	GPB1	Multistep regulator of cAMP-PKA signalling
YBL013W	0.7941395	7.664035	2.14E-04	8.56E-03	FMT1	Methionyl-tRNA formyltransferase
YCR006C	0.7802903	7.32165	7.66E-04	2.15E-02	YCR006C	Dubious ORF
YHR206W	0.7698855	8.578876	3.25E-04	1.19E-02	SKN7	Nuclear response regulator and transcription factor
YDR096W	0.753302	8.4082	7.71E-05	4.27E-03	GIS1	Histone demethylase and transcription factor
YPL148C	0.7516617	8.650217	5.28E-07	9.20E-05	PPT2	Phosphopantethrein:protein transferase
YJL017W	0.7416848	8.674153	2.02E-03	4.27E-02	<NA>	Merged ORF
YIL123W	0.7075129	8.333465	1.18E-04	5.53E-03	SIM1	Protein of the SUN family
YBR148W	0.699351	8.701616	8.63E-06	7.75E-04	YSW1	Protein required for normal prospore membrane formation
YOR267C	0.6864597	8.614525	3.50E-04	1.25E-02	HRK1	Protein kinase
YMR075C-A	0.6839848	8.173032	1.64E-04	7.00E-03	YMR075C-A	Dubious ORF
YMR037C	0.6818021	8.285859	1.56E-05	1.28E-03	MSN2	Stress-responsive transcriptional activator
YGL194C	0.6774102	7.898106	1.05E-04	5.23E-03	HOS2	Histone-deacetylase and subunit of Set3 and Rpd3L complexes
YDR259C	0.674842	9.130055	2.08E-05	1.56E-03	YAP6	Transcriptional factor
YJL168C	0.6564513	7.212665	2.18E-03	4.53E-02	SET2	Histone methyltransferase with a role in transcriptional elongation
YLL015W	0.6508324	8.273196	6.41E-04	1.88E-02	BPT1	ABC type transmembrane transport of MRP/CFTR family
YLR304C	0.6239353	7.395869	8.88E-04	2.37E-02	ACO1	Aconitase
YNL116W	0.6238826	8.487863	4.90E-05	3.05E-03	DMA2	Ubiquitin-protein ligase (E3)
YPL203W	0.6201166	7.955273	9.36E-04	2.44E-02	TPK2	cAMP-dependent protein kinase catalytic subunit
YHR163W	0.6198133	7.620024	3.23E-04	1.19E-02	SOL3	6-phosphogluconolactonase
YGL151W	0.6183187	8.184705	1.24E-03	3.00E-02	NUT1	Component of the RNA polymerase II mediator complex
YNL105W	0.6155233	8.708582	3.48E-05	2.37E-03	RRT16	Dubious ORF
YLR393W	0.6132971	7.785249	9.55E-04	2.48E-02	ATP10	Assembly factor for the F0 sector of mitochondrial F1F0 ATP synthase
YJL057C	0.6105927	7.989382	8.98E-04	2.39E-02	IKS1	Protein kinase of unknown cellular role

To validate the Bar-seq results, we grew the 90 homozygous gene deletion strains with the lowest logFC values (FDR < 0.05) in the presence and absence of the methanolic extract (0.0002% v/v) compared to the growth of the BY4743 WT strain. Of the 90 strains, 30 exhibited significantly reduced growth in the methanolic extract (Fig 4.8). The most hypersensitive gene deletion detected with approximately 80% growth inhibition compared to WT growth inhibition at 10% was *HDA3*, a component of the *HDA1* histone deacetylase complex (Carmen *et al.*, 1996). The deletion of *RPL12A*, the 12A subunit of the 60S ribosomal subunit (Planta & Mager, 1998), was found to be the next most hypersensitive gene deletion, exhibiting approximately 70% growth inhibition. Other gene deletions significantly sensitive to the methanolic extracts were involved in ribosomal structure and biogenesis (*RPL19B*, *RPP1B*, *RPL37A*), GTPase activation (*YPT7*, *GYP1*, *MOG1*, *LST4*, *SAC7*), and also calcium, sodium and phosphate transport (*FLC2*, *PHO89*). Gene deletions related to the iron chelation phenotype in Chapter 3 were also recovered, such as *DAP1*, *WHI2*, *BUD14*, *DID2* and *NAP1*. These gene deletions are particularly interesting since the homozygous diploid deletion strains (this chapter) and the haploid deletion strains (Chapter 3) independently identified iron metabolism as a mechanism of action of *P. insularum* extracts.

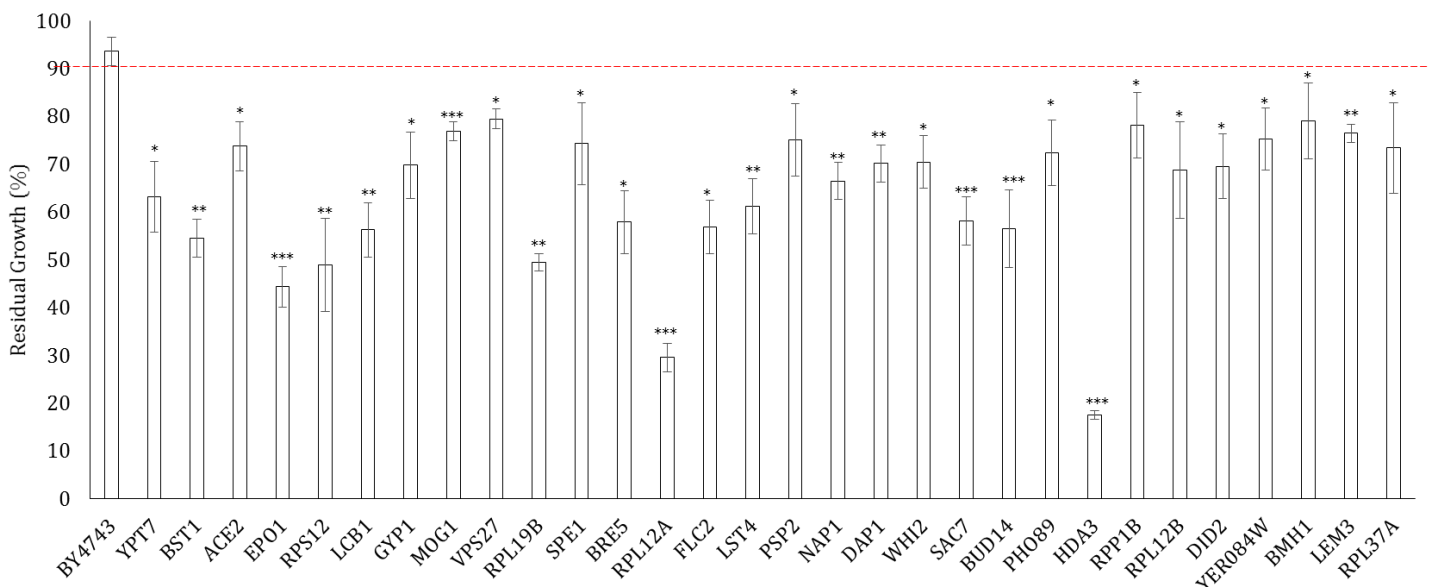


**Figure 4.8: Validations of the HOP hits of the methanolic extract of *P. insularum*.** The 90 gene deletions with the lowest logFC values were selected for liquid-based growth validations, the residual growths of which were compared to the BY4743 WT control. The red line indicates the 90% residual growth mark for the WT control, and the 30 gene deletions plotted were those with residual growths less than 90% consistently across the three triplicates are plotted, reported is mean residual growth  $\pm$  SD. Plotted is the average across the three triplicates, the error bars signifying the standard deviation. The p-values were calculated using a one tailed Student's t-test (\*: p-value < 0.05, \*\*: p-value < 0.01, \*\*\*: p-value < 0.001).

---

#### 4.4. Discussion

This chapter employed genome-wide, barcode sequencing-based HIP-HOP analyses to elucidate the genes and pathways regulated by the aqueous and methanolic extracts of *P. insularum*. Homozygous and heterozygous gene deletions were identified as hypersensitive to the extracts based on barcode sequence abundance. Specifically, the HIP analysis of the aqueous extract of *P. insularum* identified a total 51 mutants with altered growth, 25 of which were identified as hypersensitive, while 26 were identified as having improved growth in the presence of the extract. Similarly, the HIP analysis of the methanolic extract also identified 51 mutants with altered growth, although 20 were identified as hypersensitive, with the remaining 31 exhibiting positive logFC indicative of improved growth. The HOP analysis of the aqueous extract produced 30 genes with affected growth in the presence of the aqueous extract of *P. insularum*, with 18 having reduced growth, and 12 with improved growth. Contrastingly, the HOP analysis of the methanolic extract identified a large number of 307 gene deletions with affected growth, 182 of which were hypersensitive, 106 of which exhibited improved growth. However, the results for the heterozygous mutants did not validate when the strains were grown independently in contrast to the competitive pool condition in the Bar-seq analysis. Intriguingly, growth defects of 30 of the top 90 homozygous mutants with negative logFC were validated when grown independently.

Our lack of identifying the physical targets of the extracts in the HIP analyses is possibly the consequence of employing too high a concentration for the Bar-seq analyses. Screening a drug against its drug target at too high of a concentration risks the failure to identify the drug target. For example, *TUB2*, the known target of benomyl was not identified when benomyl was screened at 50 $\mu$ g/mL (IC<sub>90</sub>) although it was identified when the heterozygous library was screened at 25  $\mu$ g/mL (IC<sub>20</sub>) (Giaever *et al.*, 1999). Likewise, when tunicamycin was screened at 2.0  $\mu$ g/mL (IC<sub>80</sub>), its target *ALG7* was not identified because it was equally hypersensitive as the WT control, although it was identified when the concentration for the screen was reduced to 0.5  $\mu$ g/mL (IC<sub>20</sub>) (Giaever *et al.*, 1999). However, it is unlikely that this is the case observed here, as consideration was taken to

ensure that IC<sub>20</sub> concentrations of the aqueous and methanolic extracts of *P. insularum* were employed in our Bar-seq analyses. Alternatively, it is plausible that based on work carried out in Chapter 3, the bioactive components of the *P. insularum* extracts do not possess a genetic target, as the extracts directly bind iron.

Interestingly, despite the lack of a genetic target identified from these HIP analyses, the additional gene deletions that were identified from the HOP analyses are buffering mechanisms that include mechanisms related to the iron chelating mechanism of action identified in chapter 3. For instance, *ERG2* involved in the heme-dependent pathway of ergosterol synthesis, was found to be significantly hypersensitive to the aqueous and methanolic extracts. Although this may be a consequence of reduced membrane rigidity resulting from defective ergosterol biosynthesis under low iron conditions (Abe & Hiraki, 2009; Shakoury-Elizeh *et al.*, 2010), it is also likely that this hypersensitivity is a consequence of the vacuolar defect of the *erg2Δ* mutant, as mutants with vacuolar defects are hypersensitive under iron deficient conditions (Beh & Rine, 2004; Szczypka *et al.*, 1997). Furthermore, our results are consistent with a relationship between iron-sulfur proteins and ribosomal proteins (Yarunin *et al.*, 2005) wherein a deletion of the iron-sulfur cluster requiring protein Rli1p leads to defective processing of pre-rRNA, as well as defective export of both 40S and 60S ribosomal subunits. This link may explain why genes involved in ribosomal biogenesis, ribosomal subunits and ribosomal assembly were detected from our genome-wide analyses with the extracts of *P. insularum* (e.g., *JJJ1* from aqueous extract HOP, *RPL10* from methanolic extract HIP and *RPS12* and *RPL12A* from methanolic extract HOP), our logic being that a defect in iron-sulfur cluster synthesis resulting from reduced iron content upon treatment with the extracts of *P. insularum* exacerbates a defect already brought about by the deletion of subunits of the ribosomal machinery (e.g., *RPL12A* and *RPS12*).

The gene deletion *bre5Δ* was found to be hypersensitive to the methanolic extract. The Ubp3p/Bre5p ubiquitin protease complex functions in various cellular processes including telomeric silencing, transcriptional regulation, cell wall integrity, autophagy and DNA damage (Bilsland *et al.*,

2007; Kraft *et al.*, 2008). While a buffering link between these processes and the iron chelation activity of the extracts is not apparent, it is likely that iron chelation exacerbates these phenotypes resulting from the above gene deletions. For instance, iron chelation can reduce the effectiveness of iron-dependent proteins in their function to repair damaged DNA (Shakoury-Elizeh *et al.*, 2004), which coupled with the deletion of *BRE5* can lead to accumulated DNA damage resulting in hypersensitivity.

Another gene of interest arising from the HOP analysis of the methanolic *P. insularum* extract is *DAP1*, which encodes a heme-binding protein in which mutations of which result in mitochondrial defects (Hand *et al.*, 2003; Mallory *et al.*, 2005). Interestingly, *dap1Δ* is hypersensitive under iron-limiting conditions, possibly due to a defect in vacuolar morphology, which was previously reported to cause hypersensitivity in iron limited conditions (Craven *et al.*, 2007; Szczypka *et al.*, 1997). The same can be proposed for *did2Δ* involved in the vacuolar protein sorting pathway (Amerik *et al.*, 2000).

The homozygous deletion of *HDA3*, a subunit of the *HDA1* histone deacetylase complex (Carmen *et al.*, 1996), conferred the greatest hypersensitivity to the methanolic extract of *P. insularum*. This result suggests that the homeostasis between histone acetylation and deacetylation is disrupted by one or multiple compounds of the crude methanolic extract. Interestingly, the deletion of *HDA3* appears more sensitive against the methanolic extract of *P. insularum* at 0.0002% v/v with a growth inhibition of ~80%, compared to the deletion of iron transporters *FET3* and *FTR1* which exhibited a 20% reduction in growth at similar concentrations. This may suggest fewer compensating pathways for histone acetylation than iron transport, or it may be a consequence of the different backgrounds at which these two growth inhibition levels were obtained as the *HDA3* deletion was diploid and the *FET3* and *FTR1* deletions were haploid. The homozygous deletion of *NAP1*, which is critical to the function of histone chaperones (Ishimi & Kikuchi, 1999), was also found to be hypersensitive to the methanolic extract of *P. insularum*. Intriguingly, iron deprivation induced by curcumin treatment led to modifications in histone acetylation and degradation of Sml1p, an

inhibitor of ribonucleotide reductase that also functions in regulating dNTP production (Azad *et al.*, 2013; Chabes *et al.*, 1999; Zhao *et al.*, 1998). A similar cumulative effect of iron deprivation on dNTP levels could explain why *hda3Δ* and *nap1Δ* were hypersensitive to *P. insularum* extract treatment in our HOP analysis. Additionally, given these findings, further research is required to investigate the possibility of the methanolic *P. insularum* extract being a natural histone deacetylase (HDAC) inhibitor. From a different perspective, given the nature of some iron chelators to also chelate Zn, it may not be surprising that *P. insularum* extracts induced a HDA3 response if it were a Zn chelator as well, given that Zn regulates some histone deacetylases (Tan & Liu, 2015). However, our ICP-MS data (Appendix VIII) and metal-rescue data (Fig 3.9) suggested that extracts of *P. insularum* do not chelate Zn. For instance, ICP-MS data showed that there was no significant increase or decrease in Zn levels when cells were treated with the extracts. Furthermore, addition of Zn back into media with extract-treated cells did not partially rescue the growth defect induced by the extracts, suggesting that no part of the growth defect observed was attributable to any Zn chelation.

Intriguingly, the profile obtained from this chapter shared some similarities to the findings from the haploid screen carried out in the preceding chapter. In particular, both sets of screens did not identify the iron-sensing transcription factors or transporters the various iron transport systems *FET4* excluded. Although this was identified to be an inherent caveat of agar screening in this particular instance (*i.e.*, we probed transporter and transcription factor deletion mutants on agar against the aqueous extract but the mutants did not appear hypersensitive), whether this is the case in liquid needs to be clarified, by validating the diploid strains (both heterozygous and homozygous) of the iron transporters and the transcription factors. Additionally, both sets of screens identified genes involved in ribosomal biogenesis, ribosomal subunits and ribosomal assembly. This indicates an intricate relationship between iron and these cellular processes that warrants further investigation.

Although our HIP analyses did not identify genetic targets for either the aqueous or the methanolic extracts of *P. insularum*, and albeit the iron transporters detected in the agar-based genomic analysis in Chapter 3 were not detected in the HOP analyses in this chapter, we used these Bar-seq analyses to identify new pathways that were regulated by the extracts of *P. insularum* as well as present evidence of their complementation of data in Chapter 3. For instance, ribosomal biogenesis and organization was detected from these analyses that were not previously identified in the agar-based analysis in Chapter 3. Furthermore, a possible link with histone acetylation/deacetylation was also detected here, that was not detected in Chapter 3, but is consistent with the acetylation/deacetylation effect of the iron chelator curcumin previously reported (Azad *et al.*, 2013). For future work, characterization of the validated hits to determine their mechanistic role under extract treatment is required to fully comprehend the underlying molecular response to the *P. insularum* extracts. These investigations will also provide information on iron metabolism, regulation of iron homeostasis and how cells respond to changing iron status particularly in the presence of an iron chelator. Furthermore, investigations into the gene deletions that conferred better growth in the presence of the *P. insularum* extracts will also be helpful in identifying genes that can improve growth in the absence of iron for normal cellular processes. In conclusion, this chapter provided complementary findings that we have correlated to the proposed iron chelating mechanism of action of the *P. insularum* extracts.

---

## Chapter 5:

# Identification of the Iron Chelating Condensed Tannin from the Aqueous Extract of *Psychotria insularum*

---

### 5.1. Introduction

The preceding chapters described our work in ascertaining the mechanism of action of *P. insularum* extracts and associated buffering mechanisms without any knowledge of the bioactive compound or compounds. While that part of the work was highly crucial, it was also of great importance to determine the identity of the responsible bioactive compound, to assess its novelty and potential for pharmaceutical exploitation. Plant secondary metabolites are interesting sources of bioactive compounds, and they represent a hugely diverse group of compounds that are not usually necessary for plant cell structure and function, but are produced as part of the plant defence system against stresses and contribute to plant pigmentation (Rispaill *et al.*, 2005). Secondary metabolites include terpenoids, alkaloids and phenolics, some of which are of therapeutic significance, currently used or undergoing trials for the prevention or treatment of several diseases such as respiratory infection, anxiety disorders, sleep disorders, autoimmune diseases, inflammatory bowel diseases, Alzheimer's disease and various types of cancer (Raskin *et al.*, 2002; Reddy *et al.*, 2003; Watson *et al.*, 2001). Indeed, condensed tannins, epicatechins and flavanols possess an iron binding moiety which bears resemblance to the catechol motif that has been shown to bind iron (Baker *et al.*, 2003; Heim *et al.*, 2002). However, natural iron chelators are chemically diverse, and may also include iron siderophores that iron-dependent microorganisms have evolved to secrete to scavenge iron from their surrounds like the well-known iron chelator Deferoxamine (DFX) in clinical use (Hatcher *et al.*, 2009). There is also gathering evidence of phytochemicals, chemicals of plant origin, being potent antioxidants and iron chelators (Hatcher *et al.*, 2008; Hider *et al.*, 2001; Kell, 2009; Morel *et al.*, 1993).

Bioassay guided fractionation is a compound isolation technique that makes use of the step-wise fractionation of extracts directed by the bioactivity of the fractions obtained from each fractionation step (Fig 5.1). Indeed, this fractionation approach has led to the isolation and identification of bioactive compounds from crude plant extracts. For instance,  $\alpha$ -glucosidase inhibitors were successfully isolated and identified following bioassay-guided fractionation of leaf extracts from the plant *Aquilaria sinensis*, with a potential clinical significance in the therapy of diabetes (Feng *et al.*, 2011). Additionally, fractionated compounds from the crude leaf extracts of the garden croton (*Codiaeum variegatum*) used by Cameroons to treat bloody diarrhoea, were shown to be bioactive, via a unique mechanism of action, by targeting ceramide, a lipid involved in cell membrane function (Njoya *et al.*, 2014). The antibacterial compound okundoperoxide was isolated from crude extracts of the medicinal plant *Scleria striatinux* following a bioassay guided fractionation approach (Mbah *et al.*, 2012). Most importantly, this bioassay guided fractionation approach was used to isolate compounds bearing the iron-binding catechol moiety from flowers of the *Spartium junceum* plant used in Turkish folk medicine (Yeşilada *et al.*, 2000).

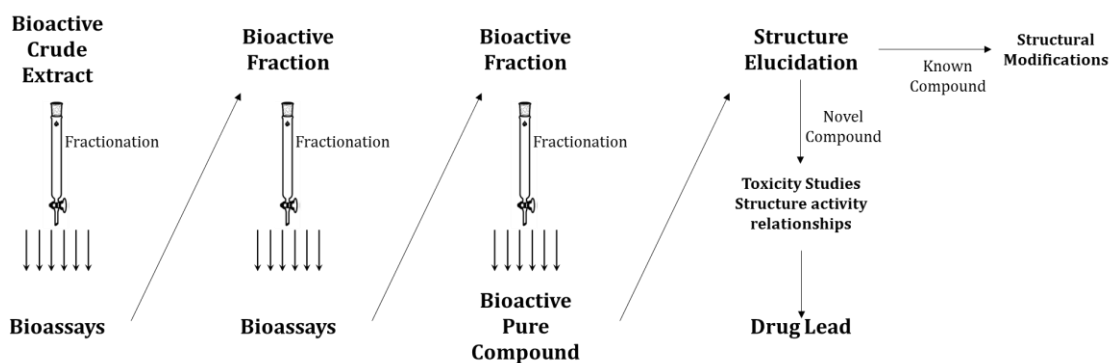


**Figure 5.1: Schematic of bioassay guided fractionation.** Further purification of each subsequent fraction is dictated by its bioactivity.

Given the success of bioassay guided fractionation of crude medicinal plant extracts to isolate bioactive compounds (some of which with iron chelating capacity), this approach was adopted for the determination of the bioactive component of the crude aqueous extract of *P.*

*insularum* leaves responsible for its iron chelation activity. Our approach incorporated yeast growth inhibition and iron chelation assays to track the compound responsible for the iron rescue activity. Polar fractionation and size-exclusion chromatography were used for the fractionation of our aqueous extract. In conjunction with our bioassays, NMR spectra were also obtained. Further, the protein expression profiles of the high affinity iron transporters Fet3p and Ftr1p were evaluated in the presence of the fractions of interest, via monitoring the GFP intensity of their GFP-tagged counterparts. We found that the fractions with the iron chelating activity of interest tracked to a 6-7ppm resonance using  $^1\text{H}$  NMR, which was subsequently determined to be a condensed tannin. Further, the expression levels of the iron transporters were up-regulated in the presence of the fractions displaying bioactivity, similar to the result obtained when cells were treated with the crude extracts.

## 5.2. Methods

### 5.2.1. HP20 column chromatography fractionation

Supelco Diaion® HP20 resin columns were prepared based on the principle that 1 mL of HP20 resin binds approximately 25 mg of extractable compounds. The aqueous extract of *P. insularum* was passed through the column four times at a flow rate of 4 mL/min. The HP20 column was eluted with three column volumes of 30%, 75% and 100% acetone in water. The 100% acetone fraction was evaporated under reduced pressure while the 30% and 75% fractions were subjected to backloading.

### 5.2.2. Backloading

Backloading of fractions eliminates long evaporating times particularly with samples of larger volumes and reduces bumping arising from samples containing water such as those eluted with 30% and 75% acetone/methanol in water. The 30% and 75% fractions that required backloading were diluted two-fold with dH<sub>2</sub>O before passing them through a column with half the column volume of resin as the previous fractionation step. Fractions were diluted two-fold and passed through the column to a final concentration of 12.5% acetone. The column was eluted with three column volumes of 100% acetone, essentially exchanging the aqueous solvent elution to a purely organic solvent, and dried under pressure as previously described. The mass of the fraction was determined by solubilising in methanol: dichloromethane (4:1), followed by transferring and drying into a pre-weighed vial.

### 5.2.3. HP20ss column chromatography fractionation

Columns for HP20ss fractionation were prepared similar to HP20 columns at a ratio of 1 mL of resin to 25 mg extractable compounds. Loaded HP20ss was transferred to a larger column bed of

HP20ss (nine times the volume of the loaded resin). Columns were eluted with the relevant acetone concentration as described in specific sections.

#### 5.2.4. LH20 column chromatography fractionation

LH20 size-exclusion chromatography fractionation was achieved by soaking 100 mL of LH20 resin in 90% methanol in water overnight before set up. The relevant fraction was passed through the column at approximately 0.3 mL/min flow rate, and 5 mL fractions were collected in 10 mL test tubes (330 x 5 mL fractions) using an automated fraction collector. To ensure all material was eluted, 2 x 1L bulk collections were subsequently collected.

#### 5.2.5. Thin Layer Chromatography (TLC)

To determine the complexity of samples and to ascertain those with similar composition, TLC analyses were carried out to permit the pooling of multiple samples in order to reduce the number of samples to be subsequently assayed for bioactivity and NMR spectroscopy. TLC was performed using Polygram® SilG/UV254 plates (Machery-Nagel) in 30% methanol in dichloromethane as the running solvent, followed by 0.1% w/v vanillin in ethanol, heated for analyses, and visualized under UV light (254 nm and 350 nm).

#### 5.2.6. Nuclear Magnetic Resonance spectroscopy

NMR spectra were acquired using a Varian DirectDrive spectrometer with triple resonance HCN cryogenic probe operating at 600 MHz for  $^1\text{H}$  using deuterated methanol (Cambridge Isotope Laboratories Inc).

### 5.2.7. Tannin test

The tannin test was conducted as previously described (Dhandapani & Sabna, 2008). Briefly, approximately 2 mg of a fraction was dissolved in 3 mL methanol, to which three drops of 100 mM FeCl<sub>3</sub> was added. The sample colour was then observed ranging from a brownish green to blue-black colouration.

### 5.2.8. Condensed tannin test

The hydrolysis of proanthocyanidin by condensed tannin assay was conducted as previously described (Porter *et al.*, 1986). Concisely, butanol:hydrochloric acid (95:5 v/v) solution was added to the fraction, leading to the auto-oxidation and hydrolysis of proanthocyanidin, detected as the red coloured anthocyanidin monomer precipitate.

### 5.2.9. Bioactivity assay

Liquid-based growth assays of bioactivity were carried out as previously described in **Section 2.2.3**.

### 5.2.10. Iron supplementation assay

Rescue of growth defects via iron supplementation was carried out as previously described in **Section 3.2.4**.

### 5.2.11. Protein expression

Monitoring of the abundance of GFP-tagged proteins was carried out as described previously in **Section 3.2.6**.

## 5.3. Results

### 5.3.1. The 30% and 75% acetone fractions are bioactive

The first fractionation step of the aqueous extract of *P. insularum* involved reversed-phase column chromatography utilizing HP20 resin. Fractions were eluted with 30%, 75% and 100% acetone in water. Upon evaporation of the samples, it was determined that the 100% fraction did not contain sufficient material for bioassays. The fractionated 30% and 75% material was solubilized in DMSO and assayed for bioactivity as well as the iron rescue assay to determine if they retained the bioactivity profile described in the preceding chapter. The 30% and 75% fractions of the aqueous extract of *P. insularum* reduced the growth of BY4741 WT yeast strain (Fig 5.2). At their lowest tested concentration of  $6.4 \times 10^{-5}$  v/v, the 30% HP20 fraction inhibited growth of BY4741 by approximately 15%, while the 75% HP20 fraction inhibited growth of BY4741 by approximately 30%, compared to the control. Interestingly, both fractions reduced growth of BY4741 by close to 100% at  $1.6 \times 10^{-3}$  v/v. Supplementation with 100  $\mu$ M exogenous  $\text{FeCl}_3$  rescued the growth defect induced by both fractions, suggesting that the bioactivity determined from treatment with the fractions alone is mediated by the iron chelation mechanism that was previously established in Chapter 3. Further, these findings indicate that both the 30% and 75% fractions contain the bioactive, iron chelating component.

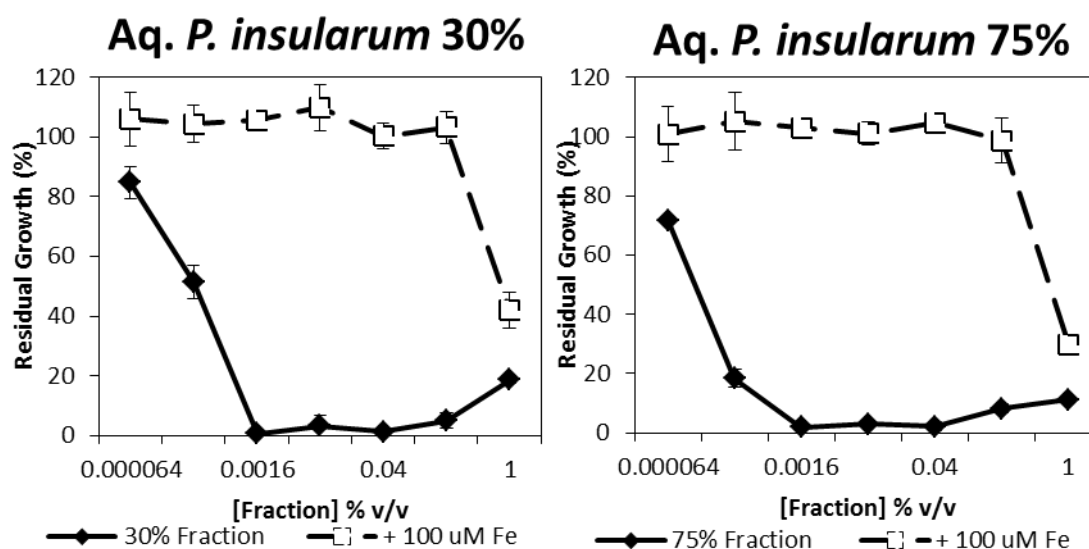


**Figure 5.2: Bioassays of the 30% and 75% HP20 fractions of the aqueous *P. insularum* extract.**

Liquid based bioactivity and iron rescue assays of the 30% and 75% HP20 fractions of the aqueous extract of *P. insularum* was achieved by exposing BY4741 WT yeast to increasing concentrations of the fractions, and grown with (open squares) or without (closed diamonds) supplementation with 100  $\mu\text{M}$   $\text{FeCl}_3$ . Residual growth was obtained by comparing the growth of treated cells against DMSO control. The solid black lines indicate treatment with the fraction alone, while the dashed lines indicate fraction treatment with 100  $\mu\text{M}$   $\text{FeCl}_3$  supplementation.

---

5.3.2. The  $^1\text{H}$  NMR analyses of the 30% and 75% fractions from HP20 fractionation show similar spectra profiles

$^1\text{H}$  NMR spectroscopy is a technique that provides information regarding the chemical composition of a given sample based upon the different 3D spatial environments that each hydrogen atom exists in the so-called “chemical environment”. In this work, NMR spectroscopy was employed to complement the bioassay-guided fractionation, to provide insight into the possible composition and complexity of the fractions. As such, sub-samples of the bioactive 30% and 75% HP20 fractions were solubilized in deuterated methanol and run at 600 MHz for  $^1\text{H}$  using a Varian DirectDrive spectrometer. The spectra of 30% and 75% HP20 fractions showed similar profiles (Fig 5.3), a result that is consistent with these fractions exhibiting similar bioactivity profiles. Similarities between the two samples (black dashed boxes in Fig 5.3) were observed at 2-3 ppm where hydrogen atoms adjacent to double bonds often resonate, and at 6-7 ppm where alkene hydrogen atoms resonate. However, there also existed a difference between the samples. This difference (red dashed box in Fig 5.3) was noted between 3-4 ppm where the hydrogen attached to oxygenated carbon atoms (*e.g.*, carbohydrates) normally resonate. The fact that these resonances were missing in the 75% acetone fraction imply they were irrelevant to the observed bioactivity. The large peaks observed at 4.90 ppm and 3.31 ppm correlate to water and the residual protons of deuterated methanol, respectively.

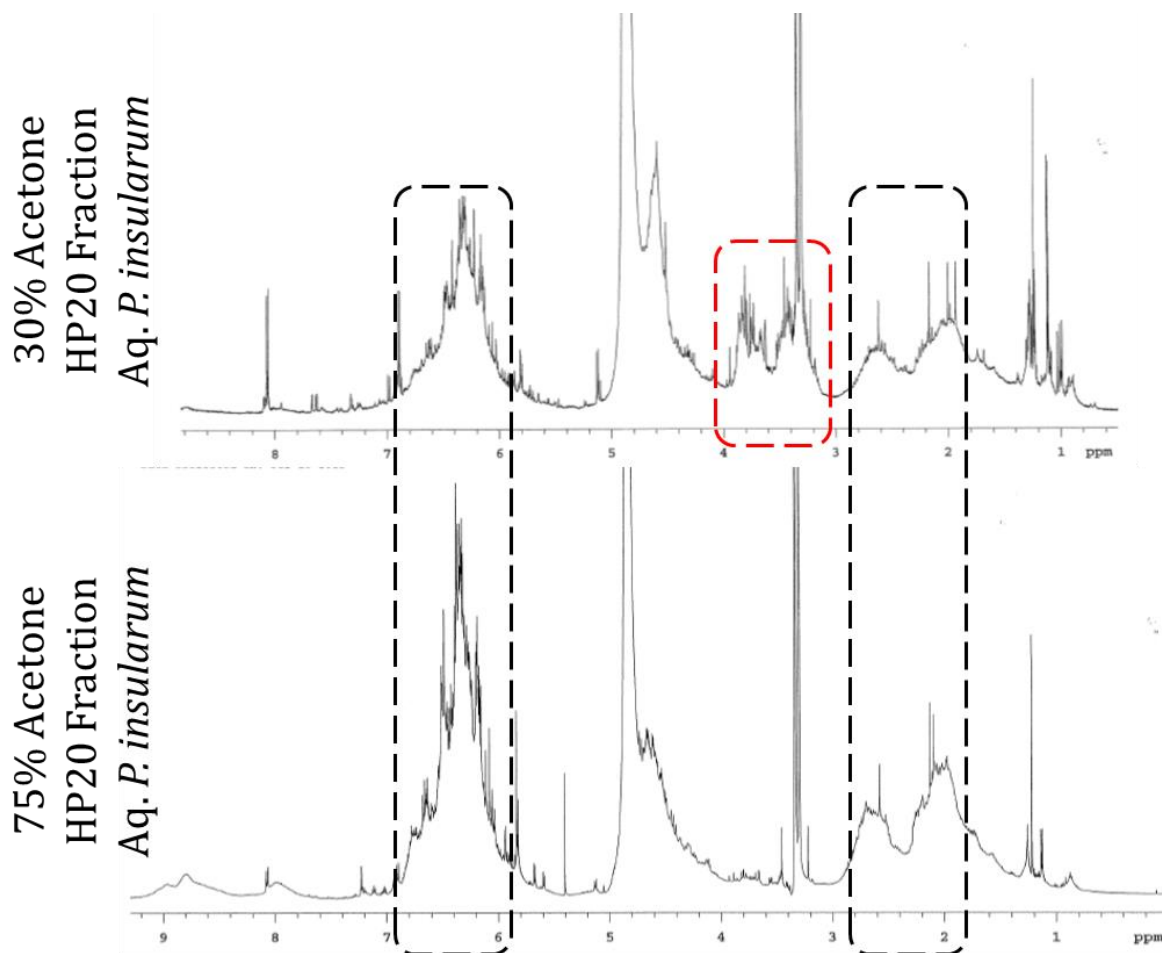


**Figure 5.3:** NMR spectra of the 30% and 75% HP20 fractions of the aqueous extract of *P. insularum*. NMR spectra of the 30% and 75% HP20 fractions of the aqueous extract of *P. insularum*, solubilized in deuterated methanol, and obtained from a Varian DirectDrive spectrometer with a triple resonance HCN cryogenic probe run at 600 MHz for  $^1\text{H}$ . The large peaks observed at 4.90 ppm and 3.31 ppm correlate to water and the residual protons of deuterated methanol, respectively.

### 5.3.3. Sub-fractions of HP20ss fractionation of 30% fraction are bioactive and variably potent

To further purify the components of the 30% HP20 fraction, it was processed through a HP20ss column and eluted with 10%, 20%, 30%, 50% and 100% acetone in water. The fractions were backloaded and dried *in vacuo* before solubilizing in DMSO. Minimal material (< 0.5 mg) was obtained from the 10%, 20% and 30% fractions and work with these fractions thus stopped at this stage. However, to determine if the 30-50 (50% HP20ss fraction of the 30% HP20 fraction of the aqueous extract of *P. insularum*) and the 30-100 (100% HP20ss fraction of the 30% HP20 fraction of the aqueous extract of *P. insularum*) fractions were bioactive, growth inhibition and iron-

supplementation assays were conducted against the BY4741 WT yeast strain. The 50% and 100% HP20ss fractions of the 30% HP@0 fraction of the aqueous extract of *P. insularum* were bioactive based on inhibited growth of the yeast strain illustrated by the downward slope of the residual growth curves (solid black line in Fig 5.4). Interestingly, the 100% HP20ss fraction caused an approximate 30% inhibition in BY4741 growth at  $6.4 \times 10^{-5}$ % v/v, while the 50% HP20ss fraction caused an approximate 10% inhibition at the same concentration. This suggests the 100% HP20ss fraction was marginally more potent than the 50% HP20ss fraction. Supplementation of fraction treatments with 100  $\mu\text{M}$   $\text{FeCl}_3$  greatly improved BY4741 WT growth, indicating the bioactive component responsible for the iron chelation activity is present in both fractions. Interestingly,  $\text{FeCl}_3$  rescued the 100% HP20ss fraction better than the 50% HP20ss fraction, where 100  $\mu\text{M}$   $\text{FeCl}_3$  supplementation of the 1% v/v concentration of the 100% HP20ss fraction treatment rescued residual growth from 20% to 80%, while the same concentration of 50% HP20ss fraction treatment only produced a residual growth rescue from 30% to 50%.

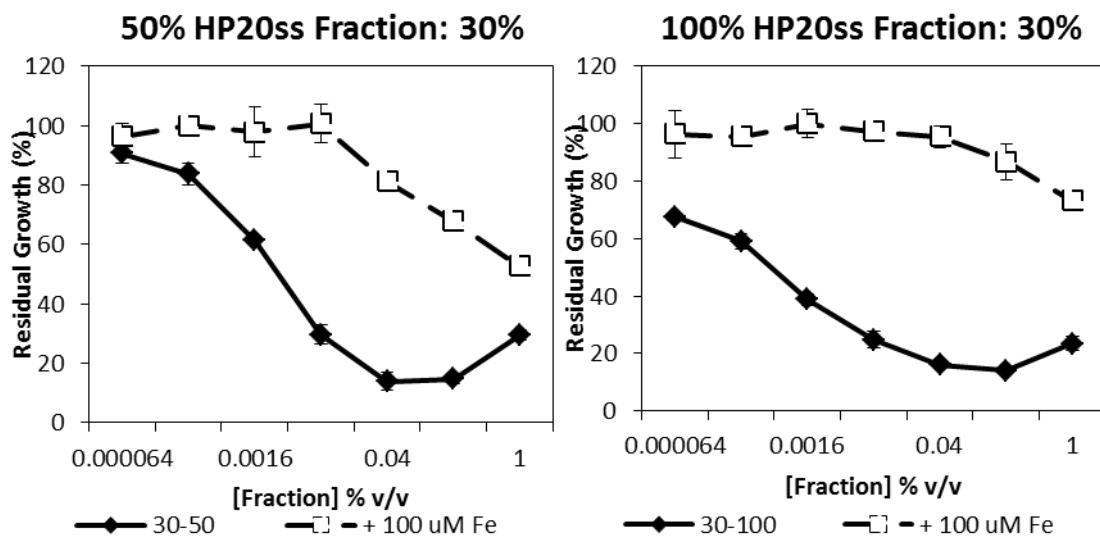


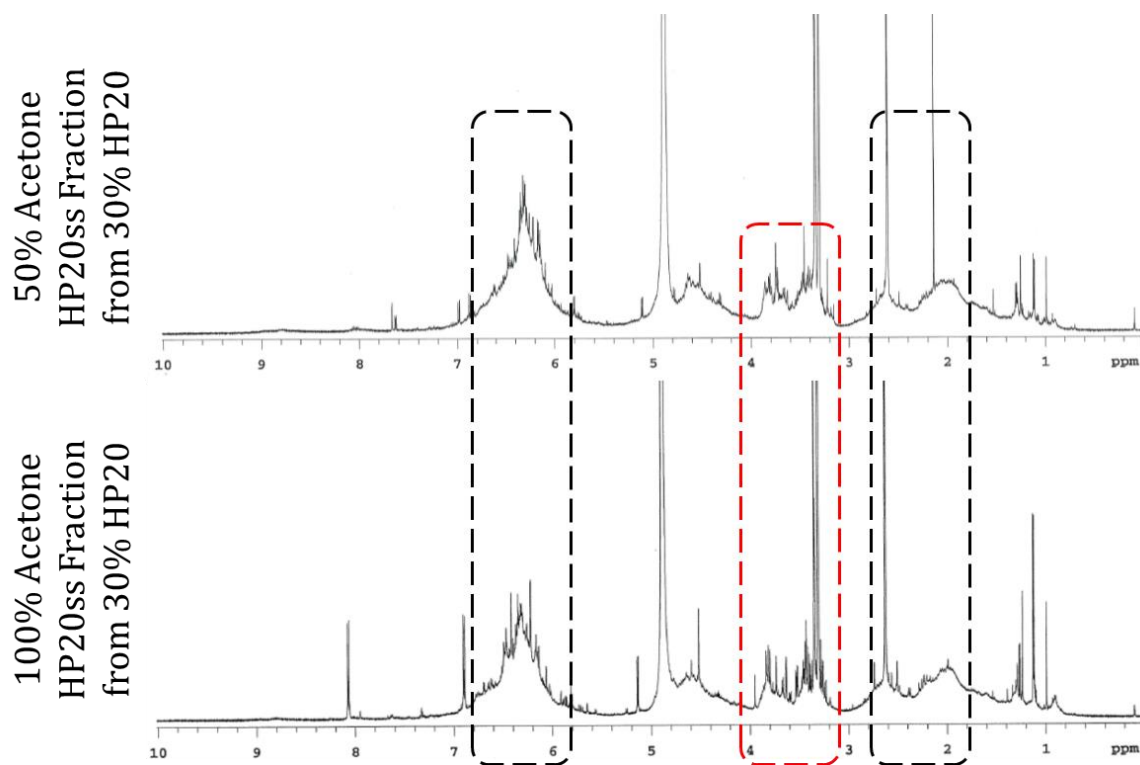
**Figure 5.4: Bioactivity and iron rescue assays of the HP20ss fractions of the 30% HP20 fraction of the aqueous extract of *P. insularum*.** BY4741 WT yeast strain was grown in the presence of the 50% (30-50) and 100% (30-100) HP20ss fractions of the 30% HP20 fraction, across a concentration range of  $6.4 \times 10^{-5}$  to 1% v/v. Cells were grown in either the fraction alone to determine its bioactivity (solid black line), or the fraction treatment with 100  $\mu\text{M}$   $\text{FeCl}_3$  supplementation (dashed black line) to assess iron rescue. Residual growth in each case was calculated by comparison to the DMSO control.

#### 5.3.4. The NMR spectra of the 50% and 100% HP20ss fractions of the 30% aqueous extract fraction show highly similar profiles

The activities of both the 50% and 100% HP20ss fractions as shown above suggest that both fractions contain a similar bioactive component with the iron chelation activity of interest. To assess the chemical composition of the fractions, the  $^1\text{H}$  NMR spectrum of each fraction was acquired using a Varian DirectDrive spectrometer at 600 MHz for  $^1\text{H}$ . The NMR spectra of the 50% and 100% HP20ss fractions from the 30% HP20 fraction of the aqueous extract of *P. insularum* showed near identical spectral profiles (Fig 5.5). The two areas of similarity previously identified from the bioactive 30% and 75% HP20 fractions of the aqueous *P. insularum* are again present in these two fractions (highlighted in black in Fig 5.5). The area which differentiated the 30% and 75% HP20 fractions (highlighted in red) was present in both fractions although it is hypothesized that because it was uniquely present in the 30% fraction but not in the 75% HP20 fraction, it is unlikely to contribute to the bioactivity of the extracts despite its presence in both the 50 and 100% fractions. However the HP20ss fractionation did not appear to have separated out any other components of the mixture from its 30% HP20 fractionation form.

---

**Figure 5.5:** NMR spectra of the 50% and 100% HP20ss fractions from 30% HP20 fraction of the aqueous *P. insularum* extract. NMR spectra of the 50% and 100% HP20ss fractions of the 30% HP20 fraction of the aqueous extract of *P. insularum*, solubilized in deuterated methanol, and obtained with a Varian DirectDrive spectrometer at 600 MHz for  $^1\text{H}$ . The black dashed boxes indicate areas of similarity. The red box indicates the area that was unique to the 30% HP20 fraction.



### 5.3.5. Sub-fractions of HP20ss fractionation of 75% fraction are bioactive and variably potent

To further purify the 75% HP20 fraction of the aqueous extract of *P. insularum*, it was loaded onto a HP20ss column and eluted with three column volumes of 30%, 40%, 50%, 60%, 75% and 100% acetone in water. TLC was performed to identify fractions that had similar chemical compositions in order to pool chemically similar samples for subsequent biological and chemical characterization of the fraction (data not shown). Samples of similar composition were pooled and evaporated *in vacuo*. However, insufficient material was recovered from the 30% and 40% HP20ss fractions and work with these fractions ceased. The 60%, 75% and 100% HP20ss fractions however were pooled. Growth inhibition bioactivity assays and iron rescue assays were carried out on the 50% and pooled 60-100% fractions. Bioactivity assays of the 50% and 60-100% pooled fractions from the HP20ss fractionation of the 75% HP20 fraction from the aqueous extract of *P. insularum* clearly showed bioactivity, demonstrated through the decreasing residual growth of BY4741 WT as the concentration of the fractions increased to 1% v/v (Fig 5.6). The potency between the two fractions was comparable as these fractions both reduced growth of the yeast cells by 90% at 0.04% v/v

compared to untreated cells. Further, supplementation of both fraction treatments with 100  $\mu\text{M}$   $\text{FeCl}_3$  rescued the growth defect. These findings indicate that both fractions were bioactive, and that their bioactivity was most likely due to a bioactive component with the iron chelation activity of interest.

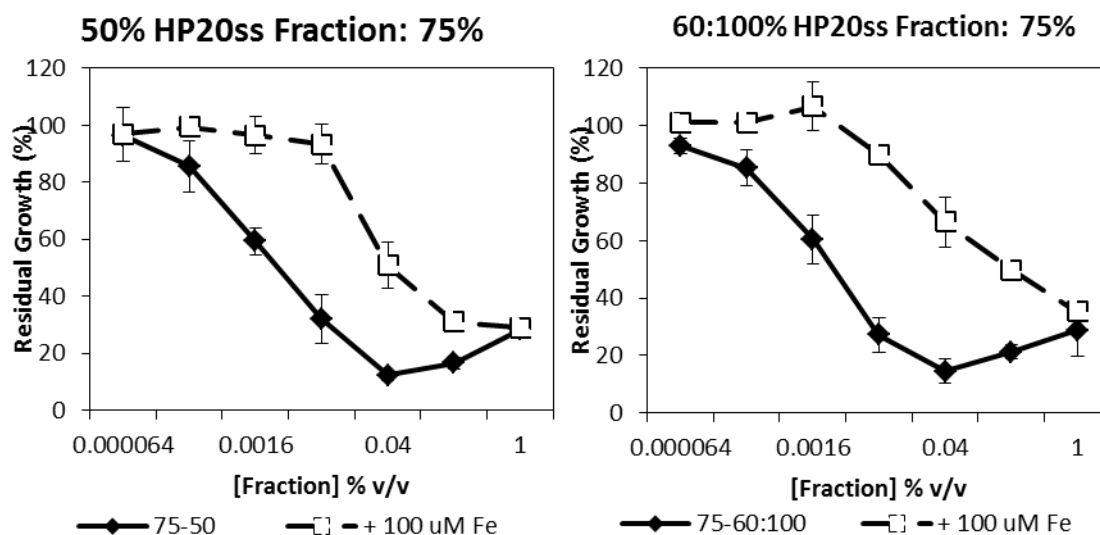


**Figure 5.6:** HP20ss fractions of the 75% HP20 fraction from the aqueous extract of *P. insularum*. Bioactivity and iron rescue assays of the 50% and 60:100% pooled fractions from HP20ss fractionation of the 75% HP20 fraction of the aqueous extract of *P. insularum*. Solid black lines indicate WT grown in the presence of increasing concentrations of the fractions. Dashed black lines indicate fraction treatment with 100  $\mu\text{M}$   $\text{FeCl}_3$  supplementation.

### 5.3.6. NMR spectra of the 50% and 60-100% HP20ss fractions of the 75% HP20 fraction display extremely similar profiles

To obtain insight into the chemical complexity of the 50% and 60-100% fractions from the HP20ss fractionation of the 75% HP20 fraction from the aqueous extract of *P. insularum*,  $^1\text{H}$  NMR spectroscopy was carried out on the two fractions at 600 MHz for  $^1\text{H}$  using a Varian DirectDrive spectrometer (Fig 5.7). Both the 50% and 60-100% pooled fractions displayed the previously observed areas of interest, at 2-3 and 6-7 ppm. These two areas have been consistently observed across all bioactive fractions, and may singly or together contribute to the iron chelation bioactivity

of the aqueous extract of *P. insularum*. Also observed from the spectra was the apparent lack of separation of the two broad resonances of interest that have both been consistently present in the bioactive fractions, which may suggest that these peaks form part of one suite of compounds, or are from different groups of compounds but with similar polarity, owing to their co-isolation in the bioactive fractions using polarity-based fractionation.

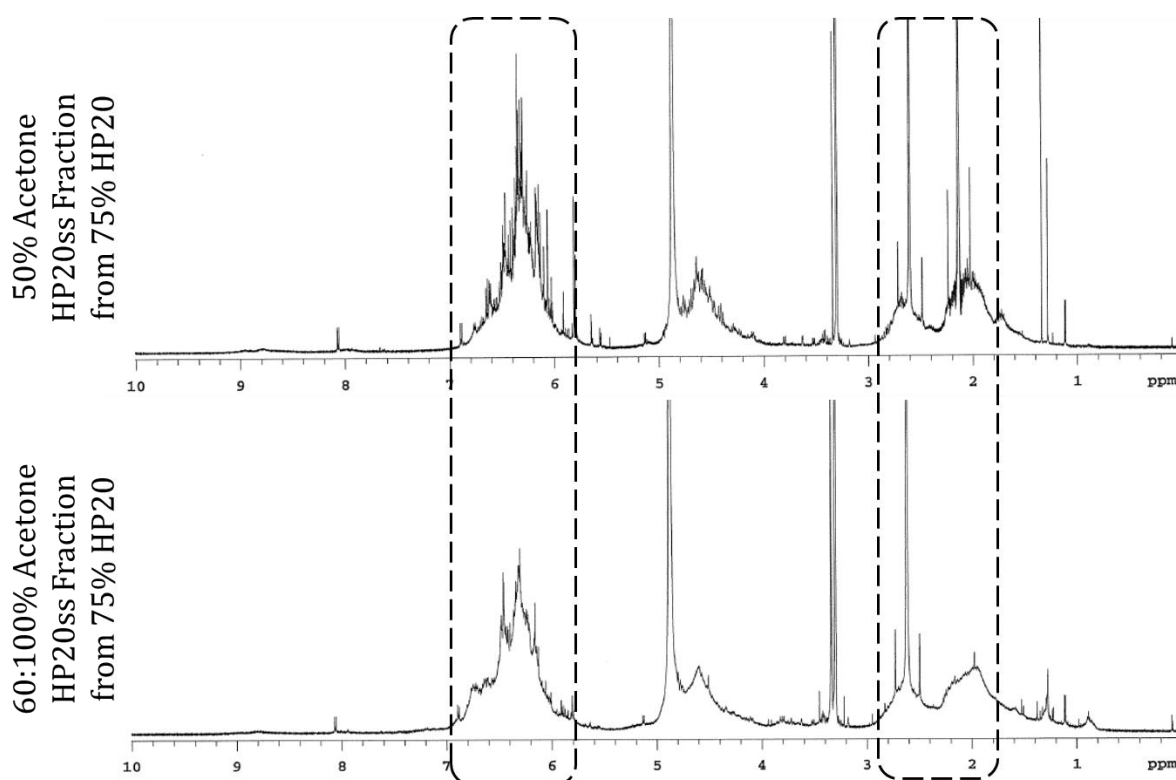


**Figure 5.7:** NMR spectra of the 50% and 60:100% HP20ss fractions of the 75% HP20 fraction of the aqueous extract from *P. insularum*. Sub samples of the 50% HP20ss fraction and the 60:100% pooled fractions from the HP20ss fractionation of the 75% HP20 fraction of the aqueous extract of *P. insularum* were dissolved in deuterated methanol then exposed to NMR spectroscopy using a Varian DirectDrive spectrometer at 600 MHz for  $^1\text{H}$ . The black dashed lines indicate areas identified from the original 75% HP20 fraction.

### 5.3.7. The 75-50% LH20 pooled fractions A, E, F, G, H, I, K and P are not bioactive

It was evident from the HP20ss fractionation and their respective NMR spectra that separation of extract components based on their polarity was not efficiently separating extract constituents from the bioactive component. It was thus determined that a size exclusion column be used to separate extract components by molecular size for the next step of fractionation. This approach, utilizing LH20 resin, permits larger molecular entities to pass through the column before smaller molecules are eluted due to the smaller compounds being temporarily trapped within pores on the resin surface. The attempt to further purify the iron chelating bioactive compound of *P. insularum* extract via LH20 size exclusion column chromatography was carried out on the 50% HP20ss fraction of the 75% HP20 fraction from the aqueous extract of *P. insularum*. This partial purification approach produced 330 5 mL eluents, which were pooled to eight fractions. Growth inhibition bioactivity assay and NMR spectral analyses were conducted for the eight pooled fractions, from which it was determined that none of the eight pooled fractions was able to inhibit yeast growth sufficiently past the 80% residual growth cut-off at the 0.0001% v/v, 0.0005% v/v and 0.001% v/v concentrations (Fig 5.8). Interestingly, the NMR spectra of the 8 fractions clearly showed the absence of the peaks of interest at 2-3 ppm and 6-7 ppm, suggesting that one or both of these peaks are responsible for the iron chelation bioactivity.

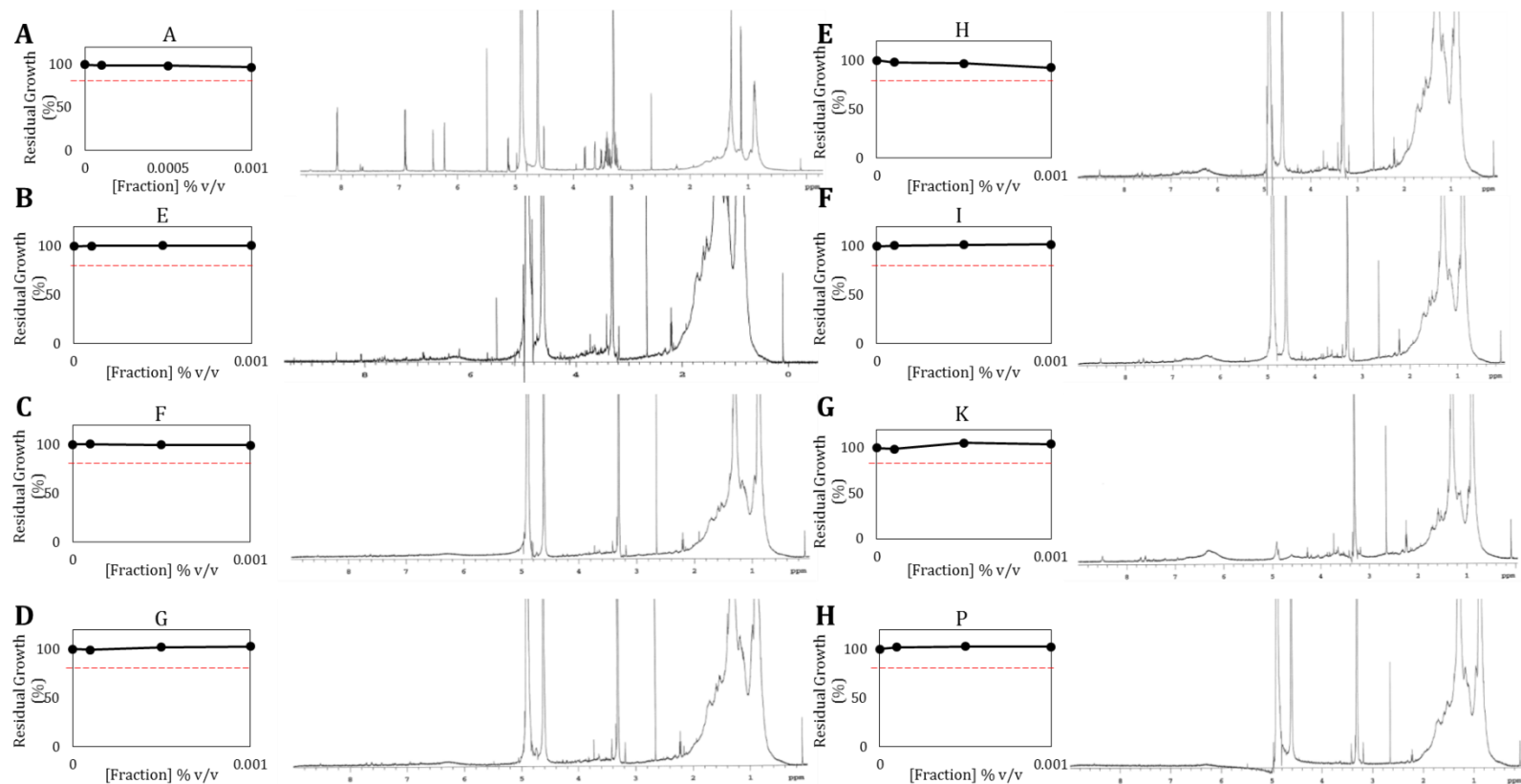


**Figure 5.8: Bioactivity assay and NMR spectra of the pooled fractions from the LH20 fractionation of the 75-50 fraction from the aqueous extract of *P. insularum*.** **A:** Bioassay and NMR spectra of fraction 75-50-A. **B** Bioassay and NMR spectra of fraction 75-50-E. **C:** Bioassay and NMR spectra of fraction 75-50-F. **D:** Bioassay and NMR spectra of fraction 75-50-G. **E:** Bioassay and NMR spectra of fraction 75-50-H. **F:** Bioassay and NMR spectra of fraction 75-50-I. **G:** Bioassay and NMR spectra of fraction 75-50-K. **H:** Bioassay and NMR spectra of fraction 75-50-P. Bioassays was carried out using BY4741 WT cells, grown in three concentrations of the fractions dissolved in DMSO, and growth profiles of fraction treated cells were compared to the growth profile of the DMSO control (0% v/v fraction). Red dashed lines indicate 80% residual growth. NMR spectra were obtained by dissolving sub samples of each pooled fraction in deuterated methanol, and spectroscopy was carried out using a Varian DirectDrive spectrometer, at 600 MHz for  $^1\text{H}$ .

### 5.3.8. The 75-50% LH20 1L bulk fractions are bioactive

The two remaining fractions (at 1L each) from the LH20 fractionation of the 75-50% fraction of the *P. insularum* aqueous extracts were hypothesized to contain the bioactive component of the extracts. This was assessed by bioassays including analyses for yeast growth in presence and absence of iron supplementation. Furthermore, NMR spectroscopic analyses were carried out on sub-samples of the fractions at 600 MHz for  $^1\text{H}$  using a Varian DirectDrive spectrometer. Fractions Q and R obtained from the LH20 size exclusion column chromatography of the 75-50% fraction of the aqueous extract of *P. insularum* were able to reduce yeast growth (Fig 5.9). Further, this growth inhibition was rescued with the addition of exogenous  $\text{FeCl}_3$  (Fig 5.9). Interestingly, the 75-50-R fraction was marginally more bioactive than the 75-50-Q fraction. The NMR spectra of both fractions displayed similar profiles (Fig 5.9). Of most importance is the presence of the broad peak resonating at 6-7 ppm (red dashed box). This broad peak was not present in the fractions tested in the previous experiment (Fig 5.8) and may indicate the area of the spectra corresponding to the compound or compounds exhibiting the iron chelation bioactivity of interest.

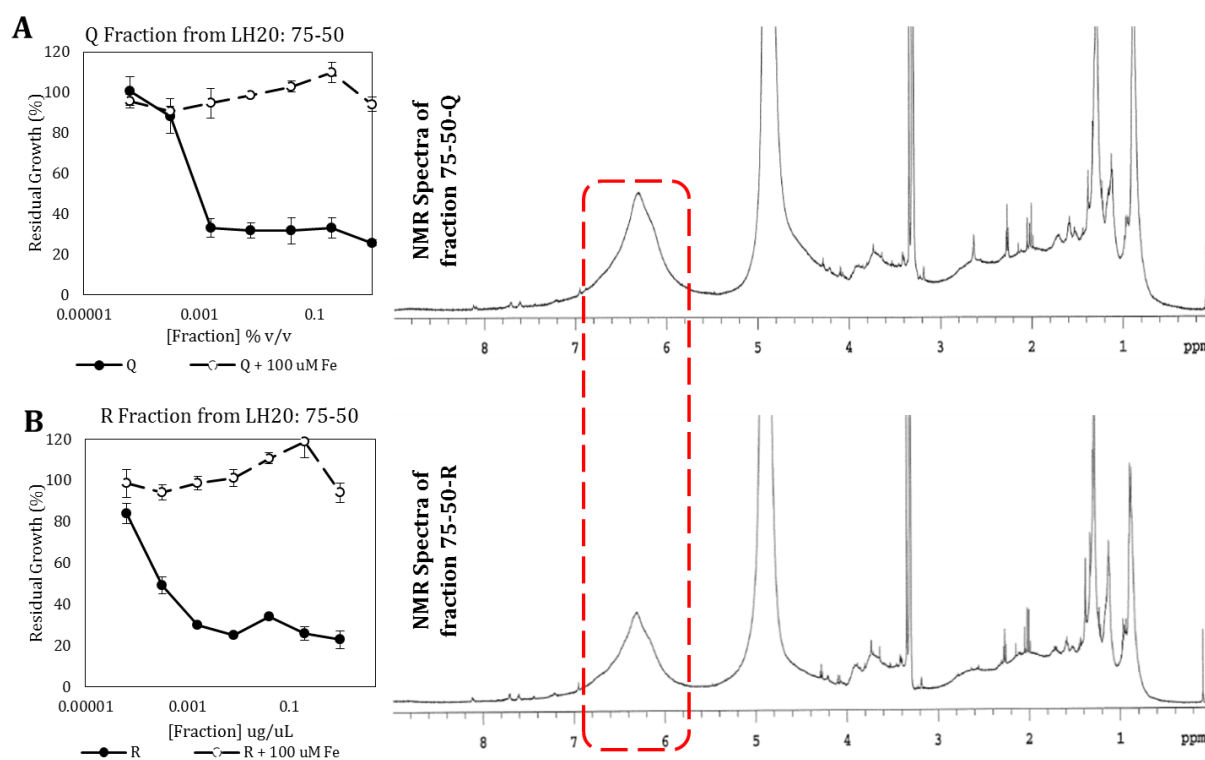


**Figure 5.9: Bioassays and NMR spectra of the 75-50-Q and 75-50-R LH20 fractions.** **A:** Bioassay and <sup>1</sup>H NMR spectrum of fraction 75-50-Q. **B:** Bioassay and <sup>1</sup>H NMR spectrum of fraction 75-50-R. Bioassays were carried out using BY4741 WT yeast strain, grown in the presence of increasing concentration of the fractions, ranging from 6.4 x 10<sup>-5</sup> to 1 % observed in the A, E, F, G, H, I, K and P fractions.

---

### 5.3.9. Expression of Fet3p and Ftr1p iron transporters are upregulated in the presence of the selected bioactive fractions

The expression levels of the high-affinity iron transport system of yeast in the presence of the selected bioactive fractions were monitored as previously described in Chapter 3. Tracking the intensity of the green fluorescence resulting from the GFP tagged onto the protein of interest, we observed that Fet3p and Ftr1p forming the high-affinity iron transport system of yeast at the plasma membrane, were shown to be upregulated when yeast cells were treated with the aqueous extract of *P. insularum* (Fig 3.11). To determine if the fractions leading to fractions Q and R elicited the same effect on the expression of iron transporters as the aqueous extract of *P. insularum*, Fet3p-GFP and Ftr1p-GFP yeast strains were grown in the presence of each of the fractions of interest (*i.e.*, 75% fraction, 75-50% fraction, 75-50-Q and 75-50-R fractions) as well as iron free media and the iron chelator control (Fig 5.10). The crude extract was also included for comparative purposes. The intensity of green fluorescence observed from the GFP tagged onto Fet3p and Ftr1p were visually monitored, and we visually detected increased green fluorescence from GFP tagged onto both Fet3p (Fig 5.10A) and Ftr1p (Fig 5.10B) when treated with all the tested fractions, as well as the crude extract, compared to the control.

The expression profiles of Fet3p-GFP showed significantly increased expression levels in the presence of the crude aqueous extract as well as the fractions from the various steps of column chromatography (Fig 5.10A). While treatment of Fet3p-GFP with 0.05% v/v of the crude aqueous extract of *P. insularum* elicited a significant 30% increase in the expression of Fet3p, treatment with 0.01% v/v of the 75% HP20 fraction, or the 50% HP20ss fraction produced a significant 60% increase

in the expression of Fet3p. Impressively, treatment with 0.01% v/v of the Q and R fractions from LH20 column chromatography led to increases of more than 100% in the expression of Fet3p which were statistically significant. Significant increases were also observed from Fet3p-GFP strains grown in iron free media and in the presence of the iron chelator by approximately 60% and 30%, respectively. These findings indicate that fractions 75% and 75-50% induced an upregulation of Fet3p similar to that observed under iron-free conditions, while the crude aqueous extract elicited a response similar to that of the iron chelator control.

The expression of Ftr1p-GFP was also increased in the presence of the crude extract as well as the fractions, as observed from the higher intensity of the GFP signal from the extract treatments compared to the control (Fig 5.10B). Treatment with 0.05% v/v of the crude aqueous extract produced a significant approximate 30% increase in the expression of Ftr1p, whilst treatment with 0.01% of the fractions produced statistically significant increased expression ranging from 70-100%. Growth in iron free media or in the presence of the iron chelator produced approximately 30% increased Ftr1p expression which were statistically significant. Together, the Fet3p and the Ftr1p results indicate that the step-wise fractionation carried out did not compromise the activity of the chemical components of interest, and that the fractions isolated with bioactivity retained the iron-mediated activity of interest.

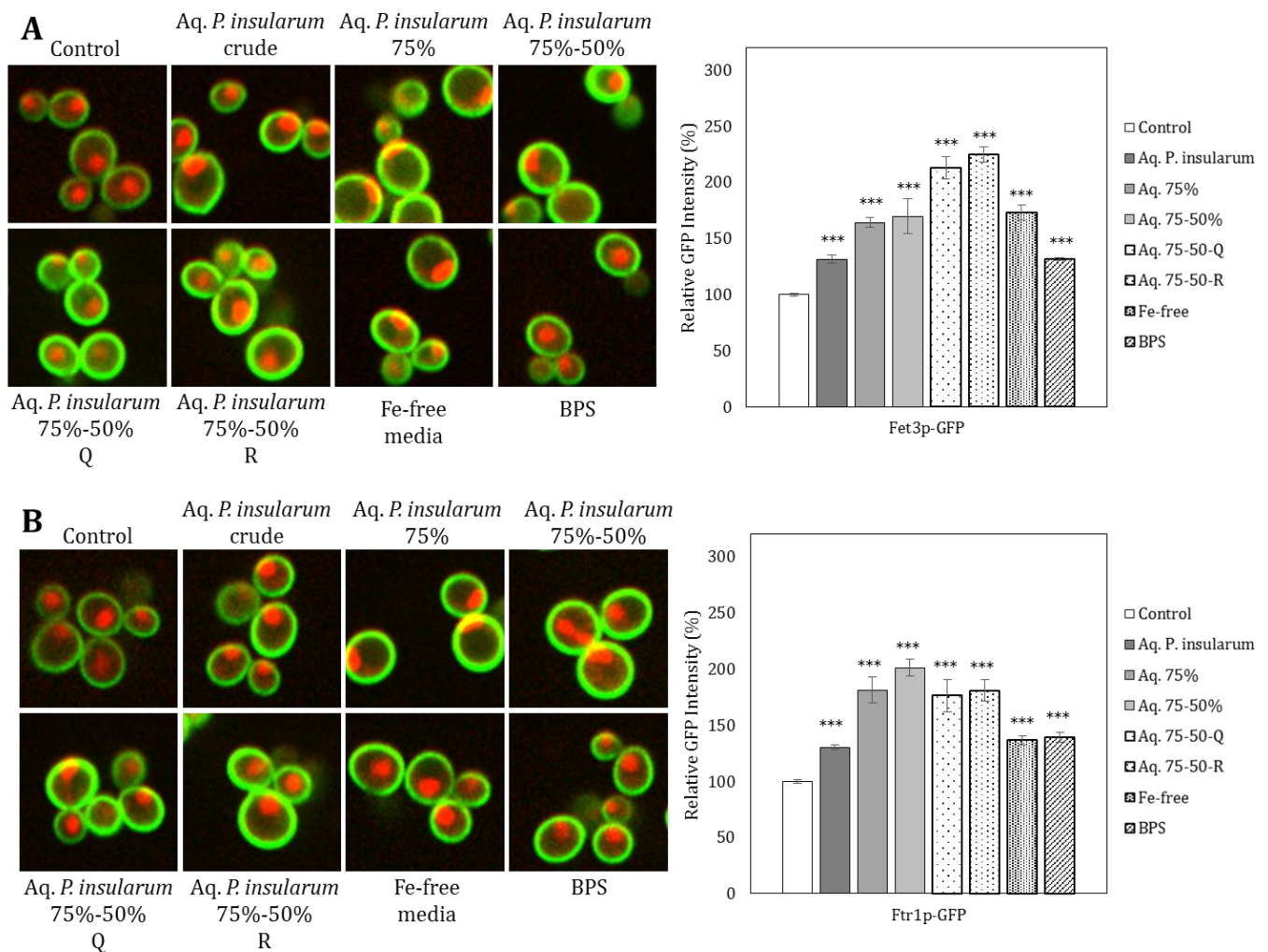


**Figure 5.10: Effects of the fractions leading to partially purified LH-20 bioactive fractions on the expression of the high affinity iron transporters Fet3p and Ftr1p. A:** GFP profile of Fet3p-GFP across the 8 treatments tested, including control, 0.05% v/v of the crude aqueous extract of *P. insularum* extract (Aq. *P. insularum* crude), 0.01% v/v of the 75% HP20 fraction from the aqueous extract (Aq. *P. insularum* 75%), 0.01% v/v of the 50% HP20ss fraction from the 75% HP20 fraction (Aq. *P. insularum* 75%-50%), 0.01% v/v of Q and R fractions from the LH20 fractionation of 75-50% fractions (Aq. *P. insularum* 75%-50% Q and Aq. *P. insularum* 75%-50% R), and Fet3p-GFP grown in iron free media (Fe-free media) and in the presence of BPS. **B:** GFP profile of Ftr1p-GFP across the 8 treatments tested. Microscopy images were obtained using a Perkin Elmer Evotec spinning disc Opera confocal microscope. Quantification shown in the bar-graphs was obtained using Acapella software. To determine if the increase in GFP intensity observed was significant, statistical analyses were carried out using Microsoft Excel paired two sample for means, one tailed t-test. (\*\*\*) = p-value < 0.001).

### 5.3.10. Fraction R from LH20 column chromatography is a condensed tannin

The NMR profiles obtained from the aqueous extracts of *P. insularum* are characteristic of tannins (Lavoie *et al.*, 2015). The tannin assay employs ferric chloride, which leads to the formation of tannin-iron complexes that are brownish-green or blue-black in colour (Dhandapani & Sabna, 2008) was used to determine if fraction R contained tannins. Indeed, when assayed against this simple colorimetric test, fraction R produced the blue-black colour indicative of the presence of tannins in fraction R (Fig 5.11A). Tannins are polyphenolic secondary metabolites that are widely distributed in plants. The three classes of tannins include hydrolysable tannins, condensed tannins and complex tannins (Cos *et al.*, 2003). As NMR analyses of fraction R showed that it did not contain the typical building blocks of hydrolysable tannins (data not shown), we sought to determine if the tannin is a condensed tannin. An easy colorimetric assay that can distinguish condensed tannin from the others is the acid-butanol assay (Fig 5.11B), which results in the hydrolysis of the condensed tannin and formation of red anthocyanidin precipitate (Schofield *et al.*, 2001). To determine if fraction R comprises condensed tannins, it was exposed to the acid-butanol test, which resulted in the formation of the positive reaction and the red precipitate (Fig 5.11C). However, despite these promising findings, due to the time limitation of this work, we were not able to continue with further purification and identification efforts.

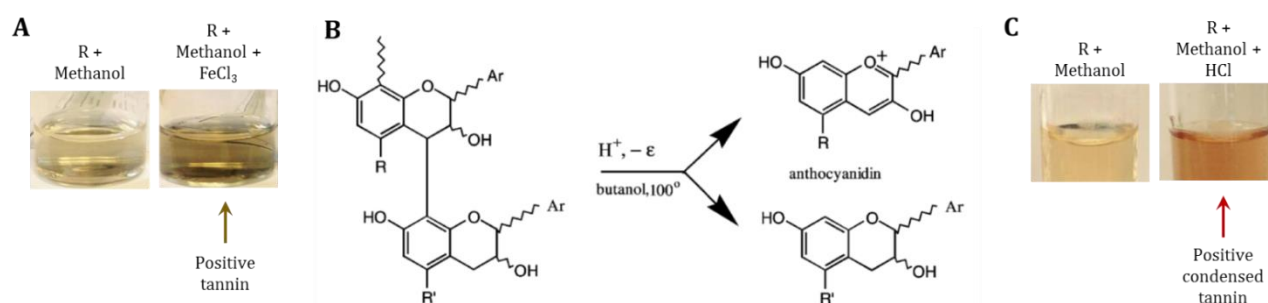


**Figure 5.11: Tannin and condensed tannin tests.** **A:** Tannin test of the R fraction from LH20 column chromatography. The ferric chloride test indicates positive for tannins with a brownish-green/blue-black colouring (brown arrow). **B:** The chemical basis of the acid-butanol condensed tannin test. The reaction involves oxidation of the condensed tannin and the formation of the red coloured anthocyanidin unit (Schofield *et al.*, 2001). **C:** Condensed tannin test of fraction R from the LH20 column chromatography. The red precipitate is indicative of a positive results is highlighted by red arrow.

## 5.4. Discussion

The aim of this chapter was to identify the compound responsible for the iron chelation activity that was determined to be the mechanism of action of the *P. insularum* extracts investigated in Chapter 3. The findings that have been presented herein traced the iron chelation activity of the aqueous extract through several column chromatography fractionations to a compound or compounds with  $^1\text{H}$  NMR resonance at 6-7 ppm indicative of condensed tannins (Fig 5.12).

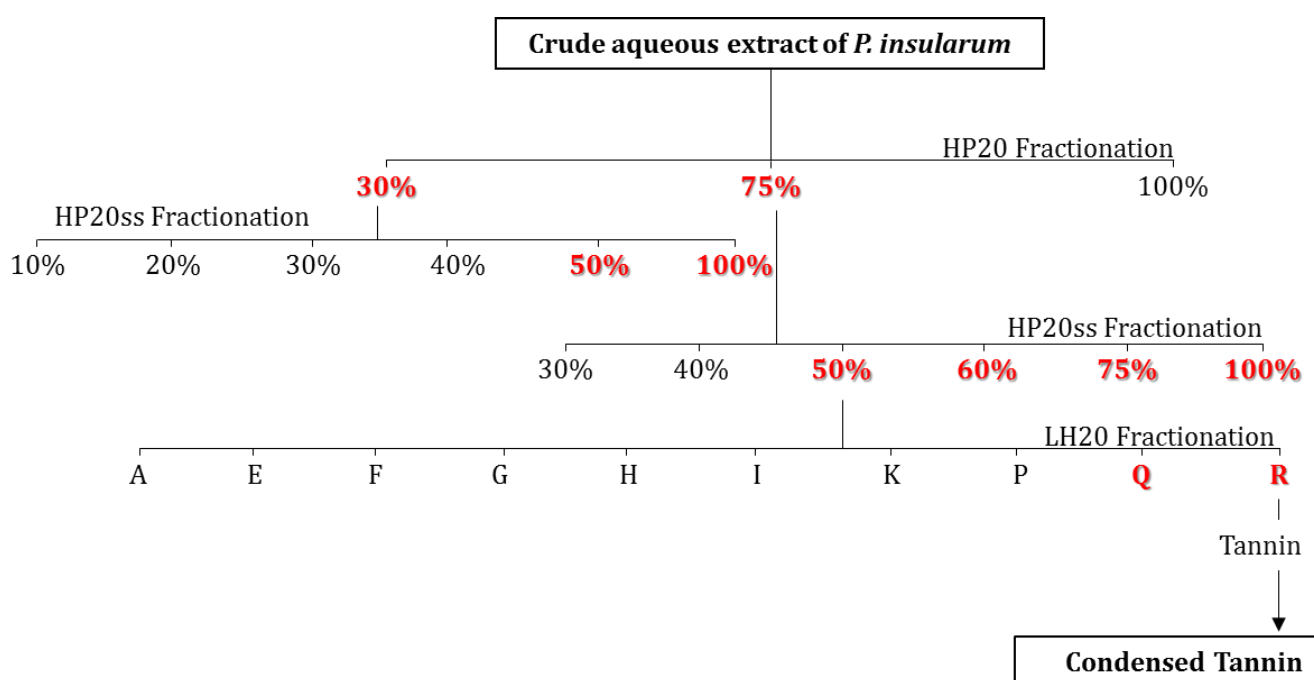


**Figure 5.12: Summary of the bioassay guided fractionation of the crude aqueous extract of *P. insularum*.** HP20 fractionation produced 30% and 75% fractions that were bioactive (in red). The 30% fraction was further fractionated with an HP20ss column, producing bioactive (in red) 50% and 100% fractions. HP20ss fractionation of the 75% HP20 fraction produced bioactive (in red) fractions 50% and 60-100% which were pooled. The 50% fraction from the HP20ss fractionation of the 75% was further fractionated with an LH20 column, producing 10 fractions, from which only Q and R were shown to be bioactive (in red). Fraction R tested positive for tannin and condensed tannin.

The fractionation scheme utilized in the first two fractionation steps here were on the basis of polarity of extract components (Fig 4.13). Essentially, most of the components of the extract elute at higher polarity elution solvent (*i.e.*, low acetone concentration) and are often composed of polysaccharides, sugars, soluble proteins and nucleotides. At lower polarity elution concentrations (*i.e.*, high acetone concentration), lipids and fatty acids are eluted. The area highlighted (red dashed

box in Fig 4.13) is often the area of most interest because this is the polarity range where secondary metabolites elute that are often responsible for bioactivity of small molecules. Interestingly, detecting the iron chelation bioactivity from the original 30% and 75% acetone HP20 fractions, and later from the 50% acetone HP20ss fraction, correlated to the area of the basic concept of polarity fractionation curve of natural products where plant secondary metabolites often elute. This suggested the compound responsible for the activity of interest is a plant secondary metabolite.

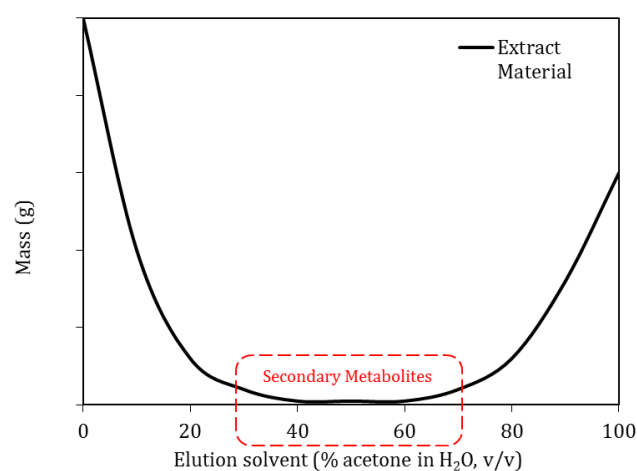


**Figure 5.13: Basic concept of polar fractionation of crude extract material.** Polysaccharides and sugars elute at higher polarity (*i.e.*, low acetone concentrations) while lipids elute at lower polarity (*i.e.*, high acetone concentrations). The area highlighted by the red dashed box is the area of most interest where secondary metabolites elute, around 30-70% acetone in water, v/v (West, 2001).

LH20 column chromatography employing separation on a size exclusion basis separated components based on size, where larger molecules pass through the columns more quickly than the smaller molecules. The lack of bioactivity from the originally collected 5 mL fractions (330 fractions) indicated that the larger molecules and subsequently smaller molecules that were eluted during these fractions were not responsible for the bioactivity. Further, it suggested that the molecular entity responsible for the iron chelation bioactivity of interest was one that was problematic to elute off an LH20 column with methanol most likely due to the strong adsorption of aromatic (benzene) components to the resin surfaces. This is in line with tannins, which often require a combination of acetone or alcohol in water for their elution off an LH20 column (Dai & Mumper, 2010).

Our bioassay guided fractionation approach required a well characterized bioassay probing a biological activity of interest. Given our previous findings, we employed two assays: the yeast growth inhibition assay, and the iron rescue assay. As such, our approach allowed the tracking of the iron chelating bioactivity of interest throughout the different fractionation steps. However, this approach is also disadvantageous; because of its inherent pursuit of a specific bioactivity, this approach ignores novel compounds that do not exhibit the activity of interest. Further, in instances where bioactivity is a consequence of the synergistic activities of two or more compounds, fractionation leads to the loss of activity. Additionally, this approach often leads to the isolation of already known compounds, although this can be rectified, as was carried out here, through the incorporation of spectroscopic analyses to prevent further fractionation where an already known compound is identified as the bioactive component.

Tannins are a type of secondary metabolite that belong to the phenolics group, and have been widely reported to have antimicrobial and anti-inflammatory properties used in medicinal application as diuretics, astringents and antiseptics (Kabera *et al.*, 2014; Khanbabaee & van Ree, 2001). Mechanisms by which tannins exert their effects include enzyme inhibition and substrate deprivation, activity on cellular membranes and metal complexation (Scalbert, 1991). Indeed, iron chelation has been reported from various tannins including tannic acid, procyanidin and catechins (Hagerman *et al.*, 1998; South & Miller, 1998). The presence of condensed tannins in our final fraction producing the iron chelation activity of interest is therefore consistent with the long history behind the metal deprivation activity of tannins (Scalbert, 1991). It is also of interest given the positive result obtained from our iron chelation assay (Fig 3.15) meaning that it is likely that another plant extract possessing iron-chelating tannins would have produced a similar positive result from this CAS assay. Also of interest and requiring consideration is the ability of tannins to precipitate proteins. This is of interest because bioactivities depending on proteins could be confounded by this activity of tannins. However, this cannot be the case here, because we have demonstrated that iron chelation carried out in a non-cell lysate environment (*i.e.*, in chemical solutions only with the

extract) exhibited iron chelation, indicating that iron chelation of *P. insularum* is independent of proteins, and therefore cannot be attributed to the protein precipitation activity of tannins.

Condensed tannins have a wide array of therapeutic functions in mammalian models of various human diseases. For instance, condensed tannins isolated from cacao inhibited the development of cataracts in diabetic rats (Osakabe *et al.*, 2003). Additionally, condensed tannins from grapeseed protected cardiomyocytes from ischemia, reduced cardiotoxicity resulting from Doxorubicin treatment, and reduced angiogenesis resulting from colon cancer (Huang *et al.*, 2012; Li *et al.*, 2010; Shao *et al.*, 2009). Other biological activities that have been observed from condensed tannins include antimicrobial (Avorn *et al.*, 1994; de Bryune *et al.*, 1999; Howell *et al.*, 2002; Kolodziej *et al.*, 1999; Kontiokari *et al.*, 1999), antiviral (Barnard *et al.*, 1993; de Bruyne *et al.*, 1999; Ma *et al.*, 2000; Shahat *et al.*, 2002), and antiprotozoal activities (Calzada *et al.*, 1999; Calzada *et al.*, 2000; Kolodziej *et al.*, 2001). Antioxidant effects of condensed tannins have also been studied and attributed to their ability to scavenge radicals (Nanjo *et al.*, 1996; Plumb *et al.*, 1993; Yokozawa *et al.*, 1998), inhibit pro-oxidant enzymes such as lipoxygenase (Moini *et al.*, 2002; Schewe *et al.*, 2001; Schewe *et al.*, 2002) and chelate metals (Facino *et al.*, 2002; Yoneda & Nakatsubo, 1998). Anti-inflammatory effects of condensed tannins have also been investigated and proposed to be mediated through the NF- $\kappa$ B pathway (Park *et al.*, 2000; Saliou *et al.*, 2001; Yang *et al.*, 1998), which is the same pathway proposed herein to mediate the iron chelating anti-inflammatory activities demonstrated by the aqueous extract of *P. insularum*.

Up to this point, we have not considered the possibility of multiple bioactive compounds in the extracts from *P. insularum*. The findings from our LH20 bioassay guided fractionation however showed that bioactivity was completely absent from fractions without the 6-7 ppm hump (Fig 5.8). These findings support the premise that bioactivity is restricted to the unresolved 6-7 ppm hump. However, the possibility that the unresolved hump may contain more than one compound still suggests that there may be more bioactive compounds, although this will be further clarified upon further purification of the unresolved hump or the R fraction.

In summary, we have identified condensed tannins as the chemical group of secondary metabolites that mediate the iron-chelating bioactivity of *P. insularum* extracts in yeast and mammalian cells. However, the complex nature of the condensed tannin isolated from the aqueous extract of *P. insularum* is currently unknown and requires further investigation to identify the condensed tannin. Furthermore, the applicability of the condensed tannin isolated herein as a lead compound needs to be investigated, where for instance, modifications to its structure which is yet to be determined, may improve its activity and drug potential.

---

## Chapter 6:

# Implications & Future Directions

---

### 6.1 Summary

The overall aim of this project was to ascertain the pharmaceutical potential of traditional Samoan medicinal plants via determining their mechanism of action and their chemical composition. In Chapter 2, the bioactivity of Samoan medicinal plants was assessed from which 15 of 22 extracts were shown to be bioactive in yeast. More significantly, 10 of 11 plants produced an extract that reduced yeast growth to an extent amenable to genome-wide analyses to identify gene deletions that significantly enhance bioactivity. Extracts from the medicinal plant *Psychotria insularum* were identified as the most potent against yeast growth. In Chapter 3, iron chelation was established as the mechanism of action for the extracts from *P. insularum*. This iron chelation activity was also shown to mediate the anti-inflammatory effects of the extracts in murine macrophages. In Chapter 4, it was further determined that the iron chelation mechanism does not include targeting a single gene, a result consistent with the extracts targeting iron directly. In Chapter 5, bioassay-guided fractionations were used to determine that condensed tannins were the class of compounds responsible for the iron chelation activity of the extract. In this chapter, the implications of the findings presented thus far will be discussed.

### 6.2 Implications on *P. insularum* as a potential pharmaceutical

Leaf extracts of the Samoan medicinal plant *P. insularum* have been used since the 1800's to treat supernaturally induced ailments, abdominal distress and ailments associated with inflammation (*e.g.*, wounds, infections, fevers) (Cox *et al.*, 1989; Whistler, 1996). Various studies have demonstrated extracts from *P. insularum* reduced hypertension, motor function, ear oedema as well as prostaglandin synthesis, and were toxic at high concentrations in mice (Cox *et al.*, 1989;

Dunstan *et al.*, 1997; Norton *et al.*, 1974). However, the underlying molecular mechanism by which *P. insularum* extracts mediated these different effects was not investigated. In this thesis, the iron chelation mechanism of action of the *P. insularum* extracts was identified, and in combination with available literature, can account for these activities. For instance, it has been demonstrated that iron chelation promoted vasodilation and subsequently lowered blood pressure (Duffy *et al.*, 2001), thus providing a tentative connection between the iron chelation mechanism of action identified in this dissertation and the hypotensive activity of *P. insularum* (Norton *et al.*, 1974). Additionally, the work described herein proposed a NF- $\kappa$ B dependent link between iron chelation and the anti-inflammatory response detected in murine macrophages treated with *P. insularum* extracts. Indeed, this link corroborates the previous report that *P. insularum* reduced prostaglandin biosynthesis (Dunstan *et al.*, 1997), since cyclooxygenase-2 (COX-2) that regulates prostaglandin synthesis is in turn regulated by NF- $\kappa$ B (Inoue & Tanabe, 1998, Newton *et al.*, 1997; Schmedtje *et al.*, 1997). Therefore, a reduction in NF- $\kappa$ B activation caused by iron chelation would lead to reduced COX-2 activity and prostaglandin synthesis. In contrast, work by Tanji *et al.* (2001) on the iron chelator desferroxamine (DFX) demonstrated that DFX upregulated the production of prostaglandin, which promoted the inflammatory process. The discrepancy between the results of the iron chelator DFX and the iron chelation activity of *P. insularum* may be a consequence of the different cells used, as the work described herein utilized primary murine macrophages, while Tanji *et al.* (2001) used the immortalized U937 human macrophage cell line.

Although elucidating the MOA of the *P. insularum* leaf extracts is a novel contribution of this thesis to the fields of genetics and molecular biology, identification of the class of bioactive compounds responsible for the iron chelating activity as condensed tannins is also a noteworthy outcome of this thesis. Condensed tannins have a wide array of therapeutic functions in mammalian models such as inhibiting the development of cataracts in diabetic rats (Osakabe *et al.*, 2003); protection of cardiomyocytes from ischemia, reduced cardiotoxicity resulting from Doxorubicin treatment, and reduced angiogenesis resulting from colon cancer (Huang *et al.*, 2012; Li *et al.*, 2010;

Shao *et al.*, 2009); as well as antimicrobial (Avorn *et al.*, 1994; de Bryune *et al.*, 1999; Howell *et al.*, 2002; Kolodziej *et al.*, 1999; Kontiokari *et al.*, 1999), antiviral (Barnard *et al.*, 1993; de Bruyne *et al.*, 1999; Ma *et al.*, 2000; Shahat *et al.*, 2002), and antiprotozoal activities (Calzada *et al.*, 1999; Calzada *et al.*, 2000; Kolodziej *et al.*, 2001). Condensed tannins have also been to chelate metals (Facino *et al.*, 2002; Yoneda & Nakatsubo, 1998) and have anti-inflammatory properties (Park *et al.*, 2000; Saliou *et al.*, 2001; Yang *et al.*, 1998).

Iron chelators are largely becoming of great interest as drug candidates in regulating diseases exhibiting iron overload. Primarily, excess iron in the body often arises from a genetic condition (*e.g.*, hereditary haemochromatosis), but can also result from chronic blood transfusion (*e.g.*, to treat  $\beta$ -thalassemia major patients) (Faa & Crispon, 1999). In addition, iron deposits accumulate to toxic levels in neurodegenerative disorders such as Alzheimer's disease (Connor *et al.*, 1992), Parkinson's disease (Sofic *et al.*, 1988), Huntington's disease (Dexter *et al.*, 1991) and HIV encephalopathy (Miszkiel *et al.*, 1997). While DFX has been the iron chelator of choice for the treatment of hereditary haemochromatosis and  $\beta$ -thalassemia major patients, it requires extended subcutaneous infusion because it has a short half-life and is inactive when administered orally (Aouad *et al.*, 2002). Deferiprone (DFP) is another iron chelator that is approved for use in the EU, Canada and the US particularly in  $\beta$ -thalassemia major patients who do not respond to other iron chelation therapy (Poggiali *et al.*, 2012). Interestingly, analogues of DFP have been investigated for potentially treating neurodegenerative diseases (Molina-Holgado *et al.*, 2008). Deferasirox (DFS) is the most orally-administered iron chelator approved and can be used in patients as young as two years old (Piga *et al.*, 2006). However, despite these successes in the development of iron chelators as therapeutic agents, these drugs elicit toxic adverse effects such as growth retardation, proteinuria, elevated liver enzymes and allergic reactions (Poggiali *et al.*, 2012). This highlights the need for a new iron chelator in the clinic, which ideally should be able to cross the gastro-intestinal tract, be selective for iron and have low toxicity but should not be able to cross the blood-placenta

barrier for the treatment of general iron imbalance; in the cases of neurodegenerative diseases, the iron chelator should also be able to cross the blood-brain barrier (Faa & Crisponi, 1999).

Condensed tannins have demonstrated great potential as drug candidates given primary beneficial effects on basic cellular processes such as oxidative stress and secondary health effects on complications arising from diseases. By extension, this makes the condensed tannin isolated from the aqueous extract of *P. insularum* a potential drug candidate, made even more convincing given its applicability as an iron chelator. However, the applicability of compounds such as condensed tannins as iron chelators in modern day medicine has not yet been investigated. Indeed, there is contradicting literature regarding the uptake of condensed tannins from the intestinal environment into the bloodstream and given the size complexity of condensed tannins, this may be a hindrance. Further investigation is warranted into identifying the compositional complexity of the condensed tannin and establishing a connection between iron chelation arising from *P. insularum* extracts and the proposed downregulation of NF- $\kappa$ B manifesting in the anti-inflammatory effects of the *P. insularum* extracts.

### 6.3 Implications on *P. insularum* application in Samoan medicine

While the demonstrated anti-inflammatory effects of *P. insularum* extracts are in line with the application of the plant to treat inflammation-related ailments in Samoa, this research has also brought to light that *P. insularum* may treat additional diseases given its iron chelating activity and the relevance of iron chelating agents to diseases with iron imbalance. As mentioned previously, hereditary haemochromatosis is a genetic condition that manifests in iron overload (Faa & Crisponi, 1999). From a sample of 169 Polynesian individuals, there was a 0.89% prevalence of a mutation that results in this condition (Cullen *et al.*, 1998). By extrapolation, this suggests that of the whole population of Samoa (~200,000 people), approximately 1,780 people have haemochromatosis specific to this mutation, not including haemochromatosis of other mutations. Alzheimer's disease, which has increasing evidence of iron imbalance (Connor *et al.*, 1992), recorded a move up in

ranking for the cause of premature death in Samoa, from 56<sup>th</sup> in 1990 to 25<sup>th</sup> in 2010 (“GBD Profile: Samoa”, 2010), indicative of increasing prevalence in Samoa. Overall, there is increasing prevalence of diseases including disrupted iron homeostasis in Samoa, and there is no better place to turn than to one of Samoa’s own traditional medicinal plants.

## 6.4 Implications on the *P. insularum* plant

Whistler (1986) reported the *Psychotria* genus of the Rubiaceae family as one of the most diverse genera across the Pacific, with the Samoan archipelago home to 20 *Psychotria* species. Although this genus was reported as abundant in 1986, a more recent report of its abundance, or more specifically that of *P. insularum*, is not available. To that end, the medicinal plant *P. insularum* has not yet been assessed by the International Union for Conservation of Nature (IUCN) for their list of endangered and threatened plant species ([www.iucnredlist.org](http://www.iucnredlist.org)). When plants were being collected for this study, *P. insularum* was not particularly abundant in national parks and had to be sourced from a single private property owned by local healers actively cultivating the species. Barring the possibility of this was not due to environmental factors (*e.g.*, seasonal fluctuation) this suggests that the abundance of the species in the wild is reduced. Therefore, the wild populations of *P. insularum* need to be evaluated particularly to avoid the future scenario where pharmaceutical potential is realized but wild populations are endangered.

This study utilized a single source of *P. insularum* from a private property of relatively low elevation (40-50 m). The study cannot however report on the bioactivity of leaves obtained from *P. insularum* plants at higher elevations or from different locations. Indeed, different populations of the Samoan medicinal plant *Homalanthus nutans* contained different amounts of the anti-HIV compound prostratin (Johnson *et al.*, 2008). Therefore, to broaden the applicability and the validity of the findings from this project, it is important to perform similar bioactivity studies on extracts from additional *P. insularum* plants. We recommend that yeast growth assays, iron rescue assays and NMRs be conducted to determine if the iron chelating activity of condensed tannins that we

identified in *P. insularum* extracts from one location (Chapters 3 & 4) are also active in new extracts from additional locations and elevations in Samoa. In addition, it would be interesting to quantify the iron-chelating potency of condensed tannins in plant parts other than *P. insularum* leaves, particularly since different parts of *H. nutans* plant contained varying amounts of prostratin (Johnson *et al.*, 2008).

## 6.5 Implications on natural products in Samoa

Previous work demonstrated the great potential of Samoan medicinal plants, illustrating bioactivity in animal and human cells, albeit with minimal knowledge on the underlying molecular mechanisms mediating their bioactivities (Cox *et al.*, 1989; Dunstan *et al.*, 1997; Norton *et al.*, 1974). This thesis on *P. insularum* has produced results that further corroborates the pharmaceutical potential of Samoan medicinal plants via the determination of the mechanism of action of *P. insularum* leaf extracts, and thus warrants extension of this research into under-studied Samoan medicinal plants. Perhaps it may also warrant an investigation into other Samoan resources as sources of natural products as a whole (*e.g.*, marine products). A Samoan saying goes “*E fofo ele alamea le alamea*”, which translates into “An injury from a crown-of-thorns starfish will be cured by the crown-of-thorns starfish” because the crown-of-thorns starfish (*Acanthaster planci*), when placed onto the injury site, will suck the toxin out itself. Indeed, bioactive compounds have been isolated from the toxins of *A. planci* that induce apoptosis, oxidative stress and ER stress (Lee *et al.*, 2014; Lee *et al.*, 2015). These findings reiterate that there is traditional knowledge to be exploited in Samoa regarding native plants and marine organisms, specifically with realizing the pharmaceutical potential of native natural products isolated from these sources.

## 6.6 Future Experiments

In Chapter 3, we identified a link between iron chelation and inflammation work, and had proposed a NF- $\kappa$ B mediated connection. This relationship requires further investigation, potentially

by monitoring kinase activities of inhibitors of NF- $\kappa$ B in the presence of the extract, control treatment, as well as in high iron conditions. It is postulated that the kinase activity of IKK (inhibitor of NF- $\kappa$ B kinase) will be reduced in the presence of the *P. insularum*, preventing the inhibitors of NF- $\kappa$ B dissociating from NF- $\kappa$ B and ultimately inhibiting the downregulation of IL-10, thereby resulting in an anti-inflammatory response. In Chapter 4, it was determined that a similarity between the diploid pooled genome-wide analyses of the extracts of *P. insularum* and the agar-based haploid screen was the absence of iron transporters and their transcription factor from hypersensitive mutants. To confirm that this was a caveat of the assay as observed in agar, we propose a validation of diploid iron transporter mutants individually against the extracts of *P. insularum*. Given that the haploid strains were hypersensitive in liquid, we expect the diploid strains will also be hypersensitive, and that the lack of detection from the pooled assays may be a consequence of high-throughput screening. Alternatively, it is also possible that in a pooled environment, there is an environment of multiple strains that may survive less well than iron-dependent mutants that were thus killed, and their waste material recycled including iron, leading to better growth of iron-related mutants. We were not able to fully isolate the bioactive component of the *P. insularum* extracts in our efforts described in Chapter 5, and we were only able to partially purify the crude extract and determine that the bioactivity was attributable to a condensed tannin. We propose further chemical analyses utilizing HPLC in combination with mass spectrometry may isolate the compound and permit its identification.

Given the potential of iron chelators to mediate diseases with aberrant iron regulation, there is a possibility our iron chelating condensed tannin may be beneficial in such diseases. For instance, iron dysregulation has been reported in diseases such as Alzheimer's, Parkinson's, obesity and diabetes. We propose that disease models for these be treated with varying concentrations of our condensed tannin to investigate whether our condensed tannin can alleviate some of these disease symptoms. Furthermore, it would be interesting to survey the prevalence of *P. insularum* use in traditional Samoan medicine, and its reported efficacy and whether the reported efficacy

correlated to the anti-inflammatory activity or iron chelating activity of *P. insularum* extracts as determined from this dissertation.

## 6.7 Conclusion

In conclusion, this dissertation used genome-wide analyses to establish the MOA of crude extracts of a medicinal plant. We established that the leaf extracts of the Samoan medicinal plant *P. insularum* mediated its bioactivity via an iron chelating mechanism. We also determined that the bioactive component of the *P. insularum* extracts mediating this activity belonged to the chemical class of condensed tannins. Indeed, findings from this work have made novel contributions to the broad fields of biology and chemistry, with multiple implications not only on the potential of this particular Samoan medicinal plant as a pharmaceutical agent, but also on its application in traditional Samoan medicine. Overall, these findings provide a strong and positive outlook for the potential for further discoveries to be made from Samoan medicinal plants.

---

## References:

---

- Abe, F. and Hiraki, T. (2009). Mechanistic role of ergosterol in membrane rigidity and cycloheximide resistance in *Saccharomyces cerevisiae*. *Biochimica et Biophysica Acta*. **1788(3)**: 743-752
- Aerts, AM.; Fracois, I.; Cammue, BPA. and Thevissen, K. (2008) The mode of antifungal action of plant, insect and human defensins. *Cellular and Molecular Life Sciences* **65**: 2069-2079
- Agne, B.; Meindl, NM.; Niderhoff, K.; Einwachter, H.; Rehling, P.; Sickmann, A.; Meyer, JE.; Girzalsky, W. and Kunau, WH. (2003). Pex8p: an intraperoxisomal organizer of the peroxisomal import machinery. *Molecular Cell*. **11(3)**: 635-646
- Alanis-Garza, BA.; Gonzales-Gonzales, GM.; Salazar-Aranda, R.; Waksman de Torres, N. and Rivas-Galindo, VM. (2007). Screening of antifungal activity of plants from the northeast of Mexico. *Journal of Ethnopharmacology*. **114(3)**: 468-471
- Alexander, DB. and Zuberer, DA. (1991). Use of chrome azurol S reagents to evaluate siderophore production by rhizosphere bacteria. *Biology and Fertility of Soils*. **12**: 39-45
- Ali-Shtayeh, MS. and Abu Ghdeib, SI. (1999). Antifungal activity of plant extracts against dermatophytes. *Mycoses* **41(5-6)**: 243-248
- Alves, RRN. and Albuquerque, UP. (2013). Animals as a source of drugs: bioprospecting and biodiversity conservation. In Alves, RRN and Rosa, IL (eds). *Animals in Traditional Folk Medicine*. Springer-Verlag Berlin Heidelberg. pp 67-89
- Amerik, AY.; Nowak, J.; Swaminathan, S. and Hochstrasser, M. (2000). The Doa4 deubiquitinating enzyme is functionally linked to the vacuolar protein-sorting and endocytic pathways. *Molecular Biology of the Cell*. **11(10)**: 3365-3380
- Aouad, F.; Florence, A.; Zhang, Y.; Collins, F.; Henry, C.; Ward, RJ. and Crichton, RR. (2002). Evaluation of new iron chelators and their therapeutic potential. *Inorganic Chimica Acta*. **339**: 470-480
- Archin, NN. and Margolis, DM. (2014). Emerging strategies to deplete the HIV reservoir. *Current Opinion in Infectious Diseases*. **27(1)**: 29-35
- Aronson, JK. (1977). Medicine in Staffordshire. *British Medical Journal* **16(1)**: 1031-1032

- Arthington, BA.; Hoskins, J.; Skatrud, PL. and Bard, M. (1991). Nucleotide sequence of the gene encoding yeast C-8 sterol isomerase. *Gene*. **107(1)**: 173-174
- Askwith, C.; Eide, D.; van Ho, A.; Bernard, PS.; Li, L.; Davis-Kaplan, S.; Sipe, DM.; Kaplan, J. (1994). The FET3 gene of *S. cerevisiae* encodes a multicopper oxidase required for ferrous iron uptake. *Cell*. **76(2)**: 403-410
- Atheron, J. and Jefferies, B. (2012). *Rapid biodiversity assessment of upland Savaii, Samoa*. Apia, Samoa: Ministry of Natural Resources & Environment, Secretariat of the Pacific Regional Environment Programme (SPREP), retrieved from [www.cepf.net/SiteCollectionDocuments/poly\\_micro/59745\\_TechnicalReport\\_RAP\\_Upland\\_Savaii.pdf](http://www.cepf.net/SiteCollectionDocuments/poly_micro/59745_TechnicalReport_RAP_Upland_Savaii.pdf)
- Amberg, DC.; Burke, DJ. and Strathern, JN. (2005). *Methods in Yeast Genetics: A Cold Spring Harbor Laboratory Course Manual*. New York: Cold Spring Harbor Lab Press
- Avorn, J.; Monane, M.; Gurwitz, JH.; Glynn, RJ.; Choodnovskiy, I.; Lipsitz, LA. (1994). Reduction of bacteriuria and pyuria after ingestion of cranberry juice. *JAMA*. **27(10)**: 751-753
- Azad, K.; Hossain, F. and Halim, MA. (2013). Screening of cellulose, pectinase and xylanase activities and optimization of radial mycelia growth of two thermophilic fungi. *Bangladesh Journal of Botany*. **42**: 207-213
- Baetz, K.; McHardy, L.; Gable, K.; Tarling, T.; Reberioux, D.; Bryan, J.; Andersen, RJ.; Dunn, T.; Hieter, P. and Roberge, M. (2004). Yeast genome-wide drug-induced haploinsufficiency screen to determine drug mode of action. *Proceedings of the National Academy of Science* **101(13)**: 4525-4530
- Baker, RT.; Tobias, JW. and Varshavsky, A. (1992). Ubiquitin-specific proteases of *Saccharomyces cerevisiae*. Cloning of UBP2 and UBP3, and functional analysis of the UBP gene family. *Journal of Biological Chemistry*. **267(32)**: 23364-23375
- Baker, HM.; Anderson, BF. and Baker, EN. (2003). Dealing with iron: common structural principles in proteins that transport iron and heme. *Proceedings of the National Academy of Science* **100**: 3579-3583
- Barnard, DL.; Smee, DF.; Huffman, JH.; Meyerson, LR. and Sidwell, RW. (1993). Antiherpes virus activity and mode of action of SP-303, a novel plant flavonoid. *Chemotherapy*. **39(3)**: 203-211
- Beh, CT. and Rine, J. (2004). A role for yeast oxysterol-binding protein homologs in endocytosis and in the maintenance of intracellular sterol-lipid distribution. *Journal of Cell Science*. **15**: 2984-2996

- Bender, A. and Pringle, JR. (1991). Use of a screen for synthetic lethal and multicopy suppressor mutants to identify two new genes involved in morphogenesis in *Saccharomyces cerevisiae*. *Molecular and Cellular Biology* **11(3)**: 1295-1305
- Benjamin, D.; Colombi, M.; Moroni, C. and Hall, MN. (2011). Rapamycin passes the torch: a new generation of mTOR inhibitors. *Nature Reviews: Drug Discovery*. **10(11)**: 868-880
- Best, HA.; Matthews, JH.; Heathcote, RW.; Hanna, R.; Leahy, DC.; Coorey, NV.; Bellows, DS.; Atkinson, PH. and Miller, JH. (2013). Laulimalinone and peloruside A inhibit mitosis of *Saccharomyces cerevisiae* by preventing microtubule depolymerisation-dependent steps in chromosome separation and nuclear positioning. *Molecular Biosystems*. **9(11)**: 2842-2852
- Bianchi, MM.; Sartori, G.; Vandenbol, M.; Kaniak, A.; Uccelletti, D.; Mazzaoni, C.; di Rago, JP.; Garignani, G.; Slonimski, PP. and Frontali, L. (1999). How to bring orphan genes into functional families. *Yeast*. **15(6)**: 513-526
- Bilsland, E.; Hult, M.; Bell, SD.; Sunnerhagen, P. and Downs, JA. (2007). The Bre5/Ubp3 ubiquitin protease complex from budding yeast contributes to the cellular response to DNA damage. *DNA Repair*. **6(10)**: 1471-1484
- Bircham, PW.; Maass, DR.; Roberts, CA.; Kiew, PY.; Low, YS.; Yegambaram, M.; Matthews, JH.; Jack, CA. and Atkinson, PH. (2011). Secretory pathway genes assessed by high-throughput microscopy and synthetic genetic array analysis. *Molecular Biosystems*. **7(9)**: 2589-2598
- Blunt, JW.; Copp, BR.; Keyzers, RA.; Munro, MHG. and Prinsep, MR. (2012). Marine natural products. *Natural Products Reports*. **29**: 144-222
- Boman, HG. (1991). Antibacterial peptides: key components needed in immunity. *Cell*. **65**: 205-207
- Boone, C.; Bussey, H. and Andrews, BJ. (2007). Exploring genetic interactions and networks with yeast. *Nature Reviews: Genetics*. **8**: 437-449
- Bordallo, J.; Bordallo, C.; Gascon, S.; Suarez-Rendueles, P. (1991). Molecular cloning and sequencing of genomic DNA encoding yeast vacuolar carboxypeptidase yscS. *FEBS Letters*. **283(1)**: 27-32
- Brackovic, A. and Harvey, JE. (2015). Synthetic, semisynthetic and natural analogues of peloruside A. *Chemical Communications (Camb)*. **51(23)**: 4750-4765
- Breter, HJ.; Ferguson, J.; Peterson, TA. and Reed, SI. (1983). Isolation and transcriptional characterization of three genes with function at start, the controlling event of the

- Saccharomyces cerevisiae* cell division cycle: CDC36, CDC37 and CDC39. *Molecular and Cellular Biology*. **3(5)**: 881-891
- Brune, K. and Hinz, B. (2004). The discovery and development of anti-inflammatory drugs. *Arthritis & Rheumatism*. **50(8)**: 2391-2399
- Cairns, BR.; Kim, YJ.; Sayre, MH.; Lauren, BC. and Kornberg, RD. (1994). A multisubunit complex containing the SWI1/ADR6, SWI2/SNF2, SWI3, SNF5 and SNF6 gene products isolated from yeast. *Proceedings of the National Academy of Science*. **91(5)**: 1950-1954
- Callegari, S.; McKinnon, RA.; Andrews, S.; de Barros Lopes, MA. (2010). Atorvastatin-induced cell toxicity in yeast is linked to disruption of protein isoprenylation. *FEMS Yeast Research*. **10(2)**: 188-198
- Calzada, F.; Cerda-Garcia-Rojas, CM.; Meckes, M.; Cedillo-Rivera, R.; Bye, R. and Mat, R. (1999). Geranins A and B, new antiprotozoal A-type proanthocyanidins from *Geranium niveum*. *Journal of Natural Products*. **62**: 705-709
- Calzada, F.; Cedillo-Rivera, R. and Mata, R. (2001). Antiprotozoal activity of the constituents of *Conyza filaginoids*. *Journal of Natural Products*. **64**: 671-673
- Campbell, WC. (2012). History of avermectin and ivermectin, with notes on the history of other macrocyclic lactone antiparasitic agents. *Current Pharmaceutical Biotechnology*. **13(6)**: 853-865
- Carbrera, M.; Arlt, H.; Epp, N.; Lachmann, J.; Griffith, J.; Perz, A.; Reggiori, F. and Ungermann, C. (2013). Functional separation of endosomal fusion factors and the class C core vacuole/endosome tethering (CORVET) complex in endosome biogenesis. *Journal of Biological Chemistry*. **288(7)**: 5166-5175
- Carmen, AA.; Rundlett, SE. and Grunstein, M. (1996). HDA1 and HDA3 are componenets of a yeast histone deacetylase (HDA) complex. *Journal of Biological Chemistry*. **271(26)**: 15837-15844
- Carroll, SY.; Stirling, PC.; Stimpson, HE.; Giesselmann, E.; Schmitt, MJ. and Drubin, DG. (2009). A yeast killer toxin screen provides insights into a/b toxin entry, trafficking, and killing mechanisms. *Developmental Cell*. **17(4)**: 552-560
- Chabes, A.; Domkin, V. and Thelander, L. (1999). Yeast Sml1, a protein inhibitor of ribonucleotide reductase. *Journal of Biological Chemistry*. **274(51)**: 36679-36683
- Chen, OS.; Crisp, RJ.; Valachovic, M.; Bard, M.; Winge, DR. and Kaplan, J. (2004). Transcription of the yeast iron regulon does not respond directly to iron but rather to iron-sulfur cluster biosynthesis. *Journal of Biological Chemistry*. **279(28)**: 29513-29518

- Collart, MA. and Struhl, K. (1994). NOT1 (CDC39), NOT2 (CDC36), NOT3 and NOT4 encode a global-negative regulator of transcription that differentially affects TATA-element utilization. *Genes & Development*. **8(5)**: 525-537
- Connor, JR.; Menzies, SL.; St. Martin, SM. and Mufson, EJ. (1992). A histochemical study of iron, transferrin, and ferritin in Alzheimer's diseased brains. *Journal of Neuroscience Research*. **31(1)**: 75-83
- Coorey, NV.; Matthews, JH.; Bellows, DS. and Atkinson, PH. (2015). Pleiotropic drug-resistance attenuated genomic library improves elucidation of drug mechanisms. *Molecular Biosystems*. **11(11)**: 3129-3136
- Cos, P.; de Bruyne, N.; Hermans, S.; Apers, D.; Berghe, V. and Vlietinck, AJ. (2003). Proanthocyanidins, in helath care current and new trends. *Current Medicinal Chemistry*. **11(10)**: 1345-1359
- Cox, PA.; Sperry LR.; Tuominen, M. and Bohlin, L. (1989). Pharmacological activity of the Samoan ethnopharmacopoeia. *Economic Botany*. **43(4)**: 487-497
- Cragg, GM. and Newman, DJ. (2013). Natural products: a continuing source of novel drug leads. *Biochimica Biophysica Acta* **1830(6)**: 3670-3695
- Cragg, GM.; Newman, DJ. and Snader, KM. (1997). Natural products in drug discovery and development. *Journal of Natural Products*. **60(1)**: 52-60
- Craven, RJ.; Mallory, JC. and Hand, RA. (2007). Regulation of iron homeostasis mediated by the heme-binding protein Dap1 (damage resistance protein 1) via the P450 protein Erg11/Cyp51. *Journal of Biological Chemistry*. **282(50)**: 36543-36551
- Cui, L. and Su, XZ. (2009). Discovery, mechanisms or action and combination therapy of artemisinin. *Expert Review of Anti-infective Therapy*. **7(8)**: 999-1013
- Cullen, LM.; Gao, X.; Easteal, S. and Jazwinska, EC. (1998). The hemochromatosis 845 G>A and 187 C>G mutations: prevalence in non-Caucasian populations. *American Journal of Human Genetics*. **62(6)**: 1403-1407
- Cushman, DW. and Ondetti, MA. (1999). Design of angiotensin converting enzyme inhibitors. *Nature Medicine*. **5(10)**: 1110-1113
- Cyr, DM.; Langer, T. and Douglas, MG. (1994). DnaJ-like proteins: molecular chaperones and specific regulators of Hsp70. *Trends in Biochemical Sciences*. **19(4)**: 176-181

- Dai, J. and Mumper, R. (2010). Phant phenolics: Extraction, analysis and their antioxidant and anticancer properties. *Molecules*. **15(10)**: 7313-7352
- Davies, MK. and Hollman, A. (2002). The opium poppy, morphine, and verapamil. *Heart*. **88**: 3
- De Bruyne, T.; Pieters, L.; Witvrouw, M.; de Clercq, E.; van den Berghe, D. and Vlietinck, AJ. (1999). Biological evaluation of proanthocyanidin dimers and related polyphenols. *Journal of Natural Products*. **62(7)**: 954-958
- De Silva, DM.; Askwith, CC.; Eide, D. and Kaplan, J. (1995). The FET3 gene product required for high affinity iron transport in yeast is a cell surface ferroxidase. *Journal of Biological Chemistry*. **270(3)**: 1098-1101
- Dexter, DT.; Carayon, A.; Javoy-Agid, F.; Agid, Y.; Wells, FR.; Daniel, SE.; Lees, AJ.; Jenner, P. and Marsden, CD. (1991). Alternations in the levels of iron, ferritin and other trace metals in Parkinson's disease and other neurodegenerative diseases affecting the basal ganglia. *Brain*. **114(4)**: 1953-1975
- Dhandapani, R. and Sabna, B. (2008). Phytochemical constituents of some Indian medicinal plants. *Ancient Science of Life*. **27(4)**: 1-8
- Dias, DA.; Urban, S. and Roessner, U. (2012). A historical overview of natural products in drug discovery. *Metabolites*. **2(2)**: 303-336
- Dittmar, JC.; Reid, RJD. and Rothstein, R. (2010). ScreenMill: a freely available software suite for growth measurement, analysis and visualization of high-throughput screen data. *BMC Bioinformatics*. **11**: 353
- Dix, DR.; Bridgham, JT.; Broderius, MA.; Byersdorfer, CA. and Eide, DJ. (1994). The FET4 gene encodes the low affinity Fe(II) transport protein of *Saccharomyces cerevisiae*. *Journal of Biological Chemistry*. **269(42)**: 26092-26099
- Dix, DR.; Bridgham, J.; Broderius, M. and Eide, DJ. (1997). Characterization of the FET4 protein of yeast. Evidence for a direct role in the transport of iron. *Journal of Biological Chemistry*. **272(18)**: 11770-11777
- Dudley, AM.; Janse, DM.; Tanay, A.; Shamir, R. and Church, GM. (2005). A global view of pleiotropy and phenotypically derived gene function in yeast. *Molecular Systems Biology*. **1**: 1-11
- Duffy, SJ.; Biegelsen, ES.; Holbrook, M.; Russell, JD.; Gokce, N.; Keaney, JF. and Vita, JA. (2001). Iron chelation improves endothelial function in patients with coronary artery disease. *Circulation*. **103**: 2799-2804

- Dunn, B. and Wobbe, CR. (2001). Preparation of protein extracts from yeast. *Current Protocols in Molecular Biology*. Chapter 13: Unit 13
- Dunstan, CA.; Noreen, Y.; Serrano, G.; Cox, PA.; Perera, P. and Bohlin, L. (1997). Evaluation of some Samoan and Peruvian medicinal plants by prostaglandin biosynthesis and rat ear oedema assays. *Journal of Ethnopharmacology*. **57(1)**: 35-56
- Eide, DJ. (1998). The molecular biology of metal iron transport in *Saccharomyces cerevisiae*. *Annual Reviews*. **18**: 441-469
- Endo, A. (2010). A historical perspective on the discovery of statins. *Proceedings of the Japan Academy, Series B Physical and Biological Sciences*. **86(5)**: 484-493
- Eng, J.; Kleinman, W.; Singh, L.; Sings, G. and Raufman, J. (1992). Isolations and characterization of exendin-4, an exendin-3 analog from *Heloderma suspectum* venom. *Journal of Biological Chemistry*. **267(11)**: 7402-7405
- Esposito, E. and Cuzzocrea, S. (2009). TNF-alpha as a therapeutic target in inflammatory diseases, ischemia-reperfusion injury and trauma. *Current Medicinal Chemistry*. **16(24)**: 3152-3167
- Esposito, AM. and Kinzy, TG. (2010). The eukaryotic translation elongation factor 1Bgamma has a non-guanine nucleotide exchange factor role in protein metabolism. *Journal of Biological Chemistry*. **285(49)**: 37995-38004
- Faa, G. and Crisponi, G. (1999). Iron chelating agents in clinical practice. *Coordination Chemistry Reviews*. **184**: 291-310
- Falagas, ME.; McDermott, L. and Snyderman, DR. (1997). Effect of pH on in vitro antimicrobial susceptibility of the *Bacteroids fragilis* group. *Antimicrobial Agents and Chemotherapy*. **41(9)**: 2047-2049
- Faulkner, DJ. (2000). Highlights of marine natural products chemistry (1972-1999). *Natural Products Reports*. **17(1)**: 1-6
- Feng, J.; Yang, XW. and Wang, RF. (2011). Bio-assay guided isolation and identification of  $\alpha$ -glucosidase inhibitors from the leaves of *Aquilaria sinensis*. *Phytochemistry*. **72(2)**: 242-247
- Ferreira, SH.; Bartlet, DC. and Greene, LJ. (1970). Isolation of bradykinin-potentiating peptides from *Bothrops jararaca* venom. *Biochemistry*. **9(13)**: 2583-2593
- Fisk, DG., Ball, CA.; Dolinski, K.; Engel, SR.; Hong, EL.; Issel-Tarver, L.; Schwartz, K.; Sethuraman, A.; Botstein, D.; Cherry, JM.; Saccharomyces Genome Database Project. (2006). *Saccharomyces cerevisiae* S288C genome annotation: a working hypothesis. *Yeast*. **23(12)**: 857-865

- Foury, F. (1997). Human genetic diseases: a cross-talk between man and yeast. *Gene*. **195(1)**: 1-10
- Fry, RC.; Begley, TJ. and Samson, LD. (2005). Genome-wide responses to DNA-damaging agents. *Annual Reviews of Microbiology*. **59**: 357-377
- Fu, D.; Beller, TJ. and Dunn, TM. (1995). Sequence, mapping and disruption of CCC2, a gene that cross-complements the Ca(2+)-sensitive phenotype of csg1 mutants and encodes a P-type ATPase belonging to the Cu(2+)-ATPase subfamily. *Yeast*. **11(3)**: 283-292
- Fu, D. and Richardson, DR. (2007). Iron chelation and regulation of the cell cycle: 2 mechanisms of posttranscriptional regulation of the universal cyclin-dependent kinase inhibitor p21CIP1/WAF1 by iron depletion. *Blood*. **110(2)**: 752-761
- Ganz, T. and Nemeth, E. (2015). Iron homeostasis in host defense and inflammation. *Nature Reviews: Immunology*. **15(8)**: 500-510
- Gardener, RG.; Swarbrick, GM.; Bays, NW.; Cronin, SR.; Wilhovsky, S.; Seelig, L.; Kim, C. and Hampton, RY. (2000). Endoplasmic reticulum degradation requires lumen to cytosol signaling. Transmembrane control of Hrd1p by Hrd3p. *Journal of Cell Biology*. **151(1)**: 69-82
- Ghaemmaghami, S. Huh, WK.; Bower, K.; Howson, RW.; Belle, A.; Dephoure, N.; O'Shea, EK. and Weissman, JS. (2003). Global analysis of protein expression in yeast. *Nature*. **425(6959)**: 737-741
- Giaever, G.; Shoemaker, DD.; Jones, TW.; Liang, H.; Winzeler, EA.; Astromoff, A. and Davis, RW. (1999). Genomic profiling of drug sensitivities via induced haploinsufficiency. *Nature Genetics*. **21(3)**: 278-283
- Giaever, G.; Chu, AM.; Ni, L.; Connelly, C.; Riles, L.; Veronneau, S.; Dow, S.; Lucau-Danila, A.; Anderson, K.; Andrew, B.; Arkin, AP.; Stromoff, A.; El-Bakkoury, M.; Bangham, R.; Benito, R.; Brachat, S.; Campanaro, S.; Curtiss, M.; Davis, K.; Deutschbauer, A.; Entian, KD.; Flaherty, P.; Foury, F.; Garfinkel, DJ.; Gerstein, M.; Gotte, D.; Guldener, U.; Hegemann, JH.; Hempel, S.; Herman, Z.; Jaramillo, DF.; Kelly, SL.; Kotter, P.; LaBonte, D.; Lamb, DC.; Lan, N.; Liang, J.; Liao, J.; Liu, L.; Luo, C.; Lussier, M.; Mao, R.; Menard, P.; Ppo, SL.; Revuelta, JL.; Roberts, CJ.; Rose, M.; Ross-MacDonald, P.; Scherens, B.; Schimmack, G.; Shafer, B.; Shoemaker, DD.; Sookhai-Mahadeo, S.; Storms, RK.; Strathern, JN.; valle, G.; Voet, M.; Volckaert, G.; Wang, CY.; Ward, TR.; Wilhelmy, J.; Winzeler, EA.; Yang, Y.; Yen, G.; Youngman, E.; Yu, K.; Bussey, H.; Boeke, JD.; Snyder, M.; Phillippsen, P.; Davis, RW. and Johnston, M. (2002). Functional profiling of the *Saccharomyces cerevisiae* genome. *Nature*. **418(6896)**: 387-391

- Giaver, G.; Flaherty, P.; Kumm, J.; Proctor, M.; Nislow, C.; Jaramillo, DF.; Chu, AM.; Jordan, MI.; Arkin, AP. and Davis, RW. (2004). Chemogenomic profiling: identifying the functional interactions of small molecules in yeast. *Proceedings of the National Academy of Science*. **101(3)**: 793-798
- Goebel, MG.; Yochem, J.; Jentsch, S.; McGrath, JP.; Varshavsky, A. and Byers, B. (1988). The yeast cell cycle gene CDC34 encodes a ubiquitin-conjugating enzyme. *Science*. **241(4871)**: 1331-1335
- Goffeau, A.; Barrell, BG.; Bussey, J.; Davis, RW.; Dujon, B.; Feldman, H.; Galiber, F.; Hoheisel, JD.; Jacq, C.; Johnston, M.; Louis, EJ.; Mewes, JW.; Murakami, Y.; Philippsen, P.; Tettelin, J. and Oliver, SG. (1996). Life with 6000 genes. *Science*. **274(5287)**: 563-567
- Gollub, EG.; Liu, KP.; Dayan, J.; Adlersberg, M. and Sprinson, DB. (1977). Yeast mutants deficient in heme biosynthesis and a heme mutant additionally blocked in cyclization of 2,3-oxidosqualene. *Journal of Biological Chemistry*. **252(9)**: 2840-2854
- Graack, HR. and Wittmann-Liebold, B. (1998). Mitochondrial ribosomal proteins (MRPs) of yeast. *Biochemical Journal*. **329 (Pt 3)**: 433-448
- Graziano, BR.; Jonasson, EM.; Pullen, JG.; Gould, CJ. and Goode, BL. (2013). Ligand-induced activation of a formin-NPF pair leads to collaborative actin nucleation. *Journal of Cell Biology*. **201(4)**: 595-611
- Gross, C.; Kelleher, M.; Iyer, VR.; Brown, PO. and Winge, DR. (2000). Identification of the copper regulon in *Saccharomyces cerevisiae*. *Journal of Biological Chemistry*. **275(41)**: 32310-32316
- Guo, W.; Grant, A. and Novick, P. (1999). Exo84p is an exocyst protein essential for secretion. *Journal of Biological Chemistry*. **274(33)**: 23558-23564
- Gustafon, KR.; Cardellin, JH 2<sup>nd</sup>, McMahon, JB.; Gluakowski, RJ.; Ishitoya, J.; Szallasi, Z.; Lewin, NE.; Blumberg, PM.; Weislow, OS.; Beutler, JA. (1992). A nonpromoting phorbol from the Samoan medicinal plant *Homalanthus nutans* inhibits cell killing by HIV-1. *Journal of Medicinal Chemistry*. **35(11)**: 1978-1986
- Hagerman, AE.; Riedl, KM.; Jones, GA.; Sovik, KN.; Rithcard, NT.; Hartzfeld, PW. and Riechel, TL. (1998). High molecular weight plant polyphenolics (tannins) as biological antioxidants. *Journal of Agricultural and Food Chemistry* **46(5)**: 1887-1892
- Hammer, KA.; Carson, CF. and Riley, TV. (1999). Antimicrobial activity of essential oils and other plant extracts. *Journal of Applied Microbiology*. **86(6)**: 985-990

- Hand, RA.; Jia, N.; Bard, M. and Craven, RJ. (2003). *Saccharomyces cerevisiae* Dap1p, a novel DNA damage response protein related to the mammalian membrane-associated progesterone receptor. *Eukaryotic Cell*. **2(2)**: 306-317
- Hartung, EF. (1954). History of the use of *colchicum* and related medicaments in gout. *Annals of Rheumatic Diseases*. **13(3)**: 190-200
- Harrington, MT. (2001). Samoan medicinal plants and their usage. 2<sup>nd</sup> ed. Agricultural Development in the American Pacific Project, Honolulu (HI). 81 pages
- Harvey, AL. (2008). Natural products in drug discovery. *Drug Discovery Today*. **13(19-20)**: 894-901
- Hassett, R.; Dix, DR.; Eide, DJ. and Kosman, DJ. (2000). The Fe(II) permease Fet4p functions as a low affinity copper transporter and supports normal copper trafficking in *Saccharomyces cerevisiae*. *Biochemical Journal*. **351 (Pt 2)**: 477-484
- Hatcher, HC.; Planalp, R.; Cho, J.; Torti, FM. and Torti, SV. (2008). Curcumin: from ancient medicine to current clinical trials. *Cell and Molecular Life Sciences* **65(11)**: 1631-1652
- Hatcher, HC.; Singh, RN.; Torti, FM. And Torti, SV. (2009). Synthetic and natural iron chelators: therapeutic potential and clinical use. *Future Medicinal Chemistry* **1(9)**: 1643-1670
- Heim, KE.; Tagliaferro, AR. and Bobilya, DJ. (2002). Flavonoid antioxidants: chemistry, metabolism and structure-activity relationships. *Journal of Nutritional Biochemistry* **13(10)**: 572-584
- Heinrich, M. and Teoh, LH. (2004). Galanthamin from snowdrop—the development of a modern drug against Alzheimer’s disease from local Caucasian knowledge. *Journal of Ethnopharmacology*. **92(2-3)**: 147-162
- Heymann, P.; Ernst, JF. and Winkelmann, G. (2000). Identification and substrate specificity of a ferrichrome-type siderophore transporter (Arn1p) in *Saccharomyces cerevisiae*. *FEMS Microbiology Letter*. **186(2)**: 221-227
- Hezareh, M. (2005). Prostratin as a new therapeutic agent targeting HIV viral reservoirs. *Drug News & Perspectives*. **18(8)**: 496-500
- Hider, RC.; Liu, ZD. and Khodr, HH. (2001). Metal chelation of polyphenols. *Methods in Enzymology* **335**: 109-203
- Hillenmeyer, ME.; Fung, E.; Wildenhain, J.; Pierce, SE.; Hoon, S.; Lee, W.; Proctor, M.; St Onge, RP.; Tyers, M.; Koller, D.; Altman, RB.; Davis, RW.; Nislow, C. and Giaever, G. (2008). The chemical genomic portrait of yeast: uncovering a phenotype for all genes. *Science*. **320(5874)**: 362-365

- Hillenmeyer, ME.; Ericson, E.; Davis, RW.; Nislow, C.; Koller, D. and Giaever, G. (2010). Systematic analysis of genome-wide fitness data in yeast reveals novel gene function and drug action. *Genome Biology*. **11(3)**: R30
- Hoyt, MA.; Totis, L. and Roberts, BT. (1991). *S. cerevisiae* genes required for cell cycle arrest in response to loss of microtubule function. *Cell*. **66(3)**: 507-517
- Huang, GZ.; Luo, SM. and Zeng, XW. (2012). Effects of plant extracts from grape seed on growth and composition of muscles of hybrid Crucian carp. *Chinese Journal of Fisheries and Science*. **31**: 433-436
- Huh, WK.; Falvo, JV.; Gerke, LC.; Carroll, AS.; Howson, RW.; Weissman, JS. and O'Shea, EK. (2003). Global analysis of protein localization in budding yeast. *Nature*. **425(6959)**: 686-691
- Inadome, H.; Noda, Y.; Adachi, J. and Yoda, K. (2005). Immunoprecipitation of the yeast Golgi subcompartments and characterization of a novel membrane protein, Svp26, discovered in the Sed5-containing compartments. *Molecular and Cellular Biology*. **25(17)**: 7696-7710
- Inoue, H. and Tanabe, T. (1998). Transcriptional role of the nuclear factor kappa B site in the induction by lipopolysaccharide and suppression by dexamethasone of cyclooxygenase-2 in U937 cells. *Biochemical and biophysical Research Communications*. **244(1)**: 143-148
- Ishimi, Y. and Kikuchi, A. (1991). Identification and molecular cloning of yeast homolog of nucleosome assembly protein I which facilitates nucleosome assembly in vitro. *Journal of Biological Chemistry*. **266(11)**: 7025-7029
- Islam, S.; Jarosch, S.; Zhou, J.; Parquet-Mdel, C.; Toquri, JT.; Colp, P. Holbein, BE. and Lehmann, C. (2016). Anti-inflammatory and anti-bacterial effects of iron chelation in experimental sepsis. *Journal of Surgical Research*. **200(1)**: 266-273
- Itokawa, H.; Wang, X. and Lee, K-H. (2005). Homoharringtonine and related compounds. In: Cragg, GM.; Kingston, DGI. and Newman, DJ. editors. Anticancer agents from natural products. CRC/Taylor & Francis; Boca Raton, Florida. Pp47-70
- Ivessa, SA.; Zhou, JQ. and Zakian, VA. (2000). The *Saccharomyces* Pif1p DNA helicase and the highly related Rrm3p have opposite effects on replication fork progression in ribosomal DNA. *Cell*. **100(4)**: 479-489
- Johnson, HE.; Banack, SA. and Cox, PA. (2008). Variability in content of the anti-AIDS drug candidate prostratin in Samoan populations of *Homalanthus nutans*. *Journal of Natural Products*. **71(12)**: 2041-2044

- Jong, AY. and Campbell, JL. (1986). Isolation of the gene encoding yeast single-stranded nucleic acid binding protein 1. *Proceedings of the National Academy of Science*. **83(4)**: 877-881
- Jurado, RL. (1997). Iron, infections, and anemia of inflammation. *Clinical Infectious Diseases: An official publication of the Infectious Diseases Society of America*. **25(4)**: 888-895
- Kabera, J.; Tuisenge, R.; Ugirinshuti, V.; Nyirabageni, A. and Munyabuhoro, S. (2014). Preliminary investigation on antihelmintic activity and phytochemical screening of leaf crude extracts of *Tithonia diversifolia* and *Tephrosia vogelii*. *African Journal of Microbiological Research*. **8(25)**: 2449-2457
- Kaplan, J.; McVey-Ward, D.; Crisp, RJ. and Philpott, CC. (2006). Iron-dependent metabolic remodeling in *S. cerevisiae*. *Biochimica Biophysica Acta*. **1763(7)**: 646-651
- Kaufman, TS. and Ruveda, EA. (2005). The quest for quinine: those who won the battles and those who won the war. *Angewandte Chemie (International ed. in English)*. **44(6)**: 854-885
- Kell, DB. (2009). Iron behaving badly: inappropriate iron chelation as a major contributor to the aetiology of vascular and other progressive inflammatory and degenerative diseases. *BMC Medical Genomics* **2**: 2
- Khandababee, K. and van Ree, T. (2001). Tannins: classification and definition. *Natural Products Reports*. **18(6)**: 641-649
- Kinzy, TG.; Ripmaster, TL. And Woolford, JL Jr. (1994). Multiple genes encode the translation elongation factor EF-1 gamma in *Saccharomyces cerevisiae*. *Nucleic Acids Research*. **22(13)**: 2703-2707
- Koehn, FE. and Carter, GT. (2005). The evolving role of natural products in drug discovery. *Nature Reviews: Drug Discovery*. **4(3)**: 206-220
- Kolodziej, H.; Kayser, O.; Latte, KP. And Ferreira, D. (1999). Evaluation of the antimicrobial potency of tannins and related compounds using the microdilution broth method. *Planta Medicine*. **65**: 444-446
- Kolodziej, H.; Kayser, O.; Kiderlen, AF.; Ito, H.; Hatano, T. and Yoshida, T. (2001). Proanthocyanidins and related compounds: Antileishmanial activity and modulatory effects on nitric oxide and tumour necrosis factor-alpha-release in the murine macrophage-like cell line RAW 264.7. *Biological & Pharmaceutical Bulletin*. **24(9)**: 1016-1021
- Kontiokari, T.; Svanberg, M.; Mattila, P.; Leinonen, M. and Uhari, M. (1999). Quantitative analysis of the effect of xylitol on pneumococcal nasal colonization in rats. *FEMS Microbiology Letters*. **178(2)**: 313-317

- Kraft, C.; Deplazes, A.; Sohrmann, M. and Peter, M. (2008). Mature ribosomes are selectively degraded upon starvation by an autophagy pathway requiring the Ubp3p/Bre5p ubiquitin protease. *Nature: Cell Biology*. **10(5)**: 602-610
- Krogan, NJ.; Kim, M.; Ahn, SH.; Zhong, G.; Kobor, MS.; Cagney, G.; Emili, A.; Shilatifard, A.; Buratowski, S. and Greenblatt, JF. (2002). RNA polymerase II elongation factors of *Saccharomyces cerevisiae*: a targeted proteomics approach. *Molecular and Cellular Biology*. **22(20)**: 6979-6992
- Kumar, VP.; Neelam, SC.; Harish, P. and Rajani, M. (2006). Search for antibacterial and antifungal agents from selected Indian medicinal plants. *Journal of Ethnopharmacology*. **107**: 182-188
- Lahlou, M. (2013). The success of natural products in drug discovery. *Pharmacology & Pharmacy*. **4**: 17-31
- Lavoie, S.; Ouellet, M.; Fleury, PY.; Gauthier, C.; Legault, J. and Pichette, A. (2015). Complete <sup>1</sup>H and <sup>13</sup>C NMR assignments of a series of pergalloylated tannins. *Magnetic Resonance Chemistry*. **54**: 168-174
- Lee, CC.; Hsieh, HJ.; Hsieh, CH. and Hwang, DF. (2014). Antioxidative and anticancer activities of various ethanolic extract fractions from crown-of-thorn starfish (*Acanthaster planci*). *Environmental Toxicology & Pharmacology*. **38(3)**: 761-773
- Lee, CC.; Hsieh, HJ.; Hsieh, CH. and Hwang, DF. (2014). Spine venom of crown-of-thorns starfish (*Acanthaster planci*) induces antiproliferation and apoptosis of human melanoma cells (A375.S2). *Toxicon: Official Journal of the International Society on Toxinology*. **91**: 126-134
- Lee, CC.; Hsieh, HJ. and Hwang, DF. (2015). Cytotoxic and apoptotic activities of the plancitoxin I from the venom of crown-of-thorns starfish (*Acanthaster planci*). On A375.S2 cells. *Journal of Applied Toxicology*. **35(4)**: 407-417
- Lehmann, C.; Islam, S.; Jarosch, S.; Zhou, J.; Hoskin, D.; Greenshields, A.; Al-Banna, N.; Sharawy, N.; Sczcesniak, A.; Kelly, M; Wafa, K.; Cheliak, W. and Holbein, B. (2015). The utility of iron chelators in the management of inflammatory disorders. *Mediators of Inflammation*. **Vol 2015**, Article 516740, 12 pages
- Lewis, TA.; Taylor, FR. and Parks, LW. (1985). Involvement of heme biosynthesis in control of sterol uptake by *Saccharomyces cerevisiae*. *Journal of Bacteriology*. **163(1)**: 199-207
- Li, WG.; Zhang, XY.; Wu, YJ. and Tian, X. (2001). Anti-inflammatory effects and mechanism of proanthocyanidins from grape seeds. *Acta Pharmacology Sin*. **22(12)**: 1117-1120

- Li, W.; Mo, W.; Shen, D.; Sun, L.; Wang, J.; Lu, S.; Gitschier, JM. and Zhou, B. (2005). Yeast model uncovers dual roles of mitochondrial in the action of artemisinin. *PLoS Genetics*. **1(3)**: e36
- Li, J. (2010). Grape seed proanthocyanidins ameliorate doxorubicin-induced cardiotoxicity. *American Journal of Chinese Medicine*. **38(3)**: 569
- Lill, R. and Mühlenhoff, U. (2008). Maturation of iron-sulfur proteins in eukaryotes: mechanisms, connected processes and diseases. *Annual Reviews* **77**: 669-700
- Lin, SJ.; Pufahl, DA.; Dancis, A.; O'Halloran, TV. and Culotta, VC. (1997). A role for the *Saccharomyces cerevisiae* *ATX1* gene in copper trafficking and iron transport. *Journal of Biological Chemistry*. **272(12)**: 9215:9220
- Lo, WS. and Dranginis, AM. (1996). FLO11, a yeast gene related to the STA genes, encodes a novel cell surface flocculin. *Journal of Bacteriology*. **178(24)**: 7144-7151
- Lopez, A.; Parsons, AB.; Nislow, C.; Giaever, G. and Boone, C. (2008). Chemical-genetic approaches for exploring the mode of action of natural products. *Progress in Drug Research*. **66(237)**: 239-271
- Lum, PY.; Armour, CD.; Stepaniants, SB.; Cavet, G.; Wolf, MK.; Butler, JS.; Hinshaw, JC.; Garnier, P.; Preswich, GD.; Leonardson, A.; Garrett-Engele, P.; Rush, CM.; Bard, M.; Schimmack, G.; Phillips, JW.; Roberts, CJ. and Shoemaker, DD. (2004). Discovering the modes of action for the therapeutic compounds using a genome-wide screen of yeast heterozygotes. *Cell*. **116(1)**: 121-137
- Ma, P.; Winderickx, J.; Nauwelaers, D.; Dumotier, F.; De Doncker, A.; Thevelein, JM. and Van Dijck, P. (1999). Deletion of SFI1, a novel suppressor of partial Ras-cAMP pathway deficiency in the yeast *Saccharomyces cerevisiae*, causes G(2) arrest. *Yeast*. **15(11)**: 1097-1109
- Mack, D.; Nishimura, K.; Dennehey, BK.; Arbogast, T.; Parkinson, J.; Toh-e, A.; Pringle, JR.; Bender, A. and Matsui, Y. (1996). Identification of the bud emergence gene BEM4 and its interactions with rho-type GTPases in *Saccharomyces cerevisiae*. *Molecular & Cellular Biology*. **16(8)**: 4387-4895
- Macpherson, M. and Macpherson, L. (1990). Samoan medical belief and practice. Auckland University Press, New Zealand. 272 pages.
- Mahmoudian, M. and Rahimi-Moghaddam, P. (2009). The anti-cancer activity of noscapine: a review. *Recent Patents on Anti-Cancer Drug Discovery*. **4(1)**: 92-97

- Mallory, JC.; Crudden, G.; Johnson, BL.; Mo, C.; Pierson, CA.; Bard, M and Craven, RJ. (2005). Dap1p, a heme-binding protein that regulates the cytochrome P450 protein Erg11p/Cyp51p in *Saccharomyces cerevisiae*. *Molecular & Cellular Biology*. **25(5)**: 1669-1679
- Malone, EA.; Clark, CD.; Chiang, A. and Winston, F. (1991). Mutations in SPT16/CDC68 suppress cis- and trans-acting mutations that affect promoter function in *Saccharomyces cerevisiae*. *Molecular & Cellular Biology*. **11(11)**: 5710-5717
- Mbah, JA.; Ngemenya, MN.; Abawah, AL.; Babiaka, SB.; Nubed, LN.; Nyongbela, KD.; Lemuh, ND. And Efange, SMN. (2012). Bioassay-guided discovery of antibacterial agents: in vitro screening of *Peperomia vulcanica*, *Peperomia fernandopoioana* and *Scleria striatinux*. *Annals of Clinical Microbiology and Antimicrobials*. **11**: 10
- McGivern, JG. (2007). Ziconotide: a review of its pharmacology and use in the treatment of pain. *Neuropsychiatric Disease & Treatment*. **3(1)**: 69-85
- Menon, VP. and Sudheer, AR. (2007). Antioxidant and anti-inflammatory properties of curcumin. *Advances in Experimental Medicine and Biology*. **595**: 105-125
- Meshnick, SR. and Dobson, MJ. (2001). The history of antimalarial drugs. In *Antimalarial Chemotherapy: Mechanisms of Action, Resistance and New Directions in Drug Discovery*. Ed Rosenthal, PJ. Totowa NJ: Humana Press Inc. pp 15-25
- Miller, EL. (2002). The penicillins: a review and update. *Journal of Midwifery & Women's Health*. **47(6)**: 426-434
- Minear, S.; O'Donnell, AF.; Ballew, A.; Giaever, G.; Nislow, C.; Stearns, T.; Cyert, MS. (2011). Curcumin inhibits growth of *Saccharomyces cerevisiae* through iron chelation. *Eukaryotic Cell*. **10(11)**: 1574-1581
- Mishra, LC.; Sing, BB. and Dagenais, S. (2001). Ayurveda-A historic perspective and principles of traditional health care systems in India. *Alternative Therapies in Health and Medicine*. **7(2)**: 36-42
- Miszkiel, KA.; Paleny, MN.; Wilkinson, ID.; Hall-Crags, MA.; Ordidge, R.; Kendall, BE.; Miller, RF. and Harrison, MJ. (1997). The measurement of R2, RE\* and RE' in HIV-infected patients using the prime sequence as a measure of brain iron deposition. *Magnetic Resonance Imaging*. **15(10)**: 1113-1119
- Moini, H.; Guo, Q. and Packer, L. (2002). Xanthine oxidase and xanthine dehydrogenase inhibition by the procyanidin-rich French maritime pine bark extract, Pycnogenol ®: A protein binding effect. In *Flavonoids in Cell Function*. Eds Buslig, B. and Manthey, J. New York: Kluwer Academic/Plenum Publishers. pp141-149

- Molan, PC. (2001). Potential of honey in the treatment of wounds and burns. *American Journal of Clinical Dermatology*. **2(1)**: 13-19
- Molina-Holgado, F.; Gaeta, A.; Francis, PT.; Williams, RJ. and Hider, RC. (2008). Neuroprotective actions of deferiprone in cultured cortical neuroles and SHSY-5Y cells. *Journal of Neurochemistry*. **105(6)**: 2466-2476
- Molinski, TF.; Dalisay, DS.; Lievens, SL. and Saludes, JP. (2009). Drug development from marine natural products. *Nature Reviews: Drug Discovery*. **8**: 69-85
- Monahan, BJ.; Villen, J.; Marguerat, S.; Bahler, J.; Gygi, SP. and Winston, F. (2008). Fission yeast SWI/SNF and RSC complexes show compositional and functional differences from budding yeast. *Nature: Structural & Molecular Biology*. **15(8)**: 873-880
- Morel, I.; Lescoat, G.; Cogrel, P.; Sergent, O.; Padeloup, N.; Brissot, P.; Cillard, P. and Cillard, J. (1993). Antioxidant and iron chelating activities of the flavonoids catechin, quercetin and diosmetin on iron-loaded rat hepatocyte cultures. *Biochemical Pharmacology* **45(1)**: 13-19
- Muren, E.; Oyen, M.; Barmark, G. and Ronne, H. (2001). Identification of yeast deletion strains that are hypersensitive to brefeldin A or monensin, two drugs that affect intracellular transport. *Yeast*. **18(2)**: 163-172
- Nanjo, F.; Goto, K.; Seto, R.; Suzuki, M.; Sakai, M. and Hara, Y. (1996). Scavenging effects of tea catechins and their derivatives on 1,1-diphenyl-2-picrylhydrazyl radical. *Free Radical Biology & Medicine*. **21(6)**: 895-902
- Nelson, ML. and Levy, ST. (2011). The history of tetracyclines. *Annals of the New York Academy of Sciences*. **124**: 17-32
- Newton, R.; Kuitert, LM.; Bergmann, M.; Adcock, IM. and Barnes, PJ. (1997). Evidence for involvement of NF-kappaB in the transcriptional control of COX-2 gene expression by IL-1 beta. *Biochemical & Biophysical Research Communications*. **237(1)**: 28-32
- Niedenthal, RK.; Riles, L.; Johnston, M. and Hegemann, JH. (1996). Green fluorescent protein as a marker for gene expression and subcellular localization in budding yeast. *Yeast*. **12(8)**: 773-786
- Nislow, C.; Ray, E. and Pillus, L. (1997). SET1, a yeast member of the trithorax family, functions in transcriptional silencing and diverse cellular processes. *Molecular & Cellular Biology*. **8(12)**: 2421-2436
- Njoya, EM.; Weber, C.; Hernandez-Cuevas, NA.; Hon, CC.; Janin, Y.; Kamini, MFG.; Moundipa, PF.; Guillen, N. (2014). Bioassay-guided fractionation of extracts from *Codeaeum variegatum*

- against *Entamoeba histolytica* discovers compounds that modify expression of ceramide biosynthesis related genes. *PLoS Neglected Tropical Diseases*. **8(1)**: e2607
- Nobel Prize Assembly. (2015). *The Nobel Prize in Physiology or Medicine 2015*. [press release] Retrieved from: [https://www.nobelprize.org/nobel\\_prizes/medicine/laureates/2015/press.html](https://www.nobelprize.org/nobel_prizes/medicine/laureates/2015/press.html)
- Norton, TR.; Bristol, ML.; Read, GW.; Bushnell, OA.; Kashiwagi, M.; Okinaga, CM. and Oda, CS. (1973). Pharmacological evaluation of medicinal plants from Western Samoa. *Journal of Pharmaceutical Sciences*. **62(7)**: 1077-1082
- O'Sullivan, D.; Green, L.; Stone, S.; Zareir, P.; Kharkrang, M.; Fong, D.; Connor, B. and La Flamme, AC. (2014). Treatment with the antipsychotic agent, risperidone, reduces disease severity in experimental autoimmune encephalomyelitis. *PLoS One*. **9(8)**: e104430
- Omura, S. and Crump, A. (2004). The life and times of ivermectin - a success story. *Nature Reviews Microbiology*. **2(12)**: 984-989
- Ondetti, MA.; Williams, NJ.; Sabo, EF.; Plluscec, J.; Weaver, ER. and Kocy, O. (1971). Angiotensin-converting enzyme inhibitors from the venom of *Bothrops jararaca*. Isolation, elucidation of structure and synthesis. *Biochemistry*. **10(22)**: 4033-4039
- Paavilainen, HM. (2009). Medieval pharmacotherapy-Continuity and change: case studies from Ibn Sina and some of his late Medieval commentations. IDC Publishers: Netherlands
- Padney, AV.; Joshi, SK.; Tekwani, BL. And Shauhan, VS. (1999). A colorimetric assay for heme in biological samples using 96-well plates. *Analytical Biochemistry*. **268(1)**: 159-161
- Park, KC.; Wook, SK.; Yoo, YJ.; Wyndham, AM.; Baker, RT. and Chung, CH. (1997). Purification and characterization of BUP6, a new ubiquitin-specific protease in *Saccharomyces cerevisiae*. *Archives of Biochemistry and Biophysics*. **347(1)**: 78-84
- Park, YK.; Koo, MH.; Ikegaki, M. and Contado, JL. (1997). Comparison of the flavonoid aglycone contents of *Apis mellifera* propolis from various regions of Brazil. *Arq. Biol. Tecnol.* **40**: 97-106
- Parsons, AB.; Brost, RL.; Ding, H.; Li, Z.; Zhang, C.; Sheikh, B.; Brown, GW.; Kane, PM.; Hughes, TR. and Boone, C. (2004). Integration of chemical-genetic and genetic interaction data links bioactive compounds to cellular target pathways. *Nature Biotechnology*. **22(1)**: 62-69
- Parsons, AB.; Lopez, A.; Givoni, IE.; Williams, DE.; Gray, CA.; Porter, J.; Chua, G.; Sopko, R.; Brostl, RL.; Ho, CH.; Wang, J.; Kertela, T.; Brenner, C.; Brill, JA.; Fernandez, GE.; Lorenz, TC.; Payne, GS.; Ishihara, S.; Ohya, Y.; Andrews, B.; Hughes, TR.; Frey, BJ.; Graham, TR.; Andersen, RJ. and

- Boone, C. (2006). Exploring the mode-of-action of bioactive compounds by chemical-genetic profiling in yeast. *Cell*. **126(3)**: 611-625
- Patridge, E.; Gareiss, P.; Kinch, MS. and Hoyer, D. (2016). An analysis of FDA-approved drugs: natural products and their derivatives. *Drug Discovery Today*. **21(2)**: 204-207
- Peterson, J.; Zheng, Y.; Bender, L.; Myers, A.; Cerione, R. and Bender, A. (1994). Interactions between the bud emergence proteins Bem1p and Bem2p and Rho-type GTPases in yeast. *Journal of Cell Biology*. **127(5)**: 1395-1406
- Philpott, CC. and Protchenko, O. (2008). Response to iron deprivation in *Saccharomyces cerevisiae*. *Eukaryotic Cell*. **7(1)**: 20-27
- Philpott, CC.; Protchenko, O.; Kim, YW.; Boretsky, Y. and Shakoury-Elizeh, M. (2002). The response to iron deprivation in *Saccharomyces cerevisiae*: expression of siderophore-based systems of iron uptake. *Biochemical Society Transactions*. **30(4)**: 698-702
- Pierce, SE.; Davis, RW.; Nislow, C. and Giaever, G. (2007). Genome-wide analysis of barcoded *Saccharomyces cerevisiae* gene-deletion mutants in pooled cultures. *Nature Protocols*. **2(11)**: 2958-2974
- Piga, A.; Galanello, R.; Forni, GL.; Cappellini, MD.; Origa, R.; Zappu, A.; Donato, G.; Bordone, E.; Lavagetto, A.; Zanaboni, L.; Sechaud, R.; Hewson, N.; Ford, JM.; Opitz, H. and Alberti, D. (2006). Randomized Phase II trial of deferasirox (Exjade, ICL670), a once-daily, orally-administered iron chelator, in comparison to deferoxamine in thalassemia patients with transfusional iron overload. *Haematologica*. **91(7)**: 873-880
- Piper, RC.; Cooper, AA.; Yang, H. and Stevens, TH. (1995). VPS27 controls vacuolar and endocytic traffic through a prevacuolar compartment in *Saccharomyces cerevisiae*. *Journal of Cell Biology*. **131(3)**: 603-617
- Pitrowski, JS.; Simpkins, SW.; Li, SC.; Deshpande, R.; McIlwain, SJ.; Ong, IM.; Myers, CL.; Boone, C and Andersen, RJ. (2015). Chemical genomic profiling via barcode sequencing to predict compound mode of action. *Methods in Molecular Biology*. **1263**: 299-318
- Planta, RJ. and Mager, WH. (1998). The list of cytoplasmic ribosomal proteins of *Saccharomyces cerevisiae*. *Yeast*. **14(5)**: 471-477
- Plumb, GW.; Pascual-Teresa, S.; Santos-Buelga, C.; Cheynier, V. and Williamson, G. (1998). Antioxidant properties of catechins and proanthocyanidins: Effect of polymerization, galloylation and glycosylation. *Free Radical Research*. **29(4)**: 351-358

- Poggiali, E.; Cassinerio, E.; Zanaboni, L. and Cappelini, MD. (2012). An update on iron chelation therapy. *Blood Transfusion*. **10(4)**: 411-422
- Polevoda, B.; Span, L. and Sherman, F. (2006). The yeast translation release factors Mrf1p and Sup45p (eRF1) are methylated, respectively, by the methyltransferases Mtq1p and Mtq2p. *Journal of Biological Chemistry*. **281(5)**: 2562-2571
- Porter, LJ.; Hrstich, LN. and Chan, BG. (1986). The conversion of procaynidins and prodelphinidins to canidin and delphinidin. *Phytochemistry*. **1**: 223-230
- Portnoy, ME.; Schmidt, PJ.; Rogers, RS. and Culotta, VC. (2001). Metal transporters that contribute copper to metallochaperones in *Saccharomyces cerevisiae*. *Molecular Genetics and Genomics*. **265(5)**: 873-882
- Potterat, O. and Hamburger, M. (2008). Drug discovery and development with plant-derived compounds. *Progress in Drug Research*. **65**: 46-118
- Prasad, T.; Chandra, A.; Mukhopadhyay, CK. and Prasad, R. (2006). Unexpected link between iron and drug resistance of *Candida* spp.: Iron depletion enhances membrane fluidity and drug diffusion, leading to drug-susceptible cells. *Antimicrobial Agents and Chemotherapy*. **50(11)**: 3597-3606
- Protchenko, O.; Ferea, T.; Rashford, J.; Tiedeman, J.; Brown, PO.; Botstein, D. and Philpott, CC. (2001). Three cell wall mannoproteins facilitate the uptake of iron in *Saccharomyces cerevisiae*. *Journal of Biological Chemistry*. **276(52)**: 49244-49250
- Pufahl, RA.; Singer, CP.; Peariso, KL.; Link, SJ.; Schmidt, PJ.; Fahrni, CJ.; Culotta, VC.; Penner-Hahn, JE. and O'Halloran, TV. (1997). Metal ion chaperone function of the soluble Cu(I) receptor Atx1p. *Science*. **278(5339)**: 853-856
- Puig, S.; Askeland, E. and Thiele, DJ. (2005). Coordinated remodeling of cellular metabolism during iron deficiency through targeted mRNA degradation. *Cell*. **120(1)**: 99-110
- Pujol, C.; Messer, SA.; Pfaller, M. and Soll, DR. (2003). Drug resistance is not directly affected by mating type locus zygosity in *Candida albicans*. *Antimicrobial Agents and Chemotherapy*. **47(4)**: 1207-1212
- Quek, NC.; Matthews, JH.; Bloor, SJ.; Jones, DA.; Bircham, PW.; Heathcott, RW. and Atkinson, PH. (2013). The novel equisetin-like compound, TA-289, causes aberrant mitochondrial morphology which is independent of the production of reactive oxygen species in *Saccharomyces cerevisiae*. *Molecular Biosystems*. **9(8)**: 2125-2133

- Quiroga, EN.; Sampietro, AR. and Vattuone, MA. (2001). Screening antifungal activities of selected medicinal plants. *Journal of Ethnopharmacology*. **74(1)**: 89-96
- Raskin, I.; Ribnicky, DM.; Komarnytsky, S.; Ilic, N.; Poulev, A.; Borisjuk, N.; Brinker, A.; Moreno, DA.; Ripoll, C.; Yakoby, N.; O'Neal, JM.; Cornwell, T.; Pastor, I.; Fridlender, B. (2002). Plants and human health in the twenty-first century. *Trends in Biotechnology*. **20(12)**: 522-531
- Rauha, JP.; Remes, S.; Heinonen, M.; Hopia, A.; Kahkonen, M.; Kujala, T.; Pihlaja, K.; Vuorela, H. and Vuorela, P. (2000). Antimicrobial effects of Finnish plant extracts containing flavonoids and other phenolic compounds. *International Journal of Food Microbiology*. **56(1)**: 3-12
- Reddy, L.; Odhav, B.; and Bhoola, KD. (2003). Natural products for cancer prevention: a global perspective. *Pharmacology & Therapeutics*. **99(1)**: 1-13
- Rispail, N.; Dita, MA.; Gonzales-Verdeho, C.; Perez-de-Lugue, A.; Castillejo, MA.; Prats, E.; Roman, B.; Jorriin J.; Rubiales, D. (2007). Plant resistance to parasitic plants: molecular approaches to an old foe. *New Phytologist*. **173(4)**: 703-712
- Robinson, JS.; Klionsky, DJ.; Banta, LM. and Emr, SD. (1988). Protein sorting in *Saccharomyces cerevisiae*: isolation of mutants defective in the delivery and processing of multiple vacuolar hydrolases. *Molecular & Cellular Biology*. **8(11)**: 4936-4948
- Robinson, DG.; Chen, W.; Stoery, JD. and Gresham, D. (2014). Design and analysis of Bar-seq experiments. *G3*. **4(1)**: 11-18
- Roncoroni, M.; Santiago, M.; Hooks, DO.; Moroney, S.; Harsch, MJ.; Lee, SA.; Richards, KD.; Nicolau, L. and Gardner, RC. (2011). The yeast IRC7 gene encodes a  $\beta$ -lyase responsible for production of the varietal thiol 4-mercapto-4-methylpentan-2-one in wine. *Food Microbiology*. **28(5)**: 926-935
- Rothman, JH. and Stevens, TH. (1986). Protein sorting in yeast: mutants defective in vacuole biogenesis mislocalize vacuolar proteins into the late secretory pathway. *Cell*. **47(6)**: 1041-1051
- Rowinsky, EK. And Donehower, RC.(1995). Paclitaxel (taxol). *New England Journal of Medicine*. **332(15)**: 1004-1014
- Sadowska-Bartosz, I.; Paczka, A.; Molon, M. and Bartosz, G. (2013). Dimethyl sulfoxide induces oxidative stress in the yeast *Saccharomyces cerevisiae*. *FEMS Yeast Research*. **13(8)**: 820-830

- Saliou, C.; Rimbach, G.; Moini, H. (2001). Solar ultraviolet-induced erythema in human skin and nuclear-factor-kappa-B-dependent gene expression in keratinocytes are modulated by a French maritime pine bark extract. *Free Radical and Biology Medicine*. **30**: 154-160
- Satish, S.; Mohana, DC.; Raghavendra, MP. and Raveesha, KA. (2007). Antifungal activity of some plant extracts against important seed borne pathogens of *Aspergillus* sp. *Journal of Agricultural Technology*. **3(1)**: 109-119
- Saveanu, C.; Fromon-Racine, M.; Harington, A.; Richard, F.; Namane, A. and Jacquier, A. (2001). Identification of 12 new yeast mitochondrial ribosomal proteins including 6 that have no prokaryotic homologues. *Journal of Biological Chemistry*. **276(19)**: 15861-15867
- Scalbert, A. (1991). Antimicrobial properties of tannins. *Phytochemistry*. **30(12)**: 3875-3883
- Schewe, T.; Sadik, C.; Klotz, LOL.; Yoshimoto, T.; Kuhn, H. and Sies, H. (2001). Polyphenols in cocoa: inhibition of mammalian 15-lipoxygenase. *Biological Chemistry*. **382(12)**: 1687-1696
- Schmedtje, JF Jr.; Ji, YS.; Liu, WL.; DuBois, RN. and Runge, MS. (1997). Hypoxia induces cyclooxygenase-2 via the NF-kappaB p65 transcription factor in human vascular endothelial cells. *Journal of Biological Chemistry*. **272(1)**: 601-608
- Schneider-Poetsch, T.; Ju, J.; Eyler, DE.; Dang, Y.; Bhat, S.; Merrick, WC.; Green, R.; Shen, B. and Liu, JO. (2010). Inhibition of eukaryotic translation elongation by cycloheximide and lactimidomycin. *Nature Chemical Biology*. **6(3)**: 209-217
- Schofield, P.; Mbugua, DM. and Pell, AN. (2001). Analysis of condensed tannins: a review. *Animal Feed Science and Technology*. **91**: 21-40
- Shahat, AA.; Cos, P.; De Bruyne, T.; Apers, S.; Hammouda, FM.; Ismail, SI.; Azzam, S.; Claeys, M.; Goovaerts, E.; Pieters, L.; Vanden Berghe, D. and Vlietinck, AJ. (2002). Antiviral and antioxidant activity of flavonoids and proanthocyanidins from *Crataegus sinaica*. *Planta Medica*. **68(6)**: 539-541
- Shakoury-Elizeh, M.; Tiedeman, J.; Rashford, J.; Ferea, T.; Demeter, J.; Garcia, E.; Rolfes, R.; Brown, PO.; Botstein, D.; and Philpott, CC. (2004). Transcriptional remodeling in response to iron deprivation in *Saccharomyces cerevisiae*. *Molecular Biology of the Cell*. **15(3)**: 1233-1243
- Shakoury-Elizeh, M.; Protchenko, O.; Berger, A.; Cox, K.; Gable, K.; Dunn, TM.; Prinz, WA.; Bard, M. and Philpott, CC. (2010). Metabolic response to iron deficiency in *Saccharomyces cerevisiae*. *Journal of Biological Chemistry*. **285(19)**: 14823-14833
- Shao, ZH.; Wojcik, KR.; Dossumbekova, A.; Hsu, C.; Mehendale, SR.; Li, CW.; Qin, Y.; Sharp, WW.; Chang, WT.; Hamann, KJ.; Yuan, CS. and vanden Hoek, TL. (2009). Grape seed

- proanthocyanidins protect cardiomyocytes from ischemia and reperfusion injury via Akt-NOS signaling. *Journal of Cellular Biochemistry*. **107(4)**: 697-705
- Shellard, EJ.; (2000). Alkaloids from snowdrops. *The Pharmaceutical Journal*. **264**: 883
- Singh, AJ.; Xu, CX.; Xu, X.; West, LM.; Wilmes, A.; Chan, A.; Hamel, E.; Miller, JH.; Northcote, PT. and Ghosh, AK. (2010). Peloruside B, a potent antitumor macrolide from the New Zealand marine sponge *Mycale hentscheli*: isolation, structure, total synthesis, and bioactivity. *Journal of Organic Chemistry*. **75(1)**: 2-10
- Siriwardana, G. and Seligman, PA. (2013). Two cell cycle blocks caused by iron chelation of neuroblastoma cells: separating cell cycle events associated with each block. *Physiological Reports*. **1(7)**: e00176
- Smith, AM.; Heisler, LE.; Mellor, J.; Kaper, F.; Thomson, MJ.; Chee, M.; Roth, FP.; Giaever, G. and Nislow, C. (2009). Quantitative phenotyping via deep barcode sequencing. *Genome Research*. **19(10)**: 1836-1842
- Smith, AM.; Ammar, R.; Nislow, C. and Giaever, G. (2010). A survey of yeast genomic assays for drug and target discovery. *Pharmacology & Therapeutics*. **127(2)**: 156-164
- Smith, AM.; Durbic, T.; Kittanakom, S.; Giaever, G. and Nislow, C. (2012). Barcode sequencing for understanding drug-gene interactions. *Methods in Molecular Biology*. **910**: 55-69.
- Sofic, E.; Riederer, P.; Heinsen, H.; Beckmann, H.; Reynolds, GP.; Hebenstreit, G. and Youdin, MBH. (1988). Increased iron (III) and total iron content in post mortem substantia nigra of parkinsonian brain. *Journal of Neural Transmission*. **74**: 199-205
- South, PK. and Miller, DD. (1998). Iron binding by tannic acid: Effects of selected ligands. *Food Chemistry* **63(2)**: 167-172
- Stearman, R.; Yuan, DS.; Yamaguchi-Iwai, Y.; Klausner, RD. and Dancis, A. (1996). A permease-oxidase complex involved in high-affinity iron uptake in yeast. *Science*. **271(5255)**: 1552-1557
- Stolc, V. and Altman, S. (1997). Rpp1, an essential protein subunit of nuclear RNase P required for processing of precursor tRNA and 35S precursor rRNA in *Saccharomyces cerevisiae*. *Genes & Development*. **11(21)**: 2926-2937
- Sugiyama, M. and Nikawa, J. (2001). The *Saccharomyces cerevisiae* Isw2p-Itc1p complex represses INO1 expression and maintains cell morphology. *Journal of Bacteriology*. **183(17)**: 4985-4993

- Szczyepka, MS.; Zhu, Z.; Silar, P.; Thiele, DJ. (1997). Saccharomyces cerevisiae mutants altered in vacuole function are defective in copper detoxification and iron-responsive gene transcription. *Yeast*. **13(15)**: 1423-1435
- Tamarit, J.; Irazusta, V.; Moreno-Cermeno, A. and Ros, J. (2006). Colorimetric assay for the quantitation of iron in yeast. *Analytical Biochemistry*. **351(1)**: 149-151.
- Tan, S. and Liu ZP. (2015). Natural products as zinc-dependent histone deacetylase inhibitors. *ChemMedChem*. **10(3)**: 441-450
- Tanji, K.; Imaizumi, T.; Matsumiya, T.; Itaya, H.; Fujimoto, K.; Cui, XF.; Toki, T.; Ito, E.; Yoshida, H.; Wakabayashi, K. and Satoh, K. (2001). Desferrioxamine, an iron chelator, upregulates cyclooxygenase-2 expression and prostaglandin production in a human macrophage cell line. *Biochimica et Biophysica Acta*. **150(2-3)**: 227-235
- Tao, L.; Zhu, F.; Qin, C.; Zhang, C.; Xu, F.; Tan, CY.; Jiang, YY. and Chen, YZ. (2014). Nature's contribution to today's pharmacopoeia. *Nature Biotechnology*. **32(10)**: 979-980
- Terkeltaub, RA. (2009). Colchicine update: 2008. *Seminars in Arthritis and Rheumatism*. **38(6)**: 411-419
- Tkach, JM.; Wimit, A.; Lee, AY.; Riffle, M.; Costanzo, M.; Jaschob, D.; Hendry, JA.; Ou, J.; Moffat, J.; Boone, C.; Davis, TN.; Nislow, C. and Brown, GW. (2012). Dissecting DNA damage response pathways by analyzing protein localization and abundance changes during DNA replication stress. *Nature: Cell Biology*. **14(9)**: 966-976
- Tong, AH.; Evangelista, M.; Parsons, AB.; Xu, H.; Bader, GD.; Page, N.; Roinson, M.; Raghiizadeh, S.; Hogue, CW.; Bussey, H.; Andrews, B.; Tyers, M.; Boone, C. (2001). Systematic genetic analysis with ordered arrays of yeast deletion mutants. *Science*. **294(5550)**: 2364-2368
- Towle, MJ.; Salvato, KA.; Budrow, J.; Wels, BF.; Kuznetsov, G.; Aalfs, KK.; Welsh, S.; Zheng, W.; Seletsky, BM.; Palme, MH.; Bahgood, GJ.; Singer, LA.; Dipietro, LV.; Wange, YC.; Quincy, DA.; Davis, A.; Yoshimatsu, K.; Kishi, Y.; Yu, MJ. and Littlefield, BA. (2001). In vitro and in vivo anticancer activities of synthetic macrocyclic ketone analogues of halichondrin B. *Cancer Research*. **61(3)**: 1013-1021
- Tu, Y. (2011). The discovery of artemisinin (qingshaosu) and gifts from Chinese medicine. *Nature Medicine*. **17**: 1217-1220
- Turi, TG. and Loper, JC. (1992). Multiple regulatory elements control expression of the gene encoding the Saccharomyces cerevisiae cytochrome P450, lanosterol 14 alpha-demethylase (ERG11). *Journal of Biological Chemistry*. **267(3)**: 2046-2056

- Uhe, G. (1974). Medicinal plants of Samoa: A preliminary survey of the use of plants for medicinal purposes in the Samoan Islands. *Economic Botany*. **28(1)**: 1-30
- van Dyke, N.; Baby, J. and van Dyke, MW. (2006). Stm1p, a ribosome-associated protein, is important for protein synthesis in *Saccharomyces cerevisiae* under nutritional stress conditions. *Journal of Molecular Biology*. **358(4)**: 1023-1031
- van Ho, A.; Ward, DM. and Kaplan, J. (2002). Transitional metal transport in yeast. *Annual Reviews in Microbiology*. **56**: 237-261
- Wade, D.; Andreu, D.; Mitchell, SA.; Silveira, AM.; Boman, A.; Boman, HG. and Merrifield, RB. (1992). Antibacterial peptides designed as analogs or hybrids of cecropins and melittin. *International Journal of Protein Research*. **40(5)**: 429-436
- Wagih, O. & Parts, L. (2014). Gitter: A robust and accurate method for quantification of colony sizes from plate images. *G3*. **4(3)**: 547-552
- Walsh, P.; Bursac, D.; Law, YC.; Cyr, D. and Lithgow, T. (2004). The J-protein family: modulating protein assembly, disassembly and translocation. *EMBO Reports*. **5(6)**: 567-571
- Wang, Q. and Chang, A. (1999). Eps1, a novel PDI-related protein involved in ER quality control in yeast. *EMBO Journal*. **18(21)**: 5972-5982
- Waters, BM. and Eide, DJ. (2002). Combinatorial control of yeast FET4 gene expression by iron, zinc and oxygen. *Journal of Biological Chemistry*. **277(37)**: 33749-33757
- Webster, D.; Taschereau, P.; Belland, RJ.; Sand, C. and Rennie, RP. (2008). Antifungal activity of medicinal plant extracts; preliminary screening studies. *Journal of Ethnopharmacology*. **115**: 140-146
- Wessecker, S.; Engel, K.; Simon-Haarhaus, B.; Wittmer, A.; Pelz, K.; Schempp, CMS. (2007). Screening of plant extract for antimicrobial activity against bacteria and yeast with dermatological relevance. *Phytomedicine*. **14(7-8)**: 508-516
- Wessling-Resnick, M. (2010). Iron homeostasis and the inflammatory response. *Annual Review of Nutrition*. **21**: 105-122
- West, LM.; Northcote, PT.; Hood, KA.; Miller, JH and Page, MJ. (2000). Mycalamide, D, a new cytotoxic amide from the New Zealand marine sponge *Mycale* species. *Journal of Natural Products*. **63**: 707-709
- Whistler, AW. (1996). *Samoan Herbal Medicine*. Isle Botanica, Honolulu: Hawaii, print.

- Whistler, AW. (2000). *Plants in Samoa Culture: the ethnobotany of Samoa*. Isle Botanica, Honolulu: Hawaii, print.
- World Health Organization (1998). *Medicinal plants in the South Pacific*. WHO Regional Publications, Western Pacific Series no. 19, WHO Regional Office for the Western Pacific, Manila.
- Wichmann, H.; Hengst, L. and Gallwitz, D. (1992). Endocytosis in yeast: evidence for the involvement of a small GTP-binding protein (Ypt7p). *Cell*. **71(7)**: 1131-1142
- Williams, SA.; Chen, LF.; Kwon, H.; Fenard, D.; Bisgrove, D.; Verdin, E and Greene, WC. (2004). Prostratin antagonizes HIV latency by activating NF-kB. *Journal of Biological Chemistry*. **279(40)**: 42008-42017
- Wilmes, A.; Hanna, R.; Heathcott, RW.; Northcote, PT.; Atkinson, PH; Bellows, DS. and Miller, JH. (2012). Chemical genetic profiling of the microtubule-targeting agent pelorudise A in budding yeast *Saccharomyces cerevisiae*. *Gene*. **497(2)**: 140-146
- Wilson, CL.; Solar, JM.; Ghaouth, AE. and Wisniewski, ME. (1997). Rapid evaluation of plant extracts and essential oils for antifungal activity against *Botrytis cinerea*. *Plant Disease*. **81(2)**: 204-210
- Winzeler, EA.; Shoemaker, DD.; Astromoff, A.; Lianh, H.; Anderson, K.; Andre, B.; Bangham, R.; Benito, R.; Boeke, JD.; Bussey, H.; Chu, AM.; Connelly, C.; Davis, K.; Dietrich, F.; Dow, SW.; El Bakkoury, M.; Foury, F.; Friend, SH.; Gentalen, E.; Giaever, G.; Hegemann, JH.; Jones, T.; Laub, M.; Liao, H.; Davis, RW.; Liedbundguth, N.; Lockhart, DJ.; Lucau-Danila, A.; Lussier, M.; M'Rabet, N.; Menard, P.; Mittmann, M.; Pai, C.; Rebischung, C.; Revuelta, JL.; Riles, L.; Roberts, CJ.; Ross-MacDonald, P.; Scherens, B.; Snyder, M.; Sookhai-Mahadeo, S.; Storms, RK.; Veronneau, S.; Voet, M.; Volckaert, G.; Ward, TR.; Wysocki, R.; Yen, GS.; Yu, K.; Zimmermann, K.; Phillippsen, P.; Johnston, M. and Davis, RW. (1999). Functional characterization of the *S. cerevisiae* genome by gene deletion and parallel analysis. *Science*. **285(5429)**: 901-906
- Wu, J.; Carmen, AA.; Kobayashi, R.; Suka, N. and Grunstein, M. (2001). HDA2 and HDA3 are related proteins that interact with and are essential for the activity of the yeast histone deacetylase HDA1. *Proceedings of the National Academy of Science*. **98(8)**: 4391-4396
- Xiong, S.; She, H.; Sung, CK and Tsukamoto, H. (2003). Iron-dependent activation of NF-kB in Kupffer cells: a priming mechanism for alcoholic liver disease. *Alcohol: An International Biomedical Journal*. **30(2)**: 107-113
- Xu, D.; Sillaots, S.; Davison, J.; Hu, W.; Jiang, B.; Kauffman, S.; Martel, N.; Ocampo, P.; Oh, C.; Trosok, S.; Veillette, K.; Wang, H.; Yang, M.; Zhang, L.; Becker, J.; Martin, CE. and Roemer, T. (2009). Chemical genetic profiling and characterization of small-molecule compounds that affect the

- biosynthesis of unsaturated fatty acids in *Candida albicans*. *Journal of Biological Chemistry*. **284(29)**: 19754-19764
- Xu, N.; Cheng, X.; Yu, Q.; Zhang, B.; Ding, X.; Xing, L. and Li, M. (2012). Identification and functional characterization of mitochondrial carrier Mrs4 in *Candida albicans*. *FEMS Yeast Research*. **12(7)**: 844-858
- Yamaguchi-Iwai, Y.; Stearman, R.; Dancis, A. and Klausner, RD. (1996). Iron-regulated DNA binding by the AFT1 protein controls the iron regulon in yeast. *EMBO Journal*. **15(13)**: 3377-3384
- Yan, Z.; Costanzo, M.; Heisler, LE.; Paw, J.; Kaper, F.; Andrews, BJ.; Boone, C.; Giaever, G. and Nislow, C. (2008). Yeast Barcoders: a chemogenomic application of a universal donor-strain collection carrying bar-code identifies. *Nature Methods*. **5(8)**: 719-725
- Yang, H.; Bard, M.; Bruner, DA.; Gleeson, A.; Deckelbaum, RJ.; Aljinovic, G.; Pohl, TM.; Rothstein, R. and Sturley, SL. (1996). Sterol esterification in yeast: a two-gene process. *Science*. **272(5266)**: 1353-1356
- Yang, CS.; Yang, GY.; Landau, JM.; Kim, S. and Liao, J. (1998). Tea and tea polyphenols inhibit cell hyperproliferation, lung tumorigenesis and tumor progression. *Experimental Lung Research*. **24(4)**: 629-639
- Yarunin, A.; Panse, VG.; Petfalski, E.; Dez, C.; Tollervey, D. and Hurt, EC. (2005). Functional link between ribosome formation and biogenesis of iron-sulfur proteins. *EMBO Journal*. **24(3)**: 580-588
- Yesilada, E.; Tsuchiya, K.; Takaishi, Y. and Kawazoe, K. (2000). Isolation and characterization of free radical scavenging flavonoid glycosides from the flowers of *Spartium junceum* by activity-guided fractionation. *Journal of Ethnopharmacology* **73**: 471-478
- Yibmantasiri, P.; Leahy, DC.; Busby, BP.; Angemayr, SA.; Sorgo, AG.; Boeger, K.; Heathcott, R.; Barber, JM.; Matthews, JH.; Northcote, PT.; Atkinson, PH. and Bellows, DS. (2012). Molecular basis for fungicidal action of neothyonidioside, a triterpene glycoside from the sea cucumber, *Australostichopus mollis*. *Molecular Biosystems*. **8(3)**: 902-912
- Yokozawa, T.; Chen, CP.; Dong, E.; Tanaka, T.; Nonaka, GI. and Nishioka, I. (1998). Study on the inhibitory effect of tannins and flavonoids against the 1,1-diphenyl-2-picrylhydrazyl radical. *Biochemical Pharmacology*. **56(2)**: 213-222
- Yompakdee, C.; Ogawa, N.; Harashima, S. and Oshima, Y. (1996). A putative membrane protein, Pho88p, involved in inorganic phosphate transport in *Saccharomyces cerevisiae*. *Molecular & General Genetics*. **251(5)**: 580-590

- Yoneda, S. and Nakatsubo, F. (1998). Effects of the hydroxylation patterns and degrees of polymerization of condensed tannins on their metal-chelating capacity. *Journal of Wood Chemistry and Technology*. **18(2)**: 193-205
- Yoshida, A.; Yoshino, F.; Tsubata, M.; Ikeguchi, M.; Nakamura, T. and Lee, MC. (2011). Direct assessment by electron spin resonance spectroscopy of the antioxidant effects of French maritime pine bark extract in the maxillofacial region of hairless mice. *Journal of Clinical Biochemical Nutrition*. **49(2)**: 79-86
- Youdell, ML.; Kizer, KO.; Kisseleva-Romanova, E.; Fuchs, SM.; Duro, E.; Strahl, BD. and Mellor, J. (2008). Roles for Ctk1 and Spt6 in regulating the different methylation states of histone H3 lysin 36. *Molecular and Cellular Biology*. **28(16)**: 4915-4926
- Yu, C.; Kennedy, NJ.; Chang, CCY. and Rothblatt, JA. (1996). Molecular cloning and characterization of two isoforms of *Saccharomyces cerevisiae* acyl-CoA:sterol acyltransferase. *Journal of Biological Chemistry*. **271(39)**: 24157-24163
- Yuan, DS.; Dancis, A.; Klausner, RD. (1997). Restriction of copper export in *Saccharomyces cerevisiae* to a late Golgio or post-Golgi compartment in the secretory pathway. *Journal of Biological Chemistry*. **272(41)**: 25787-25793
- Zakharova, M. and Ziegler, HK. (2005). Paradoxical anti-inflammatory actions of TNF-alpha: inhibition of IL-12 and IL-23 via TNF receptor 1 in macrophages and dendritic cells. *Journal of Immunology*. **175(8)**: 5024-5033
- Zhang, T.; Lei, J.; Yang, J.; Xy, K.; Wang, R. and Zhang, Z. (2011). An improved method for whole protein extraction from yeast *Saccharomyces cerevisiae*. *Yeast*. **28(11)**: 795-798
- Zhang, C.; and Zhang, F. (2014). Iron homeostasis and tumorigenesis: molecular mechanisms and therapeutic opportunities. *Protein & Cell*. **6(2)**: 88-100
- Zhao, S.; Douglas, NW.; Heine, MJ.; Williams, GM.; Winther-Larse, HC. and Meaden, PG. (1994). The STL1 gene of *Saccharomyces cerevisiae* is predicted to encode a sugar transporter-like protein. *Gene*. **146(2)**: 215-219
- Zhao, X.; Muller, EG. and Rothstein, R. (1998). A suppressor of two essential checkpoint genes identifies a novel protein that negatively affects dNTP pools. *Molecular Cell*. **2(3)**: 329-340

---

## Appendix I: Media

---

### 1. Yeast-Extract Peptone Dextrose (YPD) Media:

Ingredient	Weight (w/v)
Yeast Extract	1%
Bacto-Peptone	2%
Adenine	0.012%
Glucose	2%
Agar	2%

### 2. Synthetic Complete Media

Ingredient	Weight (w/v)
Yeast nitrogen base (without amino acids or ammonium sulfate)	1%
Monosodium glutamate	0.17%
Amino acid mixture	0/2%
Glucose	2%
Agar	2%

#### *Amino Acid Mixture:*

3 g adenine, 2 g uracil, 2 g inositol, 0.2 g para-aminobenzoic acid, 2 g alanine, 2 g arginine, 2 g asparagines, 2 g aspartic acid, 2 g cysteine, 2 g glutamic acid, 2 g glutamine, 2 g glycine, 2 g histidine, 2 g isoleucine, 10 g leucine, 2 g lysine, 2 g methionine, 2 g phenylalanine, 2 g proline, 2 g serine, 2 g threonine, 2 g tyrosine, 2 g tryptophan, 2 g valine

## Appendix II: Bioactivity at 70°C

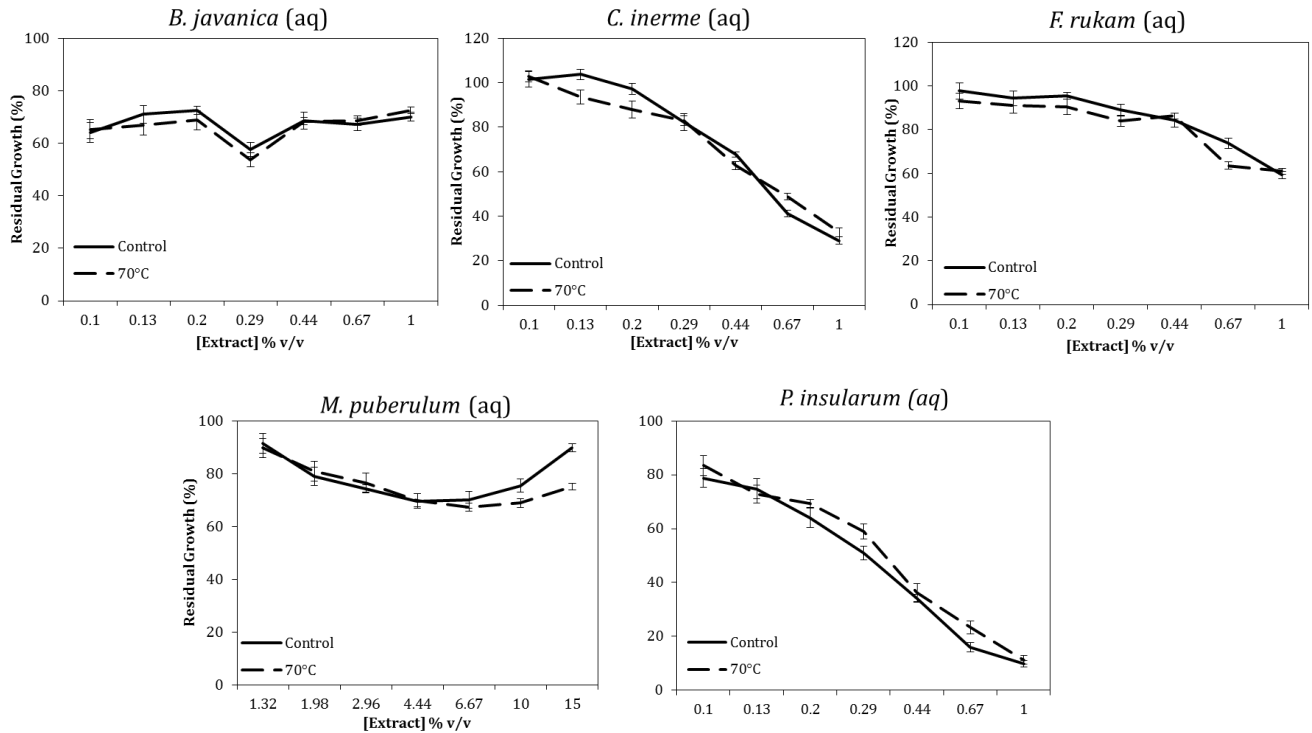


**Figure A2: Bioactivity of the five bioactive aqueous extracts after heating at 70°C.** Subsamples of the extracts were aliquot into Eppendorf tubes and heated at 70°C overnight, before cooling to RT and serial diluted. WT yeast were inoculated at  $5 \times 10^5$  cells/mL and grown in increasing concentrations of the heated extracts (dashed black lines, labelled 70°C), and their growth was compared to subsamples of the same extract stored at -20°C overnight (solid black lines, Control). Bioactivity of WT yeast in the aqueous extracts of **A:** *B. javanica*. **B:** *C. inerme*. **C:** *F. rukam*. **D:** *M. puberulum*. **E:** *P. insularum*.

## Appendix III: Genotypes of Strains Used in this Thesis

All yeast strains used in this thesis are derived from S288c and maintained at -80°C as glycerol stocks.

Strain	Name	Genotype	Reference
Y7092	WT	<i>MATα</i> ; can1Δ::STE2pr-Sp_his5; lyp1Δ; his3Δ1 leu2Δ0 ura3Δ0 met15Δ0 LYS2+	Starting strain from Boone Lab
BY4741	WT	<i>MATα</i> ; his3Δ0 leu2Δ0 met15Δ0 ura3Δ0	Biosystems
BY4742	WT	<i>MATα</i> , his3Δ1 leu2Δ0 lys2Δ0 ura3Δ0	Biosystems
BY4743	WT	BY4741 x BY4742	Biosystems
GFP strains with RedStar2 and mCherry		<i>MATα</i> ; can1Δ::STE2pr-URA3; lyp1Δ::mCherry- Nat; his3Δa; leu2Δ0; ura3 Δ0::NLS-RedStar2- HPH; LYS2+ and mated to the GFP Collection (BioSystems)	Bircham, P (2014)
Libraries Used			
GFP strains with RedStar2 and mCherry		<i>MATα</i> ; can1Δ::STE2pr-URA3; lyp1Δ::mCherry-Nat; his3Δa; leu2Δ0; ura3 Δ0::NLS-RedStar2-HPH; LYS2+ and mated to the GFP Collection (BioSystems)	Bircham, P (2014)
Haploid <i>MATa</i> deletion mutant array			Boone Lab
Diploid Heterozygous Library			Biosystems
Diploid Homozygous Library			Biosystems

## Appendix IV: 128 Mutants from Agar-Based Screen

Replicate 1		Replicate 2		Replicate 3		Combined
p-value	Gene	p-value	Gene	p-value	Gene	<b>Unique</b>
0.00857	AIF1	0.01233	ADE5,7	0.01305	ADE5,7	ADE5,7
0.01292	ARG3	0.01833	ANT1	0.02313	AIF1	AIF1
0.03925	ARO3	0.01733	ARO7	0.04954	ANT1	ANT1
0.00854	ARO7	0.00109	BEM1	0.02185	ARG3	ARG3
0.00325	BEM4	0.0028	BEM4	0.0411	ARO3	ARO3
0.02948	BUB3	0.01229	CAR1	0.04114	BEM1	ARO7
0.0477	BUD7	0.01689	CBC2	0.02041	BUB3	BEM1
0.02	CBC2	4.22E-06	CHO2	0.04793	BUD7	BEM4
5.5E-06	CHO2	0.02872	CIK1	0.03811	CAR1	BUB3
0.00085	CNE1	0.01327	CMK2	0.00226	CBC2	BUD7
0.00166	COX10	0.01357	CNE1	3.5E-08	CHO2	CAR1
0.01695	CPA2	6.30E-06	COX10	0.0172	CIK1	CBC2
0.02398	CPA2	7.62E-08	CPA2	0.03695	CMK2	CHO2
0.03022	CSF1	0.03209	CSF1	0.00584	CNE1	CIK1
0.00427	CSH1	0.00592	CTF19	0.00193	COX10	CMK2
0.02999	CUE3	0.01909	CUE3	0.00752	CPA2	CNE1
0.00607	DAL1	0.0013	DDR48	0.0304	CSH1	COX10
0.00613	DDR48	0.00969	ERP6	0.0169	CTF19	CPA2
0.04756	ERP6	0.04449	FKH2	0.00603	DAL1	CSF1
0.03747	FKH2	0.01493	FZF1	0.01425	DDR48	CSH1
0.00998	FZF1	0.04381	GEM1	0.02929	ERP6	CTF19
3.8E-05	GSH2	0.02898	GPG1	0.02103	GEM1	CUE3
0.01683	GUP1	0.04958	GSH2	0.03436	GPG1	DAL1
0.04171	HAT1	0.02748	GYP1	0.00812	GSH2	DDR48
0.04706	IDH1	0.04955	HAT1	0.03107	GUP1	ERP6
0.0125	INO2	0.04276	IPK1	0.03141	GYP1	FKH2
0.03005	IPK1	0.00826	ITT1	0.01754	IDH1	FZF1
0.04336	KAR3	0.0465	KAP122	0.02762	INO2	GEM1
0.02958	KNS1	0.0269	KNS1	0.02413	IPK1	GPG1
0.00741	LYS1	0.01553	LYS12	0.008	ITT1	GSH2
0.00208	LYS12	0.03222	MET10	0.03748	KAP122	GUP1
0.02378	NRK1	0.00057	NRK1	0.00311	KAR3	GYP1
0.02889	NUP60	0.01654	NUP60	0.03422	KNS1	HAT1
8E-07	OPI3	7.61E-06	OPI3	0.00154	LYS1	IDH1
0.03521	OSH6	0.02464	OSH6	0.03296	MET10	INO2
0.0148	OST3	0.01998	OST3	0.00012	OPI3	IPK1
0.01776	PAC10	0.01884	PAA1	0.0292	OST3	ITT1
0.01503	PDC6	0.03422	PDC6	0.02689	PAA1	KAP122
0.01995	PNT1	0.00643	PH086	0.02545	PAC10	KAR3
0.03209	RIM8	0.03064	PNT1	0.04876	PDC6	KNS1
0.02146	RPL11B	0.005	REC8	0.00699	PH086	LYS1
0.04292	RPL16B	0.0377	RIM8	0.046	REC8	LYS12
0.00919	RPL37B	0.00382	ROX1	0.01277	ROX1	MET10
0.00857	RPL6B	0.02055	RPA34	0.01023	RPA34	NRK1
0.00077	RPL9B	0.00819	RPL11B	0.00193	RPL11B	NUP60
0.00491	SET6	0.03323	RPL37B	0.00225	RPL16B	OPI3

0.00739	SKO1	0.00973	RPL6B	0.00643	RPL6B	OSH6
3.8E-05	SLG1	8.51E-06	RPL9B	0.03652	RPL9B	OST3
0.0077	SMM1	0.02599	RPS0A	0.01321	RPS0A	PAA1
0.02712	SNF5	0.03142	RPS6A	0.02147	RPS6A	PAC10
0.0004	SPE1	0.00972	SAP155	0.00589	SAP155	PDC6
1.4E-11	SPE2	0.03332	SET6	0.03305	SET6	PHO86
1.9E-06	SPE3	0.03808	SIN3	0.00025	SIN3	PNT1
0.01733	SSH1	0.00488	SKO1	0.04681	SKO1	REC8
0.02559	SWS2	0.00017	SLG1	3.5E-05	SLG1	RIM8
0.04713	TBS1	0.00022	SMM1	0.00072	SNF5	ROX1
1.9E-06	TCO89	0.00114	SNF5	4.9E-06	SPE1	RPA34
0.00822	TEF4	2.50E-05	SPE1	3.8E-08	SPE2	RPL11B
0.00049	TGS1	1.48E-06	SPE2	8.2E-07	SPE3	RPL16B
0.00895	THR1	4.96E-07	SPE3	0.00451	SSD1	RPL37B
2.6E-08	THR4	0.01567	SSD1	0.01809	SWD1	RPL6B
0.04284	UIP4	0.00298	SSH1	0.00233	TCO89	RPL9B
0.02907	VPS1	0.02748	SWD1	0.02615	TEF4	RPS0A
0.00114	VPS4	0.00344	SWS2	0.00174	TGS1	RPS6A
0.03658	YDC1	0.03969	TBS1	0.00139	THR1	SAP155
0.03277	YDL199C	0.00204	TGS1	9.5E-07	THR4	SET6
0.04523	YDR056C	0.00011	THR4	0.02946	TRF4	SIN3
0.00953	YDR269C	0.00498	TRF4	0.00293	VPS4	SKO1
0.02305	YDR459C	0.04601	UIP4	0.01986	YDC1	SLG1
0.00431	YER066W	0.04099	VPS1	0.01982	YDL199C	SMM1
0.00177	YFL032W	0.0385	YDC1	0.01926	YDR056C	SNF5
0.01374	YGL261C	0.03322	YDR056C	0.04055	YDR269C	SPE1
0.01722	YGL262W	0.01406	YFL032W	0.03471	YDR459C	SPE2
0.00379	YGR107W	0.00804	YGL118C	0.00259	YER066W	SPE3
0.04067	YGR168C	0.01854	YGL140C	0.0016	YFL032W	SSD1
0.04586	YIL086C	0.02066	YGL177W	0.02785	YGL118C	SSH1
0.03528	YIL158W	0.04415	YGL235W	0.0028	YGL140C	SWD1
2.5E-05	YJL046W	0.00038	YGR107W	0.02448	YGL177W	SWS2
8.4E-06	YJL135W	0.02944	YGR168C	0.01714	YGL235W	TBS1
0.04164	YMR124W	0.0409	YIL158W	0.04381	YGL261C	TCO89
0.00504	YMR269W	0.02638	YJL046W	0.0178	YGL262W	TEF4
0.02437	YMR326C	0.01895	YJR003C	0.0073	YGR107W	TGS1
0.00125	YNL080C	0.04061	YLR446W	0.04287	YIL086C	THR1
0.03575	YNL146W	0.02878	YLR460C	0.00106	YJL135W	THR4
0.02758	YNL190W	0.02881	YMR124W	0.00334	YJR003C	TRF4
0.04168	YNR004W	8.13E-08	YMR269W	0.01558	YLR446W	UIP4
0.01745	YOL092W	0.00269	YMR326C	0.04547	YLR460C	VPS1
3.2E-05	YOR008C-A	2.78E-11	YNL080C	0.01789	YNL080C	VPS4
0.00168	YOR309C	0.04126	YNL146W	0.0311	YNL146W	YDC1
0.02709	YPL102C	0.04364	YNL190W	0.01758	YNR020C	YDL199C
0.01382	YPL158C	9.17E-05	YNR004W	0.00215	YOR008C-A	YDR056C
0.02174	YPL272C	0.02135	YNR020C	1.8E-05	YOR309C	YDR269C
0.03033	YPT11	0.01932	YOL092W	0.0173	YPL017C	YDR459C
		0.01174	YOR008C-A	0.00036	YPL158C	YER066W
		1.01E-06	YOR309C	0.02065	YPL182C	YFL032W
		0.00738	YPL017C	0.03569	YPL245W	YGL118C
		0.04518	YPL102C	0.02222	YPL272C	YGL140C
		0.00029	YPL158C			YGL177W
		0.03051	YPL182C			YGL235W
		0.04497	YPL245W			YGL261C

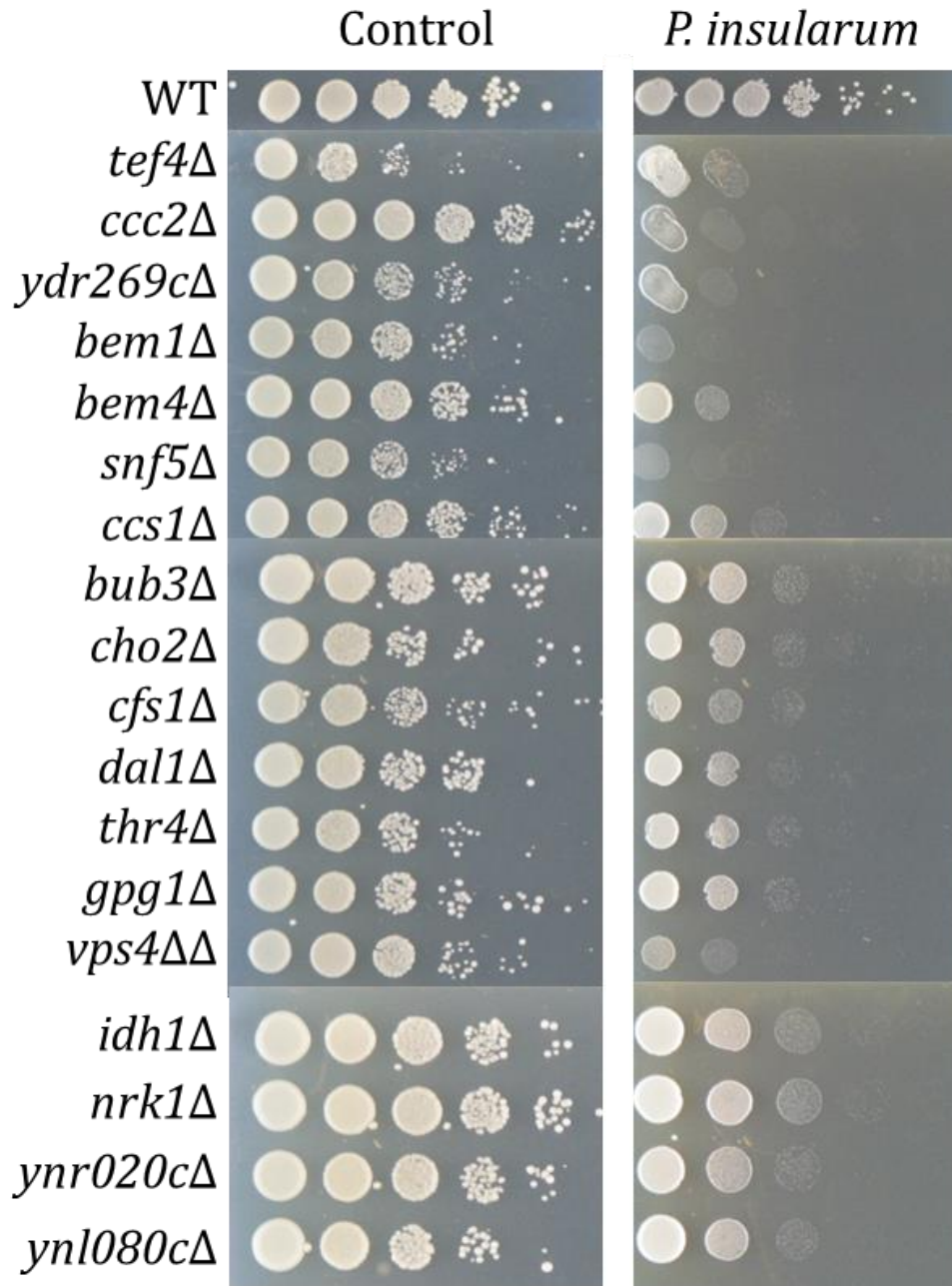
0.0018 YPT11

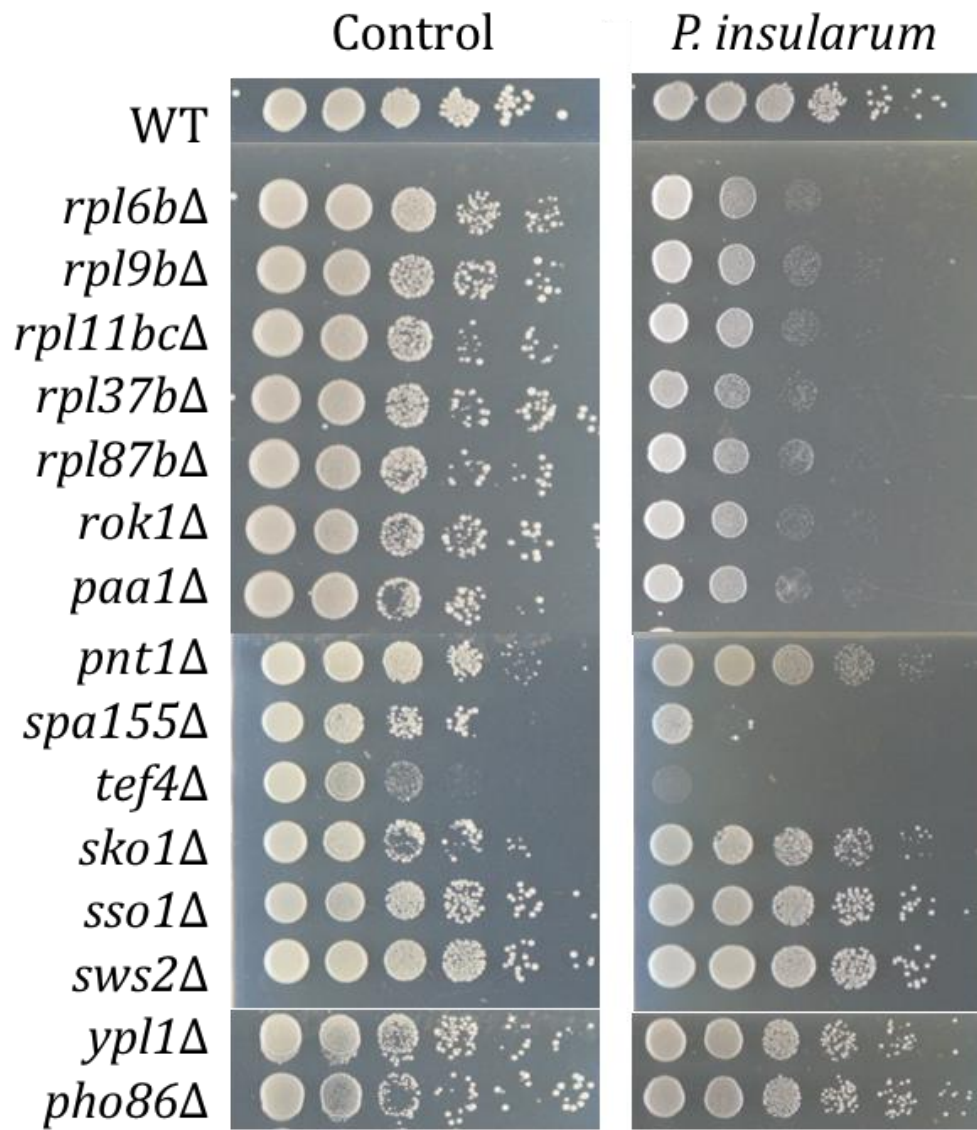
YGL262W  
YGR107W  
YGR168C  
YIL086C  
YIL158W  
YJL046W  
YJL135W  
YJR003C  
YLR446W  
YLR460C  
YMR124W  
YMR269W  
YMR326C  
YNL080C  
YNL146W  
YNL190W  
YNR004W  
YNR020C  
YOL092W  
YOR008C-A  
YOR309C  
YPL017C  
YPL102C  
YPL158C  
YPL182C  
YPL245W  
YPL272C  
YPT11

---

## Appendix V: Spot Dilution of Sensitive Strains

---





---

## Appendix VI: Script for Acapella GFP Quantification

---

```
SingleWell()
MBF_getInfo3()
CombineStack(NumberOfFields=2, MaxProjection=no, ImageAddition=no)
Nuclei_ID(CombinedPack.comimage_focus_c2_f1)
testcyto(CombinedPack.comimage_focus_c2_f1, CellDensity=no)
CalcIntensity(CalcStdDev=no, Image=CombinedPack.comimage_focus_c1_f1,
objects=Wholecells)
Set(obj1=objects)
Nuclei_ID(CombinedPack.comimage_focus_c2_f2)
testcyto(CombinedPack.comimage_focus_c2_f2, CellDensity=no)
CalcIntensity(CalcStdDev=no, Image=CombinedPack.comimage_focus_c1_f2,
objects=Wholecells)
AddObjects(Obj1, CheckOverlap=no, DeleteGeometry=yes)
If(objects.@count>20)
MAD2(objects.intensity)
Output(Objects.intensity.median, "GFP")
Output(MAD, "MAD")
End()
Output(objects.@count, "Cell Count")
```

## Appendix VII: Optimized Concentrations for HIP/HOP

**Table A7: Summary of optimization of concentrations for the aqueous and methanolic extracts for pooled diploid mutants analyses for HIP and HOP profiling.** Three concentrations for both the aqueous and methanolic extracts were assessed, including 0.0005% v/v, 0.001% v/v and 0.005% v/v for the aqueous extract, and 0.00005% v/v, 0.0001% v/v and 0.0005% v/v for the methanolic extract. The residual growth from pooled diploid libraries (heterozygous and homozygous) were compared to control conditions to determine the best concentration producing a growth inhibition of 10-20%, or a residual growth of 90-80%. Red indicates minimal growth inhibition, blue indicates too much growth inhibition, and green indicates ideal growth inhibition.

		Heterozygous Pool			Homozygous Pool		
		Control	<b>0.0005</b>	Residual %	Control	<b>0.0005</b>	Residual %
Aqueous Extract of <i>Psychotria insularum</i>	Rep-1	0.574	0.573	96.0	0.679	0.667	103.6
	Rep-2	0.656	0.631	105.7	0.644	0.661	102.6
	Rep-3	0.597	0.541	90.6	0.621	0.611	94.9
	Median	<b>0.597</b>		<b>96.0</b>	<b>0.644</b>		<b>102.6</b>
	StDev			<b>6.3</b>			<b>4.8</b>
	Control		<b>0.001</b>	Residual %	Control	<b>0.001</b>	Residual %
	Rep-1	0.574	0.475	79.6	0.679	0.576	89.4
	Rep-2	0.656	0.506	84.8	0.644	0.536	83.2
	Rep-3	0.597	0.479	80.2	0.621	0.537	83.4
	Median	<b>0.597</b>		<b>80.2</b>	<b>0.644</b>		<b>83.4</b>
	StDev			<b>2.4</b>			<b>3.5</b>
	Control		<b>0.005</b>	Residual %	Control	<b>0.005</b>	Residual %
	Rep-1	0.574	0.343	57.5	0.679	0.448	69.6
	Rep-2	0.656	0.333	55.8	0.644	0.439	68.2
	Rep-3	0.597	0.391	65.5	0.621	0.409	63.5
Median	<b>0.597</b>		<b>57.5</b>	<b>0.644</b>		<b>68.2</b>	
StDev			<b>4.4</b>			<b>3.2</b>	
Methanolic Extract of <i>Psychotria insularum</i>	Control		<b>0.00005</b>	Residual %	Control	<b>0.00005</b>	Residual %
	Rep-1	0.581	0.530	93.8	0.645	0.624	96.7
	Rep-2	0.565	0.551	97.5	0.611	0.648	100.5
	Rep-3	0.522	0.549	97.2	0.669	0.631	97.8
	Median	<b>0.565</b>		<b>97.2</b>	<b>0.645</b>		<b>97.8</b>
	StDev			<b>2.1</b>			<b>1.9</b>
	Control		<b>0.0001</b>	Residual %	Control	<b>0.0001</b>	Residual %
	Rep-1	0.581	0.461	81.6	0.645	0.497	77.1
	Rep-2	0.565	0.475	84.1	0.611	0.506	78.4
	Rep-3	0.522	0.490	86.7	0.669	0.495	76.7
	Median	<b>0.565</b>		<b>84.1</b>	<b>0.645</b>		<b>77.1</b>
	StDev			<b>2.6</b>			<b>0.908</b>
	Control		<b>0.005</b>	Residual %	Control	<b>0.005</b>	Residual %
	Rep-1	0.581	0.330	58.4	0.645	0.401	62.2
	Rep-2	0.565	0.364	64.4	0.611	0.431	66.8
Rep-3	0.522	0.373	66.0	0.669	0.415	64.3	
Median	<b>0.565</b>		<b>64.4</b>	<b>0.645</b>		<b>64.3</b>	
StDev			<b>4.0</b>			<b>2.3</b>	

---

## Appendix VIII: Primer Sequences used for Bar-Seq

---

**Illumina P5 Primer:**

5'-A ATG ATA CGG CGA CCA CCG AGA TCT ACA CTC TTT CCC TAC ACG ACG CTC TTC CGA TCT-3'

**Illumina Sequencing Primer:**

5'-ACA CTC TTT CCC TAC ACG ACG CTC TTC CGA TCT-3'

**(Robinson *et al.*, 2015)**

---

## Appendix IX: ICP-MS quantifying Zinc

---

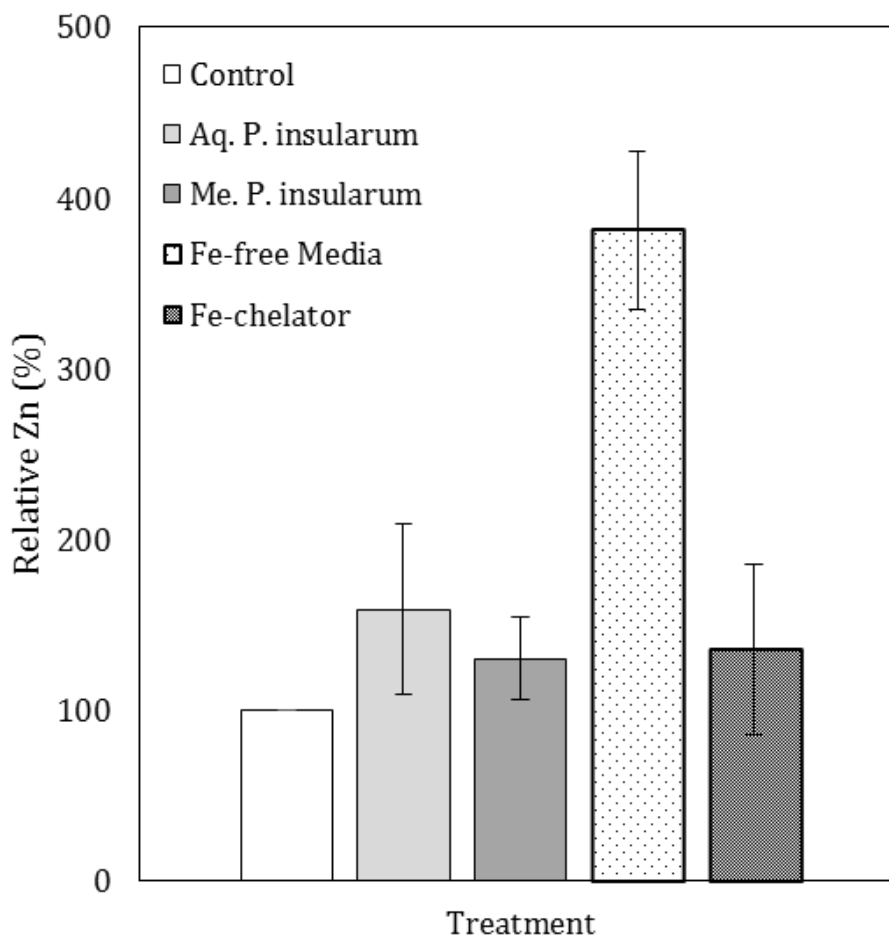


**Figure A9: Quantified intracellular zinc levels in WT yeast.** BY4741 cells were grown in control media (Control) as well as in treatment media containing 0.05% v/v of aqueous extract (Aq. *P. insularum*), 0.005% v/v of methanolic extract (Me. *P. insularum*), iron-free media (Fe-free media) and media containing 0.1  $\mu$ M bathophenanthroline disulfonic acid iron chelator control (Fe-chelator). Quantified iron is reported as relative total intracellular iron, compared to control BY4741 obtained from the average and standard deviation of two biological replicates. To determine if any increased levels of Zn were statistically significant, a one-tailed Student's t-test was carried out (\*\*: p-value < 0.01).

